PART I

DEACTIVATION OF TRIPLET PHENYL ALKYL KETONES BY CONJUGATIVELY ELECTRON-WITHDRAWING SUBSTITUENTS

PART II

REGIOELECTRONIC CONTROL OF INTRAMOLECULAR CHARGE-TRANSFER QUENCHING IN VARIOUS EXCITED TRIPLET PHENYL KETONES

By

Elizabeth Jane Siebert

A DISSERTATION

Submitted to
Michigan State University
in partial fulfillment of the requirements
for the degree of

DOCTOR OF PHILOSOPHY

Department of Chemistry

1981

ABSTRACT

PART I

DEACTIVATION OF TRIPLET PHENYL ALKYL KETONES BY CONJUGATIVELY ELECTRON-WITHDRAWING SUBSTITUENTS

PART II

REGIOELECTRONIC CONTROL OF INTRAMOLECULAR CHARGE-TRANSFER QUENCHING IN VARIOUS EXCITED TRIPLET PHENYL KETONES

By

Elizabeth Jane Siebert

PART I

Substituent effects on both photoreactivity (γ-hydrogen abstraction) and triplet energies (n,π^* and π,π^*) of phenyl alkyl ketones were determined for conjugatively electron-withdrawing substituents (cyano, carbomethoxy, and acyl). Spectroscopic results indicate that para (-R) substituents stabilize the π,π^* triplet much more than the n,π^* triplet, resulting in π,π^* lowest triplets. Conversely, meta (-R) substituents do not stabilize π,π^* triplets sufficiently to invert the triplet levels. Ortho (-R) substituents are dominated by steric factors: o-cyano stabilizes the n,π^* triplet, whereas o-carbomethoxy stabilizes the π,π^* triplet. These results support a largely

1,4-biradical structure for the π,π* triplet and suggest resonance stabilization by the para (-R) substituents.

Since only the n,π* triplet is reactive toward hydrogen abstraction, substituent effects on triplet energies can also be determined from triplet photoreactivities. In agreement with the spectroscopic results, para (-R) substituents and ortho-carbomethoxy (π,π* lowest triplets) decrease triplet reactivity, while meta (-R) substituents and ortho-cyano (n,π* lowest triplets) increase reactivity in both benzene and acetonitrile.

All (-R) substituted ketones undergo charge transfer quenching at nearly diffusion controlled rates. Various correlations involving Hammett parameters, reduction potentials, and n,π* triplet energies for various substituted valerophenones are presented.

PART II

Intramolecular charge transfer (CT) quenching rates were determined for amino-ketones in which the amine moiety was permitted only limited access to the site of triplet excitation. Rapid internal quenching ($k_{CT} \sim 5 \times 10^8\ s^{-1}$) was found in para-valeryl β-dimethylaminoethyl benzoate (p-2VB), which has a π,π* lowest triplet. The conformationally similar para-benzoyl β-dimethylaminoethyl benzoate, p-2BB, (n,π* lowest triplet) displayed slower internal quenching ($k_{CT} \sim 10^5\ s^{-1}$) as determined from its phosphorescence lifetime and quantum yield. Para-valeryl γ-dimethylaminopropyl benzoate (π,π* lowest triplet) also undergoes rapid CT quenching whereas both m-2VB and m-2BB (n,π* lowest triplets) undergo little internal quenching. Since the amine moiety cannot possibly come into contact with the carbonyl in any of these molecules, the results suggest that excitation in π,π* triplets is centered on the phenyl ring and excitation in n,π* triplets is localized on the carbonyl.

Rapid CT quenching was observed for p-methoxy-γ-dimethylaminobutyrophenone in both benzene and acetonitrile ($k_{CT} \sim 10^8 - 10^9\ s^{-1}$), while significant internal CT quenching ($k_{CT} \sim 10^7\ s^{-1}$) was observed for p-(3-dimethylaminopropoxy)valerophenone only in acetonitrile. These results suggest charge separation in the π,π* triplet, stabilized by polar solvents.

To Mom and Dad

and Barney

ACKNOWLEDGMENTS

The author wishes to thank Professor Peter J. Wagner for his guidance and support throughout the course of this endeavor. His advice to emulate his chemistry and not his desk hopefully will be heeded in the future. Also, the memos "signed" by Peter J. Wagner will always be remembered.

The author would like to thank the members of the Wagner Group for all the memorable times shared at MSU. Special thanks to (M. A. Meador)^2 for all the late night discussions, to the Kondili for their lasting friendship, and to R. Young for all the nickels. Also, hearty thanks to F. D. for the new beginning.

The author would also like to thank both relatives and friends for their encouragement and Mrs. Peri-Anne Warstler for the excellent typing of this dissertation.

Finally, the author would like to thank the Chemistry Department at MSU for the financial support and use of its facilitites and the National Science Foundation for the research assistantships administered by Dr. Wagner.

TABLE OF CONTENTS

LIST OF TABLES

Table Page

Table Page

Table Page

Table Page

LIST OF FIGURES

Figure Page

INTRODUCTION

A. Photophysical Processes

Molecules can undergo a wide variety of photophysical and photochemical processes upon the absorption of light. In order to understand better the photochemical reactions that phenyl alkyl ketones undergo, the many available photophysical processes will be discussed briefly.

A modified Jablonski diagram[1] for phenyl alkyl ketones shows the photophysical processes which can occur in the absence of photochemical reactions (Figure 1). In this diagram the absorption and

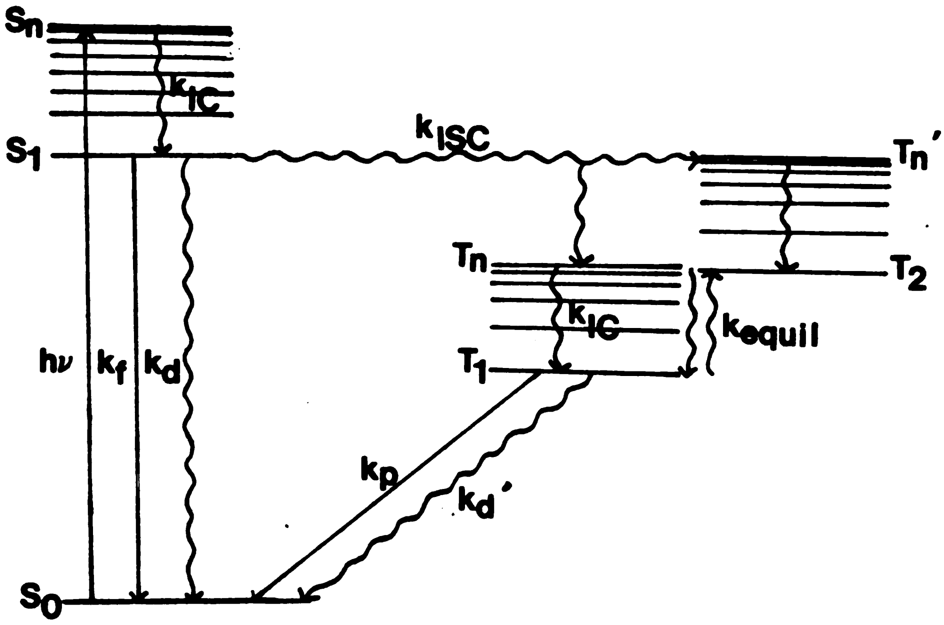

Figure 1. Modified Jablonski Diagram for Phenyl Alkyl Ketones.

emission of light are depicted by straight lines whereas radiationless transitions are shown as wavy lines. A molecule absorbs a photon and is excited to an upper singlet state which rapidly undergoes internal conversion ($k_{ic} \sim 10^{12}$ s^{-1}) to the lowest excited singlet S_1.[2] S_1 can then undergo fluorescence ($k_f \sim 10^6$ s^{-1}), radiationless decay ($k_d \sim 10^7$ s^{-1}), or intersystem crossing to the triplet state.[3]

The rate of intersystem crossing depends on the amount of spin-orbit coupling which allows the singlet to attain some triplet character.[4] The extent of spin-orbit coupling depends both on the energy gap between S_1 and the triplet state[3] and the nature of the singlet and triplet states.[4a] Both experimental observations and selection rules derived from electronic overlap integrals suggest that intersystem crossing from an n,π^* singlet to a π,π^* triplet is approximately 10^3 times faster than from an n,π^* singlet to an n,π^* triplet.[4b,c]

For phenyl alkyl ketones, which possess n,π^* lowest singlets, the rate of intersystem crossing is extremely fast ($k_{ISC} \sim 10^{10}$ s^{-1}).[5] Thus, fluorescence and radiationless decay are too slow to be competitive singlet processes. Essentially all the singlets undergo spin inversion to populate the upper vibrational states of the triplet(s). Again, rapid internal conversion ($k_{ic} \sim 10^{12}$ s^{-1}) leads to population of the lowest vibrational level of the triplet(s).[2] In many phenyl alkyl ketones, two triplets (n,π^* and π,π^*) are in close proximity and undergo vibronic coupling[5] or thermal equilibration[6] before undergoing reaction or decay. The triplet(s) can then undergo phosphorescence ($k_p \sim 10^{-1}$ to 10^3 s^{-1}) or radiationless decay if other photochemical processes are unavailable.[3] For many phenyl alkyl ketones, hydrogen abstraction is very fast compared to both radiationless decay and phosphorescence, and thus photochemical reaction leading to product formation is the major pathway for deactivation of the triplet state.

B. Norrish Type II Photochemical Reaction

The Norrish Type II photochemical reaction is the major decay process for most phenyl alkyl ketones possessing γ-hydrogens. This reaction was first discovered in 1934 by Norrish and Appleyard[7] when they found that methyl butyl ketone photodecomposes to give acetone and propene in the gas phase. Further investigation of other ketones showed a characteristic α,β-bond cleavage to give a smaller carbonyl compound and an olefin.[8] In 1958 Yang and Yang[9] reported the formation of cyclobutanols as minor products in addition to cleavage products and suggested the formation of a 1,4-biradical intermediate to explain the results. Further evidence supporting the intermediacy of a 1,4-biradical was provided by Wagner[10] and others.[11] Thus, γ-hydrogen abstraction by the triplet state to form a 1,4-biradical, followed by cleavage or cyclization is the generally accepted mechanism for the Norrish Type II photochemical reaction (Scheme 1).

The 1,4-biradical also can undergo reverse hydrogen transfer to give ground state ketone.[10a] The addition of a Lewis base suppresses the reversion of the biradical to starting ketone by hydrogen bonding the hydroxyl hydrogen, thus slowing down reverse hydrogen transfer

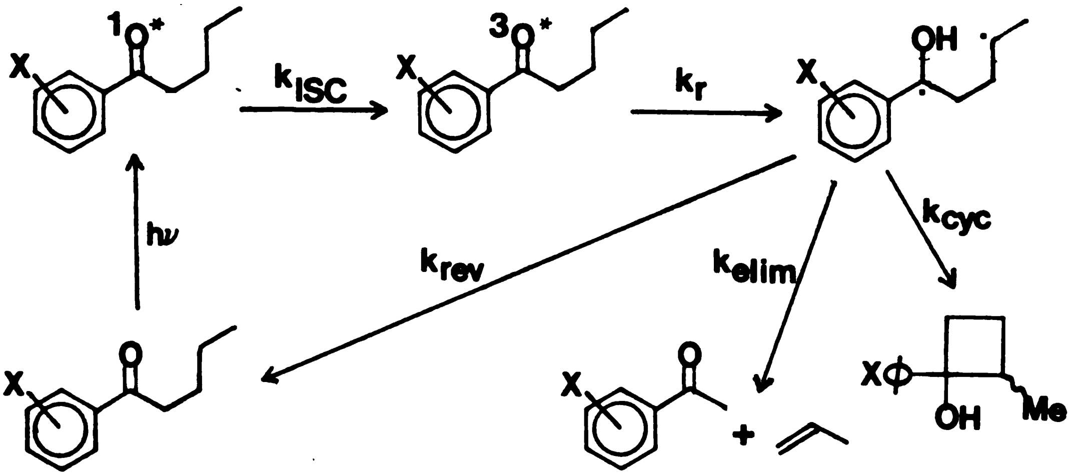

Scheme 1. Norrish Type II Photochemical Reaction.

and enabling cleavage or cyclization to occur exclusively.[10b,12] The quantum yield for cyclization products averages only approximately 10-20% of the quantum yield for cleavage products.[13] Also, the rate of γ-hydrogen abstraction is dependent on both the stability of the incipient radical center,[14,15] and the reactivity of the triplet state toward hydrogen abstraction. Both the electronic nature of the triplet state and the effects of substituents determine the reactivity of phenyl alkyl ketones.[11b,16-26]

C. Triplet States of Phenyl Alkyl Ketones

Phenyl alkyl ketones possess two triplet states which differ significantly in their electronic distribution. An n,π* triplet results from excitation of a non-bonding electron of the carbonyl to a π-antibonding orbital, thus producing electron deficiency at the oxygen atom. The n,π* triplet resembles an alkoxy radical and undergoes typical radical reactions such as hydrogen abstraction.[16,17] Analogously, a π,π* triplet results from excitation of a π electron to a π-antibonding orbital, resulting in increased electron density at the oxygen atom.[18,19] Consequently, the π,π* triplet is not reactive in typical electrophilic radical reactions. Valence bond representations of the two triplet states are given below.

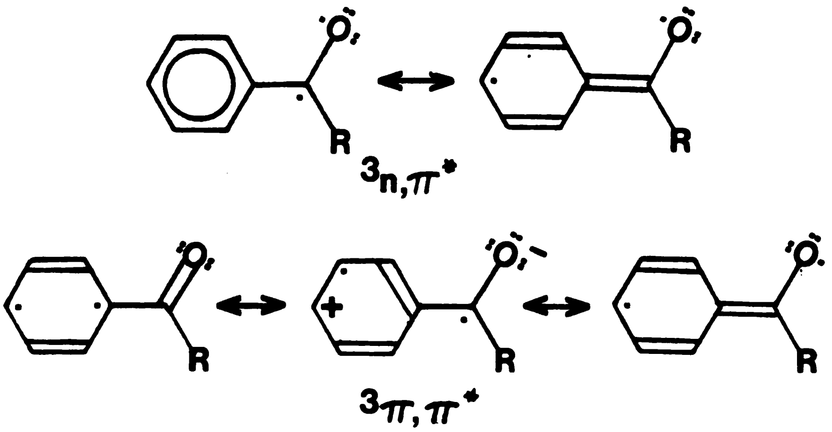

Many examples in the literature indicate that phenyl ketones with n,π* lowest triplets are reactive towards hydrogen abstraction reactions; whereas, ketones with π,π* lowest triplets are either unreactive or display substantially decreased reactivities. Yang and Dusenbery[20] reported that substituted benzophenones (4-methyl or 4-trifluoromethyl) that retain an n,π* lowest triplet are easily photoreduced by 2-propanol. Conversely, 4-phenylbenzophenone, which possesses a π,π^* lowest triplet,[21] displays a 10^3-fold decrease in reactivity compared to benzophenone itself.[22] Similarly, the photoreduction of 4-trifluoromethylacetophenone (n,π^* lowest triplet) displays a six-fold increase in the rate of hydrogen abstraction, whereas 4-methylacetophenone (π,π^* lowest triplet) shows a tenfold decrease in reactivity, both compared to acetophenone.[23,24] Likewise, the Norrish Type II photochemical reactions of substituted butyrophenones and valerophenones follow a similar trend: ketones with n,π^* lowest triplets undergo intramolecular γ-hydrogen abstraction readily, while ketones with definite π,π^* lowest triplets are essentially unreactive.[11b,25-29]

In the past two decades the determination of substituent effects on the photochemistry of phenyl ketones has received considerable attention. The effects of ring-substituents on both the triplet energies and triplet-state photoreactivity have been investigated extensively.[11b,21,23,24,27,28,30] In general, the effects of ring-substituents on the energies of both triplets, thus determining the nature of the lowest triplet, overshadow their electronic effects on the individual triplet states. In benzophenone the n,π^* triplet is far enough below the π,π^* triplet such that most substituents do not cause an inversion of the two triplet states.[31] In unsubstituted phenyl alkyl ketones the n,π^* triplet lies only approximately 2.8 kcal below the π,π^* triplet in nonpolar solvents.[30b] Polar solvents stabilize the π,π^* triplet and destabilize the n,π^* triplet, since the n,π^* triplet has a lower dipole moment and the π,π^* triplet has a higher dipole moment than the ground state.[11b,30d] Electron-donating substituents stabilize the π,π^* triplet and destabilize the n,π^* triplet, resulting in inversion of the two triplets and decreased reactivity.[28] Conversely, electron-withdrawing substituents stabilize the n,π^* triplet relative to the π,π^* triplet and also make the n,π^* triplet more electrophilic, thus making such triplets more reactive than those of unsubstituted ketones (Scheme 2).

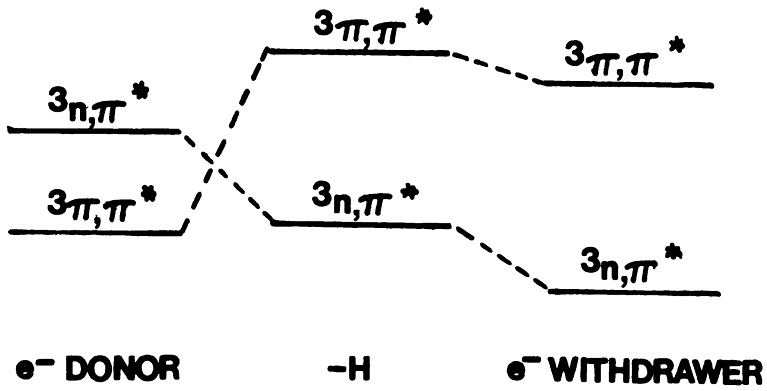

Scheme 2. Substituent Effects on Triplet Energies for Phenyl Alkyl Ketones.

It is generally accepted that π,π^* triplets are much less reactive than n,π^* triplets towards hydrogen abstraction, and ketones with π,π^* lowest triplets derive their reactivity primarily from equilibrium populations of upper n,π^* triplets.[28,32] Wagner[28] has provided evidence for photoreactivity from upper n,π^* triplets for p-methoxyphenyl alkyl ketones, since their rates for hydrogen abstraction exactly parallel the rates for unsubstituted phenyl alkyl ketones (n,π^* lowest triplets) with similar γ- or δ-substitution. Also, the variation of photoproduct distribution with temperature for 1-benzoyl-4-p-anisoylbutane is consistent with thermal equilibration of the two nonconjugated chromophores, and reaction of the anisoyl moiety from an equilibrium population of its n,π^* triplet.[32b] At a certain temperature, T, the equilibrium population of both triplets is dependent upon the energy separation between the two triplets, ΔE_T, and follows a Boltzmann distribution (Equation 1)

$$\frac{\chi_{n,\pi}}{\chi_{\pi,\pi}} = e^{-\Delta E_T/RT} \qquad (1)$$

where χ is the equilibrium fractional population of a given triplet state. At room temperature the two triplets must be in close proximity ($\Delta E_T \leq 3$ kcal) in order for thermal equilibration to occur. If the observed rate of hydrogen abstraction reflects reactivity from both triplets, then Equation (2) describes the reaction kinetics.

$$k_H^{obs} = \chi_{n,\pi} k_H^{n} + \chi_{\pi,\pi} k_H^{\pi} \qquad (2)$$

When $\Delta E_T \leq 3$ kcal, reaction occurs primarily from population of the upper n,π^* triplet.[28]

$$k_r^{obs} = \chi_{n,\pi} k_r^{n} \qquad (3)$$

If the two triplets are in close proximity then vibronic coupling can induce some n,π* character into the π,π* triplet and vice versa.[5] Therefore, the wave function Ψ of the lowest triplet is a linear combination of the two unperturbed wave functions ψ, with the mixing coefficients a and b dependent upon both the energy gap between the triplets and symmetry considerations.[5]

$$\Psi_{T_1} = a\psi(\pi,\pi^*) + b\psi(n,\pi^*) \qquad (4)$$

Thus, some reactivity possibly can occur from the vibronically induced n,π* character of the π,π* triplet.[23b]

D. Energy Transfer and Charge Transfer Processes

1. Energy Transfer Processes

a. Intermolecular - Energy transfer is an important photochemical process involving a radiationless transfer of electronic excitation from a donor molecule to a suitable acceptor molecule. Triplet-triplet energy transfer (Equation 5) is the most common type of energy transfer, since the lowest triplet state of a molecule is longer-lived than the corresponding lowest singlet state and therefore has a greater probability of transferring its electronic excitation energy to a suitable acceptor molecule.[32]

$$D^*(T_1) + A(S_0) \rightarrow D(S_0) + A^*(T_1) \qquad (5)$$

Triplet energy transfer can occur when the acceptor has a lower triplet energy than the donor molecule.[33] Usually, the efficiency of an acceptor or quencher is determined solely by the position of its lowest triplet level and not by its molecular structure.[34] In general, triplet energy transfer in solution occurs via an electron-exchange mechanism which requires diffusion of the donor and acceptor molecules to within collisional separation as a rate-limiting step.[33]

Thus, in relatively viscous solvents is triplet energy transfer diffusion controlled and described by a modified Debye equation.[35,36]

$$k_{et} = k_{dif} = 8RT/2000\,\eta \;\; \mathrm{l \cdot mol^{-1} \cdot s^{-1}} \qquad (6)$$

Only in solvents of low viscosity, the exothermic transfer of triplet excitation energy is not completely efficient, and an excited donor and an acceptor molecule can diffuse apart before energy transfer can occur.[33,37] Since every collision between donor and acceptor does not result in energy transfer, then a conformational requirement for effective orbital overlap may be necessary in order for energy transfer to occur.[38] Wagner and coworkers[39] have indicated that efficient energy transfer occurs at van der Waals separation (approximately 4 Å for π-system overlap with a carbonyl moiety) between donor and acceptor molecules. In order to gain more insight into the conformational requirements involved in energy transfer, several researchers have studied intramolecular energy transfer in systems containing isolated chromophores having known spatial dispositions relative to each other.[40-43]

b. Intramolecular - There are many examples of intramolecular triplet-triplet energy transfer reported in the literature. Hammond *et al.*[40] found that triplet energy transfer from a benzophenone chromophore to a naphthalene moiety separated by one to three methylene units (the distance between the carbonyl carbon and the center of the naphthalene group is at most 10 Å in all three cases) occurs with 100% efficiency with a rate constant greater than 10^{10} s^{-1}. Likewise, Cowan and Baum[41] investigated a series of compounds in which acetophenone and trans-β-styryl chromophores were separated by one to four methylene units and found efficient isomerization of the styryl group upon irradiation of the benzoyl chromophore. However, the reported 20-fold decrease in the rate of triplet energy transfer in going from two to four methylene groups ($k_{et} = 7.2 \times 10^{10}$ s^{-1} for $n = 2$ and $k_{et} = 3.3 \times 10^{9}$ s^{-1} for $n = 4$) suggests that an increase in the number of methylene units results in a decrease in the number of desirable conformations (donor and acceptor in close proximity) relative to the number of available conformations. Thus, it appears that the two chromophores have to be in close contact in order for energy transfer to occur.

Also, there are a few examples of intramolecular triplet-triplet energy transfer occurring in compounds containing two isolated chromophores held at fixed distances in rigid molecules. Zimmerman and McKelvey[42] investigated the phosphorescence emission of 1-benzoyl-4-(α-naphthyl)-bicyclo[2.2.2]octane, in which the benzoyl chromophore (donor) and naphthyl moiety (acceptor) are separated by approximately 7 Å, and found that intramolecular triplet energy transfer occurs with 100% efficiency. In contrast, Keller and Dolby[43] found that the rate constant for triplet energy transfer from benzophenone to a naphthalene group held approximately 14 Å apart by a rigid steroid bridge was only 25 s^{-1}. Of even greater interest is the fact that these authors[43] also discovered that energy transfer from a carbazole donor (π,π^* lowest triplet) to a naphthalene acceptor held at a comparable separation (approximately 15 Å) was 10^3 times slower ($k_{et} = 0.04\ s^{-1}$). Thus, the conclusion was reached that triplet-triplet energy transfer is not only distance dependent but also may be structure dependent, with $\pi,\pi^* \rightarrow \pi,\pi^*$ triplet-triplet energy transfer being slower by three orders of magnitude than $n,\pi^* \rightarrow \pi,\pi^*$ triplet-triplet energy transfer for the same donor-acceptor separation.

2. <u>Charge Transfer Processes</u>

a. Intermolecular - Carbonyl compounds can be photoreduced by a wide variety of hydrogen sources including alcohols,[44] alkanes,[45] alkyl benzenes,[45,46] tributylstannane,[47] ethers,[48] and amines.[49] It is well established that hydrogen abstraction from alcohols and alkanes by triplet carbonyls involves the simultaneous cleavage of the R-H bond and the formation of the O-H bond to give two radical species.[50]

$$^3R_2C = O^* + R'\text{-}H \rightarrow R_2\dot{C}\text{-}OH + R'\cdot$$

However, there are many differences in the photoreduction of ketones by amines as compared to alcohols, alkanes, and many other hydrogen donors. For example, the rate of hydrogen abstraction for triplet benzophenone with alkanes depends upon the hydrocarbon C-H bond strength,[51] whereas the photoreduction of benzophenone by N-alkylated diphenylamines displays little dependence on donor bond strength.[52] Cohen and Litt[53] reported that the photoreduction of benzophenone by triethylamine is 10^3 times faster than with isopropanol as hydrogen donor. Also, Cohen and Green[54] found that the rate of photoreduction of acetophenone with α-methylbenzylamine was twenty times greater than the rate of photoreduction with α-methylbenzyl alcohol. Both fluorenone and p-aminobenzophenone (π,π* lowest triplets) are not reduced by alcohols, but are readily photoreduced by tertiary amines.[55,56] In order to account for the greater reactivity of amines, Cohen and Cohen[56] proposed the following mechanism involving the initial transfer of an electron from the nitrogen atom to the excited carbonyl, followed by proton transfer and electron redistribution.

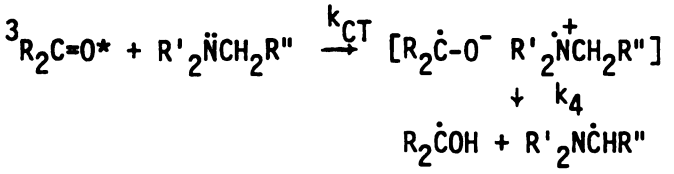

$$\begin{aligned} {}^3R_2C{=}O^* + R'_2\ddot{N}CH_2R'' \xrightarrow{k_{CT}} {} & [R_2\dot{C}\text{-}O^- \; R'_2\overset{\cdot +}{N}CH_2R''] \\ & \qquad \downarrow k_4 \\ & R_2\dot{C}OH + R'_2N\dot{C}HR'' \end{aligned}$$

The charge transfer complex can also undergo spin and charge destruction to give ground state ketone.[57] Thus, charge transfer interaction between the excited carbonyl moiety and the amine can result in

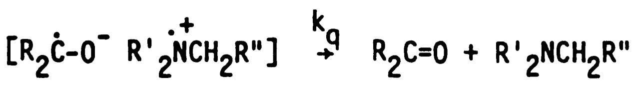

$$[R_2\dot{C}\text{-}O^- \; R'_2\overset{\cdot +}{N}CH_2R''] \xrightarrow{k_q} R_2C{=}O + R'_2NCH_2R''$$

either radical formation or deactivation to ground state ketone, depending on the nature of both the donor and acceptor molecules involved in the charge transfer complex.[58]

Rates of charge transfer interaction between donor and electronically excited acceptor have been found to be dependent on their thermodynamic properties. In 1968 Weller[59] related the rate of fluorescence quenching of aromatic hydrocarbons by amines to the change in free energy involved in electron transfer, ΔG_{CT}, which was found to be dependent on the oxidation potential of the donor, the reduction potential of the acceptor, the singlet excitation energy of the acceptor, and a Coulombic term related to the free energy gained by bringing the ions to the encounter distance (Equation 7).

$$\Delta G_{CT} = E(D/D^{+}) - E(A^{-}/A) - \Delta^{1}E(A) - e_{o}^{2}/\varepsilon_{a} \qquad (7)$$

Weller[60] determined that in solvents with large dielectric constants, the rate of charge transfer quenching of singlets produces free radical ions, and is diffusion controlled when $\Delta G_{CT} < -10$ kcal/mole. The rate constant of charge transfer quenching decreases with increasing ΔG_{CT} and becomes proportional to exp $(-\Delta G_{CT}/RT)$ when $\Delta G_{CT} > 5$ kcal/mole. Thus, when ΔG_{CT} is endothermic, a plot of log k_{CT} versus ΔG_{CT} has a slope of -16.5 eV for processes involving full electron transfer. Mataga et al.[61] observed the fluorescence from pyrene and N,N-dimethylaniline in various solvents. From the fluorescence quantum yields and lifetimes they concluded that in polar solvents the emission was due to a strong charge transfer complex, while the emission in nonpolar solvents was due to a weak CT complex (only partial electron transfer). Davis and coworkers[62] showed that the rate of fluorescence quenching of fluorenone by various amines was inversely proportional to the ionization potential of the amine. Thus, Weller's equation appeared to be applicable to a large number of systems.

A similar relationship was sought for the reaction of excited-state triplets with amines. Cohen and Stein[63] reported that for the photoreduction of sodium 4-benzoylbenzoate by tertiary aliphatic amines, the rate of interaction between ketone triplets and amines increased as the ionization potential of the amine decreased. In 1972 Guttenplan and Cohen[64] related the rate constant for donor-acceptor charge transfer interaction, k_{CT}, to the change in free energy, ΔG_{CT}, for carbonyl excited triplet states and various donors. A modified "Weller's Equation" was proposed which related ΔG_{CT} to the ionization potential of the donor, the reduction potential of the acceptor, and a constant (Equation 8).

$$\log k_{CT} \sim \Delta G_{CT} \sim IP_D - E(A^-/A) - \Delta^3E_{0,0} + C \qquad (8)$$

The use of the more readily available ionization potentials instead of the oxidation potentials of the donors only changes the value of the constant term. Thus, for a series of donors with a constant acceptor, $\log k_{CT} \sim IP_D + C'$ and for a series of acceptors with a constant donor, $\log k_{CT} \sim -E(A^-/A) - \Delta^3E_{0,0} + C''$. Guttenplan and Cohen[64b] proposed a linear correlation between $\log k_{CT}$ and the excited state reduction potential ($-E(A^-/A) - \Delta^3E_{0,0}$) for the quenching by triethylamine of various carbonyl acceptors, which possessed widely differing reduction potentials, triplet energies, and triplet configurations. These authors[64a] also reported a linear inverse relationship between log k_{CT} and the donor ionization potential for the charge transfer quenching of benzophenone by various donors including amines, sulfides, mercaptans, ethers, alcohols, aromatic hydrocarbons, and olefins. Two lines were obtained, one for aliphatic donors (slope = -0.067 mole/kcal) and the other for aromatic donors (slope = -0.105 mole/kcal), on a graph of log k_{CT} versus IP_D. The values of the slopes are much smaller than that observed in systems involving full electron transfer (slope = -0.74 mole/kcal).[65] Also, only small polar solvent effects were observed for the charge transfer quenching rate; (a factor of 2 in acetonitrile compared to benzene). A 13-fold increase in the fluorescence quenching rate for a corresponding process involving full electron transfer was reported.[66] Many studies indicate that full electron transfer is not involved in charge transfer complex formation between carbonyl triplets and amines. The small polar solvent effects and the decreased slopes of log k_{CT} versus IP_D plots suggest that at most only approximately 20% electron transfer is involved in the charge transfer complex formation.[64a,67,68] Bartholomew <u>et al</u>.[69] later conducted flash studies on the photoreduction of benzophenone with tertiary amines and found that a charge transfer complex forms in acetonitrile solvent; an exiplex may be formed in less polar solvents. Shaefer and Peters[70] used picosecond absorption techniques to confirm the initial formation of radical ions from benzophenone and triethylamine in acetonitrile, followed by either proton transfer to form the benzhydrol and amine radicals or decay back down to ground state molecules. Also, Amouyal and Bensasson[71] used laser flash absorption techniques to investigate the photoreaction of triplet duroquinone with tertiary amines and proposed that an exiplex is initially formed in both polar and nonpolar solvents, followed by the formation of a charge transfer complex in solvents of high dielectric constant.

The rate of charge transfer interaction between tertiary amines and carbonyls is fast, since these donors have relatively low ionization potentials.[72] Tertiary amines undergo charge transfer complex formation with n,π^* triplets of ketones such as benzophenone and acetophenone at nearly diffusion-controlled rates, leading to both quenching and radical formation.[57,73] Mueller[74] quenched the type II photoelimination of many ring-substituted valerophenones with triethylamine in both benzene and acetonitrile solvents and observed diffusion-controlled quenching rates for those ketones with relatively low reduction potentials. Also, Wagner and Kemppainen[75] reported an order of magnitude decrease in the quenching rate of valerophenone with triethylamine in methanol as compared to benzene and acetonitrile solvents. The decrease was attributed to the decreased availability of the hydrogen-bonded lone-pair electrons on the nitrogen atom.

In addition to amines, other types of compounds are suitable electron donors for excited ketones. Kochevar and Wagner[76] have investigated the quenching of the type II photoelimination of butyrophenone with a wide variety of olefins and determined that charge transfer quenching predominates for electron-rich olefins, while energy transfer quenching is dominant for electron-deficient olefins. Wagner and Leavitt[77] reported that in the photoreduction of α-trifluoroacetophenone with alkylbenzenes, both charge transfer complex formation and direct hydrogen abstraction are involved. Cohen and Guttenplan[78] determined that thioethers quench the triplet benzophenone in benzene and acetonitrile ($k_{CT} \sim 10^7 - 10^9\ M^{-1}\ s^{-1}$), but at a slower rate than tertiary amines, since sulfides have higher ionization potentials than tertiary amines. Also, both aromatic and aliphatic mercaptans quench the phosphorescence of benzophenone with rate constants between $10^7 - 10^9\ M^{-1}\ s^{-1}$, respectively. In addition, phosphorus, antimony, arsenic, and bismuth are thought to quench the type II photoelimination of butyrophenone by a charge transfer mechanism.[50] Thus, charge transfer complex formation is a common type of interaction between molecules capable of donating or accepting additional charge in the excited state.

b. Intramolecular - Due to the limited number of conformations possible in bifunctional molecules, the study of intramolecular charge transfer interactions in these compounds can provide insight into the structure of the CT complex and the differences in charge transfer interactions with n,π* and π,π* triplets. In the past decade a number of studies concerning intramolecular charge transfer complex formation have been published.[73,75,79-84]

The photochemical reaction of dialkylphenylacylamines was used as

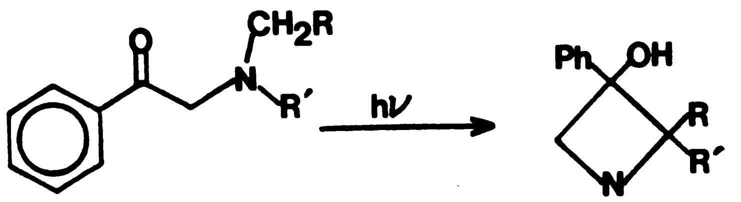

a synthetic route to 3-hydroxyazetidines in only modest yields (9-22%), since type II photoelimination products (30-55% yields) were also obtained.[79] Later, Padwa and coworkers[80] investigated two N,N-dibenzylphenacylamines having either an n,π^* or π,π^* lowest triplet and found

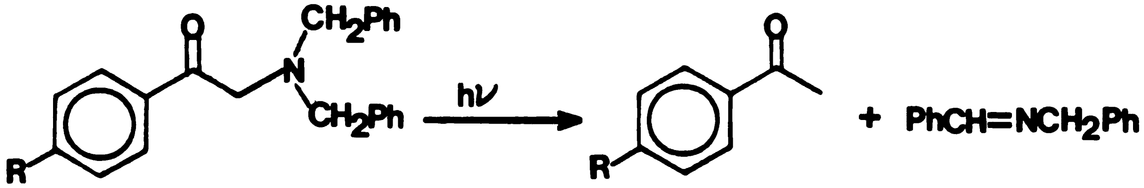

where R=H,Ph

similar type II quantum yields (Φ_{II} = 0.14 and 0.12, respectively) in ethanol. The lack of quenching by 1,3-cyclohexadiene and piperylene and the low type II quantum yields suggested that a charge transfer complex was formed at a rate exceeding diffusional quenching followed

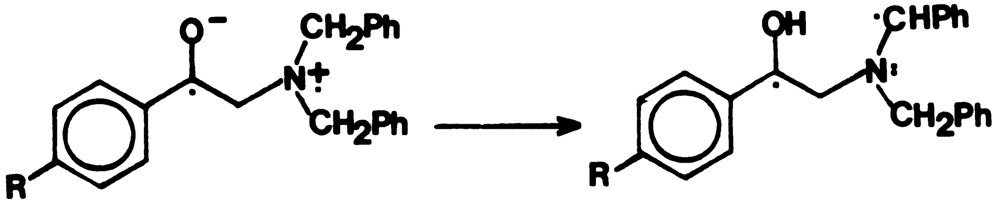

by either back electron transfer to regenerate starting ketone or proton transfer to generate a 1,4-biradical. Padwa _et al._[81] found that 3-aroylazetidines, which possess either an n,π* or π,π* triplet, give only arylpyrroles as photoproducts in low quantum yields ($\Phi \sim 0.1$). The authors proposed the rapid formation of a charge transfer complex, followed by proton transfer and electron reorganization to form a biradical, bond closure, and elimination of water to give the observed products. The corresponding hydrochloride salts

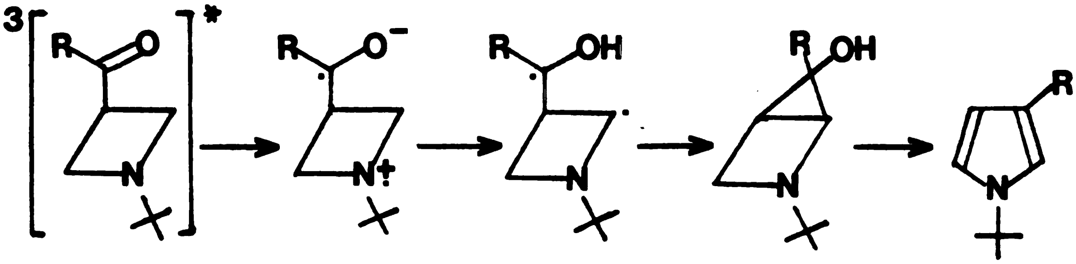

were found to be photochemically inert, since the nitrogen lone pair is no longer available. Thus, it appears that both n,π* and π,π* triplets can undergo charge transfer interactions.

Wagner and coworkers[73,75] investigated the photoreactions of α,γ, and δ-dialkylaminoketones in a variety of solvents. The intersystem crossing yields for these ketones are less than unity, with

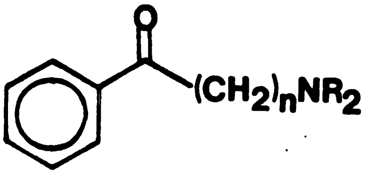

n=1,3,4

lower values for decreasing values of n ($\Phi_{ISC} \sim 0.01$ for n = 1 in benzene or acetonitrile). When n = 1, an unquenchable singlet state is responsible for all the photoelimination in benzene and acetonitrile and two-thirds of the photoelimination in methanol. In contrast, the photoelimination in compounds where n = 3 or 4 results from direct triplet-state γ-hydrogen abstraction. Rapid intramolecular charge transfer quenching is a competitive triplet-state process which results in deactivation of the triplet state to form ground-state ketone. Charge transfer quenching is 3.5 times faster for n = 3 than for n = 4, and five times faster in benzene or acetonitrile than in methanol. Since charge transfer quenching of the triplet does not result in biradical formation, the nitrogen lone pair must be held near the carbonyl and the γ-hydrogens away from the carbonyl moiety in the charge transfer complex.

Wagner and Scheve[67] also investigated 4-benzoyl-4,N-dimethylpiperidine (n,π* lowest triplet) in which the nitrogen lone pair is held approximately 4-6 Å from the carbonyl group. The two possible conformers formed distinct, non-interconverting triplets: the triplet having the benzoyl group axial underwent rapid γ-hydrogen abstraction, followed by cyclization of the 1,4-biradical, while the triplet having the benzoyl group equatorial underwent only α-cleavage. When the nitrogen lone pair is axial, the relative orientation and overlap of orbitals is poor and charge transfer quenching does not occur. The rate constant for CT quenching of the other triplet cannot exceed 2×10^6 s^{-1}. This rate is slower by a factor of 10^3 as compared to the rate of CT quenching in the acyclic γ-amino ketones.[77] From these

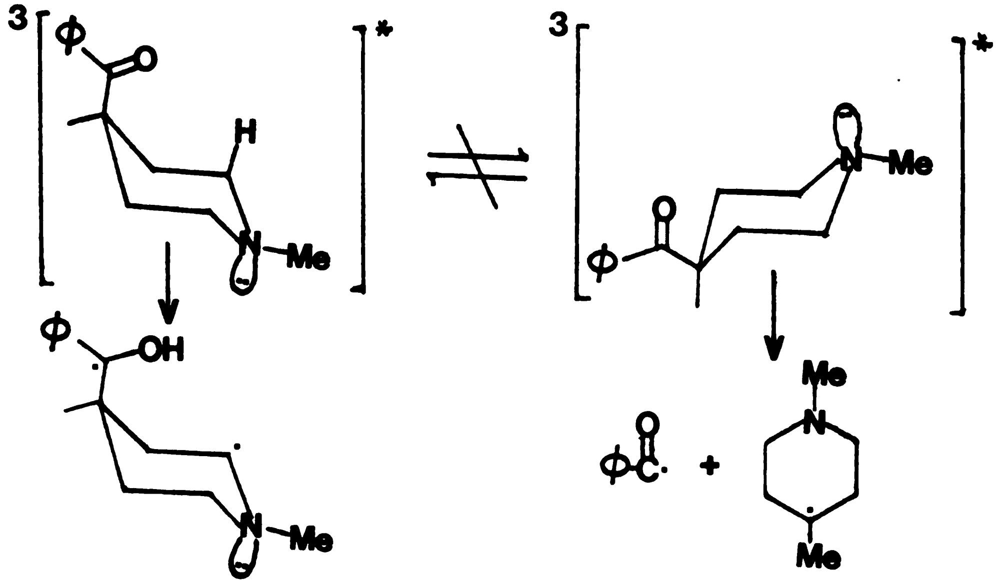

results the authors concluded that CT quenching in acyclic γ-aminoketones occurs solely by through-space rather than through-bond interactions.

Wagner and Ersfeld[67,82] photolyzed β-naphthyl-γ-dimethylaminopropyl ketone and found inefficient photoelimination (Φ_{II} = 0.008) in both benzene and acetonitrile solvents due to a π,π* lowest triplet and efficient CT interaction between the triplet state and the amine. The authors proposed that the cyclic charge transfer complex formed must be restricted to conformations in which the hydrogens α to the nitrogen are kept away from the carbonyl such that 1,5-proton transfer cannot occur. In contrast, bimolecular photoreduction of triplet

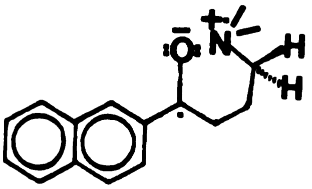

naphthyl ketones by amines results in efficient radical formation.[83] In methanol the photoelimination proceeds at moderate efficiency ($\Phi_{II} = 0.17$) and it was suggested that protonation of the oxygen atom in the CT complex by methanol leads to diradical formation and type II photoproducts.[82]

Winnik and Hsiao[84] studied a series of benzophenone derivatives in which the benzophenone chromophore and an ethenyl moiety were

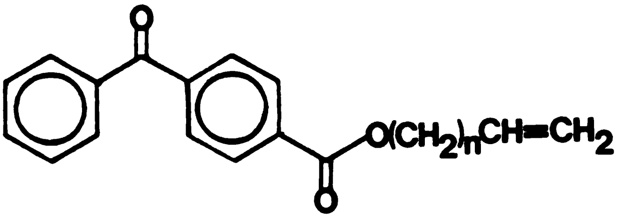

separated by one to nine methylene units and found significant intramolecular quenching of benzophenone room temperature phosphorescence emission when n = 9. The authors concluded that charge transfer quenching occurs only when the double bond approaches a van der Waals distance from the benzophenone carbonyl moiety and that CT quenching involves electron transfer to the electron deficient n orbital localized on the carbonyl oxygen. Later experiments performed by Mar and Winnik[85] with an extension of the methylene chain showed an increase in the quenching rate until n = 12, and then a rapid decrease in quenching (n = 13 to 21) due to the rapid increase in the total number of chain conformations as compared to the only modest increase in the total number of chain conformations which lead to quenching. Thus, these experiments suggest that a specific geometry is required in order for efficient charge transfer to occur.

Masuhara et al.[86] used laser spectroscopy to study systems in which benzophenone and N,N-dimethylaniline are connected by a methylene

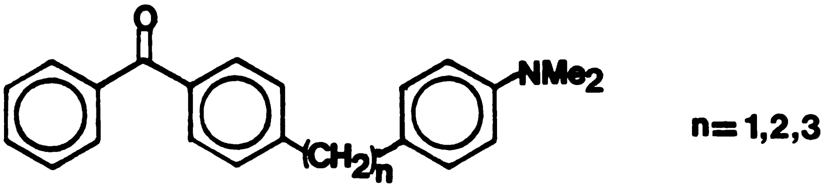

chain. The transient absorption spectra observed in acetonitrile could be reproduced by superposition of those of the benzophenone anion and DMA cation, and the spectra in benzene were similar to those of the benzophenone ketyl radical or triplet benzophenone. Thus, the authors proposed that intramolecular hydrogen abstraction resulting in the formation of benzophenone ketyl radical occurred in benzene whereas intramolecular electron transfer occurred in acetonitrile, and both processes were almost completely independent of the number of methylene units. Thus, they concluded that a definite, restricted structure was not necessary for electron transfer or hydrogen abstraction, since these processes occurred rapidly both in a loose structure (n = 1,2) or in a sandwich-type structure (n = 3). These results contradict those of previous researchers and seem suspect to error, since when n = 1 the lone pair on the amine cannot possibly come close to the carbonyl and the possibility for intramolecular hydrogen abstraction seems remote when n = 1.

Thus, many unanswered questions still remain concerning the conformational requirements involved in charge transfer complex formation.

E. Stern-Volmer Kinetics

Phenyl alkyl ketones undergo Norrish Type II photoelimination by γ-hydrogen abstraction to give a 1,4-biradical which then undergoes cleavage, cyclization, or disproportionation back to ground-state ketone (Scheme 1). The triplet lifetime, τ, is dependent on both the rate constant for γ-hydrogen abstraction, k_r, and the rate constant for radiationless decay, k_d (Equation 9).

$$\tau = (k_r + k_d)^{-1} \tag{9}$$

Quantum yields for type II photoelimination are determined by competitive excited state reactions and by partitioning of the biradical:

$$\Phi_{II} = \Phi_{ISC} \cdot k_r \cdot P_p \cdot \tau \tag{10}$$

where Φ_{ISC} is the quantum yield for intersystem crossing, k_r is the rate constant for γ-hydrogen abstraction, and P_p is the probability that the biradical will go on to form product. The addition of a Lewis base usually results in solvation of the biradical, thus inhibiting disproportionation back to ground-state ketone, and consequently maximizing the type II quantum yield (Equation 11).

$$\Phi_{max} = \Phi_{ISC} \cdot k_r \cdot \tau \tag{11}$$

Stern-Volmer quenching kinetics[87] can be used to determine triplet lifetimes:

$$\Phi^\circ/\Phi = k_q \cdot \tau \cdot [Q] + 1 \tag{12}$$

where Φ° and Φ are the quantum yields for acetophenone formation in the absence and presence of external quencher, respectively and k_q is the rate constant for bimolecular quenching by external quencher, Q.

Intersystem crossing yields can be determined by using the ketone to sensitize a well-known triplet reaction, such as the cis → trans isomerization of 1,3-pentadiene:

$$\alpha \cdot \Phi_{\text{sens}}^{-1} = \Phi_{\text{ISC}}^{-1} \left(1 + \frac{1}{k_q \cdot \tau \cdot [Q]}\right. \tag{13}$$

where $\alpha = 0.55$ and $k_q = 5 \times 10^9\ M^{-1}\ s^{-1}$ at 25° in benzene. Thus, a plot of $0.55/\Phi_{c\to t}$ versus $[\text{cis 1,3-pentadiene}]^{-1}$ gives a straight line with 1/intercept equal to Φ_{ISC} and intercept/slope equal to $k_q\tau$.[88]

F. Research Objectives

1. Part I: Deactivation of Triplet Phenyl Alkyl Ketones by Conjugatively Electron-Withdrawing Substituents

Although the effects of ring substituents on the triplet-state photoreactivity and energies of phenyl alkyl ketones have been investigated extensively,[21,23,27,28,30] one important class of substituents (conjugatively electron-withdrawing) virtually have been ignored. Since electron-withdrawing substituents stabilize the n,π* triplet by only a few kcal/mole[89] while p-CN and p-CO_2CH_3 substituents stabilize the π,π* triplet of benzonitrile and methyl benzoate by 5-6 kcal/mole,[90] the possibility exists that resonance stabilization of the π,π* triplet by these substituents can cause inversion of the two triplets. Thus, conjugatively electron-withdrawing substituents may represent a unique class which inductively make the n,π* triplet more electrophilic in all cases, while resonance stabilization of the π,π* triplet may cause inversion of the two triplets and consequently make these ketones less reactive in Type II photoelimination than the parent compound. Thus, the synthesis of a series of valerophenones containing conjugatively electron-withdrawing ring-substituents was undertaken and triplet-state reactivities and triplet energies of these ketones were determined. Suitable models were used to predict both n,π* and π,π* triplet energies (only the energy of the lowest triplet can be measured spectroscopically), so that correlation of photoreactivity with relative triplet energies could be accomplished. This investigation completes the systematic study of ring-substituent effects on the photochemistry of phenyl alkyl ketones already conducted by Wagner and coworkers.[28]

2. Part II: Regioelectronic Control of Intramolecular Charge-Transfer Quenching in Various Excited Triplet Phenyl Ketones

Charge-transfer interactions represent an important type of excited state quenching process. Even though many studies have been conducted in this area,[53-86] there are still many unanswered questions concerning both conformational and electronic requirements involved in the formation of a CT complex. The study of intramolecular charge-transfer quenching in bifunctional molecules limits the number of possible conformations between donor and acceptor. Thus, intramolecular charge transfer quenching studies of β-dimethylamino esters of valerylbenzoic acid were undertaken, since the CO_2CH_3-substituted valerophenones

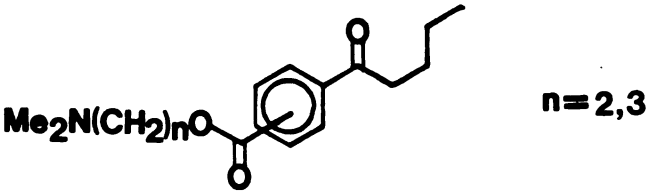

previously synthesized and studied could serve as suitable models. Consequently, both the triplet lifetime in the absence of CT quenching and the rate of intermolecular CT quenching could be determined. Since the previous studies on the m- and p-carbomethoxyvalerophenones indicated that the meta-compound has a definite n,π* lowest triplet, whereas the para isomer has a probable π,π* lowest triplet, information on CT interactions with triplets of different electronic configurations also can be obtained.

Similarly substituted benzophenones were investigated since these compounds have n,π* lowest triplets in all cases.

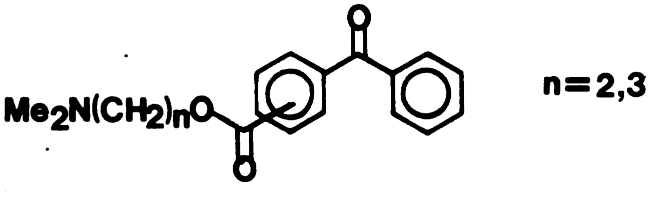

Analogously, the m- and p-CO_2CH_3 substituted benzophenones served as models for determining triplet lifetimes in the absence of CT interactions and estimating the rate of intermolecular charge transfer quenching. Triplet lifetimes can be determined by quenching the room temperature phosphorescence of these compounds.

In order to determine the general applicability of the observed intramolecular CT quenching of the π,π* triplet for para-valeryl β-dimethylaminoethyl benzoate, the corresponding ether analogue was

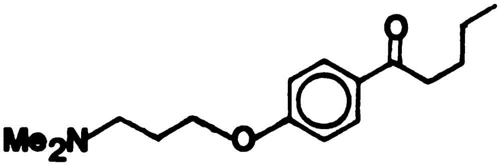

synthesized and studied. Likewise, model studies on p-methoxyvalerophenone enabled the determination of triplet lifetime in the absence of CT quenching and the rate of self-quenching. Also, solvent effects were studied for many of these ketones, and in the ether case provided somewhat surprising results.

PART I

DEACTIVATION OF TRIPLET PHENYL ALKYL KETONES BY CONJUGATIVELY ELECTRON-WITHDRAWING SUBSTITUENTS

RESULTS

A. Photokinetic Studies

1. Stern-Volmer Quenching Studies

In general, 0.04 M ketone solutions containing varying amounts of 2,5-dimethylhexa-2,4-diene or 1,3-pentadiene quencher in benzene or wet acetonitrile (2% water) solvent were irradiated at 313 nm to 5-10% conversion. Acetophenone photoproduct was measured and linear correlations were obtained for Stern-Volmer plots of $\phi°/\phi$ versus quencher concentration. The slope is equal to $k_q\tau$, where τ is the triplet lifetime of the ketone. Thus, the triplet lifetimes can be easily calculated, since $k_q = 5 \times 10^9$ M^{-1} s^{-1} in benzene[35] and 1×10^{10} M^{-1} s^{-1} in acetonitrile.[91] Duplicate runs usually agreed to within 10% of each other and the average values are reported in Table 1 and Table 2. The Stern-Volmer plots for these substituted valerophenones are depicted in Figures 2-6. Also, the experimental data for the various p-cyanophenyl alkyl ketones are given in Table 2 and plotted in Figure 15.

In order to determine the rate of charge transfer quenching, 0.04 M ketone solutions containing varying amounts of triethylamine in benzene containing 0.5 M pyridine or in wet acetonitrile were irradiated at 313 nm to <10% conversion (acetophenone photoproduct was measured). In all cases linear Stern-Volmer plots were obtained

Table 1. Photokinetic Parameters for Ring-Substituted Valerophenones.[a]

Substituent	Solvent	Φ_{II}[b]	Φ_{max}[c]	Φ_{-K}[d]	$k_q\tau, M^{-1}$ (diene)[e]	$k_q\tau, M^{-1}$ (Et_3N)[e]
H	Benzene	0.33[f]	0.85[f]	0.43[f]	47±1	11±1
H	Acetonitrile	0.85±0.01	----	----	63±2	13±1
o-CN	Benzene	0.15±0.01	----	0.14	22±1	----
o-CN	Acetonitrile	0.54	----	0.82	33	----
m-CN	Benzene	0.20±0.02	0.65	0.23±0.06	19±0.5	22±0.5
m-CN	Acetonitrile	0.68±0.05	----	0.52	20	10±0.5
p-CN	Benzene	0.19±0.02	0.43±0.04	0.27±0.05	74±1	91[g]±5
p-CN	Acetonitrile	0.74±0.06	----	0.68	87	92[g]
o-CO_2CH_3	Benzene	0.04±0.02	0.15±0.04	----	138±15	62[g]±4
o-CO_2CH_3	Acetonitrile	0.15±0.04	----	0.25±0.01	338±25	84±6
m-CO_2CH_3	Benzene	0.25±0.01	0.54	----	18±1	25[g]
m-CO_2CH_3	Acetonitrile	0.90±0.01	----	0.92±0.07	21±1	----
p-CO_2CH_3	Benzene	0.19±0.01	0.31±0.02	----	42±2	46±2
p-CO_2CH_3	Acetonitrile	0.60±0.08	----	0.82±0.01	58±5	92[g]±3
m-$CO(CH_2)_3CH_3$	Benzene	0.22±0.01	0.54±0.04	----	37±1	28[g]
m-$CO(CH_2)_3CH_3$	Acetonitrile	0.70±0.08	----	----	46	33±1
p-$CO(CH_2)_3CH_3$	Benzene	0.12±0.02	0.17±0.01	----	183±5	----

Table 1. Continued.

Substituent	Solvent	Φ_{II}[b]	Φ_{max}[c]	Φ_{-K}[d]	$k_q\tau, M^{-1}$ (diene)[e]	$k_q\tau, M^{-1}$ (Et_3N)[e]
p-$COCH_3$	Benzene	0.09±0.01	----	----	350±50	----
o-CF_3	Benzene	0.20[f]	0.90	----	38[f]	55±10[h]
m-CF_3	Benzene	0.23[f]	0.74	----	16[f]	26±3[h]
p-CF_3	Benzene	0.26[f]	0.94	----	18[f]	55[h]

[a] 0.04 M ketone irradiated at 313 nm to 5-10% conversion.

[b] Quantum yield for acetophenone formation.

[c] Quantum yield maximized with 0.5 M to 1.0 M pyridine.

[d] Disappearance quantum yield in benzene.

[e] Usually average of duplicate runs with average precision of ±7%.

[f] Values from Reference 28.

[g] $k_q\tau$ = slope/intercept.

[h] Unpublished results by Warren B. Mueller.

Table 2. Photokinetic Parameters for Phenyl Alkyl Ketones as a Function of γ-Substitution.[a]

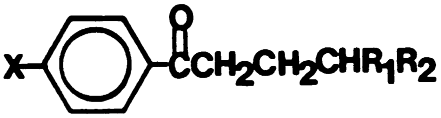

X	R_1	R_2	Φ_{II}	Φ_{max}	$k_q\tau, M^{-1}$[b]	$1/\tau, 10^7 s^{-1}$
H	H	H	0.23	----	560[c]	1.8
H	H	CH_3	0.33[d]	0.85	47±1	11.
H	CH_3	CH_3	0.25[d]	0.90	10[c]	50.
CN	H	H	0.12	0.31	400±40	2.5
CN	H	CH_3	0.17	0.47	74±1	6.7
CN	CH_3	CH_3	0.13	0.47	18	28.

[a] 0.04 M ketone in benzene irradiated at 313 nm to ∿10% conversion.

[b] Values determined from Stern Volmer runs monitoring acetophenone formation.

[c] Value in Reference 15 is 625.

[d] Values taken from Reference 15.

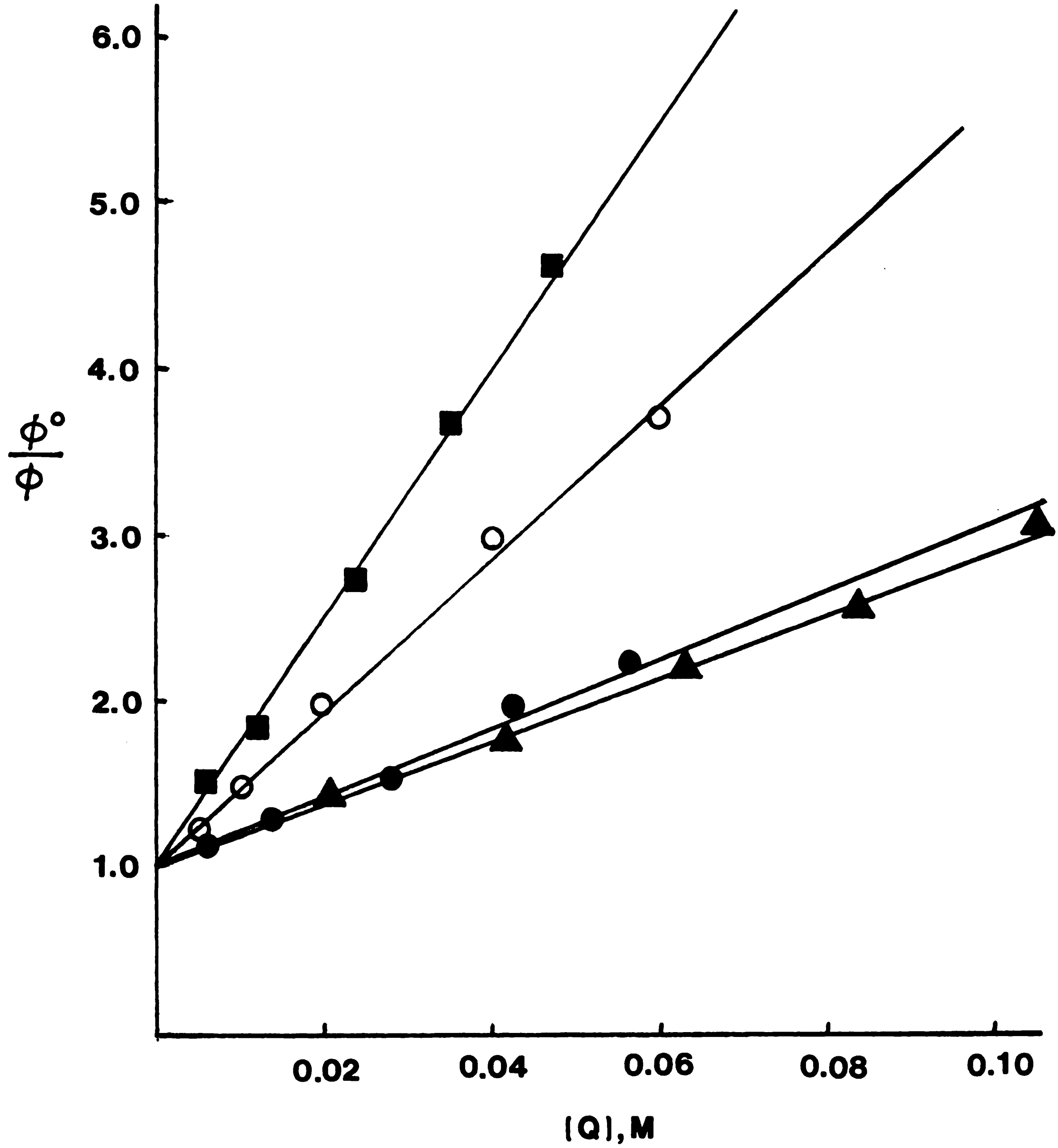

Figure 2. Stern Volmer Plots for Substituted Valerophenones in Benzene with Diene Quencher (○ H; ● o-CN; ▲ m-CN; ■ p-CN).

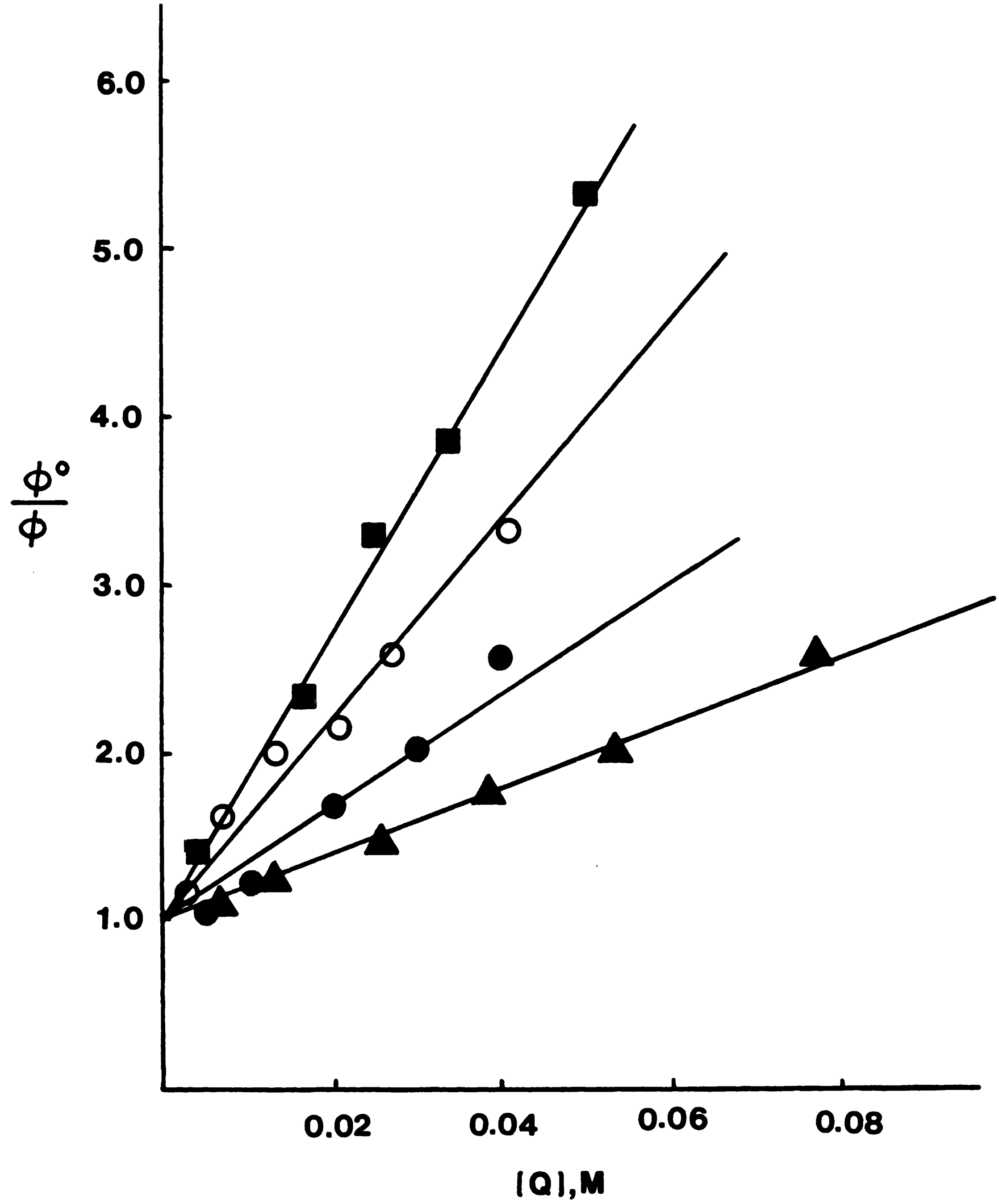

Figure 3. Stern Volmer Plots for Substituted Valerophenones in Acetonitrile with Diene Quencher (○ H; ● o-CN; ▲ m-CN; ■ p-CN).

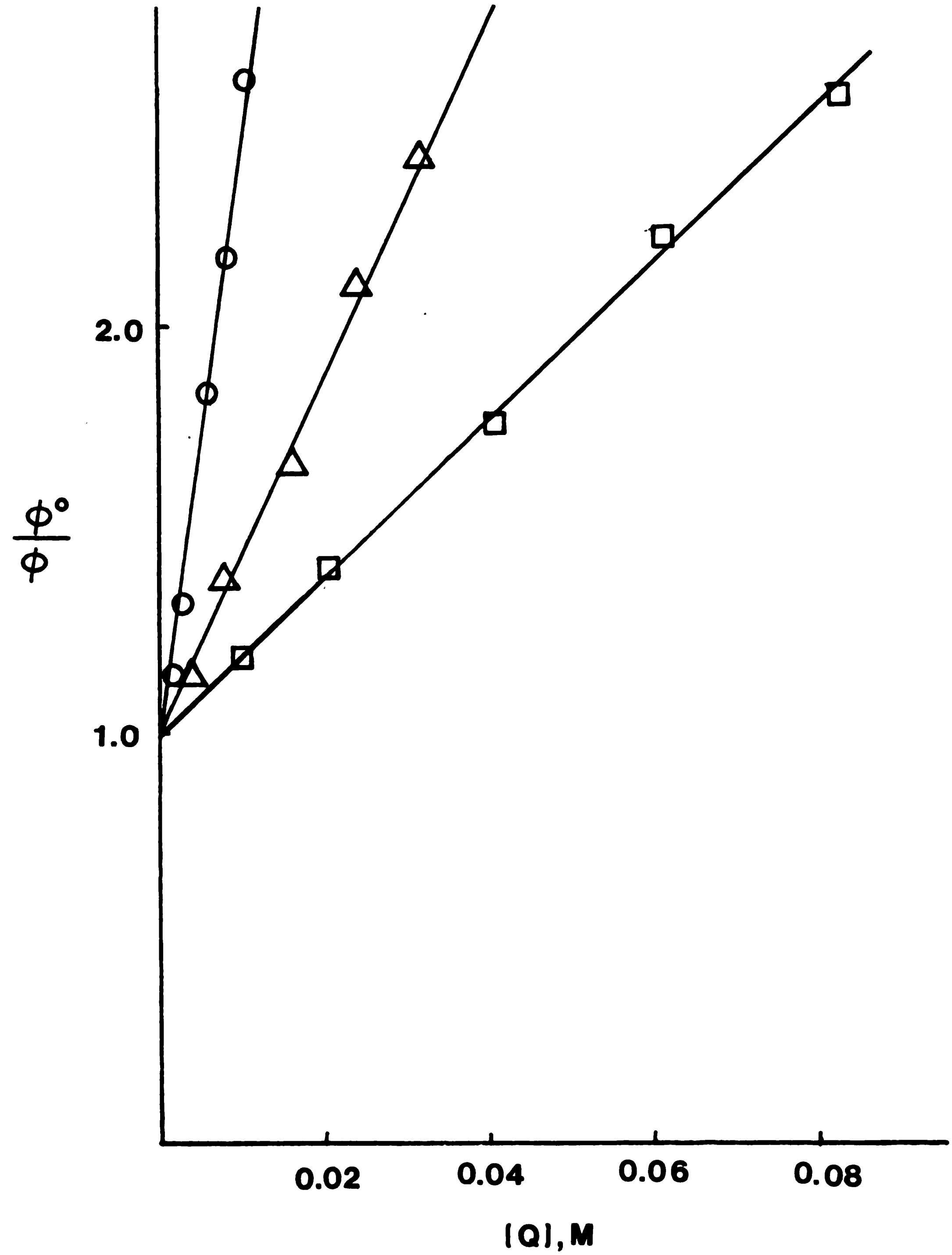

Figure 4. Stern Volmer Plots for Substituted Valerophenones in Benzene with Diene Quencher (○ o-CO_2CH_3; □ m-CO_2CH_3; △ p-CO_2CH_3).

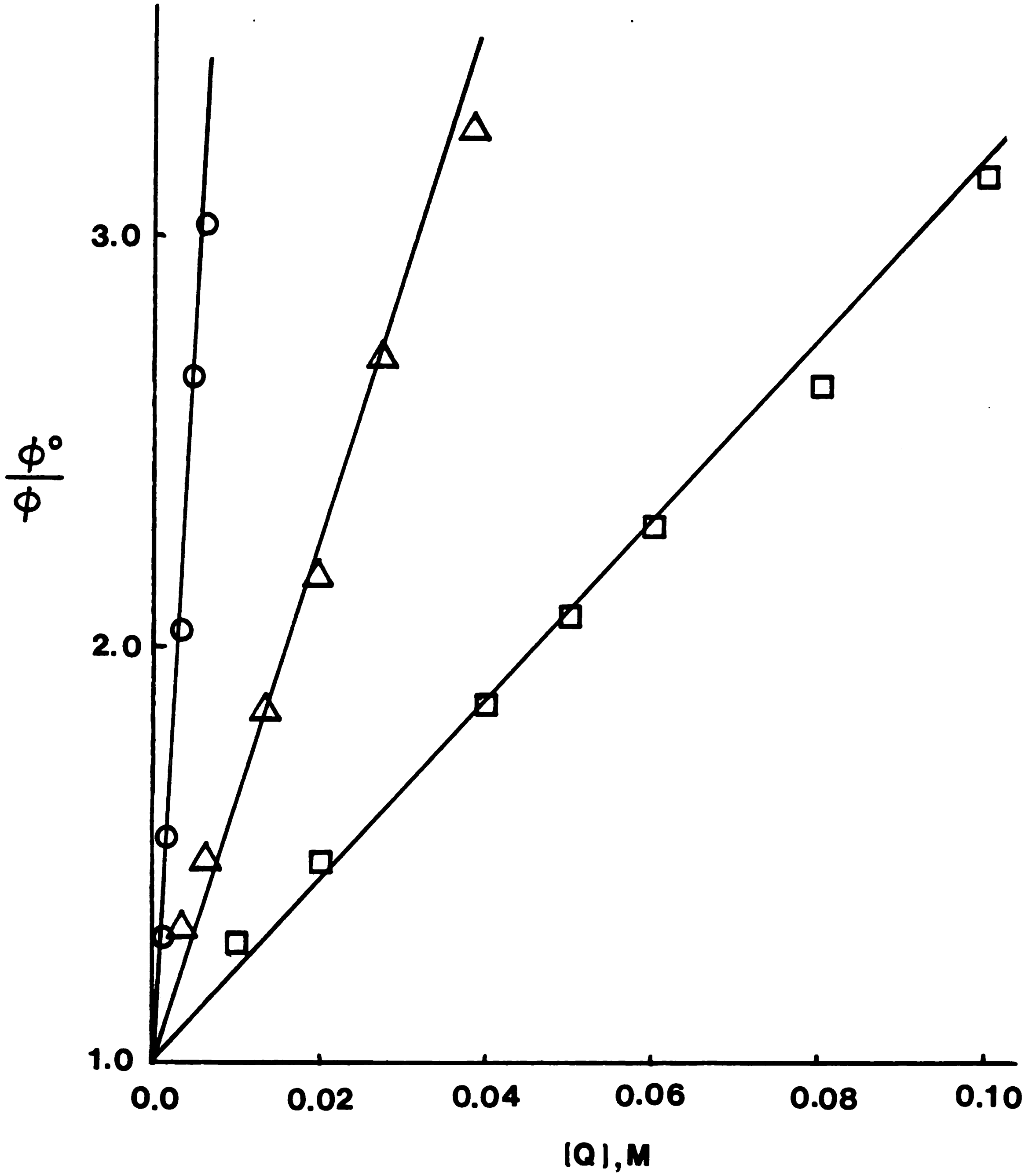

Figure 5. Stern Volmer Plots for Substituted Valerophenones in Acetonitrile with Diene Quencher (○ o-CO_2CH_3; □ m-CO_2CH_3; △ p-CO_2CH_3).

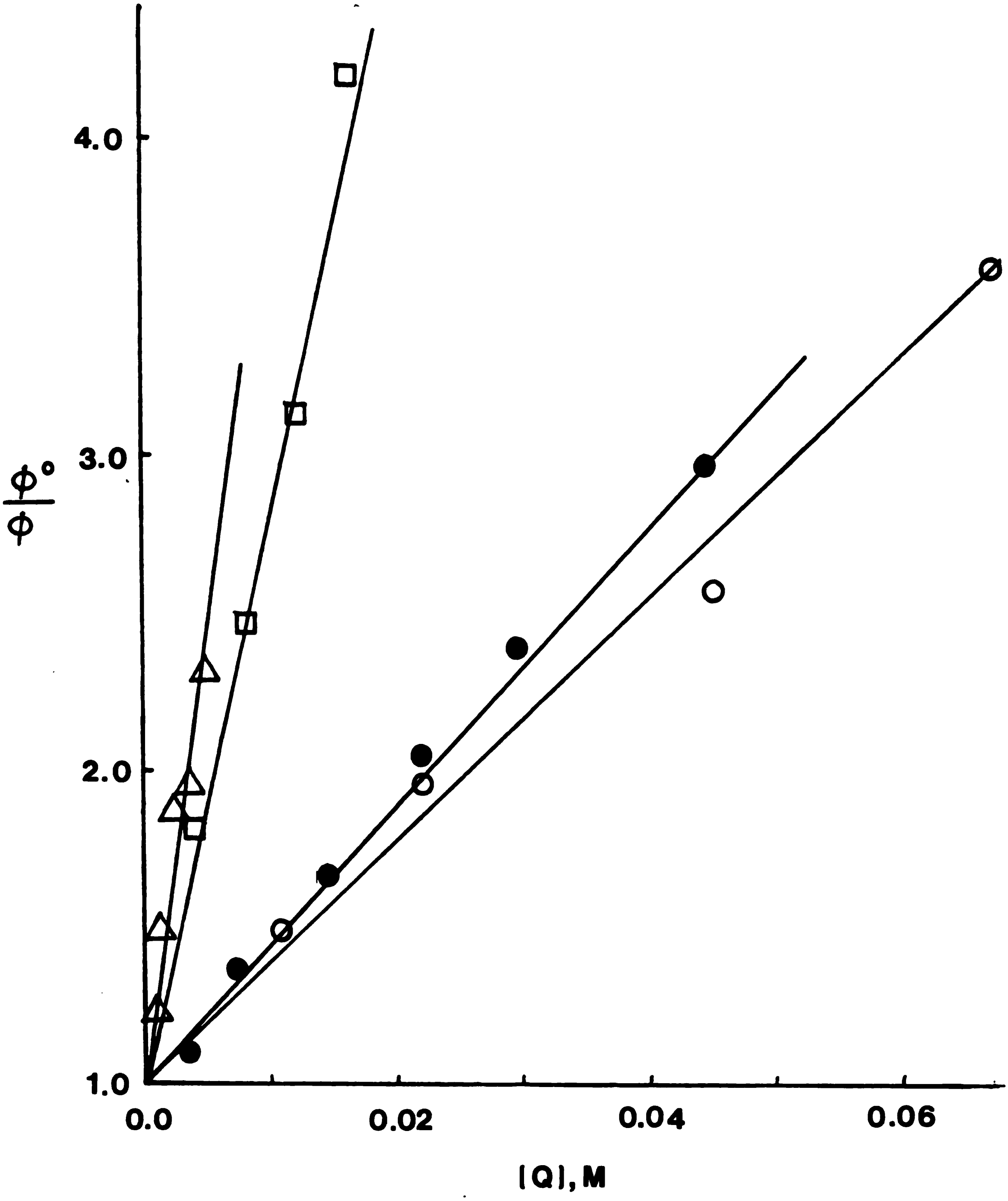

Figure 6. Stern Volmer Plots for Substituted Valerophenones in Benzene with Diene Quencher (△ p-$COCH_3$; □ p-COC_4H_9; ○ m-COC_4H_9; ● m-COC_4H_9 in acetonitrile).

(Figures 7-12). In those cases where the intercept was below 1.0, $k_q\tau$ was determined by dividing the slope by the intercept. The values obtained are also included in Table 1.

2. Quantum Yields

Quantum yields for acetophenone formation were determined by parallel irradiation at 313 nm of 0.04 M ketone solutions and usually benzene solutions of 0.1 M valerophenone as actinometer in a merry-go-round apparatus.[91] All samples were degassed prior to irradiation and conversion was usually kept below 10%. In all cases both the ketone solution and the actinometer absorbed all the incident irradiation. The values are included in Tables 1 and 2.

3. Maximum Quantum Yields

Maximum quantum yields for acetophenone formation were obtained by adding various amounts of Lewis bases to 0.04 M ketone solutions in benzene. For most ketones a maximum quantum yield of unity for total product formation could not be attained, since the addition of Lewis base up to a certain value maximized the quantum yield and further Lewis base either had no effect or slightly decreased the quantum yield. The values are given in Tables 1 and 2 and Figures 13 and 14 show the effects of added pyridine, t-butyl alcohol, and dioxane on the Type II quantum yield for p-cyanovalerophenone.

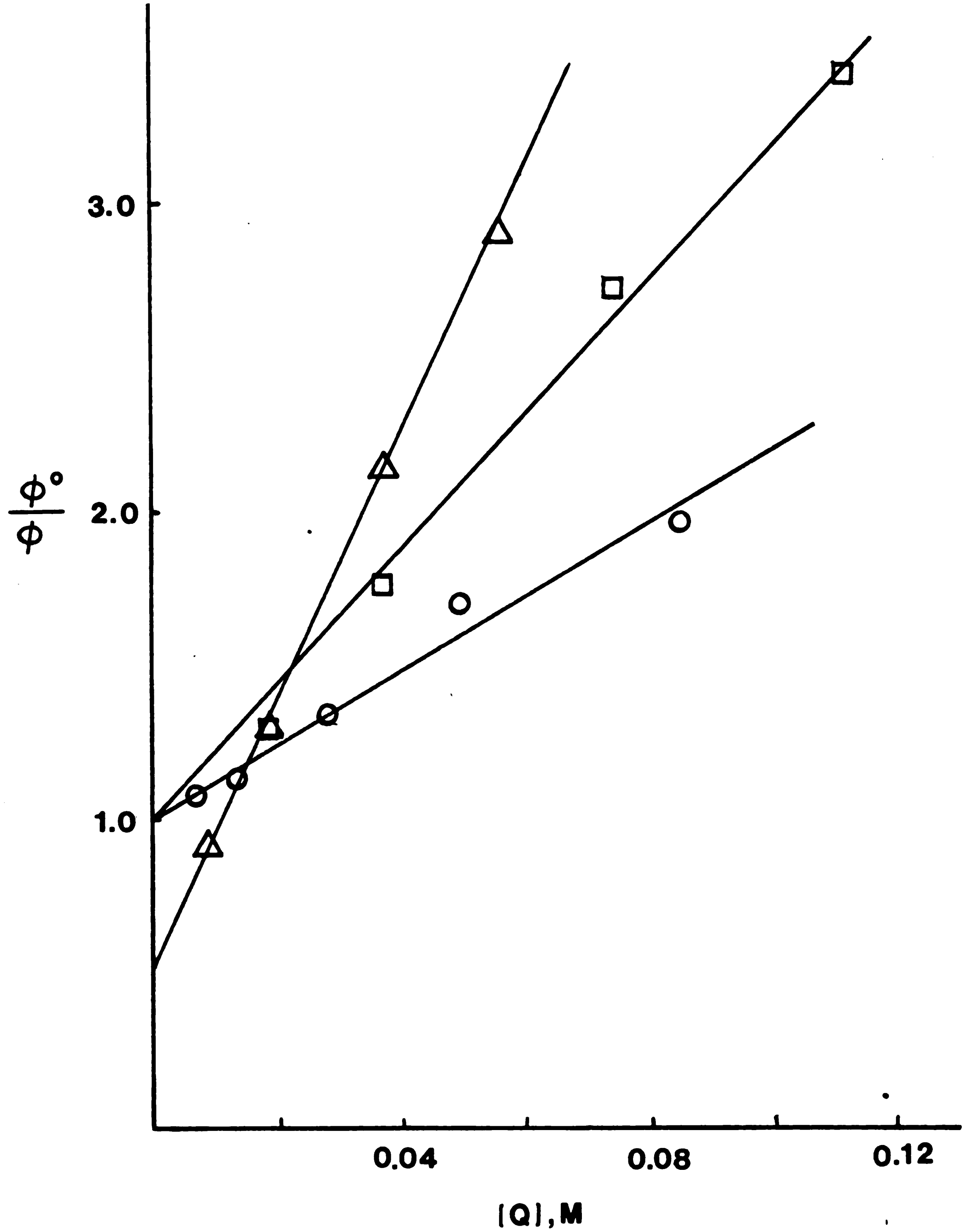

Figure 7. Stern Volmer Plots for Substituted Valerophenones in Benzene (0.5 M Pyridine) with Triethylamine Quencher (○ H; □ m-CN; △ p-CN).

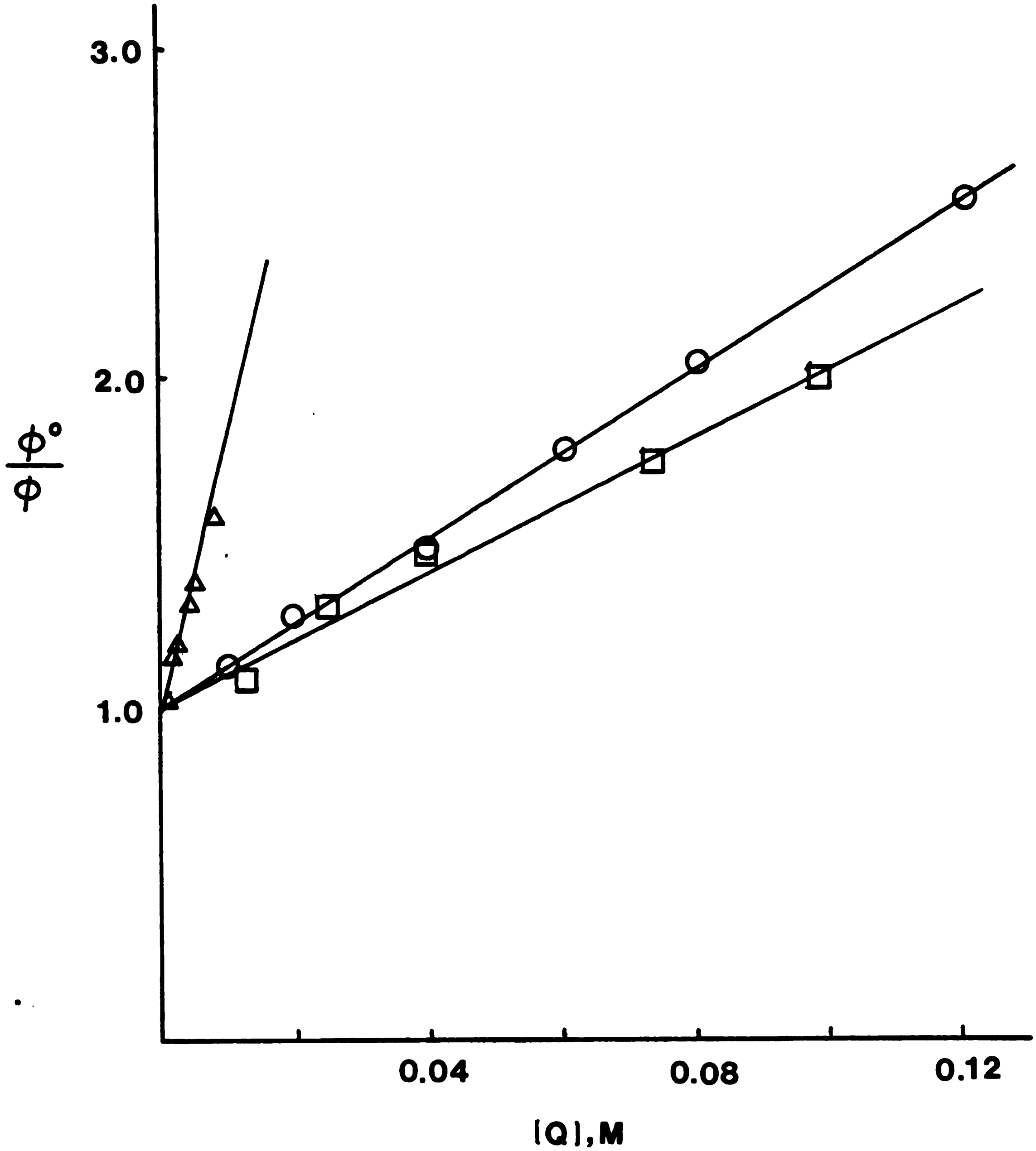

Figure 8. Stern Volmer Plots for Substituted Valerophenones in Acetonitrile with Triethylamine Quencher (○ H; □ m-CN; △ p-CN).

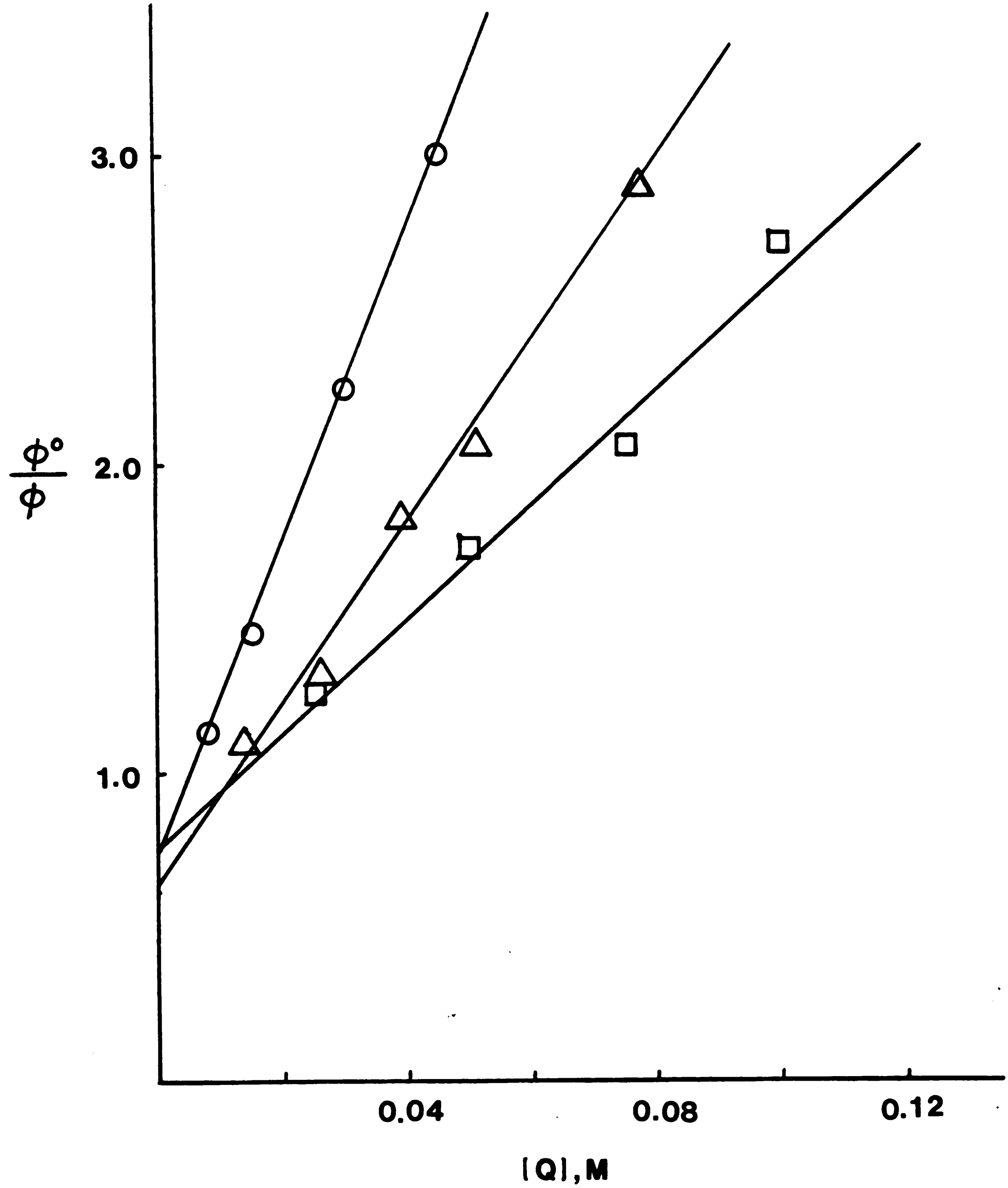

Figure 9. Stern Volmer Plots for Substituted Valerophenones in Benzene (0.5 M Pyridine) with Triethylamine Quencher (○ o-CO_2CH_3; □ m-CO_2CH_3; △ p-CO_2CH_3).

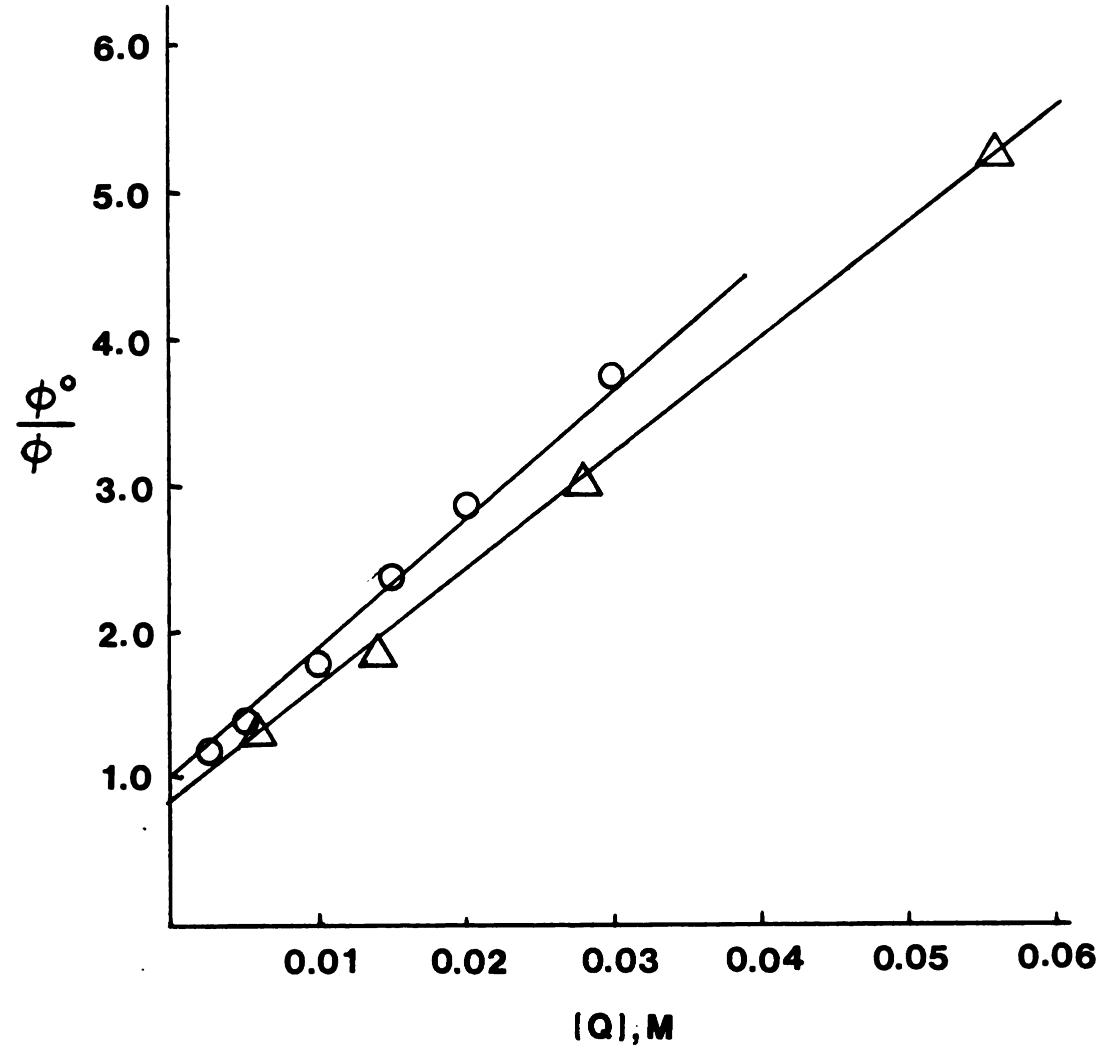

Figure 10. Stern Volmer Plots for Substituted Valerophenones in Acetonitrile with Triethylamine Quencher (○ o-CO_2CH_3; △ p-CO_2CH_3).

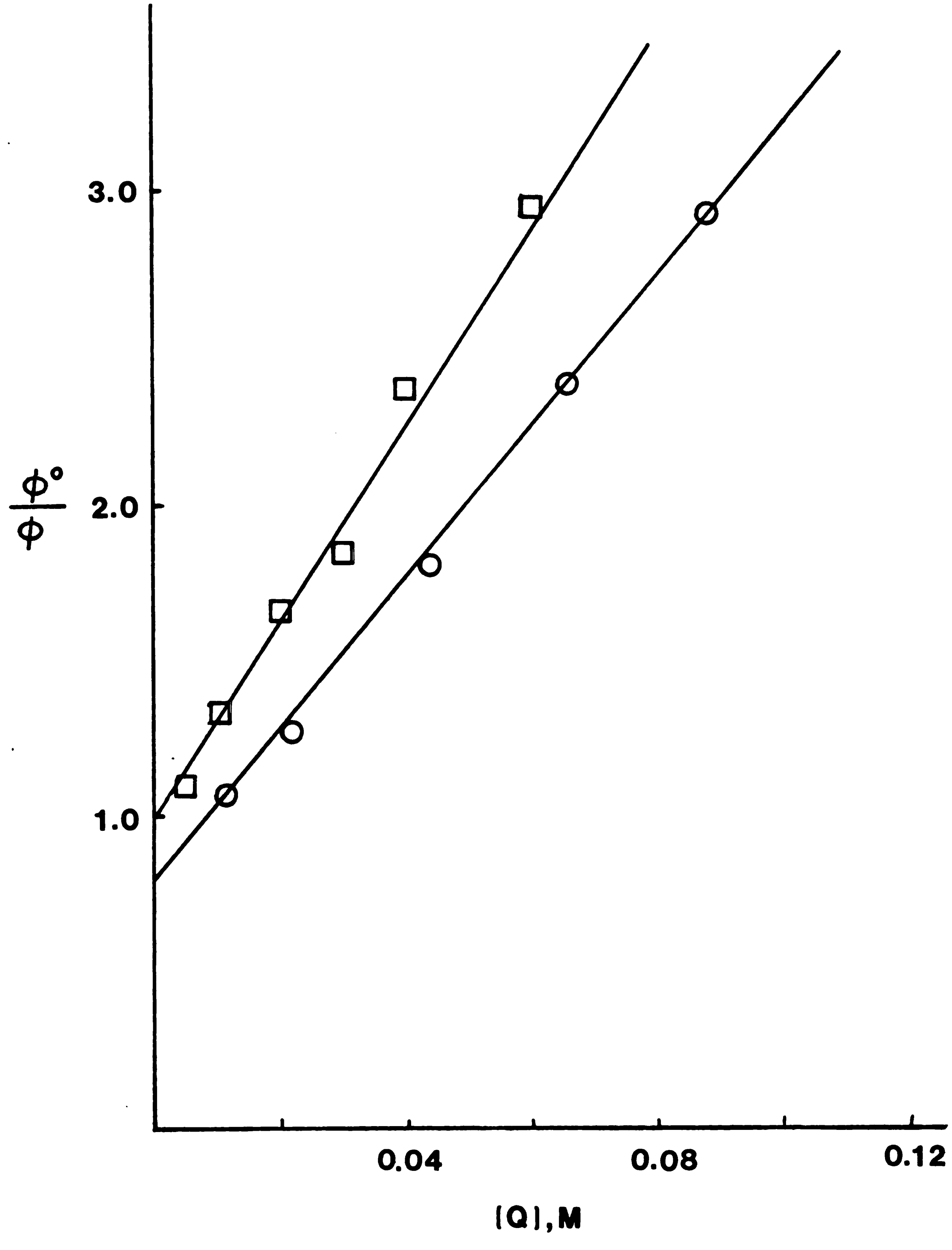

Figure 11. Stern Volmer Plots for m-Divalerylbenzene in Benzene (0.5 M Pyridine) ○ and Acetonitrile □ with Triethylamine Quencher.

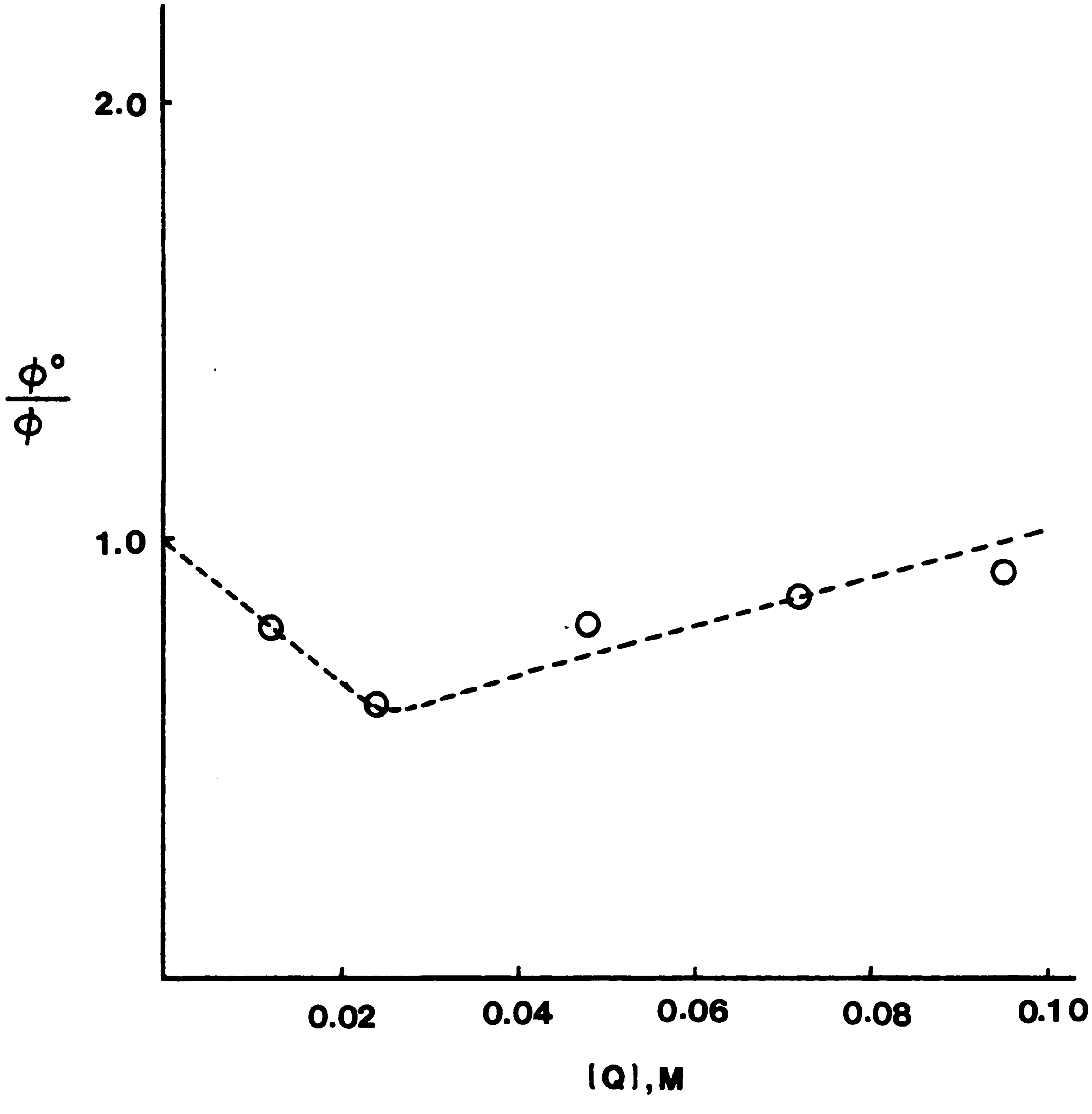

Figure 12. Stern Volmer Plot for p-Cyanovalerophenone in Benzene (0.5 M Pyridine) and Low Triethylamine Quencher Concentrations.

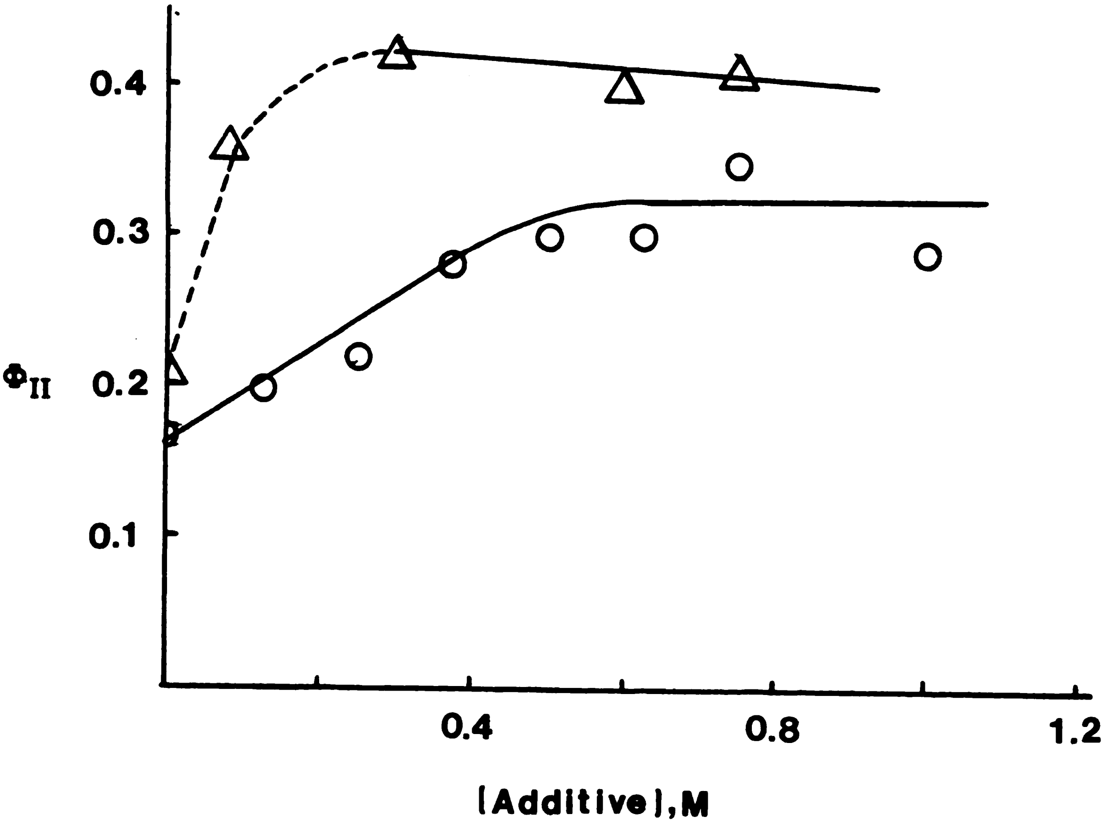

Figure 13. Maximization of Φ_{II} for p-Cyanovalerophenone in Benzene with Added t-Butyl Alcohol ○ and Added Pyridine △ .

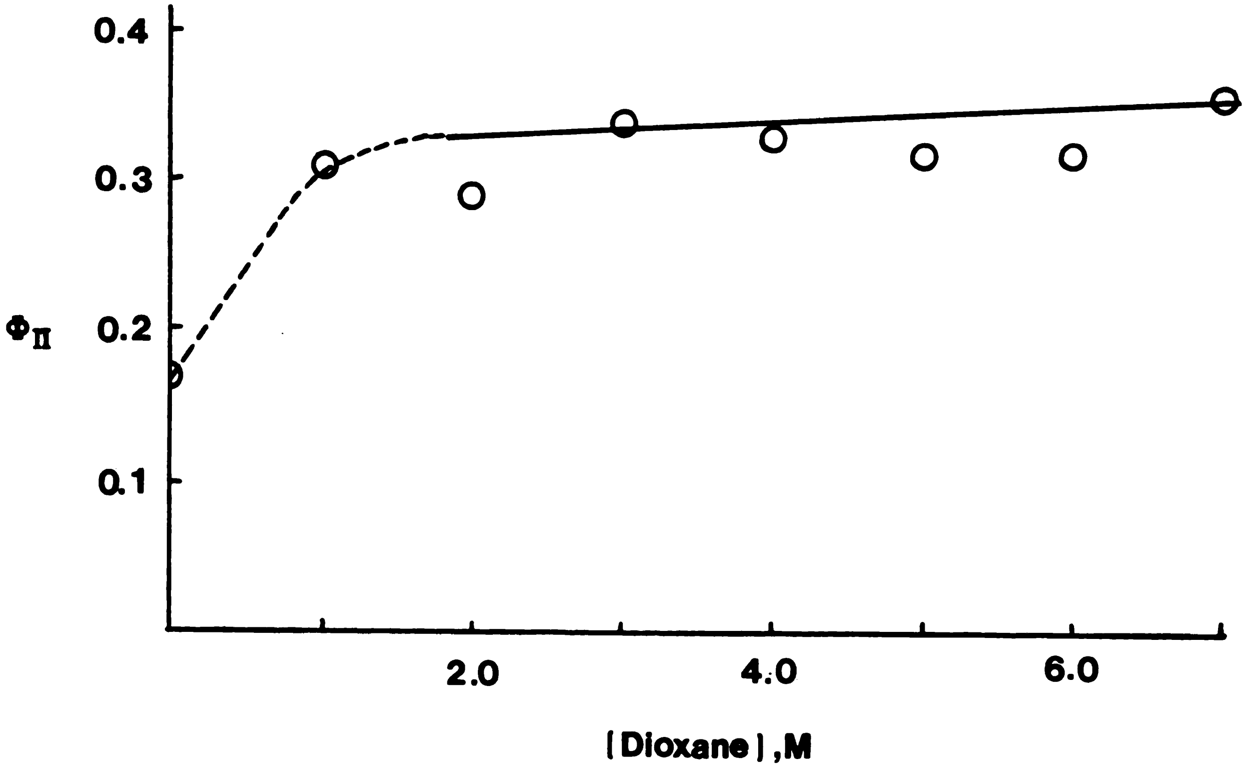

Figure 14. Maximization of Φ_{II} for p-Cyanovalerophenone in Benzene with Added Dioxane.

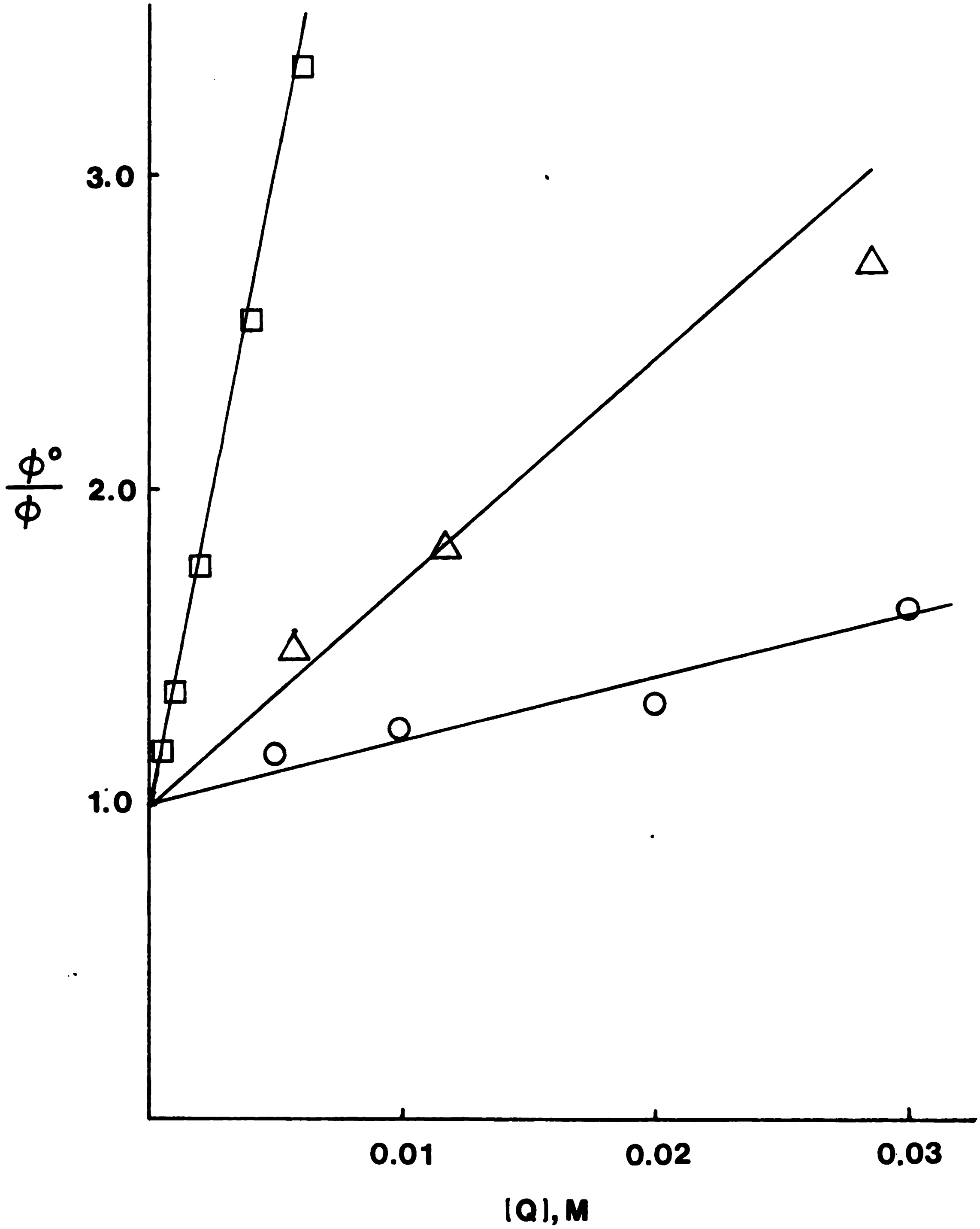

Figure 15. Stern Volmer Plots for p-Cyanophenyl Alkyl Ketones in Benzene with Diene Quencher (□ p-Cyanobutyrophenone; △ p-Cyanovalerophenone; ○ p-Cyano-γ-methylvalerophenone).

4. Disappearance Quantum Yields

Disappearance quantum yields were determined for a few of the ketones in order to confirm that the Norrish Type II reaction and normal cyclobutanol formation are the major photoreactions that occur. The errors involved are fairly large, but the results are accurate enough for this purpose. The ketones were usually photolyzed to greater than 20% conversion. The results are included in Table 1.

5. Intersystem Crossing Yields

The intersystem crossing yields for p-cyanoacetophenone and p-carbomethoxyvalerophenone were determined by comparing the relative abilities of the ketones and acetophenone or valerophenone, respectively, at sensitizing the cis-trans isomerization of 1,3-pentadiene under conditions where both the ketone and acetophenone or valerophenone absorb all the incident irradiation. The intersystem crossing yield for both acetophenone and valerophenone are known to be unity[88] and those measured for p-cyanoacetophenone and p-carbomethoxyvalerophenone were also unity. The length of the alkyl chain does not affect Φ_{ISC}. In general ring substituted valerophenones[10a] have intersystem crossing yields equal to one and since there are no structural differences which would be expected to affect the intersystem crossing yield in the other ketones studied, Φ_{ISC} for these ketones was also assumed to be unity.

6. Photoreduction Experiments

Photoreduction experiments were conducted on p-cyanoacetophenone both with toluene and p-xylene as donor, and Figures 16 and 18 show the variation in bibenzyl and di-p-tolylethane, respectively, formed as a function of donor concentration (slope/intercept = k_d/k_r). Stern-Volmer quenching studies of 0.05 M acetonitrile solutions of p-cyanoacetophenone containing 1.0 M toluene or 1.0 M p-xylene as donor and naphthalene quencher gave linear plots (Figures 17 and 19) with slopes of 2200 and 4750, respectively. Since $1/\tau = k_d + k_r$ and the results from the previous experiments gave k_d/k_r values of 10 and 0.2 for toluene and p-xylene, respectively, $k_d = 4 \times 10^5 \text{ s}^{-1}$ in both cases.

B. Spectroscopy

1. Phosphorescence Emission Spectra

Phosphorescence spectra were taken in various nonpolar and polar solvent glasses at 77°K in order to determine the energy of the lowest emitting triplet from the 0,0 band of the spectra and to observe a polar solvent effect, if any, on the triplet energies. The values are given in Tables 3 and 4. Triplet energies for the model compounds (benzonitriles,[90b] methyl benzoates,[90a] and benzophenones[89]) used in this study are presented in Table 5. Representative spectra are given in Figures 20-22.

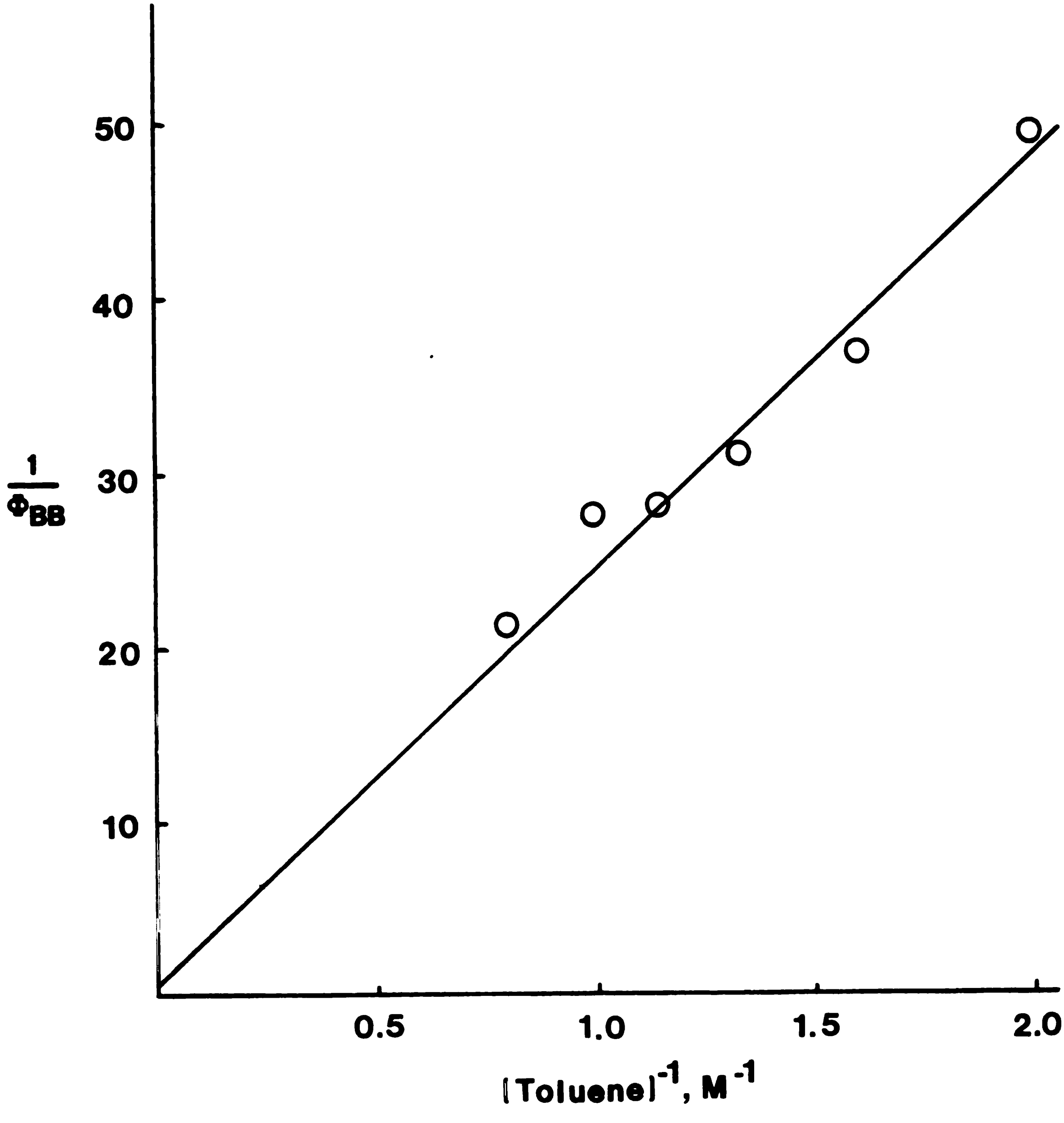

Figure 16. Results from Reaction of p-Cyanoacetophenone and Toluene in Acetonitrile (Formation of Bibenzyl Monitored).

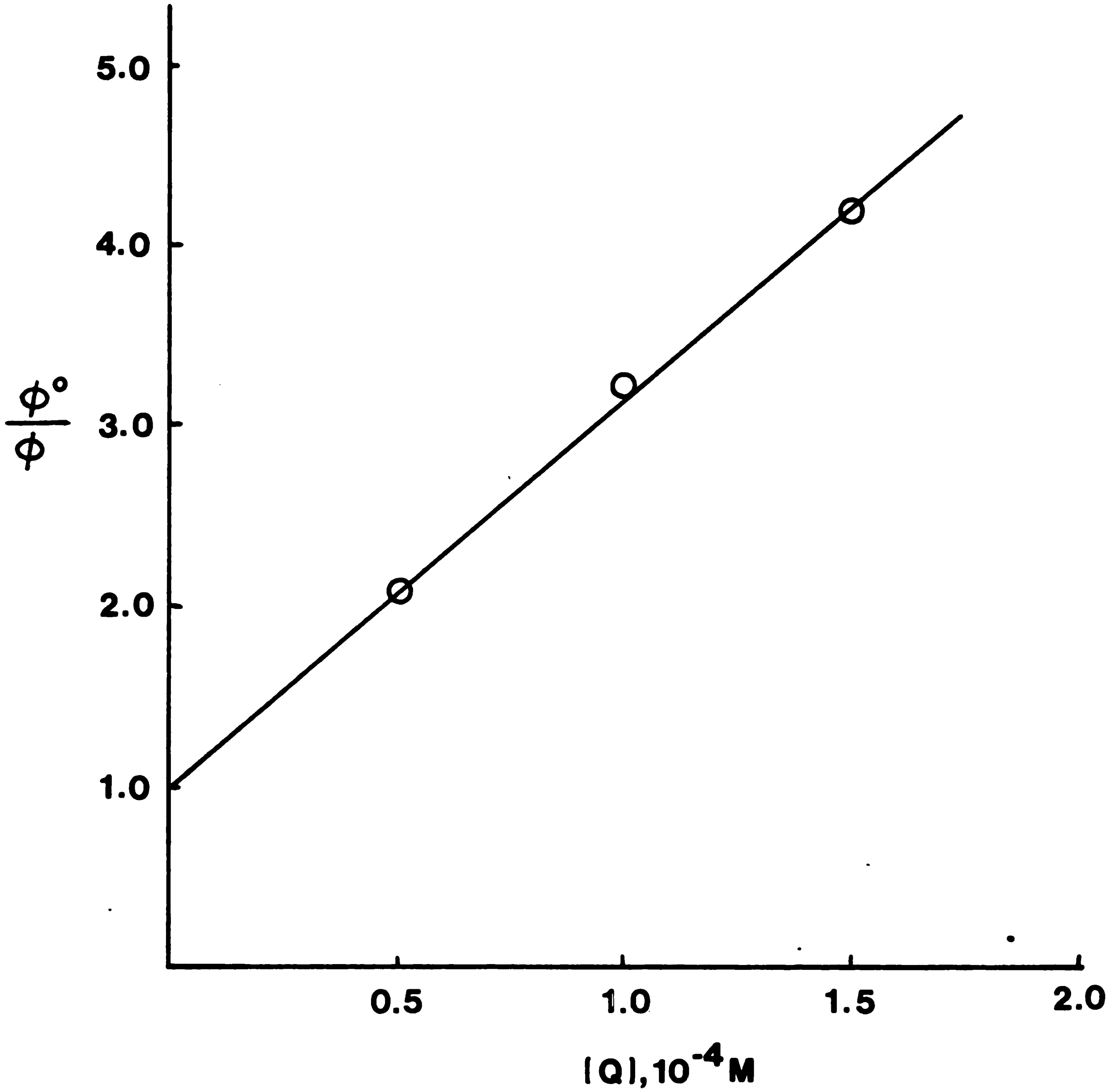

Figure 17. Stern Volmer Plot for p-Cyanoacetophenone in Acetonitrile (1.0 M Toluene) with Naphthalene Quencher (Formation of Bibenzyl Monitored).

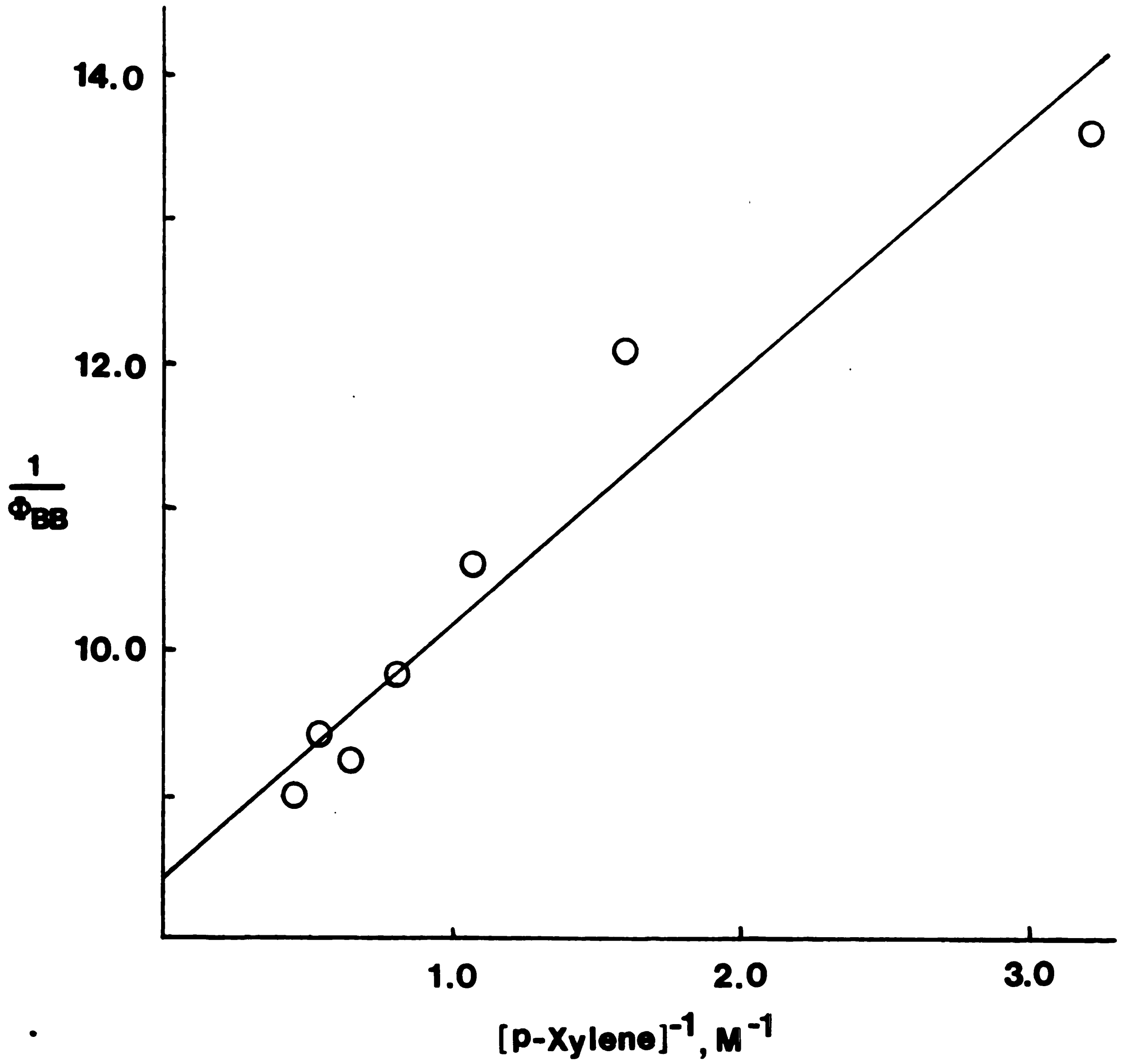

Figure 18. Results from Reaction of p-Cyanoacetophenone and p-Xylene in Acetonitrile (Formation of Di-p-tolylethane Monitored).

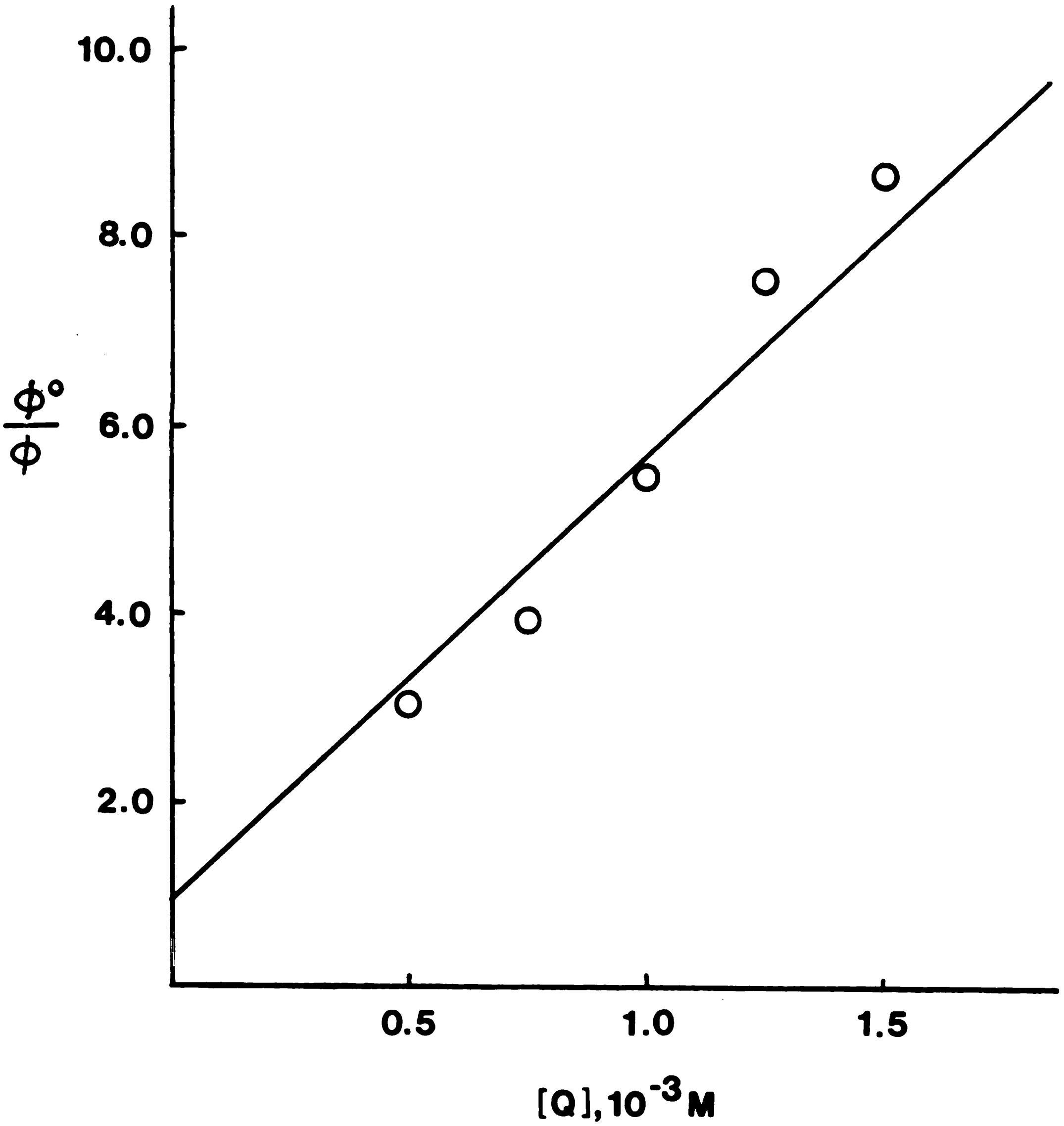

Figure 19. Stern Volmer Plot for p-Cyanoacetophenone in Acetonitrile (1.0 M p-Xylene) with Naphthalene Quencher (Formation of Di-p-tolylethane Monitored).

Table 3. Spectroscopic Data for Ring-Substituted Valerophenones.

Substituent	Isopentane E_T $(\lambda_{0,0})^a$	MCH/IP E_T $(\lambda_{0,0})^a$	Ethanol E_T $(\lambda_{0,0})^a$	$-E_{red}$,eV^b
none	71.6 (399)	74.2 (380)	73.8 (395)	2.07
o-CN	67.2 (426)	----	69.8 (409)	1.64
m-CN	70.7 (404)	73.1 (386)	73.3 (390)	1.78
p-CN	----	69.2 (414)	69.5 (412)	1.58
o-CO_2CH_3	69.6 (411)	----	∿69.1 (414)^c	1.93
m-CO_2CH_3	71.2 (402)	----	74.0 (387)	1.90
p-CO_2CH_3	68.5 (418)	70.2 (408)	70.2 (407)	1.63
m-COC_4H_9	69.1 (413)	----	71.9 (392)	1.86
p-COC_4H_9	64.3 (444)	----	67.8 (421)	1.55
p-$COCH_3$	64.3 (444)	----	67.7 (422)	1.55
o-CF_3	71.1^d	----	71.8^d	1.90
m-CF_3	71.5^d	----	74.1^d	1.86
p-CF_3	70.8^d	----	73.0^d	1.76

[a] Triplet energies (kcal/mole) determined from 0,0 band (nm) of phosphorescence spectra at 77°K.

[b] Half-wave reduction potentials in acetonitrile relative to SCE.

[c] Value in EPA solvent.

[d] Values from Reference 90b.

Table 4. Spectroscopic Data for Other Ring-Substituted Valerophenones.

Substituent	E_T $(\lambda_{0,0})$[a]	$-E_{red}$,eV[b]
o-F	72.0[c]	2.00
m-F	70.6[c]	1.93
p-F	72.4[c]	2.08
o-Cl	----[d]	1.83
m-Cl	----	1.90
p-Cl	70.6[c]	1.83
o-CO_2H	----	1.81
m-CO_2H	----	2.15
p-CO_2H	----	2.04
o-$CO_2^-Na^+$	----	1.84
m-$CO_2^-Na^+$	----	1.86
p-$CO_2^-Na^+$	----	1.77
p-$CO_2^-K^+$	----	1.86
p-phenyl	59.5 (481)	1.91
o-(N)	----	1.82
m-(N)	----	1.86
p-(N)	----	1.68
o-CH_3	69.4 (412)	2.20
m-CH_3	71.4 (401)	2.08
p-CH_3	71.5 (400)	2.15
2,4-Di-CH_3	----	2.26
3,4-Di-CH_3	----	2.16
2,4,6-Tri-CH_3(γ-CH_3)	----	2.48
2,3,5,6-Tetra-CH_3	----	2.55
o-OCH_3	69.1 (414)[e]	2.16
m-OCH_3	64.2 (445)	2.05
p-OCH_3	68.8 (416)	2.21
3,5-Di-OCH_3	----	2.04
p-OH	----	1.84

Table 4. Continued.

Substituent	E_T $(\lambda_{0,0})$[a]	$-E_{red}$,eV[b]
p-SCH_3	63.9 (448)	2.00
p-CF_3	----	1.72
p-cyclopropyl	----	2.13

[a] Triplet energies (kcal/mole) determined from 0,0 band (nm) of phosphorescence spectra at 77°K.

[b] Half-wave reduction potentials in acetonitrile relative to SCE.

[c] Values from 90b.

[d] Spectra too broad (Reference 90b).

[e] Value taken from shoulder of spectrum.

Table 5. Substituent Effects on Triplet Energies of Model Compounds.

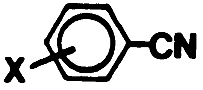

a

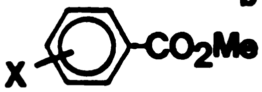

b

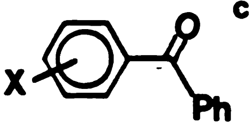

c

X	π,π*	π,π*	n,π*
H	77.3	77.9	68.6
o-CN	72.9	73.4	66.8[d]
m-CN	75.5	76.2	68.5
p-CN	70.9	72.0	66.4[f]
o-CO_2CH_3	73.4	----	69.0
m-CO_2CH_3	76.2[b]	76.9	68.8
p-CO_2CH_3	72.0[b]	72.9	66.7
p-COC_4H_9	69.5[e]	70.2[e]	----
o-CF_3	74.7	----	68.8[f]
m-CF_3	76.5	----	68.4
p-CF_3	76.1	----	67.6[f]

[a] In ethanol at 77°K, Reference 90b.

[b] In 4:1 ethanol/methanol at 77°K, Reference 90a.

[c] In 4:1 methylcyclohexane/isopentane.

[d] Estimated from E_{red}.

[e] Values measured by author.

[f] Values taken from Reference 89.

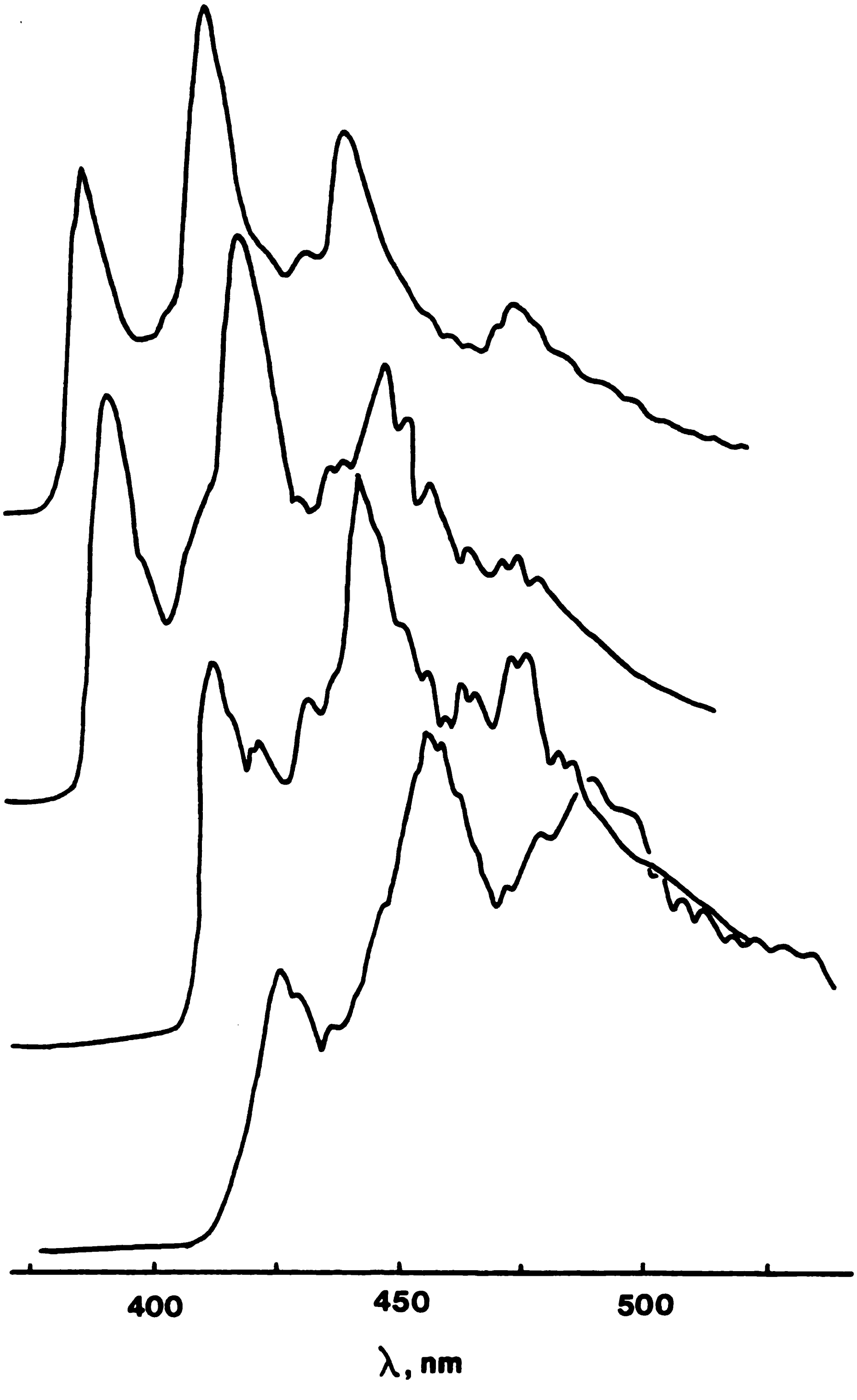

Figure 20. Phosphorescence Spectra of 10^{-4} M Valerophenones in 5:1 Methylcyclohexane/Isopentane at 77°K. Top, Valerophenone; Second, m-Cyanovalerophenone; Third, p-Cyanovalerophenone; and Bottom, o-Cyanovalerophenone in Isopentane Glass.

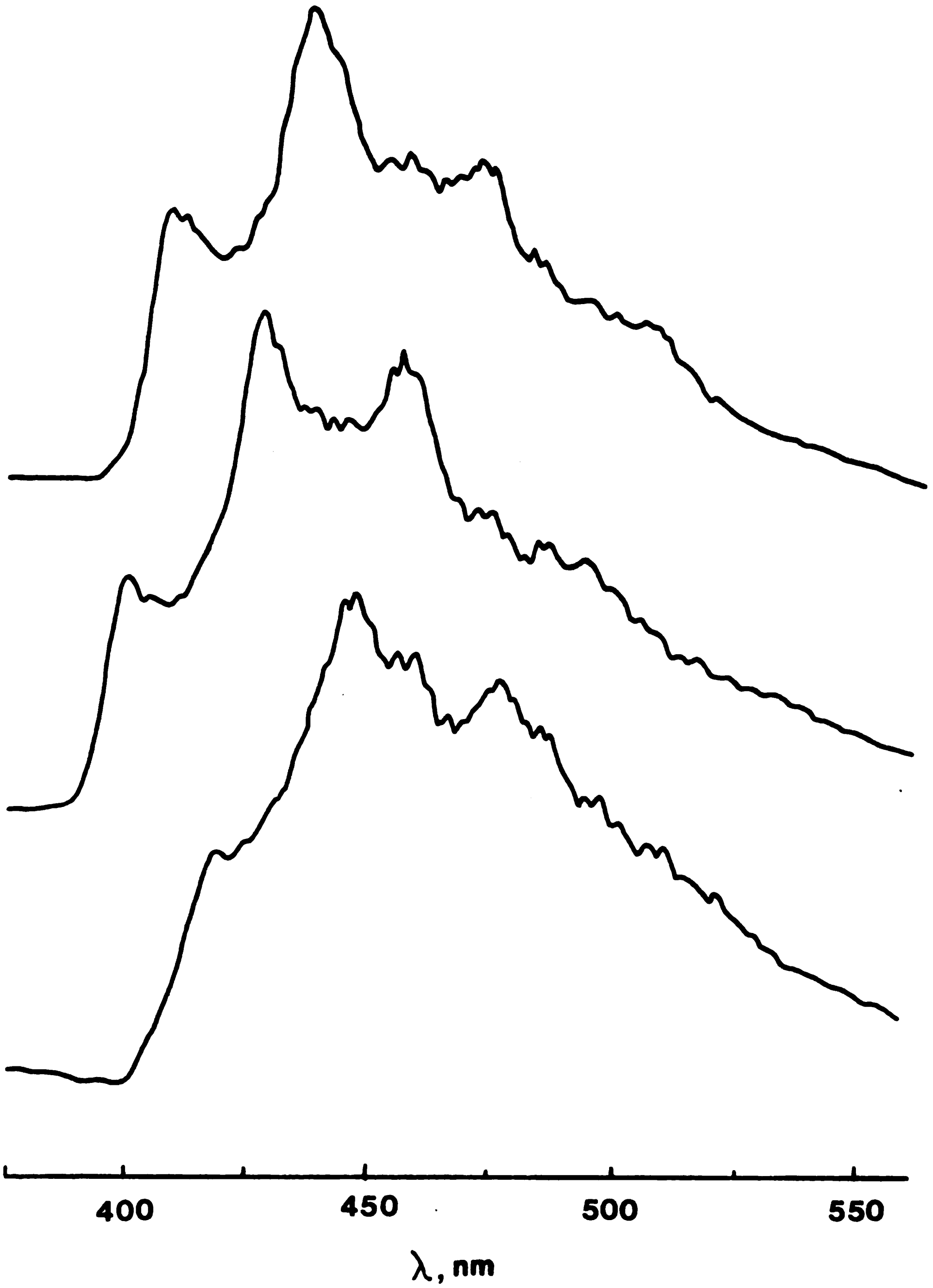

Figure 21. Phosphorescence Spectra of 10^{-4} M Valerophenones in Isopentane at 77°K. Top, o-Carbomethoxyvalerophenone; Middle, m-Carbomethoxyvalerophenone; Bottom, p-Carbomethoxyvalerophenone.

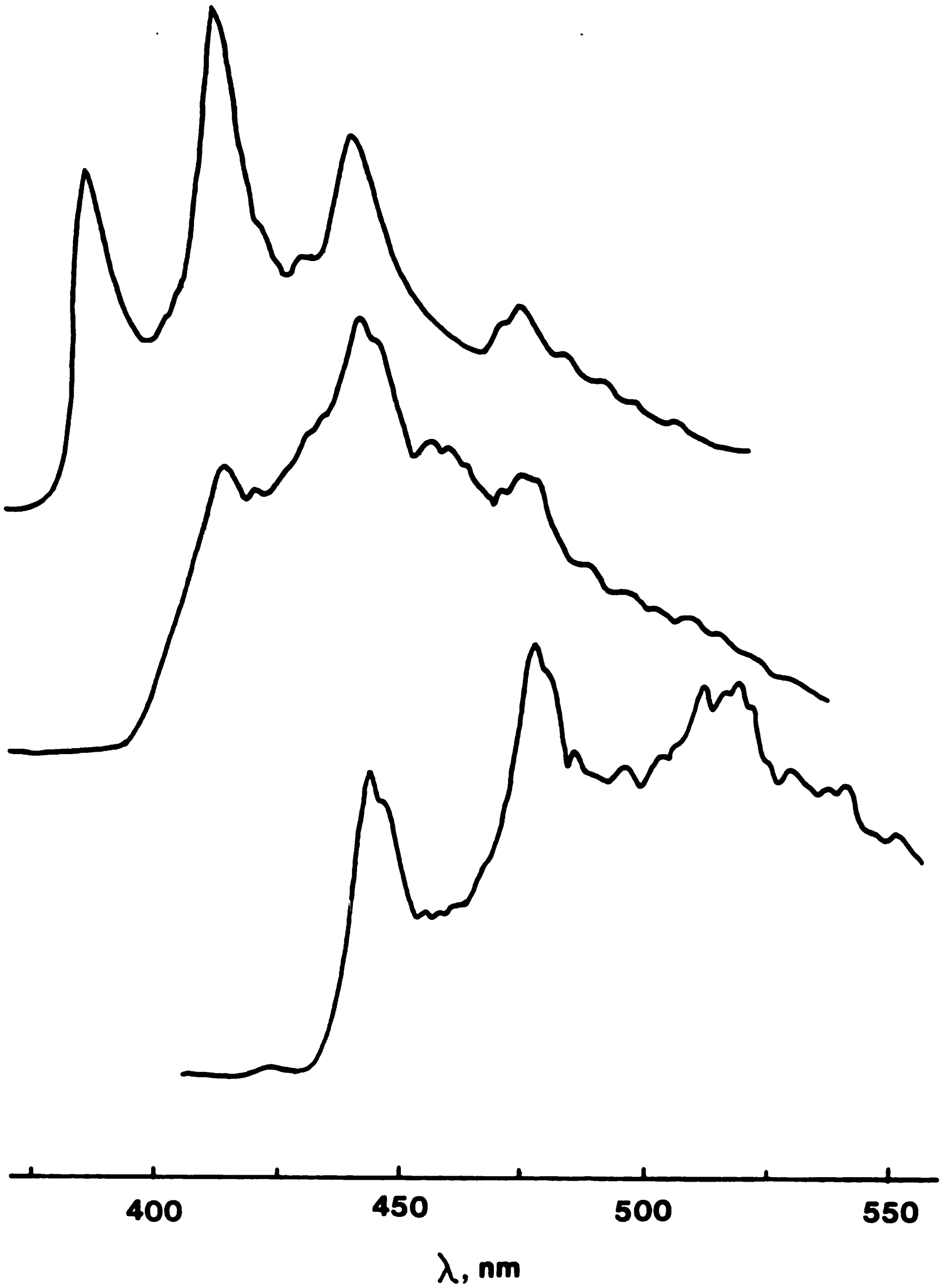

Figure 22. Phosphorescence Spectra of 10^{-4} M Valerophenones in Isopentane at 77°K. Top, Valerophenone (MCH/IP glass); Middle, m-Divalerylbenzene; Bottom, p-Divalerylbenzene.

2. Electronic Absorption Spectra

Ultraviolet absorption spectra were taken in heptane and the values for the ^1L_a bands and n,π* absorptions are given in Table 6. The extinction coefficients at 313 nm were determined in both benzene and acetonitrile solvents in order to assure that both ketone and actinometer absorbed all the incident light when quantum yields were determined, and corrections were not necessary.

3. Cyclic Voltammetry

Reduction potentials were measured for the substituted valerophenones (10^{-4} M) in dry acetonitrile containing 0.1 M tetraethylammonium perchlorate as supporting electrolyte. The half-wave reduction potentials were independent of sweep rate between 100 - 500 mV/sec, but showed greater reversibility at the higher sweep rates. Reductions were often irreversible at ketone concentrations greater than 10^{-3} M. A hanging mercury drop electrode, saturated calomel reference electrode, and platinum auxillary electrode were used. The half-wave reduction potentials were determined by taking the midpoint between the forward and reverse waves of the cyclic voltamagrams. The values obtained are given in Tables 3 and 4 and the cyclic voltammagrams are depicted in Figures 23-26.

Table 6. UV Spectroscopic Data.

Substituent	${}^1L_A\ \lambda_{max}{}^a$	$n\rightarrow\pi^*_{max}{}^a$	$\varepsilon_{313}(\phi_H)$	$\varepsilon_{313}(CH_3CN)$
H	238 (14,000)[d]	324 (42)	52	57
o-CH	236 (9,000)	324 (77)	74	67
m-CN	266 (16,000)	324 (43)	44	49
p-CN	255 (13,000)	332 (68)	74	84
$o\text{-}CO_2CH_3$	228 (9,000)	<300[e](--)	95	84
$m\text{-}CO_2CH_3$	230 (11,000)	316 (44)	48	59
$p\text{-}CO_2CH_3$	254 (13,000)	332 (70)	110	110
$m\text{-}COC_4H_9$	238 (14,000)	320 (79)	100	130
$p\text{-}COC_4H_9$	260 (18,000)	332 (180)	310	300
$p\text{-}COCH_3$	260 (17,000)	332 (160)	360	340
$o\text{-}CF_3$	218 (4,000)[d]	304 (91)	---	---
$m\text{-}CF_3$	234 (10,000)[d]	326 (41)	---	---
$p\text{-}CF_3$	234 (13,000)[d]	328 (45)	---	---

[a] Heptane solvent (extinction coefficient in parenthesis).

[b] In benzene solvent, 313 nm.

[c] In acetonitrile solvent, 313 nm.

[d] Value taken from Reference 28.

[e] Value taken from shoulder of peak.

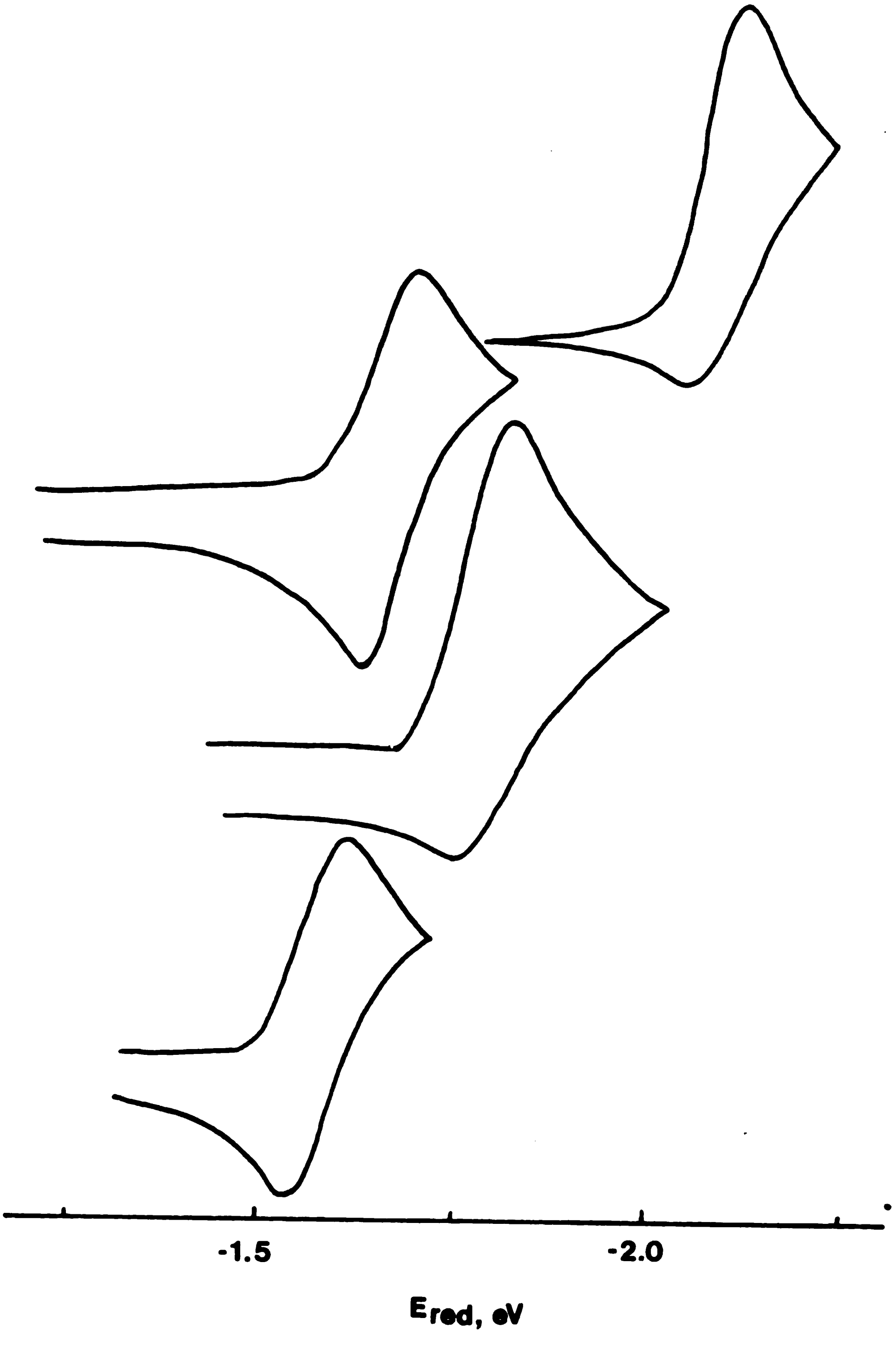

Figure 23. Cyclic Voltammagrams for 10^{-4} M Valerophenones in Acetonitrile (0.1 M TEAP) versus SCE (200 mV/sec). Top, Valerophenone; Second, o-Cyanovalerophenone; Third, m-Cyanovalerophenone; Bottom, p-Cyanovalerophenone.

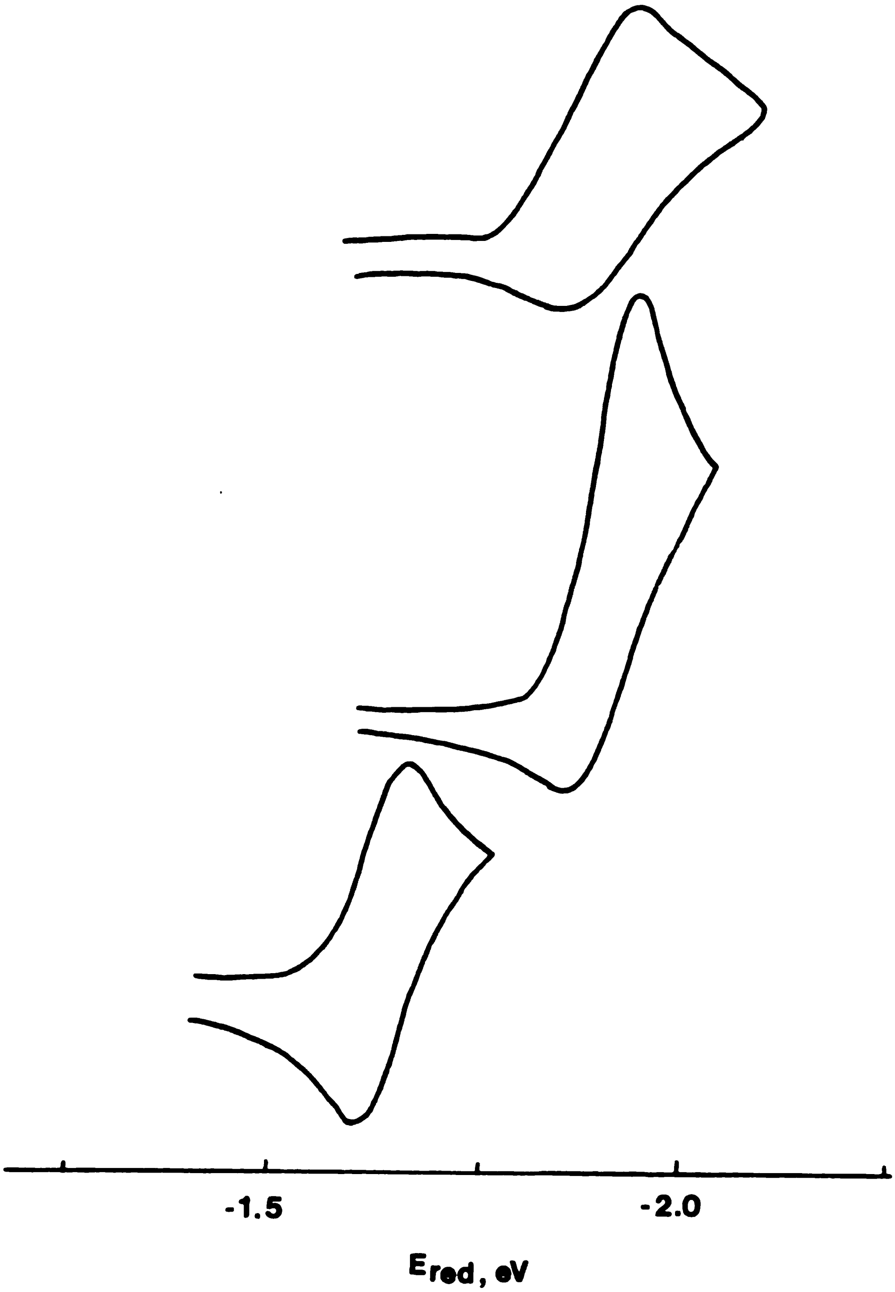

Figure 24. Cyclic Voltammagrams for 10^{-4} M Valerophenones in Acetonitrile (0.1 M TEAP) versus SCE (200 mV/sec). Top, o-Carbomethoxyvalerophenone; Middle, m-Carbomethoxyvalerophenone; Bottom, p-Carbomethoxyvalerophenone.

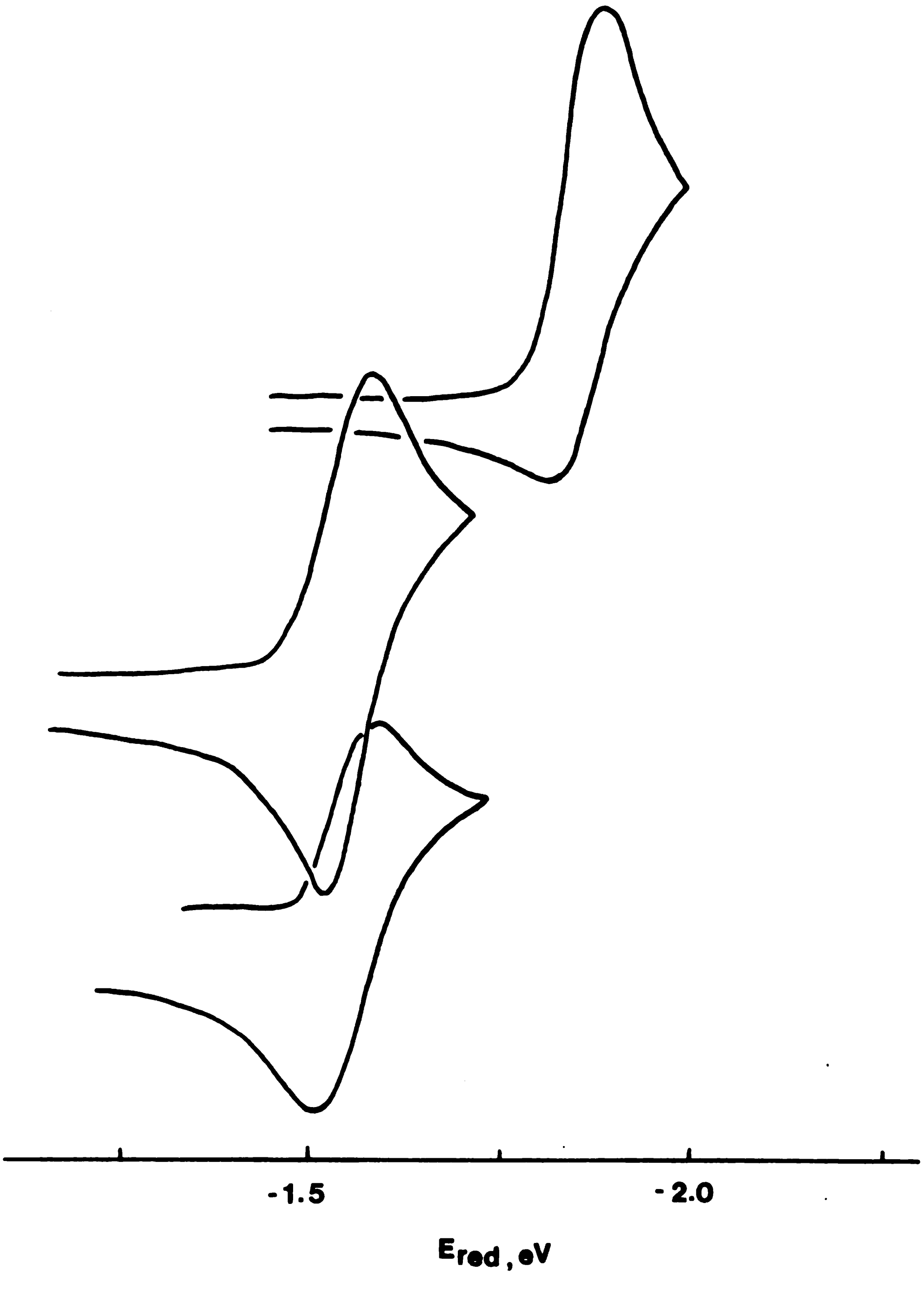

Figure 25. Cyclic Voltammagrams for 10^{-4} Valerophenones in Acetonitrile (0.1 M TEAP) versus SCE (200 mV/sec). Top, m-Divalerylbenzene; Middle, p-Divalerylbenzene; Bottom, p-Acetylvalerophenone.

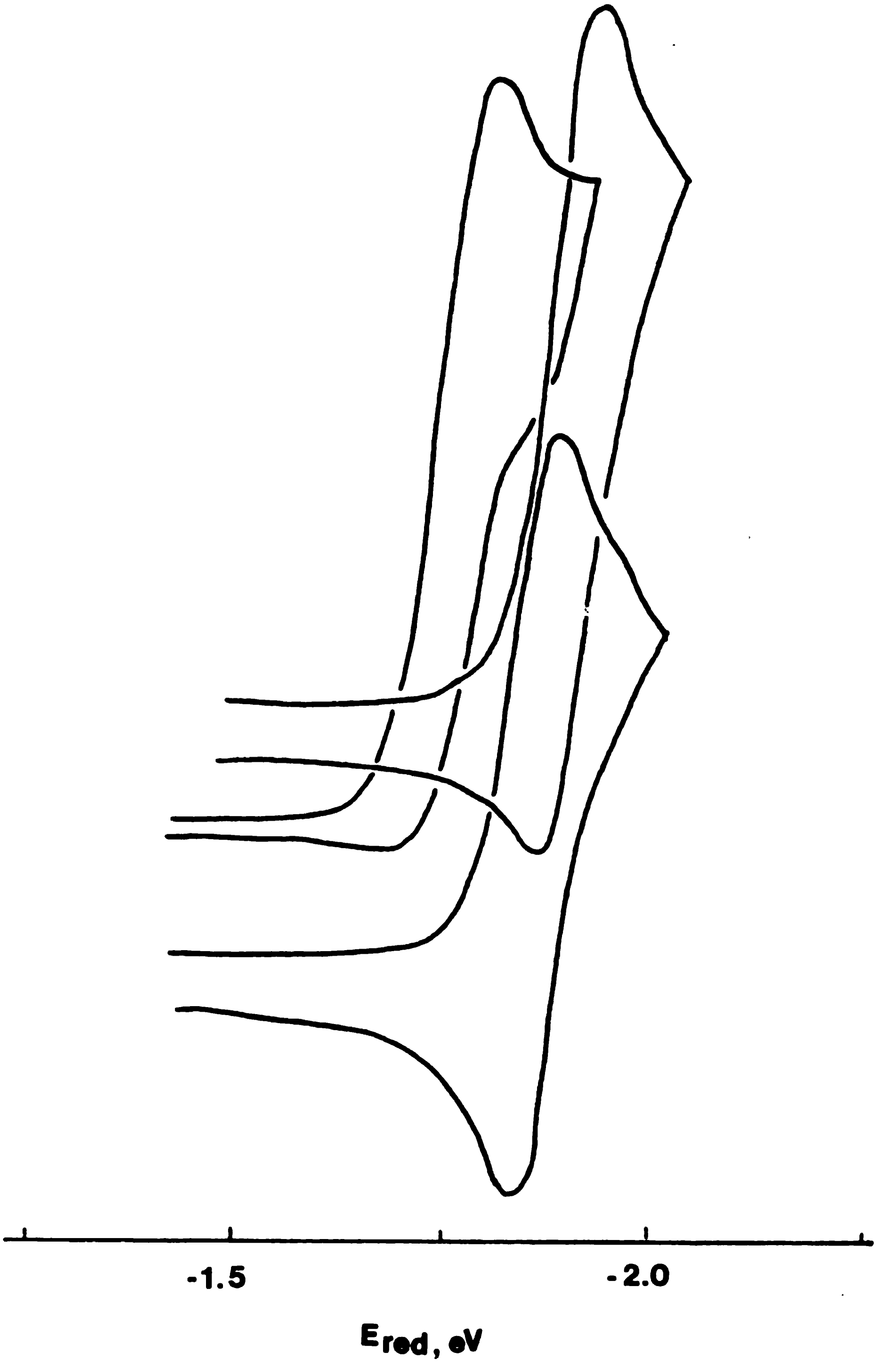

Figure 26. Cyclic Voltammagrams for 10^{-4} M Valerophenones in Acetonitrile (0.1 M TEAP) versus SCE (500 mV/sec). Top, o-Trifluoromethylvalerophenone; Middle, p-Trifluoromethylvalerophenone; Bottom, m-Trifluoromethylvalerophenone.

DISCUSSION

A. Models for Substituent Effects on Triplet Energies

Since only the energy of the lowest triplet can be measured by phosphorescence, similarly substituted compounds which do not possess both n,π* and π,π* triplets in close proximity were used as models for the ketones. Substituted benzophenones[89] have n,π* lowest triplets in all cases and thus substituent effects on purely n,π* triplets can be determined. Likewise, both benzonitriles[90b] and methyl benzoates[90a] have π,π* lowest triplets and substituent effects on purely π,π* triplets can easily be determined. The results are presented in Table 5.

All the meta-substituents studied have negligible effects on the n,π* triplet and stabilize the π,π* triplet by only 1-2 kcal/mole. Conversely, para-substituents stabilize the n,π* triplet by 1-2 kcal/mole and those substituents capable of conjugation with the phenyl ring stabilize the π,π* triplet by approximately 6 kcal/mole. In the case of ortho-substituents, steric as well as inductive and resonance factors determine the effects of substituents on triplet energies. The o-CF_3 substituent inductively stabilizes the π,π* triplet by 2 kcal/mole; both o-CN and o-CO_2CH_3 display significantly greater stabilization (4 kcal/mole), presumably through resonance stabilization, with the sterically unhindered o-CN showing a slightly larger effect. Both o-CF_3 and o-CO_2CH_3 show negligible effects on the n,π* triplet as evidenced by their effects on benzophenone. Since o-cyanobenzophenone could not be purified sufficiently to determine its phosphorescence spectra, its n,π* triplet energy was estimated using Loutfy's[92] correlation of n,π* triplet energies and reduction potentials. Since o-CN has almost the same effect on reduction potential as does p-CN, one can estimate that it will also lower the n,π* triplet energy by a similar amount, approximately 2 kcal/mole. Thus, substituent effects on both n,π* and π,π* triplets have been determined spectroscopically and these values can be used to estimate the energies of both triplets in substituted valerophenones.

B. Triplet Energies of Substituted Valerophenones

Since the photochemistry of these compounds was determined in a nonpolar solvent at room temperature, it was desirable to estimate the energies of both n,π* and π,π* triplets under similar conditions. Thus, the triplet energies for the substituted valerophenones (Table 7) were estimated by applying the substituent effects determined from the models to the estimated triplet energies of unsubstituted valerophenone in benzene at room temperature.[29] Various corrections were applied in calculating the triplet energies of valerophenone at room temperature from the data obtained at 77°K,[29] since there is a large Stokes shift between the 0,0 band of S→T absorption and phosphorescence,[30a] and n,π* triplets undergo a conformational relaxation in nonviscous solvents as compared to rigid glasses.[93]

From the spectroscopic data the meta-substituted valerophenones

Table 7. Predicted n,π* - π,π* Separations in Substituted Valerophenones in Benzene at Room Temperature.

Substituent	π,π*	n,π*
H	75.5[a]	73.4[a]
o-CN	71.0	71.6
m-CN	73.8	73.3
p-CN	69.3[b]	71.2
o-CO_2CH_3	71.5	73.4
m-CO_2CH_3	74.5	73.6
p-CO_2CH_3	70.3	71.5
m-COC_4H_9	∿73[b]	73
p-COC_4H_9	67.7[b]	71
o-CF_3	73.0	∿73[c]
m-CF_3	74.7	73.2
p-CF_3	74.3	72.4

[a] Values taken from Reference 29.

[b] Same values as measured in Reference 89.

[c] Value estimated from E_{red}.

are predicted to have n,π* and π,π* triplets closer together than in the unsubstituted compound but still maintain an n,π* lowest triplet. Conversely, the large stabilization of the π,π* triplet afforded by p-electron-withdrawing substituents capable of conjugation with the ring (p-CN, p-CO_2CH_3, and p-COR) results in inversion of the two triplet levels. For ortho-substituted compounds, steric factors play an important role in determining the nature of the lowest triplet. Sterically unhindered o-CN stabilizes both the n,π* and especially the π,π* triplet, thus making the two triplet levels nearly isoenergetic. On the other hand, o-CO_2CH_3 significantly stabilizes the π,π* triplet and has little effect on the n,π* triplet, presumably since steric bulk prevents the coplanarity of the benzoyl group.[94] Thus, o-CO_2CH_3 valerophenone is predicted to have a π,π* lowest triplet.

In summary, phenyl alkyl ketones with meta conjugatively electron-withdrawing substituents (CN, CO_2CH_3, and COR) maintain n,π* lowest triplets. Resonance stabilization of the π,π* triplet for the analogously substituted para-compounds results in inversion of the triplet levels. For both m-divalerylbenzene and o-cyanovalerophenone the triplet levels seem to be nearly isoenergetic. o-Carbomethoxyvalerophenone seems to have a π,π* lowest triplet primarily due to resonance stabilization of the π,π* triplet with little stabilization of the n,π* triplet.

The phosphorescence spectra for these substituted valerophenones were measured in various solvent glasses at 77°K and the values are included in Table 3. The spectra for valerophenone and the various substituted ketones in MCH/IP or isopentane glasses are depicted in Figures 20-22. Both valerophenone and m-cyanovalerophenone show structural emission with carbonyl progressions typically assigned to n,π* triplets;[3] whereas, p-cyanovalerophenone shows additional vibrational modes characteristic of π,π* emission.[3] The 0,0 bands measured for the para-substituted valerophenones at 77°K agree remarkably well with the predicted π,π* energy levels. Also, meta-CN, $-CO_2CH_3$, and $-CF_3$ show little effect on the energy of the emitting triplets for these substituted valerophenones, in accord with the substituent effects on n,π* triplets for the model benzophenones at 77°K. o-Carbomethoxyvalerophenone shows considerable broadening of the spectrum; o-cyanovalerophenone shows somewhat more structured emission. Thus, the measured triplet energies for the substituted valerophenones at 77°K seem to corroborate the estimated values of n,π* and π,π* triplet energies.

C. Electronic Absorption Spectra and Cyclic Voltammetry

The ultraviolet absorption spectra for these ketones were determined in heptane and the λ_{max} values and extinction coefficients for both the second benzene transition ($S_0 \rightarrow {}^1L_a$) and the n,π* absorption are given in Table 6. A moderate ${}^1L_b$ band below 310 nm is evident in the spectra. For most of the compounds the ${}^1L_a$ band appears as a shoulder on the more intense ${}^1B_a$ or ${}^1B_b$ bands. The para (-R) substituents (CN, CO_2CH_3, and COR) all show a significant stabilization of the $S_0 \rightarrow {}^1L_a$ and n,π* transitions as evidenced by a shift of λ_{max} values to higher wavelengths, as opposed to p-CF_3

which shows little stabilization of the ^1L_a band and only a small stabilization of the n,π* absorption. Since the L_a states of benzenes correspond to π,π* transitions,[28] it appears that conjugative effects are also important in stabilizing the π,π* singlet.

The cyclic voltammograms for the substituted valerophenones are depicted in Figures 23-26. The one-electron reduction of these ketones is at least partially reversible in all cases, as evidenced by the reverse wave. It is interesting to note that both o- and p-cyano substituents stabilize the incipient ketyl radical anion[95,96]

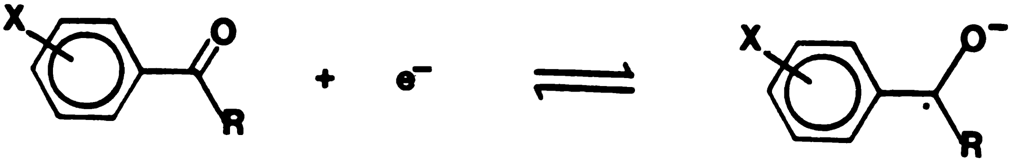

to a much greater extent than does m-cyano; whereas, only p-CO_2CH_3 shows a greater stabilization than does its ortho and meta isomers. Both p-COR substituents show greater stabilization of the radical anion than does the analogous meta substituent. A similar trend in triplet energies was observed for the ortho substituents; o-cyano stabilized the n,π* triplet while o-CO_2CH_3 had no effect, presumably due to the inability of the carbonyl to become coplanar with the phenyl ring due to steric interference. The greater stabilization of the radical anion by para (-R) substituents suggests the importance of conjugative effects. The following resonance structure depicting a fully conjugated system should contribute to the overall stability of the radical anion.

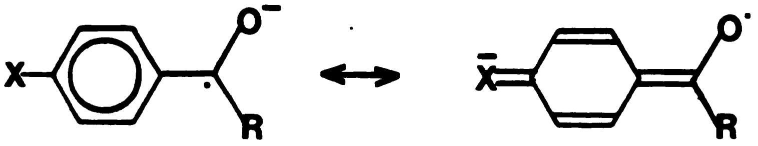

Table 8 summarizes the effects of various substituents on the half-wave reduction potentials of valerophenones in order of decreasing stabilizing effects. As expected, electron-withdrawing substituents stabilize the radical anion, whereas electron donors have the opposite effect. Both p-COR and p-CN have the largest effects on the reduction potentials. Correlations involving both Hammett σ values[96] and n,π* triplet energies[92,97] with reduction potentials have been reported in the literature and similar correlations involving these substituted valerophenones will be discussed in a later section.

D. Rationalization of Substituent Effects on Both π,π^* and n,π^* Triplet States

EPR[98,99] and theoretical studies[98,100,101] on triplet benzonitrile (model for π,π^* triplets of acylbenzenes) indicated that most of the spin density lies at the 1- and 4-positions. The L_a states of benzenes are combinations of both $\pi_a \rightarrow \pi_a^*$ and $\pi_s \rightarrow \pi_s^*$ transitions (C_{2v}) as shown in Scheme 3. A conjugatively electron-withdrawing substituent (i.e., C=O) stabilizes the π_a^* orbital and destabilizes the π_a orbital by mixing with the lower energy carbonyl π orbital[19,94] thus maximizing the contribution from the $\pi_a \rightarrow \pi_a^*$ transition to the $S \rightarrow L_a$ transition and making any contribution from the $\pi_s \rightarrow \pi_s^*$

Table 8. Relative Substituent Effects on Reduction Potentials of Substituted Valerophenones.

Substituent	ΔeV	Δkcal/mole
p-COC_4H_9	+0.52	+12.0
p-$COCH_3$	+0.52	+12.0
p-CN	+0.50	+11.4
p-CO_2CH_3	+0.44	+10.1
o-CN	+0.43	+ 9.9
p-(N)	+0.39	+ 9.0
p-SCF_3	+0.35	+ 8.1
p-CF_3	+0.31	+ 7.1
m-CN	+0.30	+ 6.8
p-$CO_2^-Na^+$	+0.30	+ 6.8
o-CO_2H	+0.26	+ 5.9
o-(N)	+0.25	+ 5.8
o-Cl	+0.24	+ 5.5
p-Cl	+0.24	+ 5.5
o-$CO_2^-Na^+$	+0.23	+ 5.2
p-OH	+0.23	+ 5.2
m-COC_4H_9	+0.22	+ 5.0
m-$CO_2^-Na^+$	+0.21	+ 4.8
m-CF_3	+0.21	+ 4.8
m-(N)	+0.21	+ 4.8
p-$CO_2^-K^+$	+0.21	+ 4.8
m-CO_2CH_3	+0.17	+ 3.9

Table 8. Continued.

Substituent	ΔeV	Δkcal/mole
o-CF_3	+0.17	+ 3.9
m-Cl	+0.17	+ 3.9
p-phenyl	+0.16	+ 3.7
o-CO_2CH_3	+0.14	+ 3.2
m-F	+0.14	+ 3.2
o-F	+0.07	+ 1.6
p-SCH_3	+0.07	+ 1.5
p-CO_2H	+0.03	+ 0.7
m-OCH_3	+0.02	+ 0.5
m-CH_3	-0.01	- 0.2
p-F	-0.02	- 0.3
p-cyclopropyl	-0.06	- 1.4
p-CH_3	-0.09	- 2.0
m-CO_2H	-0.09	- 2.0
o-OCH_3	-0.10	- 2.2
o-CH_3	-0.13	- 3.0
p-OCH_3	-0.14	- 3.2

[a] Reduction potentials measured in acetonitrile containing 0.1 M tetraethylammonium perchlorate.

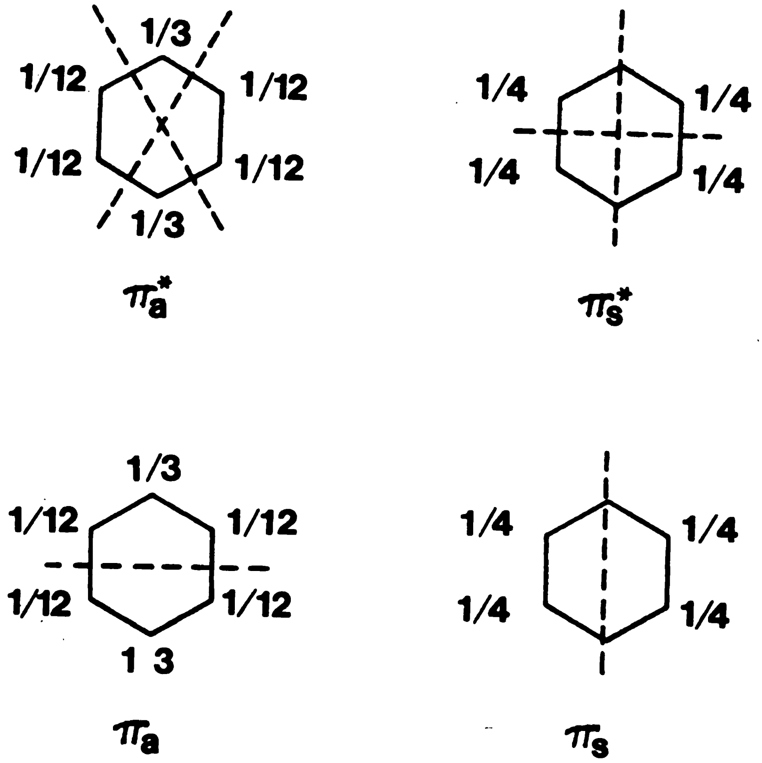

Scheme 3. M.O. Representations for π Orbitals of Benzene.

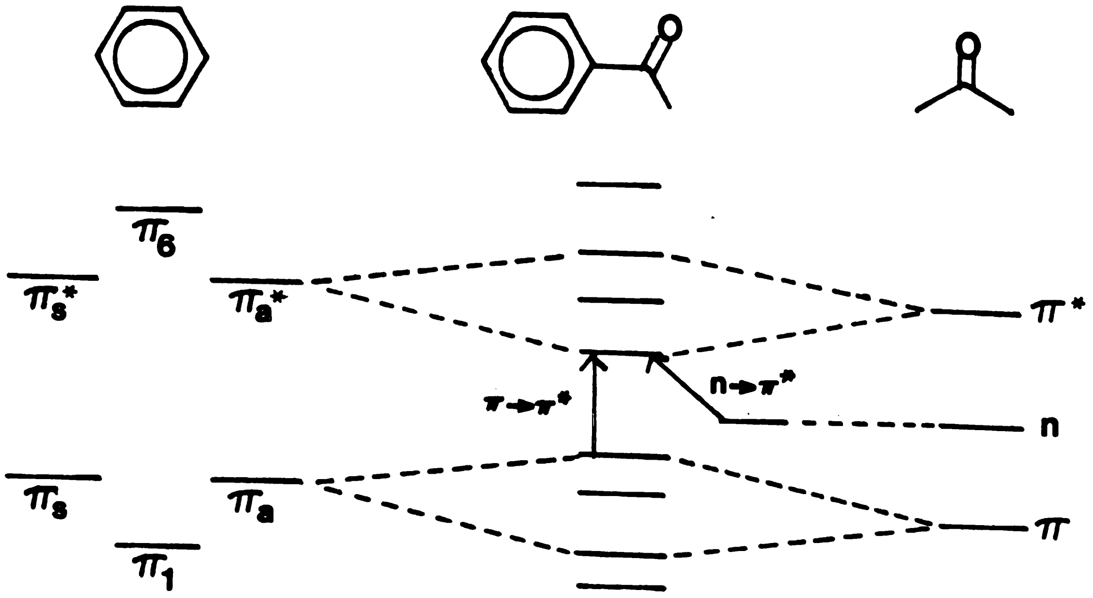

Scheme 4. Mixing of π-Orbitals in Benzoyl System.

transition negligible (Scheme 4).

Another (-R) substituent reinforces this orbital splitting, since inductive effects on transition dipoles greatly affect the ^3L_a energy level. The vector addition of individual substituent dipoles for 1,4-acceptor, acceptor substituents results in greater stabilization than does a similar 1,3 pair. The MO orbital diagram indicates that a para substituent should lower the π,π^* triplet by the same amount as the first substituent; whereas, a meta substituent should lower the triplet energy by only 1/4 the amount, if the spin density at the site affects the amount of stabilization afforded by the substituent. The π,π^* triplet energies measured for substituted benzonitriles and methyl benzoates seem to corroborate this simple MO representation of the π,π^* triplet.

The valence bond representations below describe the L_a π,π^* triplet of phenyl ketones.

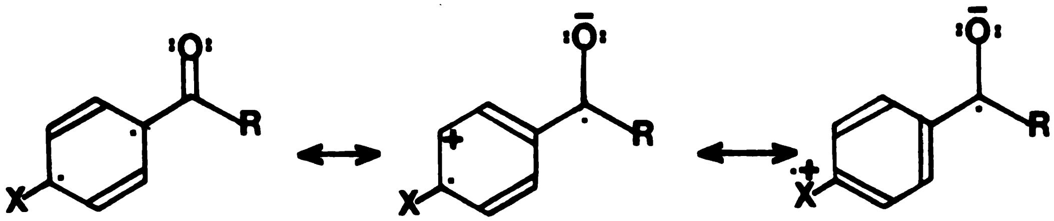

The most important resonance form is the 1,4-diradical "quinoidal" form of the triplet.[98] EPR studies[99] showed that very little charge density lies at the meta position, as is depicted in the middle valence bond structure. The third structure represents a high-energy charge-transfer state which mixes somewhat with the low-lying ^3L_a

state but to a greater extent with the high-energy ^1L_a state.[103] For phenyl alkyl ketones containing substituents capable of conjugation with the ring, the following valence bond structure depicts a fully conjugated π-system.

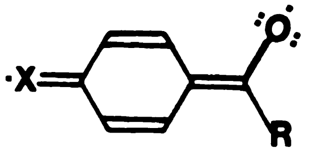

Thus, significant contribution of this structure, or the analogous ortho-structure, would account for the significantly larger stabilization of the π,π* triplet afforded by o- and p-CN, p-CO_2CH_3, and p-COR substituents as compared to the model CF_3 substituents.

As long as the n-orbital remains orthogonal to the π-system, an n,π* transition can be regarded simply as a one-electron reduction of the π-system.[104] EPR studies[105] on benzonitrile radical anions indicated that the additional electron density in the benzene ring occupies primarily the 1- and 4-positions with negligible spin density at the meta position. Thus, substituents have diminished effects in the meta position. Valence bond representations of the n,π* triplet are shown below.

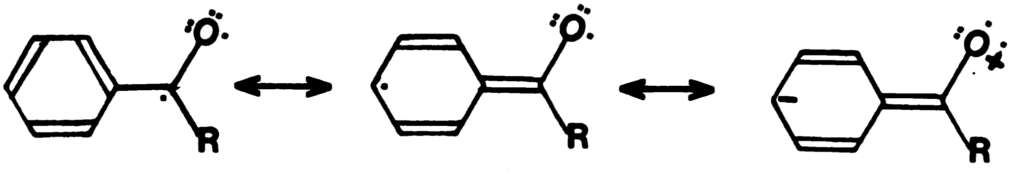

Electron-withdrawing substituents inductively stabilize the n,π^* triplet. The substituent effects determined for benzophenone n,π^* triplets confirm the larger stabilization provided by para- versus meta-substitution by electron-withdrawing substituents.

E. Type II Quantum Yields

The Type II quantum yields in benzene, wet acetonitrile, and in benzene with added Lewis base for these substituted valerophenones are given in Table 1. The quantum yields for most ring-substituted valerophenones can be maximized to unity with added Lewis base as long as there are no competing triplet processes. The Lewis base hydrogen bonds to the hydroxy proton and prevents disproportionation from occurring.[10b]

The quantum yields for these conjugatively electron-withdrawing substituted valerophenones rises to maximum values considerably less than unity with added Lewis base (i.e., pyridine, t-butyl alcohol, or dioxane) as shown in Figures 13 and 14. The quantum yields in wet acetonitrile are generally higher than with added Lewis base. The inability to sufficiently maximize the quantum yield is difficult to explain, since electron-withdrawing substituents increase the acidity of the hydroxy proton. Thus, these biradicals must be completely solvated by the added base, but for some reason do not always go on to form product. One plausable explanation involves resonance stabilization of the solvated biradical which would perhaps make disproportionation competitive with product formation.

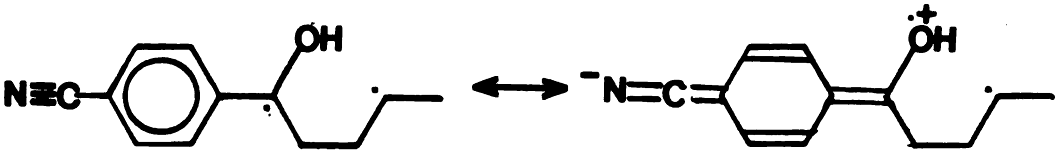

Polar solvents or Lewis bases would stabilize such charge separation.

Since the possibility remains that some other triplet decay process, k_d, could be competitive with γ-hydrogen abstraction, k_r, as in the case of p-methoxyvalerophenone,[28] suitable experiments were conducted in order to determine k_d values. Only if γ-hydrogen abstraction is found to be the only triplet process can one equate $1/\tau$ with k_r.

F. Determination of k_d Values by Various Methods

The rate of γ-hydrogen abstraction is dependent on changes in the γ-C-H bond strength.[15,28,106] Table 2 lists quantum yields in benzene, maximum quantum yields with added pyridine, and $k_q\tau$ values for both unsubstituted and p-cyanosubstituted butyrophenones (1°γ-H), valerophenones (2°γ-H), and γ-methylvalerophenones (3°γ-H). In both series the γ-methylvalerophenone is approximately four times more reactive than the corresponding valerophenone. In contrast, butyrophenone is much less reactive (factor of 6) than valerophenone, while p-cyanobutyrophenone is only 3 times less reactive than the corresponding valerophenone. The reason for the greater reactivity of p-cyanobutyrophenone than predicted by the unsubstituted models is not apparent, but appears to be real.

The Type II quantum yield for acetophenone formation is determined by competitive excited state reactions:

$$\Phi_{II} = \Phi_{ISC} \cdot k_r \cdot P_p \cdot \tau \qquad (10)$$

where Φ_{ISC} is the quantum yield for intersystem crossing, k_r is the rate for γ-hydrogen abstraction, P_p is the probability that the biradical will go on to form product, and $\tau = (k_r + k_d)^{-1}$. The intersystem crossing yields for both p-cyano and p-carbomethoxyvalerophenones were measured and found to equal unity. Within each series of compounds both P_p and k_d remain constant, since increased γ-substitution should not affect these parameters. Since the quantum yields remain nearly constant within each series, whereas, the triplet lifetimes decrease appreciably with increased γ-carbon substitution, then an increase in the rate of γ-H abstraction with increased γ-carbon substitution must be responsible. Therefore, k_d is not competitive with k_r, and k_d must be less than 10^6 s^{-1}.

In order to insure that k_d is indeed smaller than k_r, bimolecular photoreduction experiments were conducted. Photoreduction experiments on p-cyanoacetophenone using either toluene or p-xylene as donor and naphthalene as quencher in acetonitrile solvent indicate that $k_d = 4 \times 10^5$ s^{-1}. Thus, $k_d << k_r$ and $1/\tau$ can be equated to k_r. Consequently, the exceptional inability to maximize the total quantum yield to unity for these (-R) substituted valerophenones must be due to the reduced ability of the intermediate biradical to go on to form product.

G. Ketone Photoreactivity and Calculation of Relative Triplet Energies

It has been shown that the observed rate constant, k_{obs}, for ketones with π,π^* lowest triplets is described as follows:

$$k_{obs} = \chi_{n,\pi} \cdot k_r^{n,\pi} \qquad (3)$$

where $\chi_{n,\pi}$ is the thermal equilibrium fractional population of the n,π^* state and $k_r^{n,\pi}$ is the intrinsic rate of hydrogen abstraction for the appropriate n,π^* triplet. The population of the n,π^* triplet at a certain temperature can be calculated from the Boltzmann equation as follows:

$$\chi_{n,\pi} = (1 + e^{\Delta E/RT})^{-1} \qquad (14)$$

where ΔE is the energy separation between the two triplets and T is the temperature in degrees Kelvin. Thus, if one can estimate $k_r^{n,\pi}$, then calculation of the energy separation between the two triplets becomes possible.

Trifluoromethyl groups increase the energy gap between the two triplets by stabilizing the n,π^* triplet while having little effect on the π,π^* triplet such that population of the upper π,π^* triplet is essentially zero. Since CN, CO_2R, and COR all have Hammett σ values similar to that of CF_3,[107] their intrinsic $k_r^{n,\pi}$ values must nearly equal k_r for the analogous o-, m-, or p-trifluoromethylvalerophenone. Since the rate of hydrogen abstraction is enhanced only by a factor of 2-3 by the inductive effect of m- and p-CF_3 on the electrophilic n,π* triplet, the error involved in estimating the other $k_r^{n,\pi}$ values must be negligible.

From the Stern Volmer quenching studies and the other experiments verifying that γ-hydrogen abstraction is the only process responsible for triplet decay, $1/\tau = k_r^{obs}$. The data from Table 1 indicate that p-COC_4H_9, p-CN, and p-CO_2CH_3 substituents decrease triplet reactivity to 10%, 25%, and 40%, respectively, as observed for p-CF_3 valerophenone. From these $\chi_{n,\pi}$ values, the ΔE_T separations calculated are 1.3, 0.67, and 0.3 kcal/mole, respectively, in benzene at room temperature. Since $1/\tau$ increases by an average of 50% at most in acetonitrile, then these values cannot be very different in acetonitrile.

It is interesting that p-divalerylbenzene is twice as reactive as p-acetylvalerophenone. Although each compound has two chromophores capable of absorbing light, only excitation of the valeryl carbonyl can lead to γ-hydrogen abstraction. Since both carbonyls have an equal probability of becoming excited, then the decreased reactivity of p-acetylvalerophenone reaffirms the idea that excitation in the n,π* triplet is localized primarily on the carbonyl.

Both m-CN and m-CO_2CH_3 valerophenones show reactivities comparable to that of the model m-trifluoromethylvalerophenone. All three ketones have n,π* lowest triplets. Conversely, m-divalerylbenzene is only half as reactive as the model ketone, thus implying that the n,π* and π,π* triplets are isoenergetic and equally populated. The spectroscopic data seem to be in good agreement with this assignment.

The observed photoreactivity for the ortho-substituted valerophenones is more difficult to interpret, since steric factors are also involved. o-Cyanovalerophenone is twice as reactive and o-carbomethoxyvalerophenone is only 1/4 as reactive as the o-trifluoromethylvalerophenone model. Unfortunately, o-CF_3 valerophenone is not an ideal model since it displays decreased reactivity as compared to its meta and para isomers, presumably due to steric factors. Thus, calculation of the energy separation for the two ketones from the kinetics is impossible. From the spectroscopy o-cyanovalerophenone has nearly isoenergetic triplet levels; whereas, o-carbomethoxyvalerophenone has a definite π,π^* lowest triplet. At least a qualitative correlation exists between the observed reactivities and the energy separations predicted from the spectroscopic data.

Thus, the photoreactivity of these ketones provides a more sensitive method for determining the energy separation between the two triplets. In general, both photochemical and spectroscopic data agree that p- (-R) substituents stabilize the π,π^* triplet to such an extent that these ketones possess π,π^* lowest triplets.

H. Attempted Correlation of Reactivities with Hammett σ Values

Wagner et al.[29] have correlated the relative rates of γ-hydrogen abstraction of ring-substituted phenyl ketones with Hammett σ parameters (Figure 27). Both meta and para inductively electron-withdrawing (-I) substituents (n,π^* lowest triplets) (dashed line) and weakly electron-donating substituents (m-, or p-CH_3, -OCH_3) (π,π^*

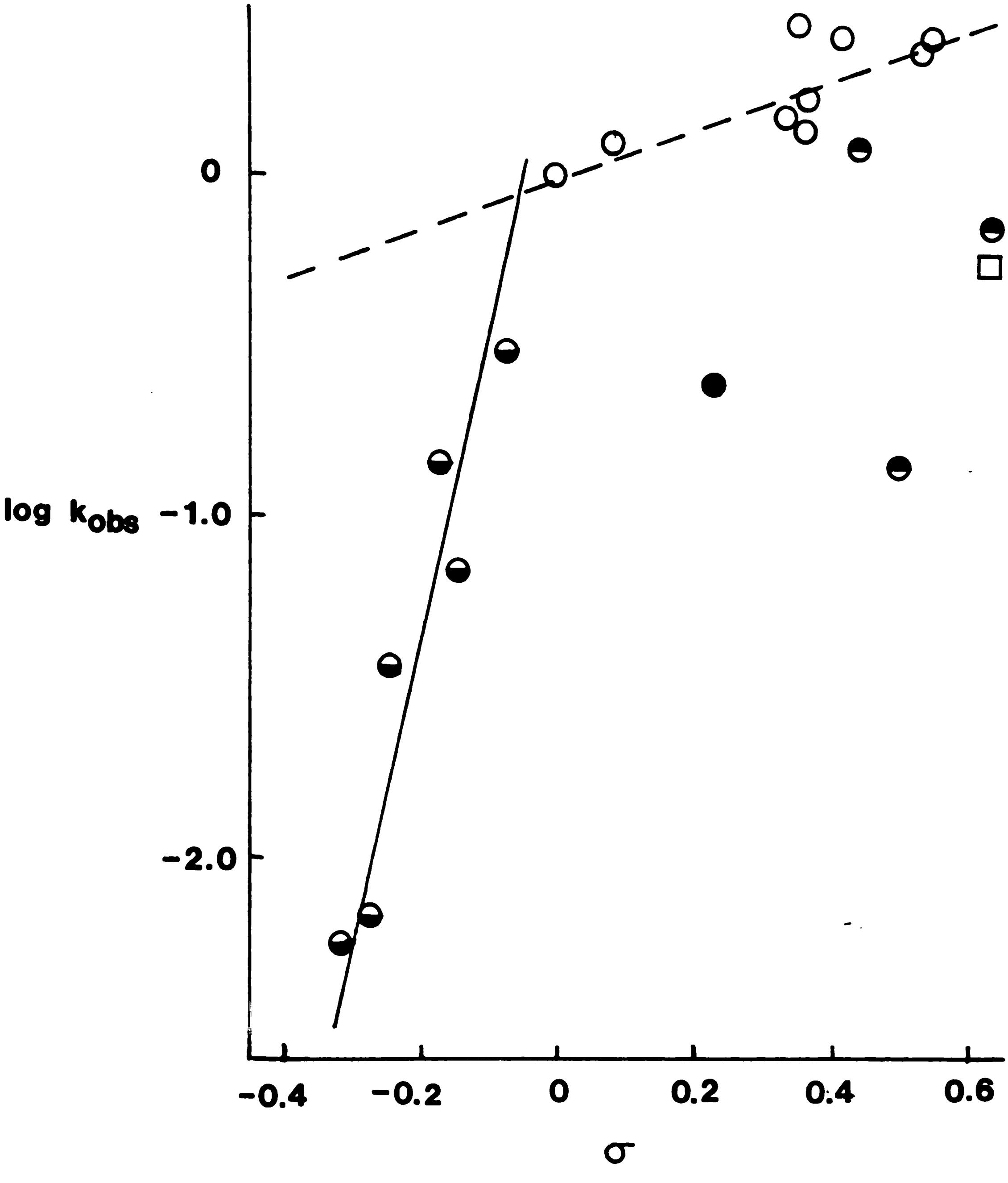

Figure 27. Plot of Relative k_{obs} Values as a Function of Ground State Hammett σ Values. ○ , -I Substituents; ◓, Electron-donating Substituents; ◓, para-R Substituents; ●, p-Cl; □, p-SCF$_3$.

lowest triplets) (solid line) gave linear correlations with different slopes. p-Cl did not fit on either line, nor does our p-CN, p-CO_2CH_3, p-COR, and m-COR, or p-SCF_3.[108] As already pointed out,[29] a Hammett plot is inappropriate for ketones with π,π^* lowest triplets where k_{obs} values are dominated by Boltzmann factors rather than by substituent effects on actual $k_r^{n,\pi}$ values. Also, since Hammett constants do not adequately describe substituent effects on π,π^* triplet energies, then ΔE_T values cannot correlate with Hammett substituent constants. Ground state σ values decrease in the order CN > COR > CO_2CH_3, whereas, conjugative effects on π,π^* triplets display a different order: COR > CN > CO_2CH_3. The coplanarity of the excited benzoyl groups compared to the twisting of the ground states[94] would explain the greater conjugating ability of acyl groups in the excited state.

I. Charge Transfer Quenching Studies

Substituted phenyl alkyl ketones can undergo charge transfer interactions with tertiary amines.

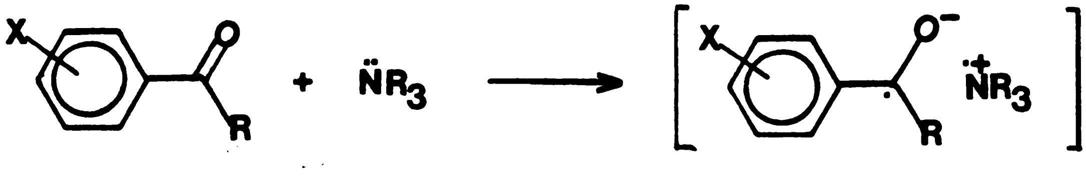

The equation developed by Weller[61] and later modified by Cohen[65] for carbonyl compounds describes the relationship between the rate constant of charge transfer quenching and the various parameters affecting the change in free energy involved.

$$\log k_{CT} \sim \Delta G_{CT} \sim IP_D - E(A^-/A) - \Delta^3E_{0,0} + C \qquad (8)$$

Since in all the experiments triethylamine was used as donor, then IP_D remains constant, as does C. Thus, if one can determine both the reduction potential and the energy of the triplet involved for the acceptor, then one can calculate relative ΔG_{CT} values.

From comparison of diene and triethylamine quenching rates under similar conditions, one can determine the rates of charge transfer quenching from the following equation:

$$k_{CT} = \frac{k_q\tau(Et_3N)}{k_q\tau(\text{diene})} \cdot k_q \qquad (15)$$

where k_q is the rate of diene quenching (5×10^9 M^{-1} s^{-1} in benzene and 1×10^{10} M^{-1} s^{-1} in acetonitrile). Table 9 contains the values of k_{CT} in both benzene and acetonitrile solvents. The parameters necessary to plot log k_{CT} versus excited state reduction potential (Figure 28) are summarized in Table 10. Assuming that the rates of charge transfer quenching of the n,π^* and π,π^* triplets are not significantly different,[83] then the energy of the lowest triplet was used in calculating the excited state reduction potentials for the graph. Even if this assumption proves to be erroneous, then only small errors are involved since most of the ketones studied possess n,π^* and π,π^* triplets in close proximity.

Table 9. Charge Transfer Quenching Data for Substituted Valerophenones.

Substituent	Solvent	k_H, $10^7 s^{-1}$	k_{CT}, $10^9 s^{-1}$
H	Benzene	11.	1.2
H	Acetonitrile	16.	2.1
o-CN	Benzene	23.	---
o-CN	Acetonitrile	30.	--
m-CN	Benzene	26.	5.8
m-CN	Acetonitrile	50.	5.0
p-CN	Benzene	6.8	6.1
p-CN	Acetonitrile	11.	11.
o-CO_2CH_3	Benzene	3.6	2.2
o-CO_2CH_3	Acetonitrile	3.0	2.5
m-CO_2CH_3	Benzene	28.	6.9
m-CO_2CH_3	Acetonitrile	48.	---
p-CO_2CH_3	Benzene	12.	5.5
p-CO_2CH_3	Acetonitrile	17.	16.
m-COC_4H_9	Benzene	14.	3.8
m-COC_4H_9	Acetonitrile	22.	7.2
p-COC_4H_9	Benzene	2.7	---
p-COC_4H_9	Acetonitrile	1.4	---
o-CF_3	Benzene	13.[a]	7.2
m-CF_3	Benzene	32.[a]	8.4
p-CF_3	Benzene	28.[a]	15.
p-CF_3	Acetonitrile	42.[a]	21.

[a] Unpublished results by Warren B. Mueller.

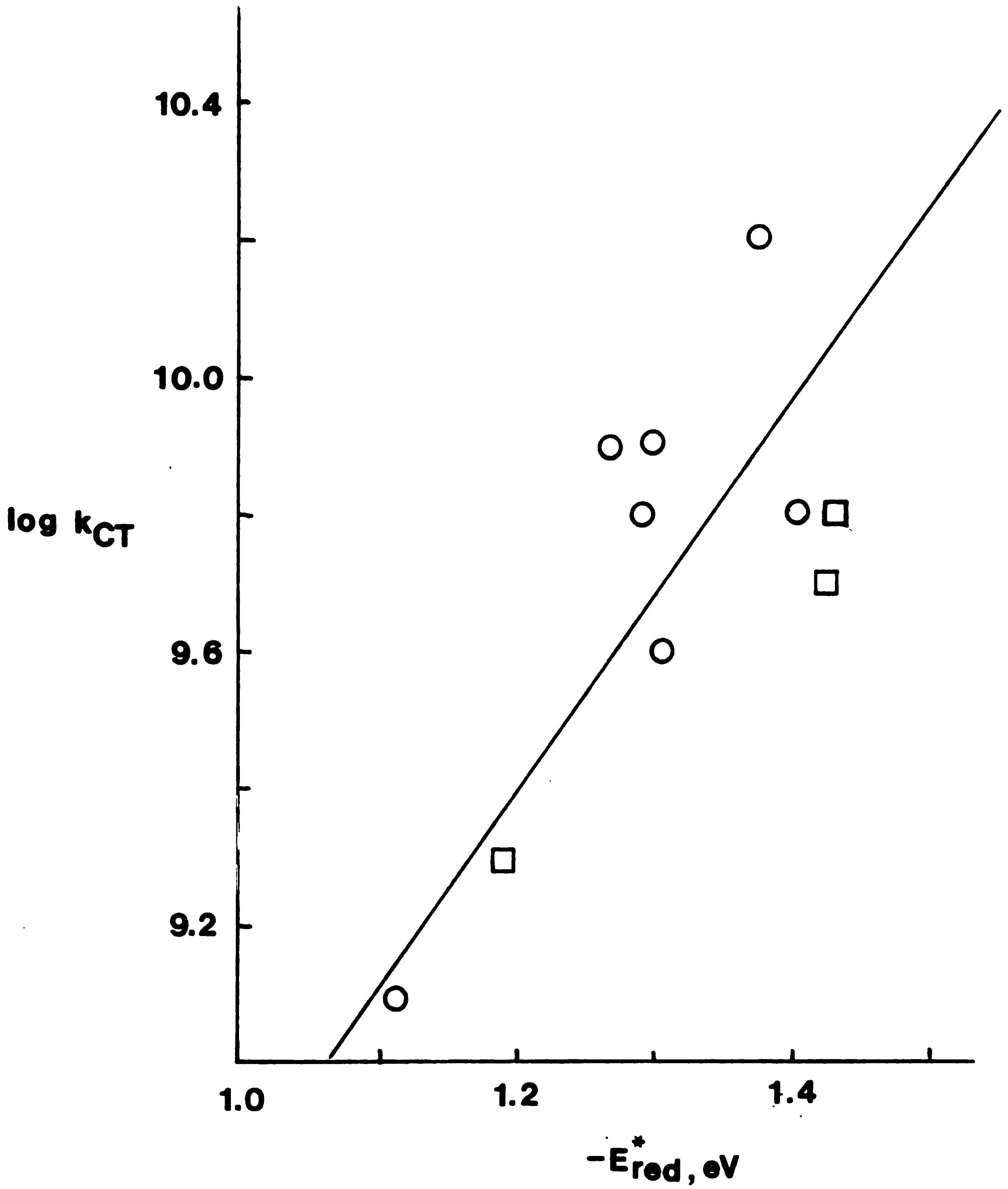

Figure 28. Correlation of Charge Transfer Quenching Rates for Substituted Valerophenones in Benzene (0.5 M Pyridine) with Excited State Reduction Potentials: ○ n,π* lowest Triplet; □ π,π* Lowest Triplet.

Table 10. Charge Transfer Quenching Parameters in Benzene.

Substituent	E_T (n,π*)	E_T (π,π*)	$-E_{red}$[a]	$-{}^*E_{red}$(eV)[b]	k_{CT} $10^9 s^{-1}$	log k_{CT}
H	73.4[c]	75.5[c]	47.7	1.11 (1.21)	1.2	9.1
o-CN	∿71.6	71.0	37.8	1.47 (1.44)	---	---
m-CN	73.3	73.8	40.9	1.41 (1.43)	5.8	9.8
p-CN	71.2	69.3	36.3	1.51 (1.43)	6.1	9.8
o-CO_2CH_3	73.4	71.5	44.5	1.25 (1.17)	2.2	9.3
m-CO_2CH_3	73.6	74.5	43.8	1.29 (1.33)	6.9	9.8
p-CO_2CH_3	71.5	70.3	37.6	1.47 (1.42)	5.5	9.7
m-COC_4H_9	73	∿73	42.8	1.31 (1.31)	3.8	9.6
p-COC_4H_9	71	67.7	35.7	1.53 (1.39)	---	---
o-CF_3	∿ 73	73.0	43.8	1.27 (1.27)	7.2[d]	9.9
m-CF_3	72.8	74.7	42.9	1.30 (1.38)	8.4[d]	9.9
p-CF_3	72.4	74.3	40.6	1.38 (1.46)	15.[d]	10.2

[a] Values in kcal/mole.

[b] Values for excited state reduction potentials for n,π* triplets; values in parentheses for π,π* triplets.

[c] Values taken from Reference 29.

[d] Unpublished results by Warren B. Mueller.

Weller's equation seems to hold for these (-R) substituted valerophenones. In all cases these compounds possess excited state reduction potentials lower than valerophenone itself and exhibit increased rates of charge transfer quenching. The rate of charge transfer quenching generally increased at most by a factor of 2 in acetonitrile. As previously determined, the separation between the two triplets cannot be significantly different in acetonitrile than in benzene. The rate of charge transfer quenching with triethylamine exceeds the rate of diene quenching for many of these (-R) substituted valerophenones.

In summary, these electron-withdrawing substituted valerophenones readily undergo charge-transfer interactions with tertiary amines, many at rates which approach diffusion control. Since the n,π^* and π,π^* triplets are close in energy and the triplet energies are estimated values, then correlation of the rates of charge-transfer quenching with the nature of the triplet undergoing the interaction is impossible. All Stern Volmer quenching experiments involving triethylamine in benzene solvent contained 0.5 M pyridine to solvate the biradical. For many ketones it is apparent that small amounts of triethylamine ($pK_a = 11$)[109] solvate the biradical to a greater extent than does pyridine ($pK_a = 5.2$)[109], since slightly more photoproduct was produced in the lowest concentration quenched tubes than in the unquenched tubes.

J. Correlation of Reduction Potentials with Hammett σ Values

Nadjo and Saveant[96] have related the reduction potentials of substituted acetophenones, fluorenones, and benzophenones to Hammett σ_m and σ_p parameters. A similar correlation was sought for the wide variety of substituted valerophenones studied. The reduction potentials and Hammett σ values for both meta and para substituted ketones are presented in Table 11. A plot of $-E_{red}$ versus σ_m or σ_p values (Figure 29) gave a linear correlation which suggests that resonance effects are indeed important in stabilizing the radical anion formed by the one-electron reduction of phenyl ketones. When Hammett σ_p values were used instead of σ_p^- values, the reduction potentials of p (-R) ketones fell well below the line. The only anomalies found were the CO_2H and CO_2^- substituted valerophenones which fell symmetrically about the line. Perhaps acid or base catalyzed reactions with the solvent or reduction of the carboxy functionality are responsible. Whatever the explanation for these discrepancies, the other ketones seem to correlate very well with Hammett parameters.

K. Correlation of n,π^* Triplet Energies for Substituted Phenyl Ketones with Hammett σ Values

Arnold[89] has published several correlations of n,π^* triplet energies for both substituted acetophenones and benzophenones with Hammett σ_m and σ_p values. The acetophenones gave a good linear correlation (no -R substituents were included). The benzophenones

Table 11. Correlation of Hammett σ Values with Reduction Potentials for Valerophenones.

Substituent	σ_m or σ_p [a]	σ_p^- [a]	$-E_{red}$ [b]
H	0		47.7
m-CN	+.56		40.9
p-CN	+.66	+.90	36.3
m-CO_2CH_3	+.37		43.8
p-CO_2CH_3	+.45	+.68	37.6
m-COC_4H_9	+.38		42.8
p-$COCH_3$	+.50	+.87	35.7
m-CF_3			42.9
p-CF_3	+.54		40.6
m-CH_3	-.07		48.0
p-CH_3	-.17		49.7
m-OCH_3	+.12		47.3
p-OCH_3	-.27	-.2	51.0
m-F	+.34		44.5
p-F	+.06	-.02	48.1
m-Cl	+.37		43.9
m-CO_2^-	-.10		42.9
p-CO_2^-	0		40.9
m-CO_2H	+.37		49.7
p-CO_2H	+.45	+.73	47.0

[a] Values taken from Reference 107.

[b] Values given in kcal/mole.

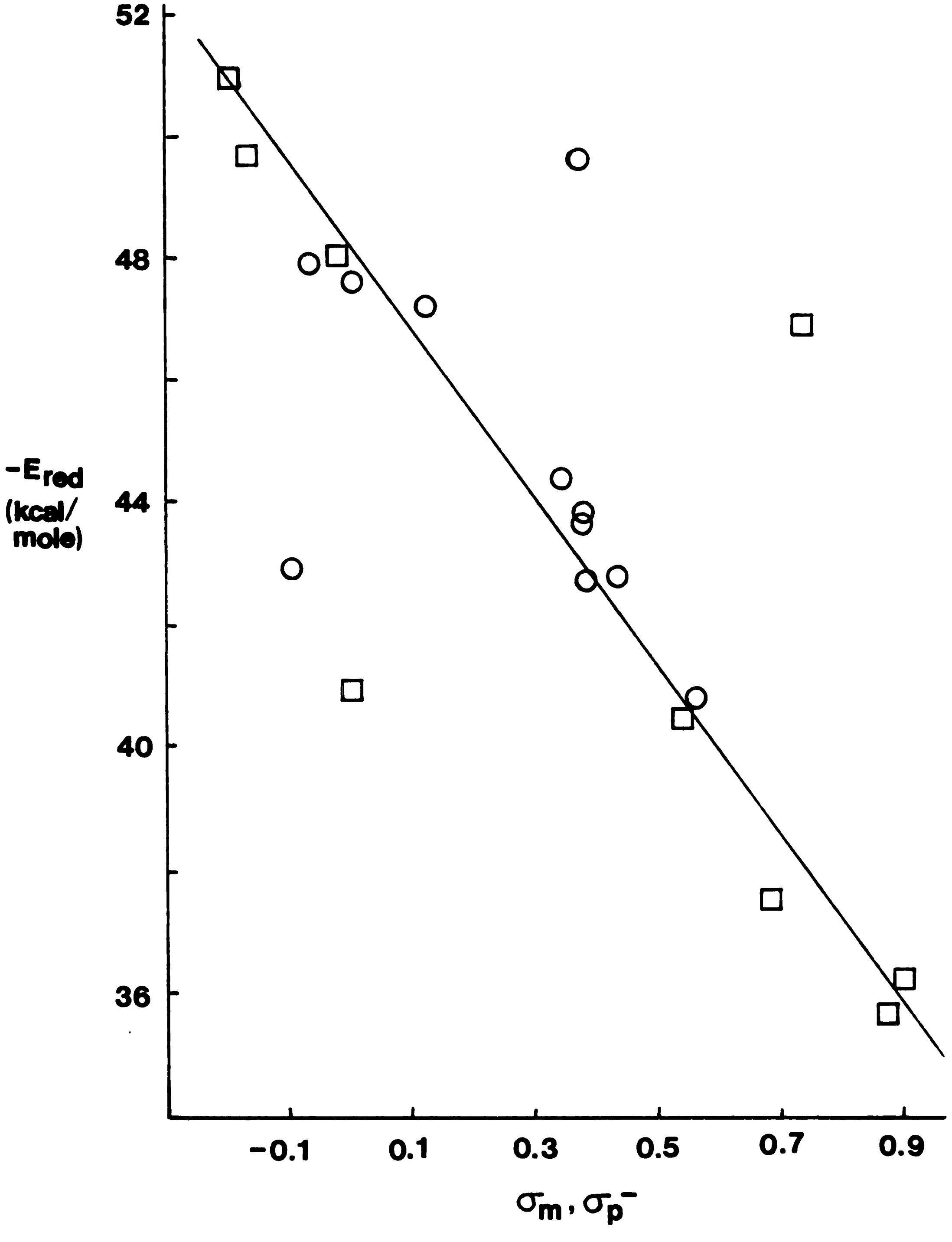

Figure 29. Correlation of Half-wave Reduction Potentials for Substituted Valerophenones with Hammett σ_m and σ_p^- Values: ○ meta-Substitution; □ para-Substitution.

(both mono- and symmetrically substituted compounds) did not correlate well with the additive Hammett parameters for disubstitution (Figure 30), but a somewhat better correlation can be obtained when Hammett σ_m and σ_p^- values are used and symmetrically substituted benzophenones are treated as monosubstituted compounds (Figure 31). Arnold[89b] later studied a wide variety of both mono- and symmetrically and unsymmetrically substituted benzophenones. They found that all the symmetric derivatives correlate fairly well with a Hammett two-parameter treatment employing both σ and $\sigma^{\cdot}$ values, indicating that both polar and radical-stabilizing effects influence the n,π^* triplet state. For unsymmetrically substituted benzophenones, the triplet energies were lower than predicted, presumably from merostabilization[110] from substituents that can stabilize charge separation in the free spin system.

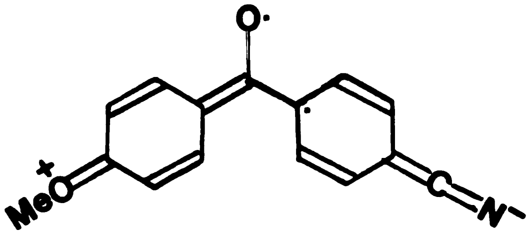

L. Correlation of n,π^* Triplet Energies with Reduction Potentials

In 1973 Loutfy and Loutfy[92] published a correlation between n,π^* triplet energies and half-wave reduction potentials for substituted acetophenones. Also, similar correlations were published for substituted benzophenones[89b] and thiophenes.[97] Since the n-orbital is orthogonal to the π-system, substitution of a group into the phenyl ring would not affect the energy of the n-orbital but would affect the energies of both the π and π^* levels.[104] Loutfy maintains that p-cyanoacetophenone has a lowest n,π^* triplet, since it lies on the line

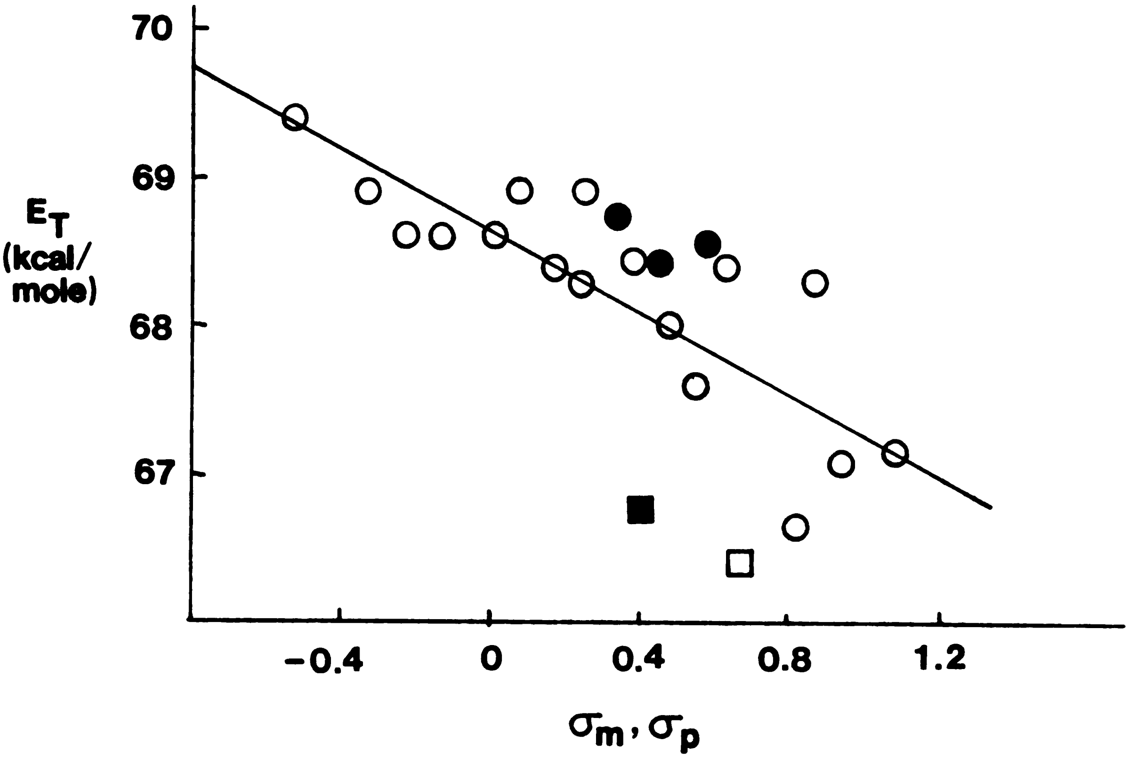

Figure 30. Correlation of n,π^* Triplet Energies (4:1 MCH/IP, 77°K of Substituted Benzophenones with Hammett Parameters.[89a] □ , ■ (-R) Substituents;●,■ Values Added From This Study.

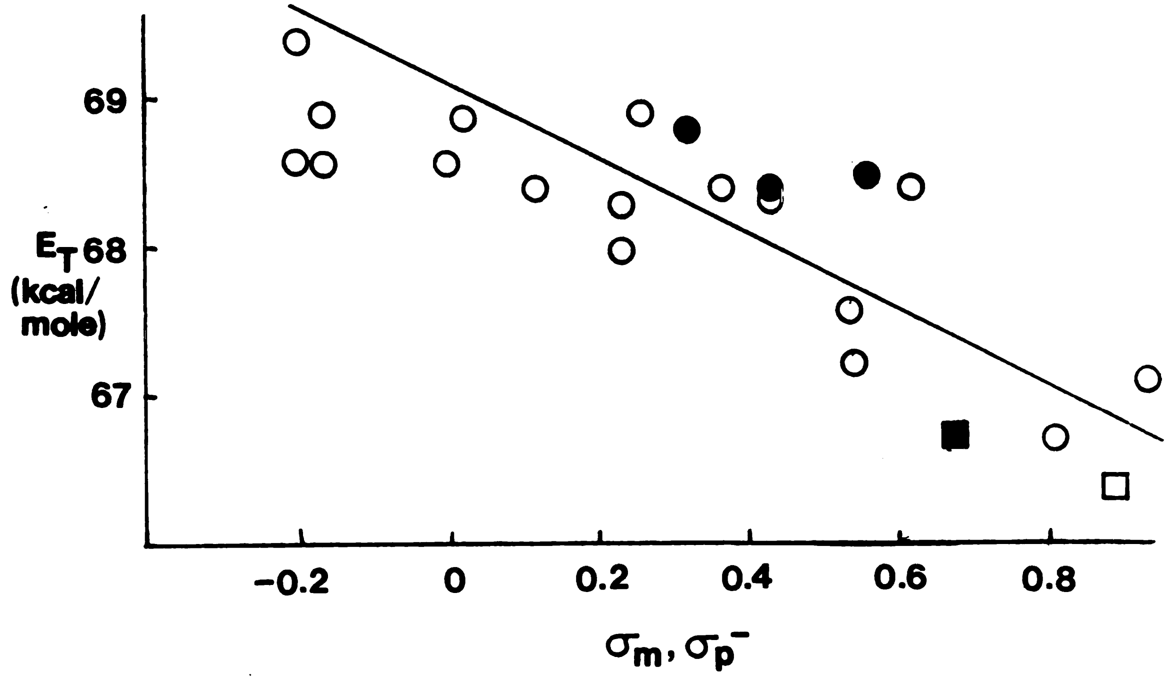

Figure 31. Correlation of n,π^* Triplet Energies (4:1 MCH/IP, 77°K) of Substituted Benzophenones with Hammett Parameters: □ ,■ (-R) Substituents;○, □ Values Taken From Ref. 89a.

formed by -H, p-Cl, p-Br, and p-CF_3 substituted acetophenones. Since the triplet energy for p-cyanoacetophenone was measured in ethanol glass, while the other ketones were measured in 4:1 methylcyclohexane/isopentane glass, we measured the triplet energy for p-cyanoacetophenone in a comparable glass and found it to be only slightly lower (0.5 kcal) than the reported value in ethanol. In contrast, our study involving both spectroscopic and photokinetic data suggests that p-cyanovalerophenone (therefore p-cyanoacetophenone also) has a π,π^* lowest triplet. In order to probe the matter further, a similar correlation was attempted on a wide variety of substituted valerophenones in both a fluid glass (isopentane) and a more rigid and polar glass (ethanol) at 77°K (Figures 32 and 33). It appears that in both isopentane and ethanol glasses, most of the ketones with n,π^* lowest triplets fall on a line and those ketones with π,π^* lowest triplets fall below the line. The most noticeable exceptions are o-CN and m-COC_4H_9 in isopentane glass, since they are predicted to have nearly isoenergetic energy levels by the other methods. In general the energy separations between the n,π^* and π,π^* triplets predicted by this correlation are much larger (isopentane glass) than those previously estimated in benzene at room temperature. Fortunately, the Boltzmann equation (Equation 1) would predict a somewhat larger energy separation at lower temperatures, and also, n,π^* triplets in solution are generally lower by approximately 2 kcal than in rigid glasses due to differences in conformation between the ground state and the excited state.[93] It appears that Loutfy's correlation is at least qualitatively correct in most cases, and gives a rough estimation at best of n,π^* triplet energies.

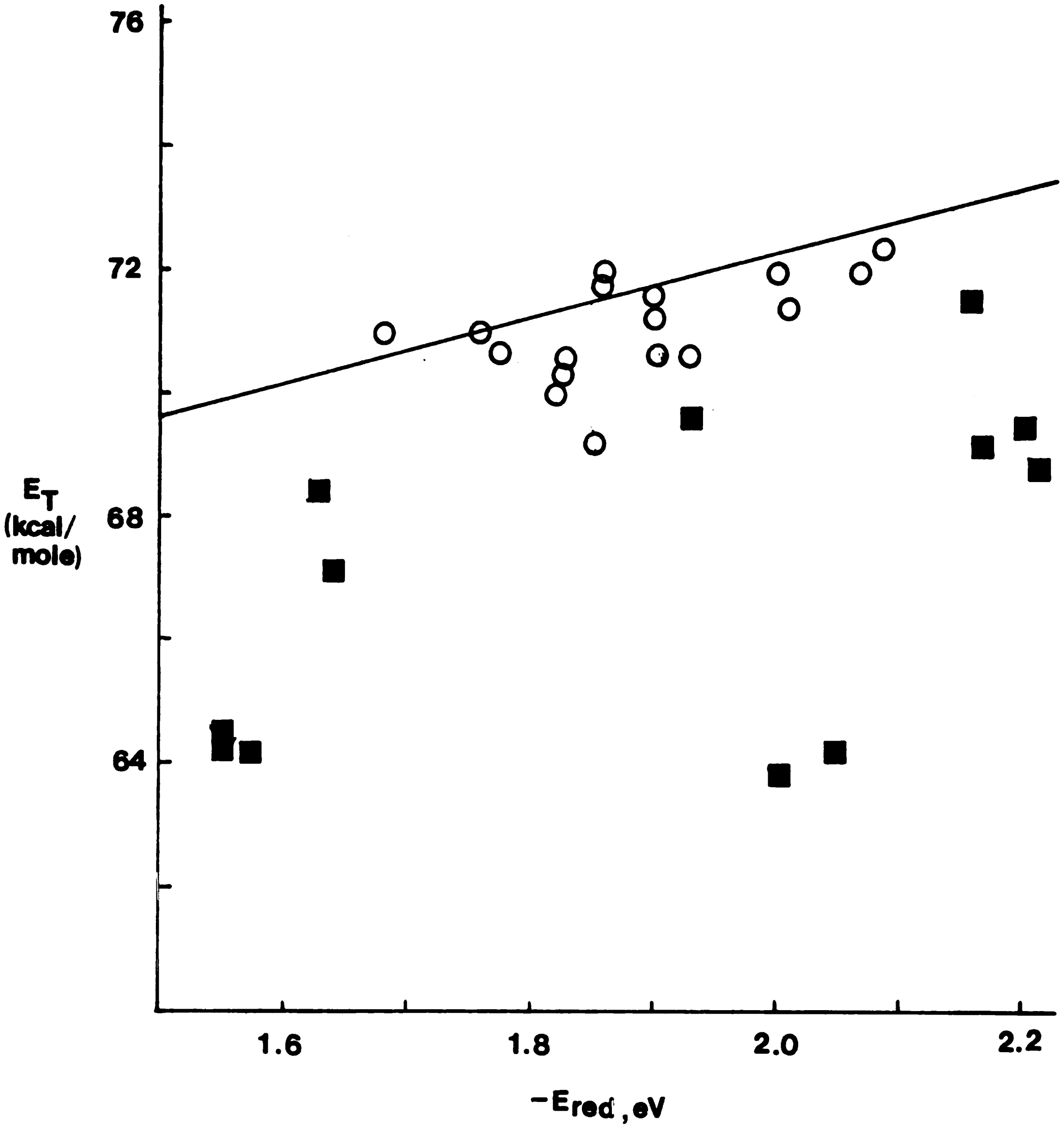

Figure 32. Attempted Correlation of n,π* Triplet Energies (Isopentane, 77°K) with Half-wave Reduction Potentials for Substituted Valerophenones: ○ n,π* Lowest Triplets; □ π,π* Lowest Triplets.

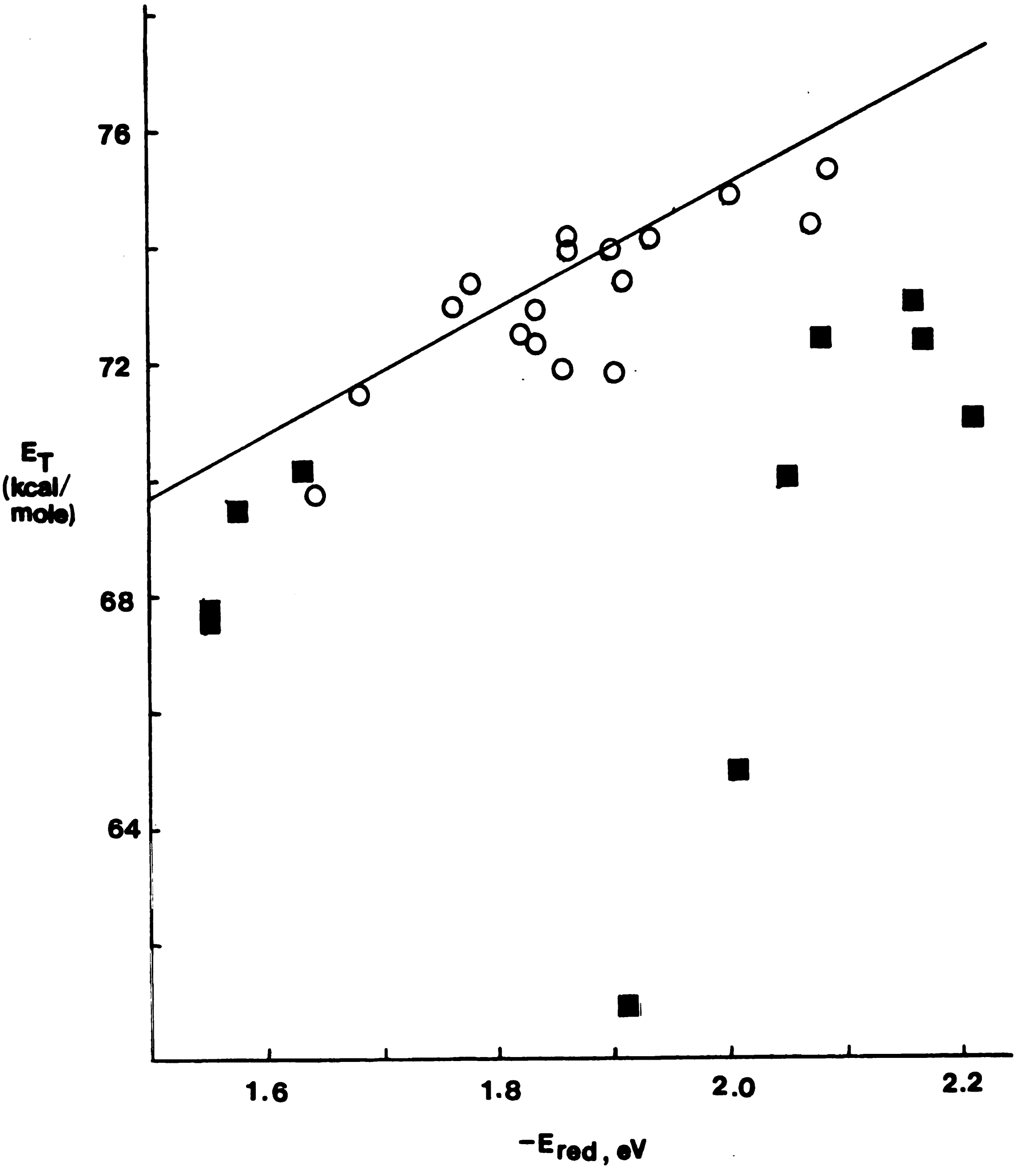

Figure 33. Attempted Correlation of n,π* Triplet Energies (Ethanol, 77°K) with Half-wave Reduction Potentials for Substituted Valerophenones: ○ n,π* Lowest Triplets; ■ π,π* Lowest Triplets.

PART II

REGIOELECTRONIC CONTROL OF INTRAMOLECULAR CHARGE TRANSFER QUENCHING IN VARIOUS PHENYL KETONES

RESULTS

A. Photokinetic Studies

1. Stern-Volmer Quenching Studies

In general 0.01 M ketone solutions containing varying amounts of quencher in benzene or wet acetonitrile (2% H_2O) were irradiated at 313 nm to 5 - 10% conversion (acetophenone photoproduct was measured). A linear correlation was obtained for Stern Volmer quenching plots of $\phi°/\phi$ versus quencher concentration (Figures 34, 35 and 36). The slope is equal to $k_q\tau$, where τ is the triplet lifetime of the ketone. The triplet lifetimes can be calculated, since $k_q = 5 \times 10^9\ M^{-1}s^{-1}$ in benzene[35] and $1 \times 10^{10}\ M^{-1}s^{-1}$ in acetonitrile.[91] Duplicate runs usually agreed to within 10% of each other. Table 12 contains the photokinetic data for the model compounds and Tables 13 and 14 contain the data for the amino-ketones studied. Also, Figure 37 depicts the extrapolation of triplet lifetimes to infinite dilution in order to eliminate intermolecular CT processes (both lines must have similar slopes since intermolecular CT quenching rates are approximately the same).

The phosphorescence lifetimes for the model m- and p-carbomethoxybenzophenones and p-2BB (1×10^{-4} M) were measured by diene quenching of the phosphorescence emission in carbon tetrachloride solution at room temperature (Figures 38 and 39). Also, emission

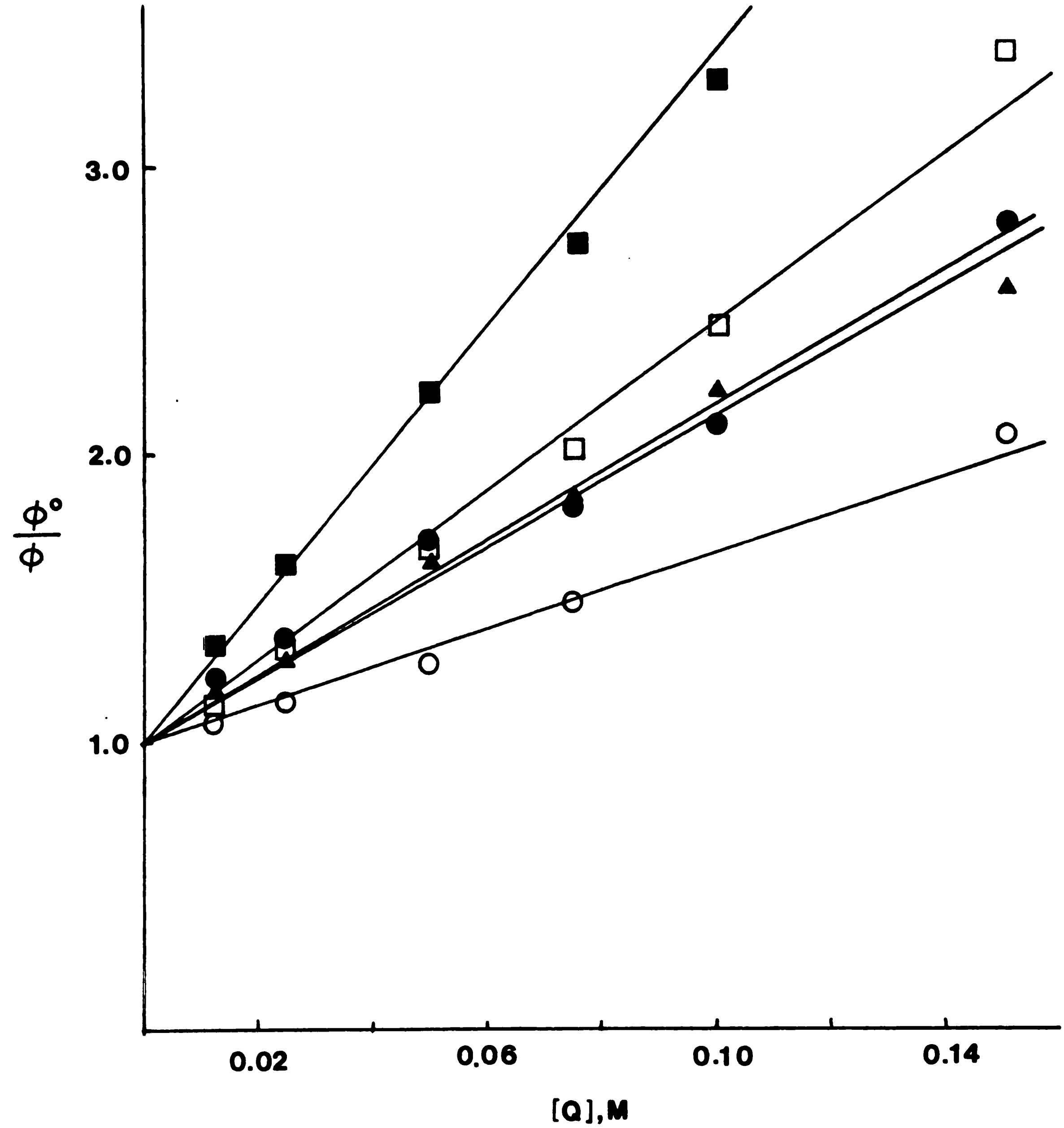

Figure 34. Stern Volmer Plots for Diene Quenching of 0.020 M Ketones: ○ p2VB in Benzene; ● p2VB in Acetonitrile; ▲ p3VB in Acetonitrile; □ m2VB in Benzene; and ■ m2VB in Acetonitrile.

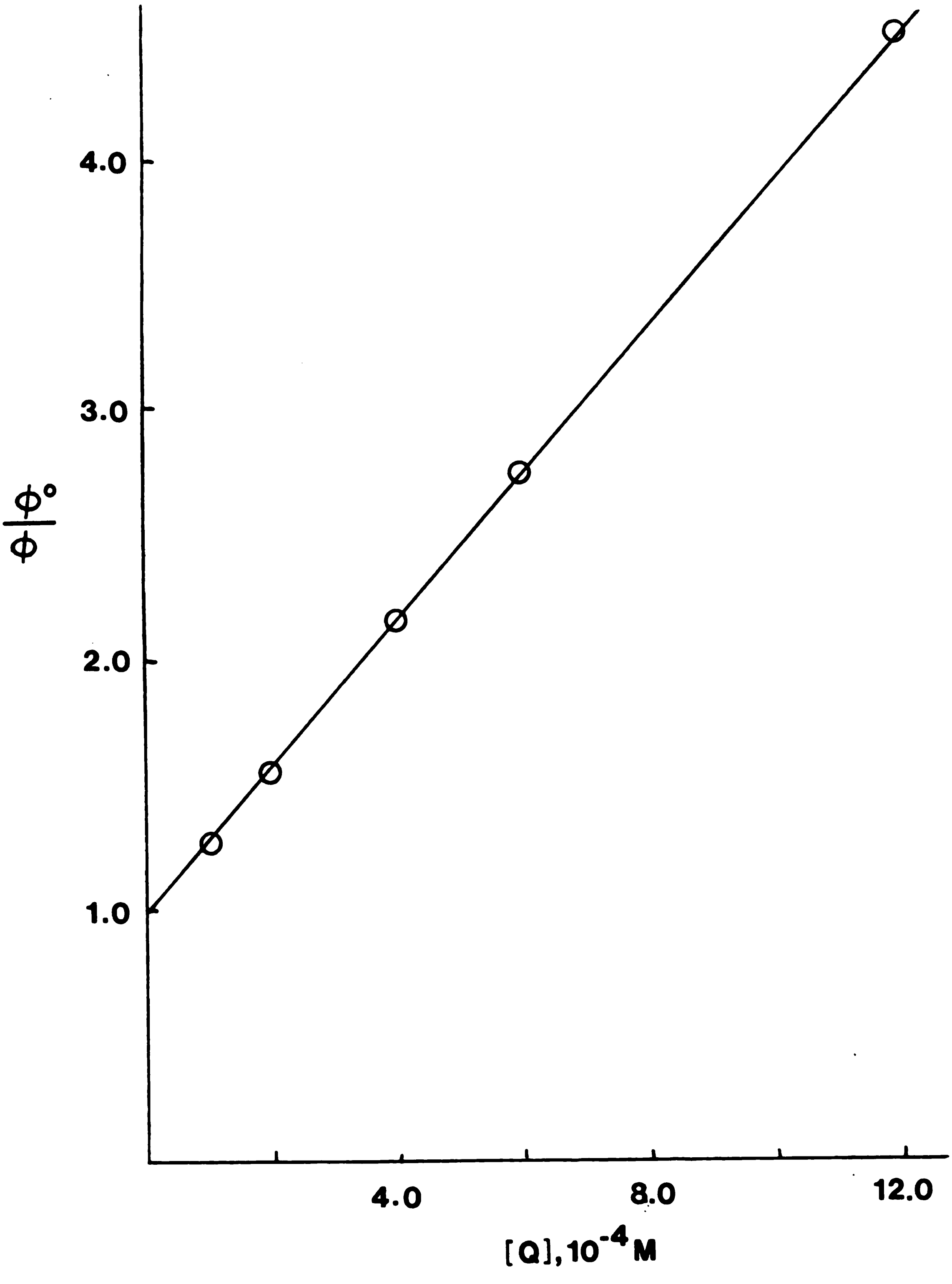

Figure 35. Stern Volmer Plot for Diene Quenching of 0.020 M p3VE in Benzene.

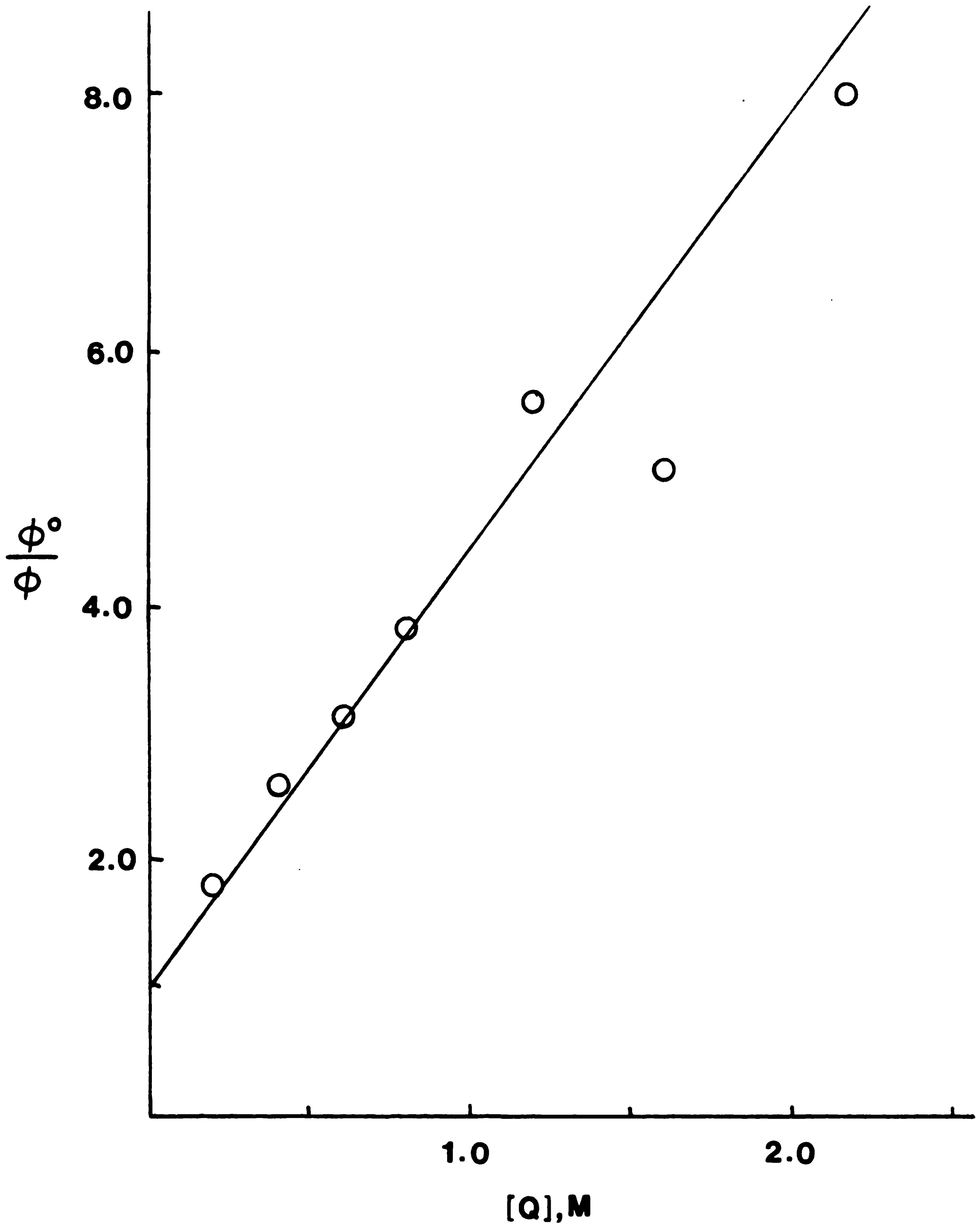

Figure 36. Stern Volmer Plot for Diene Quenching of 0.020 M p-MeO3E in Acetonitrile.

Table 12. Photokinetic Data for Valerophenone Models.[a]

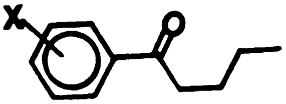

-X	Solvent	Q	Φ_{II}[g]	Φ_{max}	$k_q\tau$
p-CO_2CH_3	Benzene	Diene[b]	0.19	0.33	42±2
p-CO_2CH_3	Benzene[c]	Amine[d]	----	----	32
p-CO_2CH_3	Benzene[c]	Amine[e]	----	----	26
p-CO_2CH_3	Acetonitrile	Diene[b]	0.60	----	58±5
p-CO_2CH_3	Acetonitrile	Amine[d]	----	----	40±0.5
p-CO_2CH_3	Acetonitrile	Amine[e]	----	----	47
m-CO_2CH_3	Benzene	Diene[b]	0.25	----	18±1
m-CO_2CH_3	Acetonitrile	Diene[b]	0.90	----	21±1
m-CO_2CH_3	Acetonitrile	Amine[d]	----	----	8.0
p-OCH_3	Benzene	Diene[b]	0.11	----	4,300±500
p-OCH_3	Benzene[c]	Amine[f]	----	----	∿50[i]
p-OCH_3	Acetonitrile	Diene[b]	0.21	0.26[h]	6,400±400
p-OCH_3	Acetonitrile	Amine[f]	----	----	202

[a] 0.040 M ketone solutions irradiated at 313 nm to ≤ 10% conversion.

[b] 2,5-Dimethylhexa-2,4-diene or 1,3-pentadiene.

[c] 0.50 M Pyridine added.

[d] β-Dimethylaminoethyl benzoate.

[e] γ-Dimethylaminopropyl benzoate.

[f] N,N-Dimethylaminopropyl phenyl ether.

[g] Usually 0.10 M solutions of valerophenone in benzene used as actinometer; formation of acetophenone monitored.

[h] Value from Reference 28.

[i] Value estimated from solvent effects on quenching p-methoxyvalerophenone with triethylamine obtained by Warren B. Mueller.

Table 13. Photokinetic Data for Amino-Esters.[a]

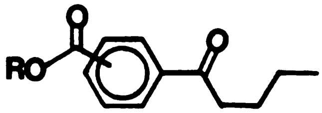

Name	Position	R	Solvent	Φ_∞[b]	$k_q\tau$[c]
p-2VB	para	$-(CH_2)_2N(CH_3)_2$	Benzene[d]	0.07	10.
p-2VB	para	$-(CH_2)_2N(CH_3)_2$	Acetonitrile[e]	0.12	14.9
p-3VB	para	$-(CH_2)_3N(CH_3)_2$	Acetonitrile[e]	0.11	11.8
m-2VB	meta	$-(CH_2)_2N(CH_3)_2$	Benzene	0.15	16.
m-2VB	meta	$-(CH_2)_2N(CH_3)_2$	Acetonitrile[e]	0.31	24.

[a] 0.01 - 0.10 M Ketone in degassed solutions at room temperature.

[b] Quantum yield for acetophenone formation, extrapolated to infinite dilution.

[c] Determined by SV quenching with 1,3-pentadiene, extrapolated to infinite dilution.

[d] 0.40 M Pyridine added.

[e] 2% H_2O added.

Table 14. Photokinetic Data for Amino-Ethers.[a]

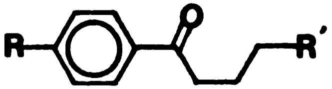

Name	R	R'	Solvent	Φ_∞[b]	$k_q\tau$[c]
p-3VE	$-O(CH_2)_3N(CH_3)_2$	$-CH_3$	Benzene	0.07	3000±100
p-3VE	$-O(CH_2)_3N(CH_3)_2$	$-CH_3$	Acetonitrile	∿0.	150±30[d]
p-MeO3E	$-OCH_3$	$-N(CH_3)_2$	Benzene	0.028[e]	9.3[e]
p-MeO3E	$-OCH_3$	$-N(CH_3)_2$	Acetonitrile	0.030	3.6
3-A	-H	$-N(CH_3)_2$	Benzene	0.025[f]	0.60[f]
3-A	-H	$-N(CH_3)_2$	Acetonitrile	0.050[f]	1.5[f]

[a] 0.02 - 0.03 M Ketone in degassed benzene or wet acetonitrile (2% H_2O) at RT.

[b] Quantum yield for acetophenone formation.

[c] Determined by SV quenching with 1,3-pentadiene.

[d] Value determined by quenching ketone disappearance with 1,3-pentadiene.

[e] Values from reference 111.

[f] Values from Reference 73.

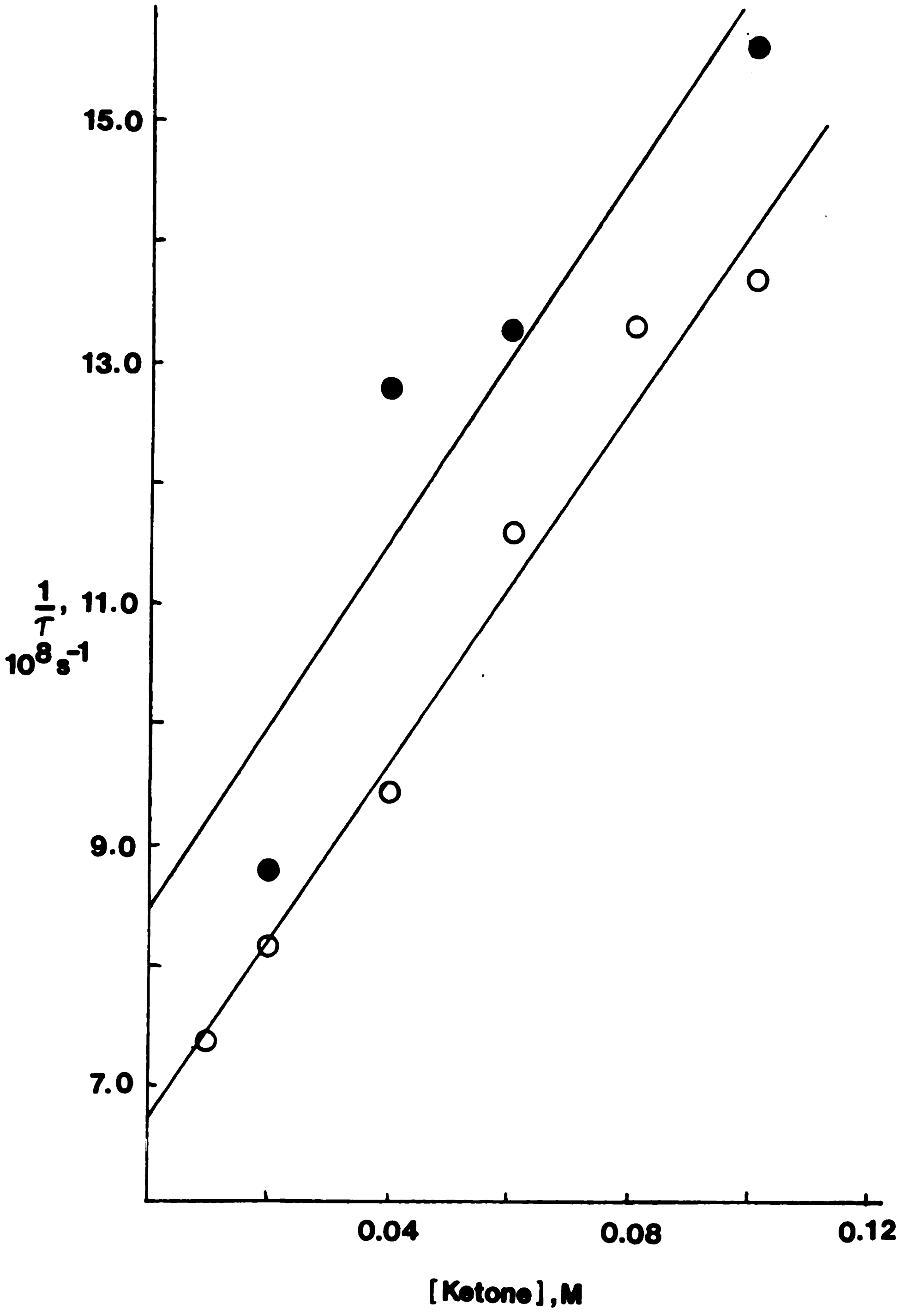

Figure 37. Extrapolation of Triplet Lifetimes of p2VB ○ and p3VB ●
in Acetonitrile.

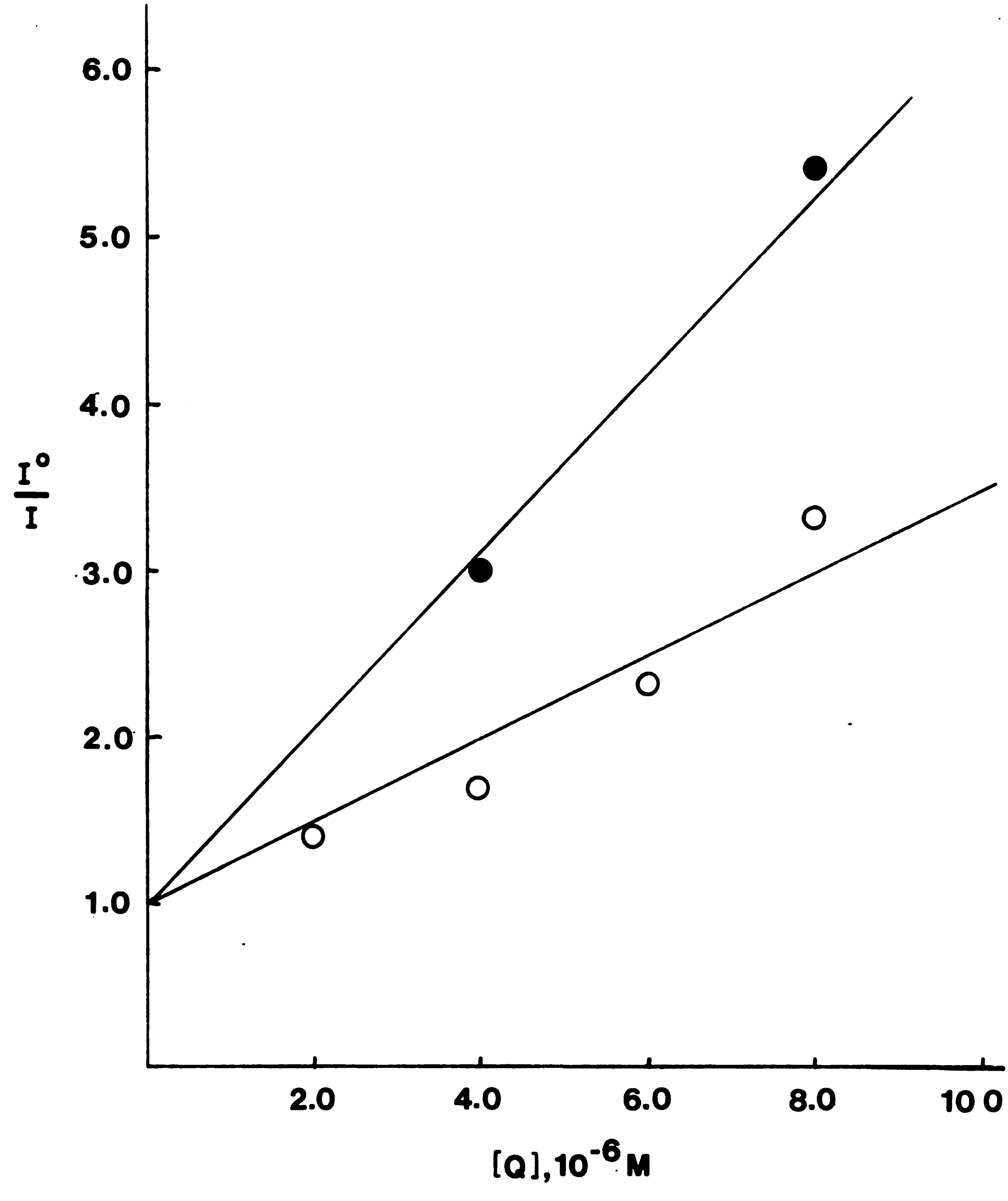

Figure 38. Stern Volmer Plot for Diene Quenching of Room Temperature Phosphorescence of m-Carbomethoxybenzophenone ○ and p-Carbomethoxybenzophenone ● in CCl_4.

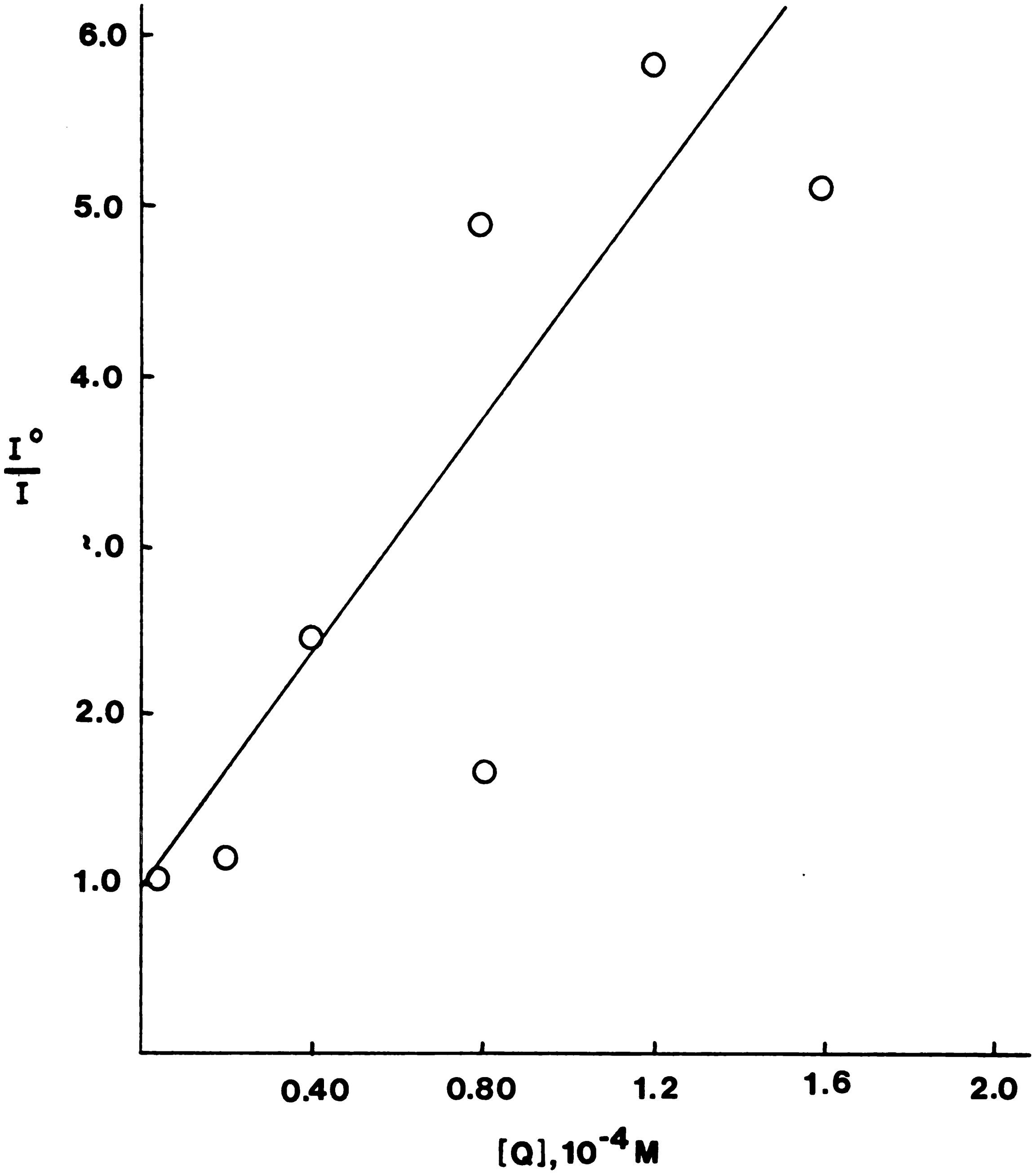

Figure 39. Stern Volmer Plot for Diene Quenching of Room Temperature Phosphorescence of p2BB in CCl_4.

from 1:1 solutions of carbomethoxybenzophenone and the model N,N-dimethylaminoethylbenzoate quencher were measured and compared to the emission from an equimolar amount of the amino-ketones in order to obtain an estimate of self-quenching by the amino-ketones. The results are summarized in Table 15. As a comparison, the rate of quenching of butyrophenone by both 2,5-dimethylhexa-2,4-diene and triethylamine in carbon tetrachloride was measured (Figure 40).

2. Quantum Yields

Quantum yields for acetophenone formation were determined by parallel irradiation at 313 nm of 0.01 - 0.10 M ketone solutions and 0.10 M valerophenone actinometer in a merry-go-round apparatus.[13] All samples were adequately degassed prior to irradiation and conversion was usually kept below 10%. In most cases both the ketone solution and the actinometer absorbed all the incident irradiation; in those cases (low ketone concentration) where some of the light was transmitted, then suitable corrections were made. The values are included in Tables 12-14 and the extrapolation of quantum yields to infinite dilution for p-2VB and p-3VB and for m-2VB in acetonitrile are shown in Figures 41 and 42.

3. Disappearance Quantum Yields

Disappearance quantum yields determined for p-2VB and p-2AB were extrapolated to infinite dilution (Figure 43) in order to determine whether the Norrish Type II photoelimination is the major

Table 15. Phosphorescence Data for Substituted Benzophenones.[a]

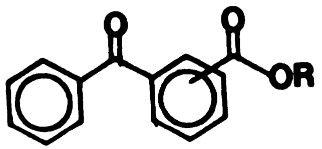

Name	Position	R	$\lambda_{0,0}$ (nm)	Φ_p^{rel}	$k_q\tau$, 10^5	$1/\tau$, 10^5 s^{-1}
	para	$-CH_3$	437	1.	5.2[c]	0.08
p-2BB	para	$-CH_2CH_2N(CH_3)_2$	440	0.08	0.35	1.3
	meta	$-CH_3$	426	1.	2.4	0.17
m-2BB	meta	$-CH_2CH_2N(CH_3)_2$	426	0.09	---	∿1.6[d]

[a] Values determined for 1.0×10^{-4} M ketone in degassed CCl_4 solutions at room temperature.

[b] Values determined by quenching with 2,5-dimethylhexa-2,4-diene ($k_q \sim 4 \times 10^9$ M^{-1} s^{-1} in CCl_4, estimated from its viscosity).

[c] Reference 85 reports a 100 μsec lifetime measured by flash spectroscopy.

[d] Value estimated from decrease in quantum yield as compared to model ester.

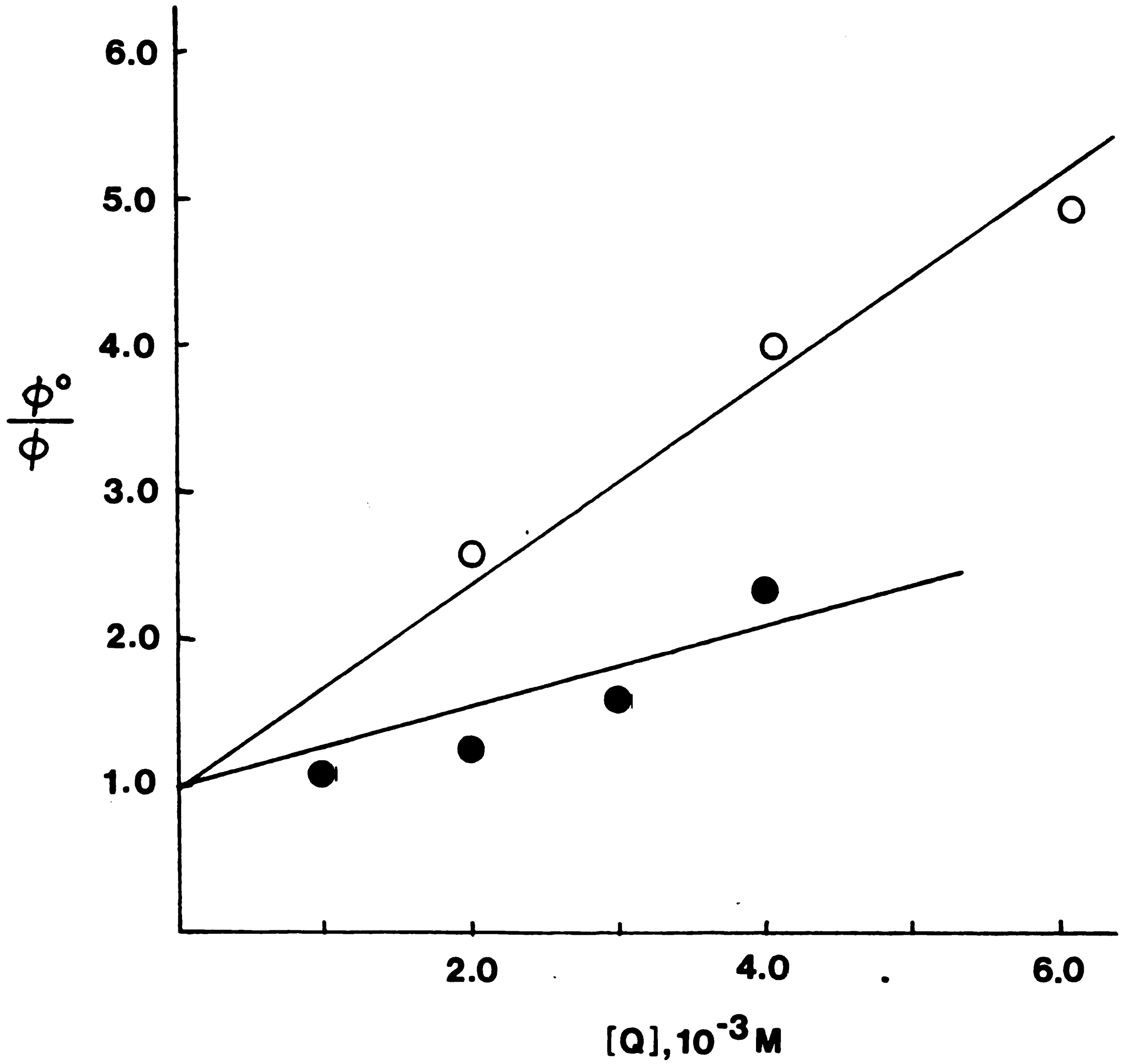

Figure 40. Stern Volmer Plot for 0.040 M Butyrophenone in CCl_4 with Hexadiene Quencher ○ or Triethylamine Quencher ●.

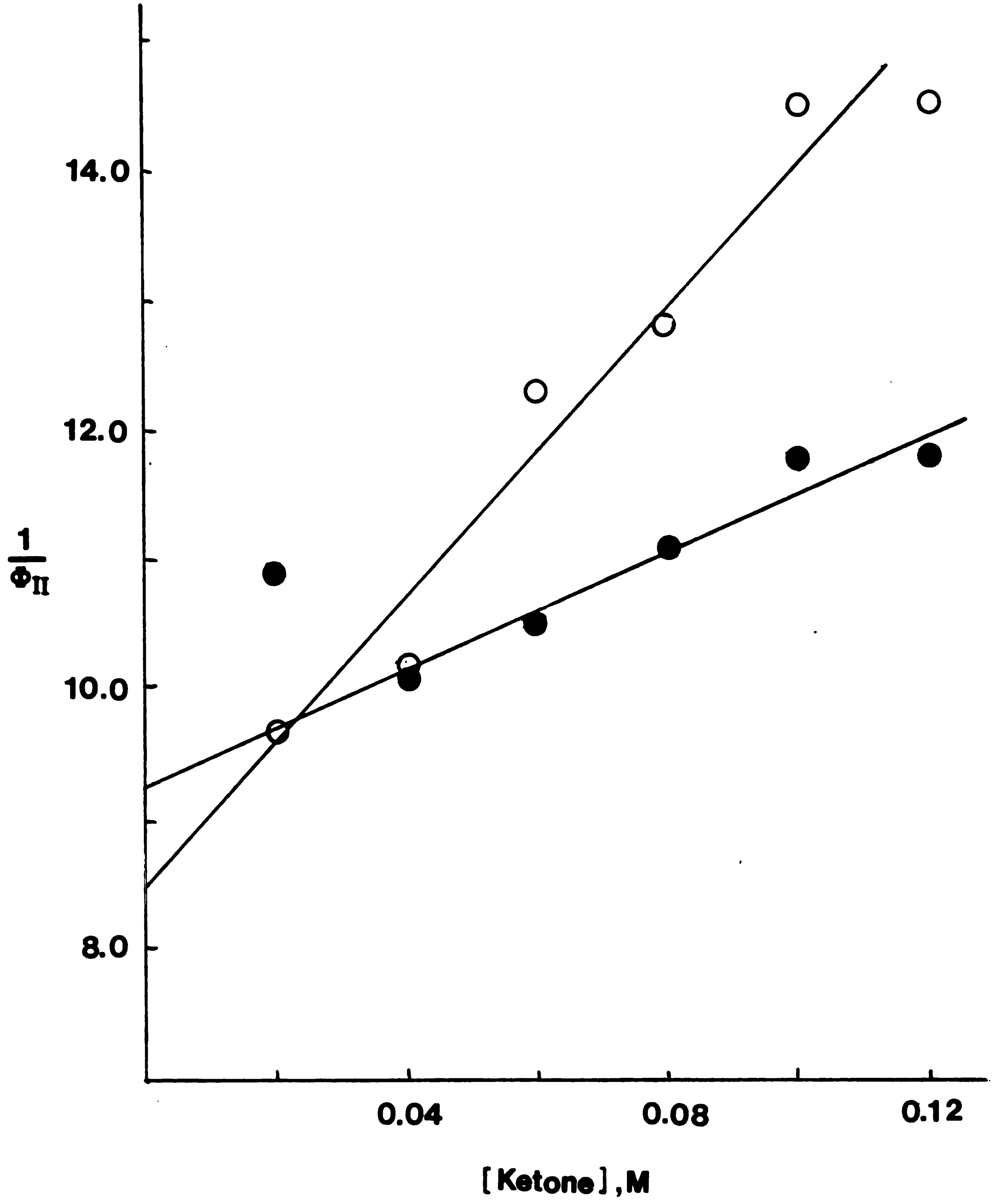

Figure 41. Extrapolation of Φ_{II} for p2VB ○ and p3VB ● in Acetonitrile to Infinite Dilution.

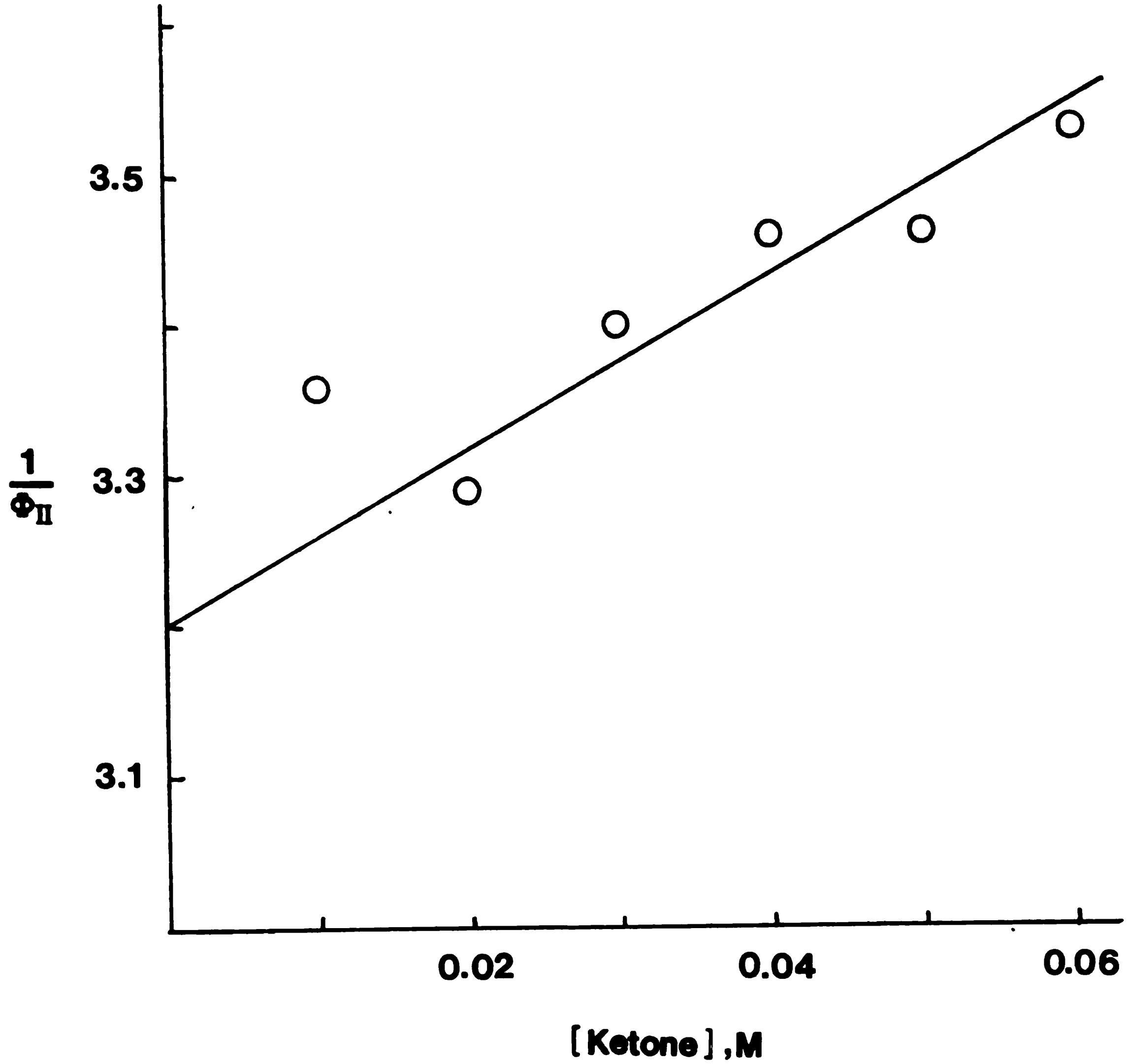

Figure 42. Extrapolation of Φ_{II} for m2VB in Acetonitrile to Infinite Dilution.

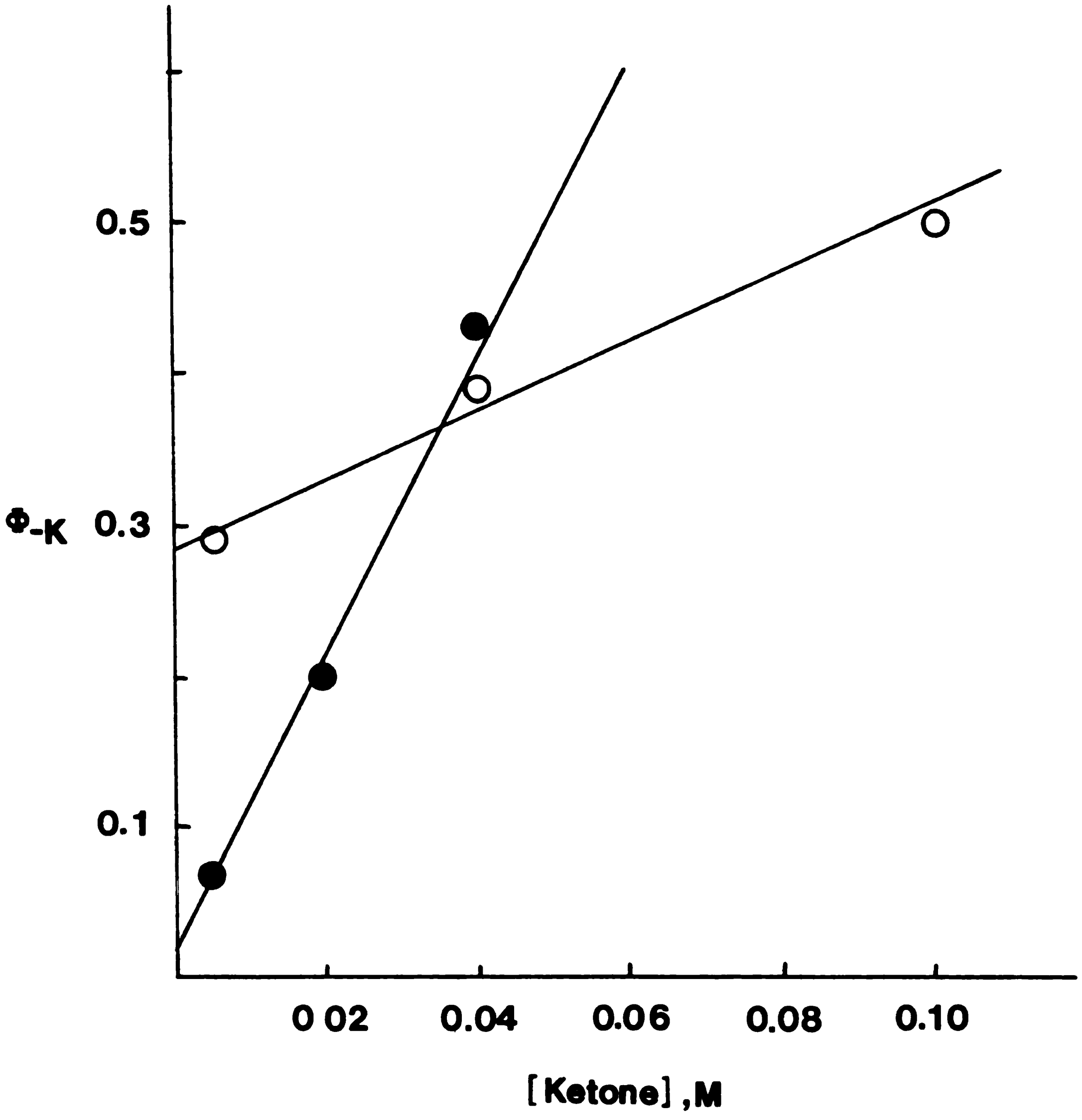

Figure 43. Extrapolation of Φ_{-K} for p2VB ○ and p2AB ● in Acetonitrile to Infinite Dilution.

source of ketone disappearance or if charge transfer processes (both intramolecular and intermolecular) efficiently lead to product formation. The errors involved are fairly large, but accurate enough for this purpose. The ketones were usually photolyzed to greater than 20% conversion.

DISCUSSION

A. Bifunctional Molecules

The study of bifunctional molecules enables one to limit the number of conformations in which the donor and acceptor orbitals overlap. In order to investigate the effect of triplet state electronic configuration on CT quenching, the following system was chosen for study, since both m-2VB and p-2BB have n,π* lowest

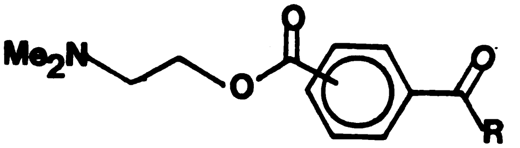

R = n-C_4H_9 (2-VB)

R = Ph (2-BB)

triplets, while p-2VB has a π,π* lowest triplet. Identical conformational restraints are present in both p-2VB and p-2BB.

Another interesting system includes the following amino-ethers

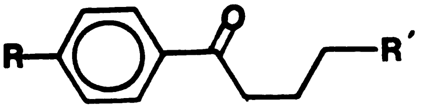

R = OMe, R' = NMe_2(p-MeO3E)

R = $O(CH_2)_3NMe_2$, R'=CH_3(p-3VB)

in which the only significant difference involves the different approach of the donor to the acceptor orbital. Both compounds possess identical energetic parameters, including a π,π* lowest triplet.

The following kinetic expression holds for these bifunctional

$$1/\tau = k_r + k_d + k_{CT\ intra} + k_{CT\ inter} \cdot [\text{Ketone}] \qquad (16)$$

molecules since the triplet lifetime, τ, is dependent on the rate constant for hydrogen abstraction, k_r, the rate constant for radiationless decay, k_d, the rate constant for intramolecular charge transfer quenching, $k_{CT\ intra}$, and the bimolecular rate constant for charge transfer quenching, $k_{CT\ inter}$. The sum of k_d and k_r can be obtained from the triplet lifetimes of the model carbomethoxy ketones and estimates for amino-ketone self-quenching rates can be obtained by quenching the carbomethoxy models with suitable tertiary amines. Extrapolation of triplet lifetimes to infinite dilution eliminates any intermolecular CT quenching by the amino-ketone and simplifies the kinetic expression.

$$1/\tau^\circ = k_r + k_d + k_{CT\ intra} \qquad (17)$$

Thus, the rates of intramolecular CT quenching in bifunctional molecules can readily be determined.

B. Amino-Esters

Winnik et al.[84,85] have studied the intramolecular CT quenching of benzophenone emission by alkenes in the following system

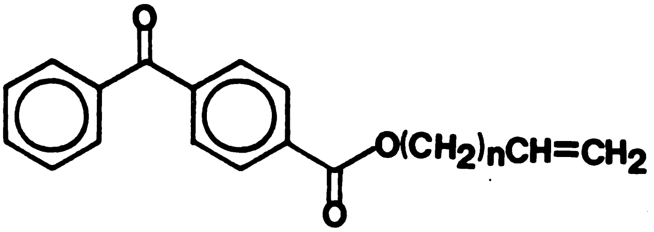

and observed no intramolecular charge transfer quenching when $n < 9$. For short methylene chains the double bond can come into contact with the phenyl ring, but cannot approach the carbonyl moiety. Thus, the lack of CT quenching in these compounds suggests that the electron-deficiency in the n,π^* excited benzophenone must be located on the carbonyl n-orbital.

Since tertiary amines are better donors than alkenes,[64a] the analogously substituted benzophenones would provide better evidence for the localization of excitation energy on the carbonyl in n,π^* triplets. Table 15 contains the phosphorescence data in carbon

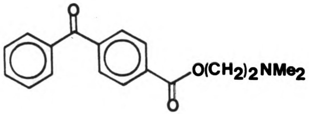

tetrachloride for p-2BB and m-2BB, as well as the data for the model p- and m-carbomethoxybenzophenones. The triplet lifetimes were measured by diene quenching of phosphorescence emission. p-2BB has a shorter triplet lifetime than the model p-carbomethoxybenzophenone (τ_p = 8 μsec and 130 μsec, respectively) and the decrease in lifetime is paralleled by a decrease in emission intensity. The triplet lifetime of m-carbomethoxybenzophenone measured was 0.6 μsec and the triplet lifetime of m-2BB, as determined by comparison of emission intensities of equimolar solutions of m-2BB and model ester, is 0.05 μsec. The rates of intermolecular CT quenching in carbon tetrachloride were determined by comparing the emission of the model compounds containing equimolar amounts of γ-dimethylaminoethyl benzoate with the emission from equimolar amounts of p-2BB or m-2BB. The values for bimolecular CT quenching for the para- and meta-amino-ketones are 3×10^7 $M^{-1}s^{-1}$ and 2×10^8 $M^{-1}s^{-1}$, respectively. These values are somewhat lower than the value one would predict on the basis that triethylamine quenches triplet butyrophenone at a slightly faster rate in carbon tetrachloride (1.6×10^9 $M^{-1}s^{-1}$) than in benzene (1.2×10^9 $M^{-1}s^{-1}$). In any case, the rate of intramolecular CT quenching is $\sim 1 \times 10^5$ s^{-1} which is 10^2-10^3 times slower than the rate for intermolecular CT quenching in carbon tetrachloride. Thus, the low rates of intramolecular CT quenching by the amine moiety in these short chain compounds support Winnik's results with the alkenyl moiety,[84,85] suggesting that the excitation of the benzophenone n,π* triplet is localized on the carbonyl moiety.

Unfortunately, since the aminobenzophenones react with trace impurities in the carbon tetrachloride or with the solvent itself to form quaternary ammonium salts (isolated and identified by NMR) upon standing, it was necessary to establish the amount of free amine in solution when the experiments were conducted. A FT-250 MHz NMR of 1.0×10^{-4} M p-2BB in carbon tetrachloride pulsed for 4 hours showed only a 15% decrease in free amine as compared to a tetrachloroethane standard. This result would imply no more than a 30% decrease in free amine over a 4 to 4-1/2 hour period, since a time-average value was obtained. Thus, within the time frame of these experiments, only a small percentage of the free amine became protonated. Also, the quaternary ammonium salt was not sufficiently soluble in the carbon tetrachloride solution to be detected in the NMR spectrum and a blank of the HCl salt of p-2BB in carbon tetrachloride showed no appreciable room temperature phosphorescence. The lifetime of the quarternary salt would be expected to be similar to the carbomethoxybenzophenone models, since the lone pair on the nitrogen atom is no longer available for CT quenching interactions. Thus, it was concluded that the observed phosphorescence emission was indeed from the free amine. Other solvents such as acetonitrile, benzene, heptane, methylene chloride, t-butyl alcohol, distilled water, and chlorobenzene also had been tried, but solvent emission prevented detection of ketone phosphorescence. Further studies to determine the triplet lifetimes of the aminobenzophenones in acetonitrile will be undertaken in this group.

Table 17 contains the Type II quantum yields, triplet lifetimes extrapolated to infinite dilution, and the rate constants for γ-hydrogen abstraction and intramolecular CT quenching for the aminoesters p-2VB, m-2VB, and p-3VB. Both p-2VB and p-3VB show rapid intramolecular CT quenching ($k_{CT\ intra} = 5.1 \times 10^8\ s^{-1}$ and $6.6 \times 10^8\ s^{-1}$, respectively, in acetonitrile), while m-2VB shows negligible intramolecular CT quenching. Also, p-2VB undergoes rapid intramolecular CT quenching ($k_{CT\ intra} = 3.8 \times 10^8\ s^{-1}$) in benzene, while the meta isomer does not. The low quantum yields for the para amino-ketones reflect the intramolecular CT quenching, but the reason for the low quantum yield for m-2VB is not fully understood.

Table 16. Charge Transfer Quenching Data for Valerophenone Models.[a]

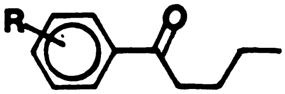

R	Solvent	$k_H, 10^7 s^{-1}$ [b]	k_{CT} inter' 10^8 $M^{-1}s^{-1}$
p-CO_2CH_3	Benzene	12.	38.[d]
p-CO_2CH_3	Benzene	12.	31.[e]
p-CO_2CH_3	Acetonitrile	17.	69.[d]
p-CO_2CH_3	Acetonitrile	17.	81.[e]
m-CO_2CH_3	Benzene	28.	---
m-CO_2CH_3	Acetonitrile	48.	38.[d]
p-OCH_3	Benzene	0.12	0.6[f]
p-OCH_3	Acetonitrile	0.16	3.2[g]

[a] 0.040 M Ketone in degassed benzene or wet acetonitrile (2% H_2O) solution.

[b] Determined by SV quenching with 1,3-pentadiene.

[c] Determined by SV quenching with various tertiary amines.

[d] β-Dimethylaminoethyl benzoate quencher.

[e] γ-Dimethylaminopropyl benzoate quencher.

[f] Estimated from solvent effects on quenching of p-methoxyvalerophenone with triethylamine obtained by Warren B. Mueller.

[g] N,N-Dimethylaminopropyl phenyl ether quencher.

Long alkyl chains are known to lessen the efficiency of product formation from the intermediate biradicals[112] and could partially explain the lower quantum yields. From the kinetic and spectroscopic studies presented in Part I, it was concluded that p-carbomethoxyvalerophenone has nearly isoenergetic triplet states. Assuming a Boltzmann population, the π,π^* and n,π^* triplets are nearly equally populated in p-carbomethoxyvalerophenone, and analogously, in p-2VB. Thus, one would estimate the rate for intramolecular CT quenching of the π,π^* triplet in these amino-esters as $\sim 1 \times 10^9$ s^{-1} in acetonitrile.

Since both carbomethoxyvalerophenones and carbomethoxybenzophenones have similar excited state reduction potentials (Table 19), these results seem to support the idea that excitation of the n,π^* triplet is localized primarily on the carbonyl, while excitation of the π,π^* triplet lies primarily on the benzene ring (Scheme 5).

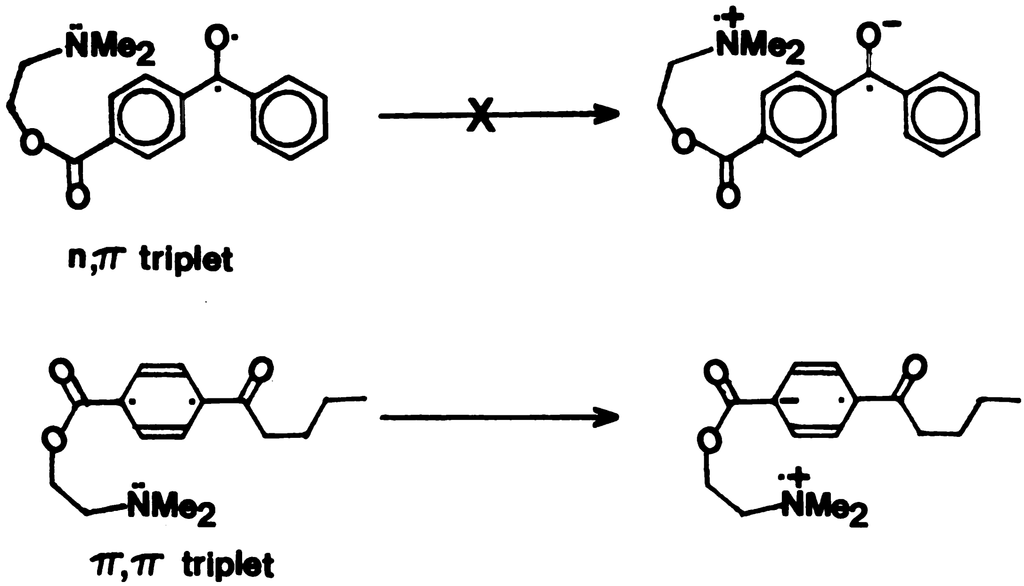

Scheme 5. Valence Bond Representations of p-2BB and p-2VB.

Table 17. Charge Transfer Quenching Data for Amino-Esters.[a]

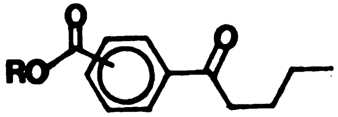

Name	Position	R	Solvent	Φ_{II}[b]	$1/\tau$, $10^8\ s^{-1}$[c]	k_H, $10^8\ s^{-1}$	$k_{CT\ intra}$, $10^8\ s^{-1}$
	para	$-CH_3$	Benzene	0.19	1.2	1.2	---
	para	$-CH_3$	Acetonitrile	0.60	1.7	1.7	---
p-2VB	para	$-(CH_2)_2N(CH_3)_2$	Benzene	0.07	5.0	1.2	3.8
p-2VB	para	$-(CH_2)_2N(CH_3)_2$	Acetonitrile	0.13	6.7	1.7	5.1
p-3VB	para	$-(CH_2)_3N(CH_3)_2$	Acetonitrile	0.11	8.5	1.7	6.9
	meta	$-CH_3$	Benzene	0.25	2.8	2.8	---
	meta	$-CH_3$	Acetonitrile	0.90	4.8	4.8	---
m-2VB	meta	$-(CH_2)_2N(CH_3)_2$	Benzene	0.15	3.1	2.8	---
m-2VB	meta	$-(CH_2)_2N(CH_3)_2$	Acetonitrile	0.32	4.2	4.2	---

[a] 0.01-0.10 M Ketone in degassed benzene or wet acetonitrile (2% H_2O) solutions at RT. [b] Quantum yield for acetophenone formation, extrapolated to infinite dilution. [c] Determined by SV quenching with 1,3-pentadiene, extrapolated to infinite dilution.

Since the para-valeryl amines undergo rapid internal and external CT quenching, it was necessary to determine whether CT quenching leads to product formation. The disappearance quantum yields for p-2VB and p-2AB (the acetophenone analogue) were measured and extrapolated to infinite dilution (Figure 42). At 0.040 M ketone Φ_{-K} = 0.39 and 0.43 for p-2VB and p-2AB, respectively, while at infinite dilution, Φ_{-K} = 0.28 and 0.02, respectively. Since Φ_{II} = 0.13 for p-2VB at infinite dilution and relatively large errors are involved in the measurement of disappearance quantum yields, then one can assume that intramolecular CT quenching leads to little, if any, nonvolatile photoproduct formation. This result is expected since the hydrogens α to the nitrogen are unavailable for intramolecular abstraction by the radical anion.

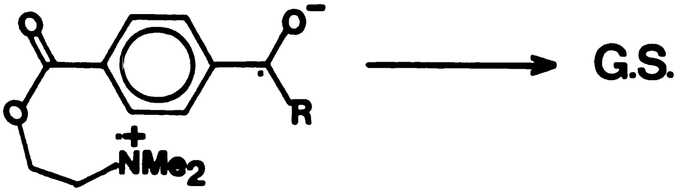

Thus, intermolecular CT interactions must lead to photoreduction products by α-hydrogen abstraction[60] and subsequent radical-coupling to give nonvolatile photoproducts.

C. Amino-Ethers

In order to determine the generality of these results, the following amino-ethers were investigated and the results are

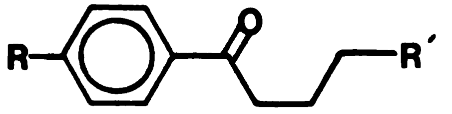

R=$O(CH_2)_3N(CH_3)_2$, R'=CH_3(p-3VB)
R= OCH_3,   R'=$N(CH_3)_2$(p-MeO3E)

presented in Table 14. In both acetonitrile and benzene solvents, p-MeO3E undergoes rapid intramolecular CT quenching ($k_{CT\ intra}$ = 2.8×10^9 s^{-1} and 5.4×10^8 s^{-1}, respectively) as compared to intermolecular CT quenching rates of 3×10^8 and 6×10^7 in acetonitrile and benzene. Conversely, p-3VE undergoes CT quenching with a rate constant of 6×10^7 s^{-1} in acetonitrile and only $\leq 1 \times 10^4$ s^{-1} in benzene, compared to rate constants for intermolecular CT quenching of 3×10^8 s^{-1} and 6×10^7 s^{-1}, respectively. The major differences between the two compounds involves the approach of the donor electron pair to the acceptor orbital, and the charge separation involved in the excited state.

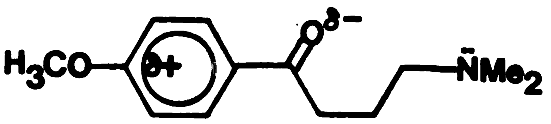

vs.

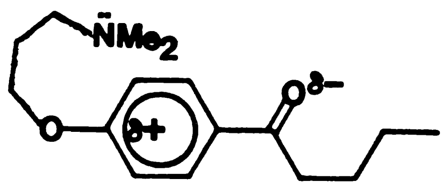

p-MeO3E

p-3VE

One would expect a polar solvent such as acetonitrile to stabilize these charge separated forms. In the case of p-MeO3E, such charge separation would not be expected to significantly increase the rate of intramolecular CT quenching, since the nitrogen lone pair does not have access to the positively-polarized portion of the phenyl

Table 18. Charge Transfer Quenching Data for Amino-Ethers.[a]

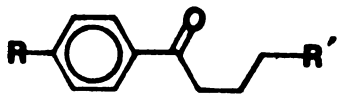

Name	R	R'	Solvent	Φ_{II}[b]	$1/\tau$, 10^6 s^{-1}[c]	k_H, 10^6	inter k_{CT}, 10^6	intra k_{CT}, 10^6
	$-OCH_3$	$-CH_3$	Benzene	0.11	1.2	1.2	----	----
	$-OCH_3$	$-CH_3$	Acetonitrile	0.21	1.6	1.6	----	----
p-3VE	$-O(CH_2)_3N(CH_3)_2$	$-CH_3$	Benzene	0.07	1.7	1.2	∿1.3	<0.01
p-3VE	$-O(CH_2)_3N(CH_3)_2$	$-CH_3$	Acetonitrile	∿0.	67.[e]	1.6	6.4	59.
p-MeO3E	$-OCH_3$	$-N(CH_3)_2$	Benzene	0.028[f]	540.[f]	1.2	∿1.9	537.
p-MeO3E	$-OCH_3$	$-N(CH_3)_2$	Acetonitrile	0.030	2800.	1.2	6.4	2800.
3-A	-H	$-N(CH_3)_2$	Benzene	0.025[g]	8300.[g]	110.		8000.
3-A	-H	$-N(CH_3)_2$	Acetonitrile	0.050[g]	6700.[g]	160.		6500.

[a] 0.02-0.03 M Ketone is degassed benzene or wet acetonitrile solution (2% H_2O) solution at RT.

[b] Quantum yield for acetophenone formation.

[c] Values determined by SV quenching with 1,3-pentadiene.

[d] Value calculated from ketone concentration and k_{SQ} determined by quenching experiments on models.

[e] Value determined by quenching ketone disappearance with 1,3-pentadiene.

[f] Values taken from Reference 111.

[g] Values taken from Reference 73.

ring. Thus, one would expect the normal polar solvent effects on the rate of intramolecular charge transfer quenching, as indicated by bimolecular CT quenching of p-methoxyvalerophenone (Table 16). Both the intermolecular CT quenching of p-methoxyvalerophenone and the intramolecular CT quenching of p-MeO3E show a 5-fold increase in acetonitrile as compared to benzene. On the other hand, the nitrogen lone pair in p-3VE can come into contact with the electron-deficient portion of the phenyl ring, and one would predict rapid intramolecular CT quenching in acetonitrile. A 10^3-fold increase in intramolecular CT quenching for p-3VE was observed in acetonitrile as compared to benzene.

D. Summary of Charge Transfer Quenching Results

Table 19 summarizes the rate constants for CT quenching of amino-ketones. Since tertiary amines have oxidation potentials of approximately 34 kcal/mole[113] these CT interactions are either slightly endothermic or thermoneutral. The rapid intramolecular CT quenching of both γ-dimethylaminobutyrophenone (3-A)[73] and p-MeO3E[111] demonstrates the ready access of the amine lone pair to the electron "hole" in the n,π^* and π,π^* triplets, respectively. The slower rate of intramolecular CT quenching in p-3VE as compared to p-MeO3E in benzene is hard to explain, except on conformational factors, while the large increase in the intramolecular CT quenching rate of p-3VE in acetonitrile as compared to benzene is probably due to charge separation in the excited π,π^* triplet state. Charge transfer quenching is thermodynamically favorable for the amino-esters and both

Table 19: Summary of Charge Transfer Quenching Results.

Ketone	Lowest Triplet	$-E_{red}^{*b}$	k_{CT}, intra s^{-1} ^{c}	k_{CT}, inter $M^{-1}s^{-1d}$
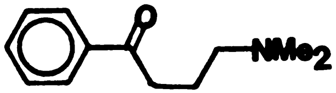 3-A	n,π*	25.7 (27.8)^{e}	8×10^{9} ^{h,i} 7×10^{9} ^{i,j}	1×10^{9} ^{h,m} 2×10^{9} ^{j,m}
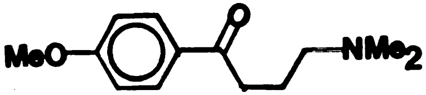 p-MeO3E	π,π*	21.1 (23.9)^{e}	5×10^{8} ^{h} 3×10^{9} ^{j}	6×10^{7} ^{h,m} 3×10^{8} ^{j}
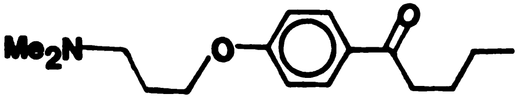 p-3VE	π,π*	21.1 (23.9)^{e}	10^{4} ^{h} 6×10^{7} ^{j}	6×10^{7} ^{h} 3×10^{8} ^{j}
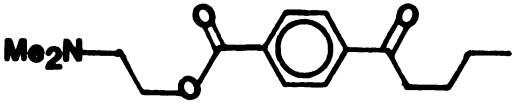 p-2VB	π,π*	32.8 (34.0)^{e}	4×10^{8} ^{h} 5×10^{8} ^{j}	4×10^{9} ^{h} 7×10^{9} ^{j}

Table 19. Continued.

Ketone	Lowest Triplet	$-E_{red}^{*b}$	$k_{CT, intra}$ $s^{-1\,c}$	$k_{CT, inter}$ $M^{-1}s^{-1\,d}$
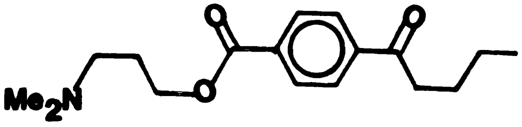 p-3VB	π,π^*	32.8 (34.0)^e	7×10^8 j	8×10^9 j
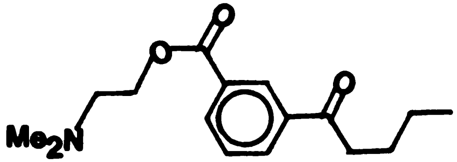 m-2VB	n,π^*	29.8 (30.7)^e	$\leq 10^6$ h $\leq 10^6$ j	$\sim 3 \times 10^9$ h 4×10^9 j
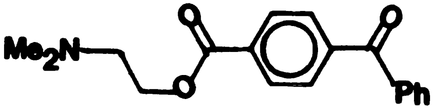 p-2BB	n,π^*	32.1^f	$\leq 1 \times 10^5$ k	$\geq 10^7$ k
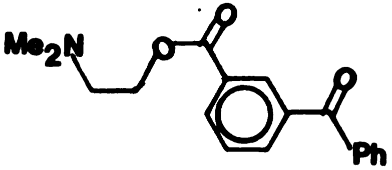 m-2BB	n,π^*	29.4^f	$\leq 1 \times 10^5$ k	$\geq 10^8$ k

Table 19. Continued.

Ketone	Lowest Triplet		k_{CT}, intra s^{-1} [c]	k_{CT}, inter $M^{-1}s^{-1}$ [d]
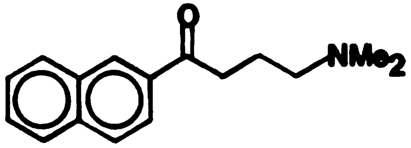 β-3N	π,π*	17.8[g]	1 x 10^5 [g,l]	

[a] Nature of lowest triplet assigned from spectroscopic and photokinetic results on models. [b] Excited state reduction potential of lowest triplet state calculated from the equation $-E_{red}^* = -E_{red} - E_T$ (kcal/mole). [c] Values calculated from Stern Volmer quenching with 1,3-pentadiene. [d] Values determined from Stern Volmer quenching of models with appropriate model tertiary amines. [e] Value in parenthesis is for second triplet state. [f] Reduction potentials for p-CO_2CH_3BP = -1.50 eV (37.6 kcal) and for m-CO_2CH_3BP = -1.71 eV (39.4) compared to -1.83 eV (42.2 kcal) for benzophenone. All values relative to S.C.E. and determined on 10^{-4} M ketone solutions in acetonitrile (0.1 M TEAP). [g] Value taken from Reference 82. [h] Benzene solvent. [i] Value taken from Reference 73. [j] Acetonitrile solvent (2% H_2O). [k] Carbon tetrachloride solvent. [l] Methanol solvent. [m] Values taken from Reference 111.

p-2VB and p-3VB show appreciable intramolecular CT quenching, presumably of the π,π^* triplet, in both benzene and acetonitrile ($k_{CT\ intra} \sim 5 \times 10^8\ s^{-1}$), while m-2VB ($n,\pi^*$ lowest triplet) shows very little if any intramolecular CT quenching ($k_{CT\ intra} \leq 10^6\ s^{-1}$). Since the benzophenone esters have excited state reduction potentials comparable to those of their valeryl analogues and undergo only slow intramolecular CT quenching ($k_{CT} \leq 1 \times 10^5\ s^{-1}$), one can conclude that the n,π^* excitation is localized primarily on the carbonyl. The naphthyl analogue of 3-A (β-3N)[82] shows only slow intramolecular CT quenching in methanol, presumably since the CT interaction is highly endothermic. Thus, although some trends in CT quenching of bifunctional molecules are evident, further research is necessary in order to understand better the conformational factors involved and the differences in CT quenching of n,π^* and π,π^* triplet states.

E. Suggestions for Further Research

1. The methylene chains on both the amino-esters and the amino-ethers could be extended in order to determine the conformational effects on electron donor and acceptor orbital-overlap on CT quenching rates.

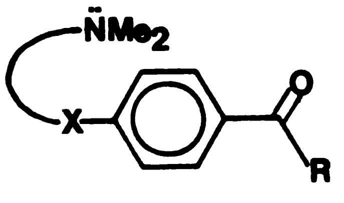

X = O or C=O

R = n-C_4H_9 or ϕ

2. The effects of other electron donors, such as other heteroatoms or alkenes, on intramolecular CT quenching could be studied.

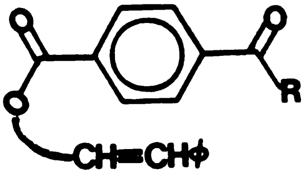

R = n-C_4H_9 or ϕ

3. Intramolecular CT interactions in 3-benzoylpropionate esters could be investigated, since both the nature of the lowest triplet and the excited state reduction potential of the ketone can be varied without affecting the orbital overlap between donor and acceptor moieties.

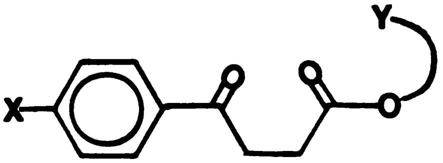

X = H, CF_3, CN, etc.

Y = $N(CH_3)_2$ or CH=CHϕ

4. Solvent effects on intramolecular CT quenching rates in bifunctional molecules could provide interesting results, especially in molecules where charge separation can occur in the excited state.

5. Since Mashuhara's[86] conclusions about internal hydrogen abstraction seem questionable, the following system could be studied.

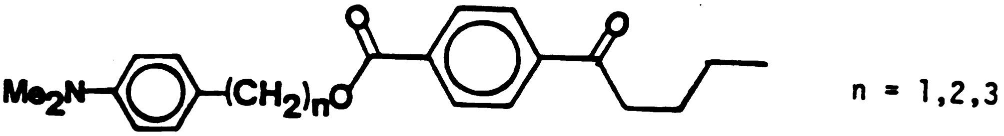

The rate of intramolecular CT quenching can be determined by quenching Type II photoproduct formation and the results compared with those of Mashuhara.

EXPERIMENTAL

A. Preparation and Purification of Chemicals

1. Solvents and Additives

Benzene. One gallon of thiophene-free Mallinckrodt reagent grade benzene was stirred repeatedly over 200 ml portions of concentrated sulfuric acid for 1 day periods until the sulfuric acid no longer discolored. The benzene was washed three times with distilled water, 4-5 times with saturated sodium bicarbonate solution (until a white precipitate no longer formed in the aqueous layer), then 4 times with distilled water, and dried over magnesium sulfate. Phosphorous pentoxide (100 g) was added and the benzene was refluxed overnight and distilled through a one-meter column packed with stainless steel helices at a rate of 100 ml/hr. The first and last 10-15% portions of the benzene were discarded.

Acetonitrile (Mallinckrodt spectrophotometric or MCB OmniSolv) was used as received.

Carbon Tetrachloride (Fisher Scientific Company - spectranalyzed) was purified following the procedure of Schuster.[114] Carbon tetrachloride (1 liter) containing 0.1 g benzophenone was photolyzed for 2 hours under an inert atmosphere (solution turned yellow). The solvent was refluxed for 4 hours and distilled through a 60 cm column packed with glass helices at a rate of 100 ml/hr. The first and last 200 ml portions were discarded.

Methanol. Mallinckrodt reagent grade methanol (1 liter) was purified by distillation from magnesium turnings (1g) through a 60 cm column packed with glass helices. The middle fraction ($\sim$60%) was collected, bp 64-65°.

Pyridine (Fisher Scientific Company reagent grade) was distilled from barium oxide through a 60 cm column packed with glass helices, and the middle fraction ($\sim$70%) was collected and redistilled, bp 114.5-115°.

Dioxane. MCB Scintillation grade dioxane (500 ml) was refluxed for 3 hours through a 50 cm column packed with stainless steel helices, followed by distillation (50 ml/hr). The first and last 100 ml portions were discarded.

tert-Butyl Alcohol. Fisher Scientific Company tert-butyl alcohol (500 ml) was distilled from magnesium turnings (1 g) through a 60 cm glass helice packed column at a rate of 50 ml/hr. The middle 60% portion was collected.

Ethanol was purified according to Riddich's Technique[115] by Dr. Harlan W. Frerking, Jr. One gallon of U.S.P. grade 190 proof ethanol was distilled from 100 ml of concentrated sulfuric acid through a one meter glass helice packed column at a rate of 40 ml/hr. The middle 70% portion was collected and distilled from 60 g of potassium hydroxide and 30 g of silver nitrate. The middle 80% portion was collected and 200 ml of distilled water was added. The ethanol was redistilled and the middle 80% portion was collected.

EPA Mixed Solvent. MCB Phosphorimetric grade EPA mixed solvent (5:5:2 ethyl ether, isopentane and ethyl alcohol) was used as received.

2-Methylbutane (Aldrich gold label spectrophotometric grade) was used as received.

Methylcyclohexane (MCB reagent grade) was purified using Forster's technique.[116] Methylcyclohexane (500 ml) was stirred over concentrated sulfuric acid until the acid no longer discolored. It was then washed with three 20 ml portions of distilled water, three 200 ml portions of saturated sodium bicarbonate, and then three 200 ml portions of distilled water. The methylcyclohexane was dried over magnesium sulfate and distilled through a 50 cm column packed with stainless steel helices. The first and last 100 ml portions were discarded.

Toluene (Mallinckrodt) was purified in the same manner as benzene. In order to prevent sulfonation of the ring, the toluene was cooled in an ice bath while being washed for only 2-3 hour periods with sulfuric acid. The middle fraction was collected, bp 110°.

p-Xylene (Mallinckrodt reagent grade) was purified in the same manner as toluene.

2. Internal Standards

Tridecane (Aldrich Chemical Company) was purified by washing with sulfuric acid, followed by distillation, bp 105° (10 Torr) by Dr. Peter J. Wagner.

Hexadecane (Aldrich Chemical Company) was purified by washing with sulfuric acid, followed by distillation, bp 146° (10 Torr) by Dr. Peter J. Wagner.

Heptadecane (Chemical Samples Company) was purified by washing with sulfuric acid, followed by distillation, bp 158° (8 Torr) by Dr. Peter J. Wagner.

Nonadecane (Chemical Samples Company) was purified by recrystallization from ethanol.

Eicosane (Eastman) was purified by recrystallization from ethanol.

Heneicosane (Chemical Samples Company) was purified by recrystallization from ethanol.

Docosane (Aldrich) was purified by recrystallization from ethanol.

Tetracosane (Aldrich) was used as received.

Hexacosane (Pfaltz and Bauer) was used as received.

n-Octadecyl benzoate was prepared by esterification of benzoyl chloride (Matheson, Coleman and Bell) with n-octadecanol (Aldrich), mp 57-58°..

3. Quenchers

1,3-Pentadiene (Chemical Samples Company) was used as received.

cis 1,3-Pentadiene (Chemical Samples Company) was used as received.

2,5-Dimethylhexa-2,4-diene (Chemical Samples Company) was allowed to sublime in the refrigerator.

Triethylamine (Matheson, Coleman and Bell) was stirred over potassium hydroxide (20 g) for 5 hours, then decanted off and distilled through a 60 cm glass helice packed column. The middle 60% portion was collected.

Naphthalene (Matheson, Coleman and Bell) was recrystallized from ethanol.

β-Dimethylaminoethyl Benzoate was synthesized in the manner described for the analogously substituted ketones. Benzoyl chloride (14.1 g, 0.1 mole) in ether was reacted with excess N,N-dimethylethanolamine (Aldrich) and subsequent workup gave the HCl salt of the desired product in 70% yield, mp 144-146°. Freeing the amine with aqueous base gave a colorless liquid. IR (neat) 1725 cm^{-1}; ^1H NMR ($CDCl_3$) 2.25 (s, 6H), 2.6 (t, 2H), 4.3 (t, 2H), 7.1-7.5 (m, 3H), 7.8-8.1 (m, 2H); MS m/e 193, 71, 58.

γ-Dimethylaminopropyl Benzoate was prepared in a similar manner to its 2-carbon analogue. The HCl salt is a white solid, mp 156-159.5°. The free amine is a colorless liquid. IR (neat) 1720 cm^{-1}; ^1H NMR ($CDCl_3$) 1.6-2.2 (m, 2H), 2.2-2.6 (m, 2H), 2.2 (s, 6H), 4.3 (t, 2H), 7.1-7.45 (m, 3H), 7.8-8.1 (m, 2H).

N,N-Dimethylaminopropyl Phenyl Ether was prepared in a similar manner as the analogously substituted ketone. Phenol (9.4 g, 0.1 mole), N,N-dimethylaminopropyl chloride (13.5g, 0.11 mole) and potassium carbonate (13.8 g, 0.1 mole) in 100 ml dry acetone were refluxed for 20 hours and subsequent workup gave the HCl salt of the desired product as a white solid (mp 144-146°) after recrystallization from MEK/hexane. The free amine is a colorless liquid. IR (neat) 1595 cm^{-1}; ^1H NMR ($CDCl_3$) δ1.58-2.55 (m, 4HO), 2.2 (s, 6H), 3.90 (t, 2H), 6.5-7.4 (m, 5H); MS m/e 179, 58.

4. Ketones

Valerophenone was prepared by the Friedel-Crafts acylation of benzene with valeryl chloride. Normal work-up procedures gave the crude product and distillation gave a colorless liquid, bp 105° (2 Torr).

o-, m-, and p-Trifluoromethylvalerophenones were available from a previous study.[28]

p-Methoxyvalerophenone was available from a previous study.[28]

Substituted Valerophenones for which only reduction potentials or triplet energies were measured were available from previous studies.[28,117]

Butyrophenone was available from a previous study.[28]

p-Methoxy-γ-dimethylaminobutyrophenone was available from a previous study.[82]

Para-Fluorovalerophenone was prepared by Friedel-Crafts acylation of Aldrich fluorobenzene with valeryl chloride. It was purified by vacuum distillation, bp 95° (0.16 Torr), mp 26°; IR (neat) 1691 cm^{-1}; ^1H NMR ($CDCl_3$) δ0.9 (t, 3H), 1.1-2.1 (m, 4H), 2.89 (t, 2H), 6.8-7.2 (m, 2H), 7.7-8.0 (m, 2H); MS m/e 180, 138, 123.

Para-Cyanovalerophenone. Sodium cyanide (20 g, 0.41 mole) was partially dissolved by heating in 300 ml of DMSO; para-fluorovalerophenone (65 g, 0.36 mole) was added slowly to the mixture. The solution was heated to 110-130° for 5 hours, the reaction being followed by NMR monitoring of the aromatic region. The viscous brown mixture was poured into 600 ml water and extracted several times with ether. The combined ether extracts were washed first with water, then with saturated sodium bicarbonate solution, and were dried over sodium sulfate. The solvent was removed under vacuum and a brown oil (58 g, 0.31 mole) was isolated in 87% yield. NMR Analysis of crude product showed $\sim$75% conversion. Vacuum distillation provided 50 g (0.27 mole) of p-cyanovalerophenone as an oil bp 114° (0.1 Torr). Recrystallization from hexane gave white crystals, mp 34-36° (lit. 32-33).[118] IR (KBr) 1696, 2225 cm^{-1}; ^1H NMR ($CDCl_3$) δ0.7-1.1 (m, 3H), 1.1-2.0 (m, 4H), 2.85 (t, 2H), 7.78 (q, 4H); MS m/e 187, 145, 130.

p-Fluorobutyrophenone was prepared by Friedel-Crafts acylation of Aldrich fluorobenzene with butyryl chloride and $AlCl_3$ catalyst. After acidic workup, the desired product was isolated as a light yellow oil in 70% yield. IR (neat) 1690 cm^{-1}; ^1H NMR ($CDCl_3$) δ0.6 (t, 3H), 1.5-2.1 (m, 2H), 2.87 (t, 2H), 6.8-7.2 (m, 2H), 7.6-8.0 (m, 2H); MS m/e 166, 138, 123, 95, 75.

Para-Cyanobutyrophenone was prepared, as described for p-cyanovalerophenone, in 70% crude yield. Vacuum distillation and recrystallization from hexane gave a white solid, mp 43.5-45°; IR (KBr) 1690, 2220 cm^{-1}; ^{1}H NMR ($CDCl_3$) δ0.8-1.2 (m, 3H), 1.5-2.0 (m, 2H), 2.91 (t, 2H), 7.74 (q, 4H); MS m/e 173, 145, 130, 102, 75.

Para-fluoro-γ-methylvalerophenone was synthesized by Freidel-Crafts acylation of Aldrich fluorobenzene with γ-methylvaleryl chloride. IR (neat) 1670 cm^{-1}; ^{1}H NMR ($CDCl_3$) δ0.6-1.1 (d, 6H), 1.2-2.0 (m, 4H), 2.8 (t, 2H), 6.7-7.2 (m, 2H), 7.6-8.0 (m, 2H); MS m/e 194, 138, 123.

Para-Cyano-γ-methylvalerophenone was prepared, as described for p-cyanovalerophenone, as a colorless liquid, bp 108° (0.8 Torr). IR (neat) 1690, 2225 cm^{-1}; ^{1}H NMR ($CDCl_3$) δ0.91 (d, 6H), 1.4-1.8 (m, 3H), 2.90 (t, 2H), 7.80 (q, 4H); MS m/e 201, 145, 130.

Meta-Cyanovalerophenone. n-Butylmagnesium bromide was prepared by adding 1-bromobutane (28 g, 0.2 mole) in 200 ml ether to Mg turnings (4.9 g, 0.2 mole) covered with ether. Aldrich m-cyanobenzaldehyde (26 g, 0.2 mole) was partially dissolved in 200 ml benzene, and the Grignard reagent was added dropwise with stirring. After being refluxed for 2 hours and then cooled, the solution was poured over dilute H_2SO_4/ice mixture. Normal work up gave 1-(3-cyanophenyl)-1-pentanol as a light yellow oil (32 g, 0.17 mole). A solution of the crude alcohol (30 g, 0.16 mole) in 85 ml benzene was added slowly to a cooled mixture of 20 g (0.07 mole) sodium dichromate, 10 ml glacial acetic acid, 30 ml conc. sulfuric acid, and 85 ml water.[119] After the solution was stirred at room temperature for three hours, the layers were separated and the aqueous layer was extracted with benzene. The combined organic layers were washed first with 5% KOH solution and then water, then were dried over sodium sulfate. The oily solid (22 g, 0.12 mole) resulting from solvent removal was recrystallized several times from hexane to give white crystals, mp 52-53°. IR (KBr) 1682, 2230, cm^{-1}; ^{1}H NMR ($CDCl_3$) δ0.7-1.1 (m, 3H), 1.1-2.0 (m, 4H), 2.94 (t, 2H), 7.2-8.3 (m, 4H); MS m/e 187, 158, 145, 130.

Para-Valerylbenzoic Acid. A solution of p-cyanovalerophenone (20 g, 0.11 mole), 30% KOH (100 ml), and ethanol (20 ml) was refluxed overnight. Careful acidification of the warm solution with dilute HCl resulted in precipitation of p-valerylbenzoic acid. Suction filtration of the solid followed by drying in a dessicator gave a white solid (16 g, 0.085 mole), mp 155-157°. IR (KBr) 1679, 1693 cm^{-1}; ^{1}H NMR ($CDCl_3$) δ0.7-1.1 (m, 3H), 1.1-2.0 (m, 4H), 2.94 (t, 2H), 8.00 (d of d, 4H), 9.7 (broad s, 1H); MS m/e 206, 189, 164, 149.

Meta-Valerylbenzoic Acid. Hydrolysis of m-cyanovalerophenone (15 g, 0.98 mole) with 100 ml 30% KOH/ethanol solution according to the above procedure resulted in precipitation of an oily solid. The solution was extracted with ether and the combined ether extracts were washed with water and dried over sodium sulfate. Evaporation of solvent, followed by recrystallization of the crude product from ethanol/water, gave white crystals (11 g, 0.053 mole), mp 115-118°. IR (KBr) 1688 cm^{-1}; ^{1}H NMR (CDCl$_3$) δ0.7-1.1 (m, 3H), 1.1-2.0 (m, 4H), 2.94 (t, 2H), 8.00 (q, 4H), 10.7 (broad s, 1H); MS m/e 206, 189, 164, 149.

Para-Carbomethoxyvalerophenone. *p*-Valerylbenzoic acid (10.3 g, 0.050 mole), sodium bicarbonate (17 g, 0.15 mole), and methyl iodide (22 g, 0.15 mole) in 100 ml dry DMF were stirred at room temperature in the dark for 18 hours.[120] The mixture was poured into 400 ml of saturated NaCl solution, and the solution was extracted with ether. The combined ether extracts were washed with water and dried over sodium sulfate. Evaporation of solvent and recrystallization of the crude product from hexane (charcoal) gave white crystals (9.4 g, 0.043 mole), mp 81-82° (lit 81°).[119] IR (KBr) 1676, 1724 cm^{-1}; ^{1}H NMR (CDCl$_3$) δ0.8-1.1 (m, 3H), 1.1-2.0 (m, 4H), 2.91 (t, 2H), 3.88 (s, 3H), 7.91 (d of d, 4H), MS m/e 220, 189, 178, 163.

Meta-Carbomethoxyvalerophenone. *m*-Valerylbenzoic acid (21 g, 0.10 mole), sodium bicarbonate (34 g, 0.4 mole) and methyl iodide (44 g, 0.3 mole) in 100 ml dry DMF were treated in a similar manner to the *para* compound. After work-up, evaporation of the solvent gave an oil (18 g, 0.8 mole) which was purified by vacuum distillation (bp 182° at 10 Torr), followed by low temperature recrystallization from hexane. IR (neat) 1690, 1729 cm^{-1}; ^{1}H NMR (CDCl$_3$) δ0.7-1.1 (m, 3H), 1.1-2.0 (m, 4H), 2.94 (t, 2H), 3.89 (s, 3H), 7.2-8.5 (m, 4H); MS m/e 220, 189, 178, 163.

Para-Divalerylbenzene was prepared by reaction of Aldrich terphthalonitrile with 4 equivalents of n-butylmagnesium bromide. Mg turnings (9.7 g) were covered with anhydrous ether and 1-bromobutane (73 ml, 0.47 mole) in 200 ml ether was added dropwise with stirring. A slurry of terephthalonitrile (12.8 g, 0.10 mole) in benzene was added slowly. After being refluxed overnight (solution turned orange), the mixture was poured into dilute HCl/ice solution and extracted with ether. A small amount of p-divalerylbenzene precipitated out of the aqueous layer and was collected. The combined organic extracts were washed with water and dried over sodium sulfate. Removal of the solvent gave a yellow, oily solid (12.6 g, 0.05 mole). The crude product was chromatographed on an alumina column using various petroleum ether/ether mixtures and the resulting eluted solid was recrystallized from hexane to give white crystals in 30% overall yield, mp 96-97°. IR (KBr) 1676 cm^{-1}; ^1H NMR ($CDCl_3$) δ0.7=1.2 (m, 6H), 1.2-2.0 (m, 8H), 2.95 (t, 4H), 7.90 (s, 4H); MS m/e 246, 204, 189, 162, 147.

Meta-Divalerylbenzene. Similar synthetic and purification methods were used as described above for the para-compound. Aldrich isophthalonitrile (12.8 g, 0.10 mole) in benzene was added slowly to n-butylmagnesium bromide (0.4 mole). After work-up, 11 g of a yellow oil was obtained (45% yield). After elution through an alumina column and repeated recrystallizations from petroleum ether, white crystals were obtained, mp 25°. IR (KBr) 1682 cm^{-1}; ^1H NMR ($CDCl_3$) δ0.7-1.1 (m, 6H) 1.1-2.1 (m, 8H), 2.98 (t, 4H), 7.2-8.5 (m, 4H); MS m/e 246, 204, 189, 162, 147.

Para-Acetylvalerophenone. A solution of Aldrich p-acetylbenzonitrile (8.0 g, 0.055 mole), ethylene glycol (10 ml), and p-toluenesulfonic acid (0.1 g) in 50 ml benzene was refluxed in a Dean-Stark trap until no more water azeotroped off. The cooled solution was washed first with water then with saturated sodium bicarbonate, and was dried over sodium sulfate. Evaporation of solvent gave the ketal as a white solid (9.8 g, 0.052 mole), mp 68-70°; ^1H NMR ($CDCl_3$) δ1.60 (s, 3H), 3.4-3.8 (m, 2H), 3.8-4.2 (m, 2H), 7.48 (s, 4H).

Magnesium turnings (1.25 g, 0.052 mole) were covered with dry ether; 1-bromobutane (7.1 g, 0.052 mole) in 200 ml ether was added dropwise to maintain reflux. A slurry of the ketal (9.0 g, 0.047 mole) in 200 ml benzene was added slowly with stirring. After being refluxed for 6 hrs the solution was poured into HCl/ice mixture and extracted with ether. Evaporation of the ether gave only starting material (2.2 g, 0.012 mole). The desired product (white solid) precipitated out of the aqueous solution (3.2 g, 0.016 mole) and, after recrystallization from hexane, gave white crystals, mp 77-78°. IR (KBr) 1676 cm^{-1}; NMR ($CDCl_3$ δ0.7-1.1 (m, 3H), 1.1-2.0 (m, 4H), 2.94 (t, 2H), 7.90 (s, 4H); MS m/e 204, 189, 162, 147.

Ortho-Bromovalerophenone. n-Butylmagnesium bromide was made by the addition of 1-bromobutane (16 g, 0.12 mole) in 200 ml ether to magnesium turnings (2.8 g 0.115 mole) in ether. A slurry of Aldrich o-bromobenzaldehyde (18.5 g, 0.10 mole) in benzene was added slowly with stirring. After being refluxed for 2 hours and cooled, the solution was hydrolyzed with dilute HCl/ice water. Normal workup gave a yellow oil (20.5 g, 0.085 mole) in 85% yield, IR (neat) 3300 cm^{-1}. The crude 1-(2-bromophenyl)-pentan-1-ol (9.7 g, 0.004 mole) was oxidized using sodium dichromate (24 g, 0.008 mole), glacial acetic acid (17 ml), and conc. sulfuric acid (30 ml) in 100 ml water following the procedure of Bruce.[35] The solution was stirred for 5 hours at room temperature and then extracted with ether. The ether extracts were washed with 5% KOH solution and water, then dried over sodium sulfate. Removal of solvent gave a yellow oil (5.1 g, 0.02 mole); IR (neat) 1700 cm^{-1}; ^{1}H NMR ($CDCl_3$) δ0.7-1.1 (t, 3H), 1.1-2.0 (m, 4H) 2.82 (t, 2H), 6.9-7.5 (m, 4H).

Ortho-Cyanovalerophenone. A solution of o-bromovalerophenone (20 g, 0.08 mole) and CuCN (10.0 g, 0.16 mole) in 25 ml pyridine was refluxed for 2 hours. The mixture was added to 75 ml water and extracted with ether. The combined ether layers were washed with water and dried over sodium sulfate. Evaporation of solvent gave a brown oil (13 g, 0.07 mole). Vacuum distillation gave a colorless oil, bp 117° (8 Torr). From low temperature recrystallization in hexane, a white solid was obtained, mp ∿25°. IR (KBr) 1690 cm^{-1}; ^{1}H NMR ($CDCl_3$) δ0.8-1.1 (t, 3H), 1.1-2.0 (m, 4H), 2.82 (t, 2H), 7.4-7.9 (m, 4H); MS m/e 187, 145, 130.

Ortho-Carbomethoxyvalerophenone. o-Valerylbenzoic acid was synthesized following a procedure for keto-acids developed by De Benneville.[121] n-Butyl magnesium bromide (0.5 mole) in ether was cooled in an ice bath, and oven-dried $CdCl_2$ (46 g, 0.25 mole) was added slowly to the mixture. The mixture was allowed to warm and was refluxed for 1.5 hours. Solid phthalic anhydride (37 g, 0.25 mole) was added slowly with stirring to the cooled (0°) solution. After being refluxed for 2.5 hours, the solution was cooled and dilute H_2SO_4/ice water was added. The organic layer was separated and combined with ether extracts of the aqueous layer. The product was extracted from the ether layer with 10% K_2CO_3 solution, which was then filtered and acidified with dilute H_2SO_4. The keto-acid was then extracted into ether; solvent evaporation left a clear oil (36.5 g, 0.17 mole). The oil eventually solidified in the refrigerator and was washed with cold hexane to give a white solid, mp 40-42°. The free acid exists mainly as its hydroxy-γ-lactone isomer; IR (KBr) 1750, 3360 cm^{-1}; ^1H NMR ($CDCl_3$) δ0.6-1.0 (m, 3H), 1.1-1.6 (m, 4H), 2.2 (broad t, 2H), 6.0 (broad s, 1H), 7.2-7.9 (m, 4H); MS m/e 206, 189, 164, 149 (base).

The crude o-valerylbenzoic acid (20 g, 0.097 mole) was esterified according to the procedure previously described involving stirring in the dark overnight with methyl iodide (30 ml, 0.48 mole) and sodium bicarbonate (15 g, 0.17 mole) in DMF (100 ml). After ether work-up, evaporation of the solvent gave an orange oil (17 g, 0.078 mole) in 80% yield. Three consecutive vacuum distillations of the crude product gave a colorless oil, bp 116° (0.4 Torr). IR (neat) 1713, 1735, cm^{-1}; ^1H NMR ($CDCl_3$) δ0.7-1.1 (t, 3H), 1.1-2.0 (m, 4H), 2.74 (t, 2H), 3.8 (s, 3H), 7.2-7.9 (m, 4H); MS m/e 220, 189, 178, 163. 146.

3-Benzoylbenzonitrile. Phenyl magnesium bromide (0.08 mole) in ether was added dropwise with stirring to Aldrich m-cyanobenzaldehyde (9.0 g, 0.075 mole) in 250 ml benzene. The solution was refluxed for 1 hour, cooled, and then added to dilute HCl/ice water. After hydrolysis was complete, the layers were separated and the aqueous layer extracted with ether. Normal workup gave a light yellow oil (12 g, 0.057 mole) in 76% yield; IR (neat) 2210, 3450 cm^{-1}; ^1H NMR ($CDCl_3$) δ2.55 (broad s, 1H), 5.7 (d, 1H), 7.0-8.0 (m, ∿9H). The crude alcohol was oxidized to 3-benzoylbenzonitrile without further purification by the method described previously for 1-(3-cyanophenyl)-1-pentanol. After benzene work-up, an oily solid was obtained which, after recrystallization from hexane, gave 3.0 g (0.14 mole) of white crystals, mp 88-90°. IR (KBr) 1710, 2200 cm^{-1}; ^1H NMR ($CDCl_3$)δ7.1-8.1 (m); MS m/e 207, 130, 105 (base).

Methyl 2-Benzoylbenzoate. Aldrich 2-benzoylbenzoic acid (9.1 g, 0.040 mole) was esterified as previously described using CH_3I (10 ml, 0.16 mole) and $NaHCO_3$ (5 g, 0.06 mole) in 100 ml DMF. Upon normal work-up, a yellow oil was isolated which was recrystallized twice from hexane to give a white solid (6.2 g, 0.026 mole), mp 48-49.5° (lit. 52°).[122] IR(KBr) 1670, 1720 cm^{-1}; ^1H NMR ($CDCl_3$) δ3.52 (s, 3H), 7.1-8.0 (m, 9H); MS m/e 240, 209, 163, 105.

Methyl 4-Benzoylbenzoate. Aldrich 4-benzoylbenzoic acid (4.0 g, 0.018 mole) was esterified by refluxing overnight in methanol (50 ml) containing sulfuric acid (1/2 ml). Most of the solvent was removed under aspirator pressure and water was added. The solution was made basic with K_2CO_3 and extracted with benzene. The combined benzene extract was washed with water and dried over sodium sulfate. Removal of solvent gave a white solid, which was recrystallized from hexane (3 g, 0.13 mole), mp 108-109°. IR (KBr) 1640, 1715 cm^{-1}; ^1H NMR ($CDCl_3$) δ3.88 (s, H), 7.0-8.1 (m, 9H); MS m/e 240, 209, 163, 105.

Methyl 3-benzoylbenzoate. 3-Benzoylbenzonitrile (1.4 g, 0.0068 mole) was hydrolyzed in 50 ml of 30% alcoholic KOH according to the procedure described previously. After work-up, 1 g (0.004 mole) of 3-benzoylbenzoic acid (tan solid) was obtained, which was recrystallized from MEK/hexane to give a solid, mp 161-163° (lit. 161-2°).[123] IR (KBr) 1650, 1685 cm^{-1}; ^1H NMR ($CDCl_3$)δ7.3-8.5 (m, 9H), 9.9 (broad s, 1H).

The ester was synthesized from 3-benzoylbenzoic acid (0.5 g, 0.003 mole) by refluxing overnight in 50 ml methanol containing a trace of sulfuric acid, the procedure previously described for the para analogue. After similar work-up and recrystallization from hexane, white crystals were obtained (∿0.2 g), mp 43-45°. IR (KBr) 1650 1725 cm^{-1}; ^1H NMR ($CDCl_3$) δ3.82 (s, 3H), 7.1-8.4 (m, 9H); MS m/e 240, 209, 163, 105.

3-Trifluormethylbenzophenone. Aldrich m-trifluoromethylbenzonitrile (4.3 g, 0.025 mole) in benzene was added dropwise to an ether solution containing 0.03 mole phenyl magnesium bromide; the mixture was refluxed for 2 hours. Dilute HCl/ice water was added and the layers were separated. The organic layer contained mostly unreacted bromobenzene. The aqueous layer was heated on the steam bath for 2 hours, followed by cooling and extraction with ether. The combined ether extracts were washed with water and dried over sodium sulfate. Evaporation of the solvent gave crude product; recrystallization from hexane gave white crystals (1.4 g, 0.006 mole), mp 49-51°. IR (KBr) 1650 cm^{-1}; ^1H NMR ($CDCl_3$) δ7.2-8.0 (m); MS m/e 250, 173, 145, 105 (base), 77.

p-Valeryl β-Dimethylaminoethyl Benzoate. p-Valerylbenzoic acid (10.0 g, 0.05 mole) and thionyl chloride (4 ml, 0.06 mole) in 50 ml benzene were refluxed under anhydrous conditions, followed by removal of excess thionyl chloride and partial removal of solvent under aspirator pressure. The solution was then cooled (0°) and 300 ml anhydrous ether was added. Excess N,N-dimethylethanolamine (Aldrich) was added dropwise with stirring with the evolution of much HCl gas. The white solid (12 g) was filtered off, and NMR analysis revealed the HCl salt of the desired product with little starting alcohol. Addition of more N,N-dimethylethanolamine to the filtrate gave very little additional solid. More product could occasionally be obtained by bubbling HCl gas through the filtrate and filtering off the precipitate (mixture of starting alcohol and the desired product). The solid was dissolved in the minimum amount of distilled water (10-20 ml) and the solution was made basic (pH ∿9) by the addition of potassium carbonate (carbon dioxide was evolved). The solution was extracted three times with benzene (20 ml) and the combined benzene solution was washed once with 5% KOH solution (to remove starting acid), four times with distilled water (to remove starting alcohol), and dried over sodium sulfate. Removal of solvent under vacuum gave a light yellow oil. The oil was dissolved in anhydrous ether and HCl gas was bubbled through the solution. The precipitated HCl salt of the amino ester (off-white solid) was filtered and washed with ether. Recrystallization of the HCl salt from MEK (charcoal) gave a white solid, mp 135-137.5°. The HCl salt was dissolved in the minimum amount of water (5-10 ml) and the solution was made basic with potassium carbonate and extracted with ether. The combined ether extracts were washed three times with distilled water and dried over sodium sulfate. Removal of solvent under vacuum gave a colorless oil. IR (neat) 1685, 1720 cm^{-1}; ^1H NMR ($CDCl_3$) δ0.7-1.1 (m, 3H), 1.1-2.0 (m, 4H), 2.30 (s, 6H), 2.64 (t, 2H), 2.92 (t, 2H), 4.36 (t, 2H), 7.92 (d of d, 4H); MS m/e 277, 248, 220, 189, 149, 104, 71, 58 (base).

<u>m-Valeryl β-Dimethylaminoethyl Benzoate</u> was prepared in a similar manner as the <u>para</u> isomer. <u>m</u>-Valerylbenzoic acid (10.0 g, 0.05 mole) and thionyl chloride (4 ml, 0.06 mole) in 100 ml benzene were refluxed for 4 hours, followed by removal of excess thionyl chloride and partial removal of solvent under aspirator pressure. The dropwise addition of excess N,N-dimethylethanolamine to the ether solution gave a yellow oil, and the solution was decanted off. Similar work-up gave the HCl salt as a light yellow oil. Attempted

low temperature recrystallization from hexane gave a "taffy-like" off-white semi-solid. The HCl salt was freed as described for the para isomer to give the desired amine and subsequent chromatography on a short alumina column using petroleum ether/ether mixtures gave a päle yellow liquid. IR (neat) 1685, 1720 cm^{-1}; ^1H NMR ($CDCl_3$) δ0.7-1.1 (m, 3H), 1.1-2.0 (m, 4H), 2.33 (s, 6H), 2.68 (t, 2H), 2.95 (t, 2H), 4.38 (t, 2H), 7.4 (t, 1H), 7.9-8.1 (m, 2H), 8.4-8.53 (m, 1H); MS m/e 277, 220, 189, 149, 104, 71, 58 (base).

p-Acetyl β-Dimethylaminoethyl Benzoate was prepared in a similar manner as the valeryl analogue. Aldrich p-acetylbenzoic acid (2.0 g, 0.01 mole) and thionyl chloride (2 ml, 0.03 mole) were refluxed for 2 hours (solution turned brown), followed by removal of unreacted thionyl chloride and partial removal of solvent under aspirator pressure. The dropwise addition of excess N,N-dimethylethanolamine to the ether solution gave a brown oil, and the solution was decanted off. Similar work-up and recrystallization from MEK/hexane gave a white solid (HCl salt), mp 168-171°. The HCl salt was freed in a similar manner to give a colorless liquid. IR (neat) 1685, 1720 cm^{-1}; ^1H NMR ($CDCl_3$) δ2.3 (s, 6H), 2.58 (s, 3H), 2.65 (t, 2H), 4.38 (t, 2H), 7.92 (d of d, 4H); MS m/e 235, 220, 147, 104, 71, 58 (base).

p-Valeryl β-Dimethylaminopropyl Benzoate was synthesized in a similar manner as the 2 carbon analogue. p-Valerylbenzoic acid (10.0 g, 0.05 mole) and thionyl chloride (4 ml, 0.06 mole) were refluxed for 4 hours, followed by removal of solvent under aspirator pressure. The dropwise addition of excess 3-(N,N-dimethylamino)-1-propanol (Aldrich) to the ether solution (25°) gave an off-white solid (12.1 g) which was filtered. Similar work-up and recrystallization from MEK/hexane gave a white solid (HCl salt), mp 203-204°. The HCl salt was freed in a similar manner to give a colorless liquid. IR (neat) 1685, 1720 cm^{-1}; ^1H NMR ($CDCl_3$) δ0.7-1.1 (m, 3H), 1.1-2.1 (m, 6H), 2.1-2.63 (m, 2H), 2.23 (s, 6H), 2.84 (t, 2H), 4.34 (t, 2H), 7.94 (d of d, 4H); MS m/e 291, 234, 147, 102, 86, 58 (base).

p-Benzoyl β-Dimethylaminoethyl Benzoate was prepared in a similar manner as the valeryl analogue. Aldrich p-benzoylbenzoic acid (3.0 g, 0.013 mole) and thionyl chloride (1.2 ml, 0.18 mole) in 100 ml benzene were refluxed for 5 hours. Ether was added and the dropwise addition of excess N,N-dimethylethanolamine (Aldrich) gave an oily white solid which was filtered and identified as N,N-dimethylethanol ammonium chloride. Additional starting alcohol was removed by bubbling HCl gas through the solution and filtering off the precipitate. The solvent was then removed under vacuo to give a yellow oil and similar work-up gave the desired HCl salt as an off-white solid. Recrystallization of the HCl salt from MEK gave a white solid, mp 168-171°. The HCl salt was freed in a similar manner to give a white solid, mp 39.5-42°. IR (KBr) 1645, 1700 cm^{-1}; ^1H NMR ($CDCl_3$) δ2.30 (s, 6H), 2.65 (t, 2H), 4.37 (t, 2H), 7.2-8.2 (m, 9H); MS m/e 297, 209, 105, 77, 71, 58 (base).

m-Benzoyl β-Dimethylaminoethyl Benzoate was synthesized in a similar manner as the para-isomer. 3-Benzoylbenzoic acid (1.0 g - synthesis previously described under methyl 3-benzoylbenzoate) and thionyl chloride (1 ml) were refluxed for 3 hours, followed by removal of excess thionyl chloride and partial removal of solvent under aspirator pressure. Similarly, the dropwise addition of excess N,N-dimethylethanolamine (Aldrich) gave an oily white solid which was filtered and identified as N,N-dimethylethanol ammonium chloride. Evaporation of solvent gave an off-white semi-solid and similar workup and attempted recrystallization from hexane gave the HCl salt as a "taffy-like", off-white semi-solid. The HCl salt was freed in a similar manner to give an almost colorless liquid. IR (neat) 1660, 1720 cm^{-1}; ^1H NMR ($CDCl_3$) δ2.30 (s, 6H), 2.65 (t, 2H), 4.37 (t, 2H), 7.2-8.4 (m, 9H); MS m/e 297, 209, 105, 77, 71, 58 (base).

p-(3-Dimethylaminopropoxy)valerophenone was synthesized following the procedure developed by Allen and Gate for phenolic ethers.[124] Eastman 4'-hydroxyvalerophenone (5.4 g, 0.030 mole), 3-dimethylaminopropyl chloride 4.3 g, 0.035 mole (obtained by freeing Aldrich HCl salt with aqueous base and extracting with ether), and potassium carbonate (4.2 g, 0.030 mole) in 100 ml dry acetone were refluxed for 16 hours under anhydrous conditions. After solvent removal under vacuo, 100 ml distilled water was added and the solution was extracted 3 times with 75 ml benzene. The combined organic extract was washed with 10% KOH, then 3 times with distilled water and dried over sodium sulfate. Removal of solvent gave an oil. The oil was dissolved in ether and HCl gas was bubbled through the solution. The profuse amount of soap-like white precipitate was filtered and recrystallized from MEK/hexane to give white solid (HCl salt of the desired amine, mp 156.5-158°. The amine was freed by dissolving the HCl salt in the minimum amount of distilled water, making the solution basic (pH ∿9) with potassium carbonate, and extracting with ether. The combined ether extract was washed with distilled water and dried over sodium sulfate. Evaporation of solvent gave a colorless liquid. IR (neat) 1600, 1675 cm^{-1}; ^1H NMR ($CDCl_3$) δ0.7-1.1 (m, 3H), 1.1-2.6 (m, 8H), 2.2 (s, 6H), 2.86 (t, 2H), 4.0 (t, 2H), 7.2 (d, 2H), 7.8 (d, 2H); MS m/e 263, 120, 86, 58 (base).

p-(3-Dimethylaminopropoxy)acetophenone was prepared in a similar manner as the valeryl analogue. Eastman 4'-hydroxyacetophenone (13.6 g, 0.10 mole), Aldrich 3-dimethylpropyl chloride (13.4 g, 0.11 mole), and potassium carbonate (13.8 g, 0.10 mole) in 100 ml dry acetone were refluxed for 20 hours. Similar work-up procedures and recrystallization of the HCl salt from MEK/hexane gave a white solid, mp 177-178°. The amine was freed in a similar manner to give a colorless liquid. IR (neat) 1600, 1675 cm^{-1}; ^1H NMR ($CDCl_3$) δ1.68-2.75 (m, 4H), 2.2 (s, 6H), 2.48 (s, 3H), 4.0 (t, 2H), 7.28 (d, 2H), 7.76 (d, 2H); MS m/e 221, 120, 92, 58 (base).

B. Photokinetic Techniques

1. General Procedure

Glassware - All photochemical glassware (class A volumetric flasks and pipets) was cleaned by first washing with acetone twice, followed by soaking in hot distilled water containing Alconox detergent for 24 hours. Then the equipment was rinsed and soaked in hot distilled water for 2 days, changing the water every 12 hours. Syringes used for transferring solutions and Pyrex culture tubes used for irradiation were also cleaned in the same manner. All glassware was dried in a 150° oven used solely for drying photochemical glassware.

Irradiation tubes were made by heating the previously cleaned Pyrex culture tubes (13 x 100 mm) near the top and drawing them out to a uniform 15 mm length (2 mm neck).

Sample Preparation - Solutions were prepared by either weighing the desired amount of compound directly into the volumetric flask and diluting to the mark with solvent or by pipetting an aliquot from a stock solution (make in the above manner) into a volumetric flask and diluting to the mark. A constant amount (2.8 ml) of the solutions were syringed into the constricted culture tubes. Usually hydrocarbon internal standard were used in irradiations, but when solubility was a problem, standards were added after photolysis by pipetting both photolyzed ketone and standard (known concentration) into vials before GC analysis.

Degassing Procedure - The filled irradiation tubes were attached to a vacuum line (10^{-4} Torr) by means of one-hole rubber stoppers (size 00) attached to a manifold containing 12 stopcocks. The solutions were frozen by slow immersion in liquid nitrogen, followed by opening of the stopcocks. After pumping on the samples for 5-15 minutes (depending on sample) the stopcocks were closed and the solutions were allowed to thaw completely. This freeze-pump-thaw cycle was repeated two to four times (depending on sample) after which the tubes were sealed while still frozen using a torch.

Pyrex tubes fitted to ground glass joints and a manifold containing 10 vacuum stopcocks with ground glass joints were used in Stern Volmer quenching experiments involving the determination of room temperature phosphorescence lifetimes. Also, six 5-8 minute freeze-pump-thaw cycles were performed and the diffusion pump was employed in the last two cycles.

Irradiation Procedure - Quantum yield and Stern Volmer quenching studies were performed by parallel irradiation of samples and actimometer in a merry-go-round apparatus immersed in a water bath maintained at 25°. A water-cooled Hanovia medium-pressure mercury lamp equipped with either an alkaline potassium chromate (0.002 M K_2CrO_4 and 1% K_2CO_3) filter solution to isolate the 313 nm band or Corning #7-83 filters to isolate the 366 nm band was used in the analyses.

Analysis of Samples - All analyses were performed on a Varian Aerograph Series 1200 or Hy-Fi Model 550 gas chromatographs (flame ionization detectors) equipped with Leeds and Northrup recorders and Infotronics CRS 309 digital integrators. On-column injection and nitrogen carrier gas (40 ml/min flow rate) were used in all analyses. The 1/8" aluminum columns used in the analyses are listed below.

Columns #1,2:	4' and 6-1/2', respectively, 4% QF-1 and 1% Carbowax 20 M on AW-Chromosorb G, with 1% KOH added.
Column #3:	8' 5% FFAP on AW-Chromosorb P.
Column #4:	3' 19.4% FFAP on AW-Chromosorb P.
Column #5:	5' 5% SE-30 on Chromosorb W.
Column #6:	25' 25% 1,2,3-Tris (2-cyanoethyl)propane on Chromosorb P.

GC response factors were determined by measuring the relative peak areas of products and standards of known concentrations. The ortho- and meta-substituted acetophenones not available were assumed to have the same response factor as their para-isomers. The response factors determined are given below.

Standard/Product	$\frac{\text{Area/Mole (std)}}{\text{Area/Mole (prod)}}$
hexadecane/acetophenone	2.33±0.03
heptadecane/acetophenone	2.39
nonadecane/p-cyanoacetophenone	2.42±0.02
eicosane/p-cyanoacetophenone	2.64±0.03
eicosane/m-cyanoacetophenone	2.49±0.03
heneicosane/p-cyanoacetophenone	2.72±0.02
eicosane/p-carbomethoxyacetophenone	2.52±0.03

Standard/Product	$\frac{\text{Area/Mole (std)}}{\text{Area/Mole (prod)}}$
eicosane/p-diacetylbenzene	2.56±0.04
heneicosane/p-acetylvalerophenone	1.82±0.02
docosane/p-acetylvalerophenone	1.93±0.03
tetracosane/p-acetylvalerophenone	2.03±0.04
eicosane/p-methoxyacetophenone	2.50±0.01
docosane/p-methoxyacetophenone	2.68±0.04
tridecane/p-trifluoromethylacetophenone	1.69±0.03
hexadecane/p-trifluoromethylacetophenone	2.01±0.02
n-octyl benzoate/p-acetyl β-dimethylaminoethyl benzoate	2.50±0.02
tetracosane/p-(3-dimethylaminopropoxy)acetophenone	2.35±0.05

Identification of Photoproducts - Samples were analyzed for acetophenone photoproducts, identified by comparison of GC retention times with those of authentic samples under identical conditions. In general, the ortho- and meta-substituted acetophenones were unavailable, and these acetophenones were assumed to have nearly identical retention times as their para isomers. As a check, p-carbomethoxyacetophenone was also identified by GC/MS in the photolysis of p-carbomethoxyvalerophenone in acetonitrile. Usually two small broad peaks with slightly longer retention times than the parent ketones were evident in the GC traces, and these peaks were assumed to correspond to the isomeric cyclobutanols typically formed in the photolysis of phenyl alkyl ketones.[28]

The para-aminoketones were also identified by comparison of GC retention times with those of the appropriate aminoacetophenones independently synthesized. m-2AB was assumed to have nearly the same GC retention time as the para isomer. Also, a 250 MHz ^1H NMR spectra of the photolyzed sample from irradiation of p-2AB in acetonitrile showed the appearance of a singlet with the same chemical shift as the corresponding acetophenone methyl group.

2. Stern-Volmer Quenching Studies and Quantum Yields

Usually stock solutions of ketone and internal standard were prepared in 10 ml volumetric flasks from which constant amounts were pipetted for both quenched and unquenched samples (1 ml/5 ml volummetric and 2 ml/10 ml volumetric, respectively). Also stock quencher solutions were made in 10 ml volumetric from which varying amounts (0.25 ml-3 ml) were pipetted. When necessary, stock solutions of additive (i.e., pyridine) were also prepared in 10 ml volumetric flasks. The various volumetric flasks were then filled to volume with solvent. Usually, three tubes without quencher and 6 tubes containing varying amounts of quencher were prepared. After the tubes were filled, degassed, and photolyzed, Φ^0/Φ was obtained for each quenched solution by dividing the average GC photoproduct/standard ratio for the unquenched tubes by the same ratio for the quenched tubes. A plot of Φ^0/Φ versus quencher concentration enables calculation of triplet lifetime from the slope.

Quantum yields were also obtained at the same time by parallel irradiation of an actinometer. The quantum yield of acetophenone formation for 0.05 M valerophenone in benzene is 0.315 and for 0.1 M valerophenone in benzene is 0.33.[13] Quantum yields can be calculated as follows:

0 Quencher Tube:

[X-Acetophenone] = [Standard] x R.F. x area X-AP/area standard

Actinometer Tube:

[Acetophenone] = [Standard] x R.F. x area AP/area standard

Φ_{II} = 0.33 ([X-Acetophenone]/[Acetophenone])

Maximum quantum yields were obtained by adding varying amounts of a stock solution of Lewis base to solutions of ketone and internal standard. Usually 0.5 M pyridine was sufficient to maximize the quantum yield and added pyridine had either no effect or slightly decreased the quantum yield.

3. Disappearance Yields

Disappearance yields were determined by comparing the ketone concentration before and after irradiation. A known concentration of external standard was added to both photolyzed and unphotolyzed samples. Since the initial ketone concentration was known, then the GC response factor was calculated and used to calculate the ketone concentration after photolysis. The disappearance yield was calculated as follows:

$$\Delta\text{Ketone} = [\text{Ketone}]_{\text{initial}} - [\text{Ketone}]_{\text{final}}$$

$$\Phi_{-K} = 0.33\,\frac{\Delta\text{Ketone}}{[\text{AP}]_{\text{act}}}$$

All samples were taken to 20% or more conversion in order to minimize the error involved in the measurements and valerophenone was used as actinometer.

4. Intersystem Crossing Yields

The intersystem crossing yields for p-cyanoacetophenone and p-carbomethoxyvalerophenone were obtained by sensitizing the isomerization of cis-1,3-pentadiene. Tubes containing 0.04 M ketone with varying amounts of cis 1,3-pentadiene were irradiated (313 nm) in parallel with 0.06 M acetophenone or valerophenone, respectively, and varying amounts of cis 1,3-pentadiene as actinometers. A plot of $\alpha/\Phi_{\text{isom}}$ versus 1/[cis1,3-pentadiene] gives a linear correlation in which 1/intercept equals Φ_{ISC}.

$$\frac{\alpha}{\Phi_{\text{isom}}} = \frac{\beta'_{\text{Act}}[\text{Quencher}]_{\text{Act}}}{\beta'_{\text{Ketone}}[\text{Quencher}]_{\text{Ketone}}},$$

where α is the photostationary state for quencher isomerization ($\alpha = 0.55$ for cis 1,3-pentadiene)[14] and β' is the fraction of newly formed isomer corrected for back-reaction.

$$\beta' = 0.55\,\ln\frac{0.55}{0.55-\beta}, \quad \text{where } \beta = \frac{\text{area trans}}{\text{area trans} + \text{area cis}}$$

5. Photoreduction

Photoreduction experiments on p-cyanoacetophenone were performed by preparing stock solutions of both ketone and donor and by adding varying amounts of donor to a constant amount of ketone (0.05 M). After photolysis, the amount of donor coupling product was determined and a plot of $1/\Phi_{\text{coupling prod}}$ versus 1/[donor] gave a linear correlation with a slope/intercept equal to k_d/k_r. Stern-Volmer quenching experiments involving varying the amount of naphthalene quencher with a constant amount of ketone and donor gave a linear correlation when Φ^o/Φ versus [quencher] was plotted (formation of coupling photoproduct was monitored). Since the lifetime, τ, can be determined from the slope and $1/\tau = k_d + k_r$, then both k_d and k_r could be determined from these experiments.

C. Spectra

1. Phosphorescence Emission Spectra

Phosphorescence spectra were recorded on a Perkin-Elmer MPF-44A Fluorescence Spectrophotometer equipped with a Differential Corrected Spectra Unit and Hitachi Phosphorescence Accessory. Spectra were run on 10^{-4} M ketone in various solvent glasses at 77°K using a quartz dewar and 5 mm quartz tubes. The corrected emission scan mode, ratio measurement mode, and DC photometric mode were used. Excitation and emission slit widths were typically 8 and 4 nm, respectively, and spectra were recorded at a scan rate of 120 nm/min.

Various sample sensitivities, excitation wavelengths, and emission responses (0.3 - 3 sec) were used, depending on sample.

2. Electronic Absorption Spectra

Ultraviolet absorption spectra were recorded on a Cary 219 spectrophotometer. MCB Omnisolv heptane was used as solvent. Extinction coefficients at 313 nm for various ketones were determined on a Gilford-Beckman spectrophotometer.

3. Infrared Spectra

IR spectra were recorded on a Perkin-Elmer Model 237 B grating infrared spectrophotometer. Samples were run as thin films or KBr pellets and polystyrene (1601.4, 2850.7 cm^{-1}) was used to calibrate each spectrum.

4. ^1H NMR Spectra

Routinely, ^1H NMR spectra of $CDCl_3$ solutions (1% TMS) of the various ketones were recorded on a Varian T-60 spectrometer. Fourier transformed ^1H NMR spectra (250 MHz) were taken of the following amino ketones, since similar chemical shifts resulted in overlapping peaks in the T-60 spectra:

p-2VB: ($CDCl_3$) δ0.960 (t, 3H); 1.42 (sextet, 2H); 1.73 (quintet, 2H); 2.45 (s, 6H); 2.73 (t, 2H); 2.99 (t, 2H); 4.46 (t, 2H); 8.01 (d, 2H); 8.12 (d, 2H).

m-2VB: ($CDCl_3$) δ0.963 (t, 3H); 1.42 (sextet, 2H); 1.74 (quintet, 2H); 2.36 (s, 6H); 2.75 (t, 2H); 3.01 (t, 2H); 4.48 (t, 2H); 7.55 (t, 1H); 8.22 (m, 2H); 8.61 (m, 1H).

p-3VB: ($CDCl_3$) δ0.958 (t, 3H); 1.42 (sextet, 2H); 1.73 (quintet, 2H); 1.98 (quintet, 2H); 2.26 (s, 6H); 2.44 (t, 2H); 2.99 (t, 2H); 4.41 (t, 2H); 8.01 (d, 2H); 8.12 (d, 2H).

p-2BB: ($CDCl_3$) δ2.83 (s, 6H); 2.77 (t, 2H); 4.49 (t, 2H); 7.50 (m, 1H); 7.60 (m, 2H); 7.82 (t, 4H); 8.17 (d, 2H).

p-3VE: ($CDCl_3$) δ0.945 (t, 3H); 1.38 (sextet, 2H); 1.72 (quintet, 2H); 1.97 (quintet, 2H); 2.25 (s, 6H); 2.45 (t, 2H); 2.90 (t, 2H); 4.08 (t, 2H); 6.92 (d, 2H); 7.93 (d, 2H).

The spectra were recorded on a Bruker WM 250 spectrometer by Michael A. Meador. Also, 250 MHz spectra of p-2BB (1.0×10^{-4} M) in carbon tetrachloride with 1% C_6D_6 and 10^{-4} M tetrachloroethane internal standard were recorded by M. A. Meador.

5. Mass Spectra

Mass spectra were run on a Finnigan 4000 GC/MS using the direct inlet mode by Ernest Oliver.

6. Cyclic Voltammetry

Reduction potentials were measured for various ketones (10^{-4} M) in Aldrich gold label acetonitrile (0.1 M TEAP) relative to SCE at a hanging mercury drop electrode with platinum auxillary electrode by cyclic voltammetry using a PAR 174A analyzer. The half-wave reduction potentials were independent of sweep rate between 100-500 mV/sec, with reversibility increasing with increasing scan rates. Most ketones showed a quasi-reversible, if not completely reversible wave.

APPENDIX

The Appendix contains the raw experimental data used to calculate the photokinetic parameters. The data are contained in tables which include: concentrations of ketone, quencher, standards, valerophenone actinometer, and photoproducts formed; product/standard ratios; quencher; solvent and additive (if any); and GC column conditions. Both descriptions of the columns and GC response factors are contained in the experimental section.

In all cases valerophenone in benzene was used as actinometer and was analyzed on column #3 at ∿130°. The GC response factor for acetophenone versus C_{16} is 2.3 and for acetophenone versus C_{14} is 2.0. All quantum yields were performed at 313 nm in a merry-go-round apparatus. Quenchers 2,5-dimethylhexa-2,4-diene, 1,3-pentadiene, and triethylamine were referred to simply as hexadiene, pentadiene, and Et_3N, respectively. All runs using acetonitrile as solvent contained 2% water, unless specifically stated as dry acetonitrile.

REFERENCES

Table 20. Quenching of 0.039 M Valerophenone by Hexadiene in Benzene.[a]

$k_q\tau$ = 47 [Q], M	AP/C_{16} Area Ratio[b]	[AP], 10^{-3} M	ϕ^o/ϕ
0.0	2.10	2.38	---
0.0050	1.69	1.92	1.24
0.0100	1.40	1.59	1.50
0.0200	1.06	1.20	1.99
0.0400	0.703	0.799	2.98
0.0600	0.566	0.643	3.71

[a] RT, 313 nm, 50 min.

[b] $[C_{16}]$ = 4.94 x 10^{-4} M; column #3, 120°.

Table 21. Quenching of Valerophenone by Hexadiene in Acetonitrile.[a]

Run #1: $k_q\tau = 61$, $\Phi_{II} = 0.87^b$

[Q], M	AP/C_{16} Area Ratio[c]	[AP], 10^{-3} M	ϕ^o/ϕ
0.0	1.31	1.84	----
0.0034	1.12	1.57	1.17
0.0068	0.796	1.12	1.64
0.0136	0.655	0.919	2.00
0.0204	0.609	0.854	2.15
0.0272	0.511	0.717	2.56
0.0408	0.395	0.554	3.32

[a] 0.041 M ketone; RT, 313 nm, 25 min.

[b] 0.10 M VP actinometer: AP/C_{16} area ratio = 0.120; $[C_{16}] = 2.69 \times 10^{-3}$ M.

[c] $[C_{16}] = 6.10 \times 10^{-4}$ M; Column #1, 90°.

Run #2: $k_q\tau = 64$

[Q], M	AP/C_{16} Area Ratio[c]	[AP], 10^{-3} M	ϕ^o/ϕ
0.0	2.19	2.05	----
0.00730	1.51	1.41	1.45
0.0150	1.17	1.00	1.87
0.0220	0.903	0.845	2.42
0.0290	0.746	0.698	2.93
0.0440	0.546	0.511	4.00

[a] 0.037 M ketone; RT, 313 nm, 25 min.

[b] $[C_{17}] = 3.90 \times 10^{-4}$ M; column #1, 105°.

Table 22. Quenching of Valerophenone by Triethylamine in Benzene.[a]

Run #1: $k_q\tau = 11$

[Q], M	AP/C_{17} Area Ratio[b]	[AP], 10^{-3} M	ϕ^o/ϕ
0.0	0.755	1.39	---
0.00714	0.701	1.29	1.08
0.0143	0.660	1.21	1.14
0.0286	0.562	1.03	1.34
0.0571	0.448	0.824	1.68
0.0857	0.383	0.704	1.97

[a] 0.021 M ketone; 0.50 M pyridine; RT, 313 nm, 20 min.

[b] $[C_{17}] = 7.66 \times 10^{-4}$ M; column #1, 100°.

Run #2: $k_q\tau = 12$

[Q], M	AP/C_{17} Area Ratio[b]	[AP], 10^{-3} M	ϕ^o/ϕ
0.0	2.21	2.07	---
0.0139	1.97	1.84	1.12
0.0278	1.66	1.55	1.34
0.0555	1.32	1.24	1.68
0.0833	1.13	1.06	1.96

[a] 0.020 M ketone; 0.50 M pyridine; RT, 313 nm, 20 min.

[b] $[C_{17}] = 3.90 \times 10^{-4}$ M; column #1, 100°.

Table 23: Quenching of Valerophenone by Triethylamine in Acetonitrile.[a]

Run #1: $k_q\tau = 13$, $\Phi_{II} = 0.85$

[Q], M	AP/C_{17} Area Ratio[b]	[AP], 10^{-3} M	ϕ^o/ϕ
0.0	1.16	2.75	----
0.0101	1.02	2.42	1.13
0.0202	0.929	2.21	1.24
0.0403	0.778	1.85	1.49
0.0605	0.649	1.54	1.78
0.0807	0.567	1.35	2.04
0.121	0.457	1.08	2.53

[a] 0.041 M ketone; RT, 313 nm.

[b] 0.099 M VP actinometer; AP/C_{17} area ratio = 0.349; [C_{17}] = 1.25 x 10^{-3} M.

[c] [C_{17}] = 9.89 x 10^{-4} M; column #3, 145°.

Run #2: $k_q\tau = 14$, $\Phi_{II} = 0.85$[b]

[Q], M	AP/C_{16} Area Ratio[c]	[AP], 10^{-3} M	ϕ^o/ϕ
0.0	1.07	2.30	----
0.00476	1.00	2.15	1.06
0.00952	0.963	2.07	1.11
0.0190	0.803	1.73	1.33
0.0286	0.781	1.68	1.37
0.0381	0.705	1.52	1.52
0.0571	0.599	1.29	1.78

[a] 0.042 M ketone; RT, 313 nm, 25 min.

[b] 0.11 M VP actinometer: AP/C_{16} ratio = 0.443; [C_{16}] = 8.80 x 10^{-4} M.

[c] [C_{16}] = 9.36 x 10^{-4} M; column #3, 145°.

Table 24. Quenching of 0.040 M Butyrophenone by Hexadiene in Benzene.[a]

$k_q\tau = 560$, $\Phi_{II} = 0.23$[b]

[Q], M	AP/C_{16} Area Ratio[c]	[AP], 10^{-3} M	ϕ^o/ϕ
0.0	3.39	5.44	----
0.00050	2.53	4.06	1.34
0.0010	2.15	3.45	1.57
0.0015	1.91	3.07	1.82
0.0020	1.63	2.62	2.08

[a] RT, 313 nm, 1 hr.

[b] 0.10 M VP actinometer: AP/C_{16} area ratio = 0.773; $[C_{16}] = 2.56 \times 10^{-3}$ M.

[c] $[C_{16}] = 6.98 \times 10^{-4}$ M; column #3, 100°.

Table 25. Quenching of o-Cyanovalerophenone by Hexadiene in Benzene.[a]

Run #1: $k_q\tau$ = 21, Φ_{II} = 0.15[b]

[Q], M	AP/C_{21} Area Ratio[c]	[AP], 10^{-3}	ϕ^o/ϕ
0.0	0.765	2.81	----
0.0071	0.669	2.46	1.14
0.0141	0.591	2.17	1.30
0.0282	0.498	1.83	1.54
0.0423	0.389	1.43	1.97
0.0564	0.344	1.26	2.23

[a] 0.040 M ketone; RT, 313 nm.

[b] 0.25 M VP actinometer: AP/C_{16} area ratio = 0.286; $[C_{16}]$ = 9.72 x 10^{-3} M; (Φ_{II} = 0.35 for 0.25 M VP in benzene).

[c] $[C_{21}]$ = 1.36 x 10^{-3} M; column #3, 195°.

Run #2: $k_q\tau$ = 23, Φ_{II} = 0.15[b]

[Q], M	AP/C_{21} Area Ratio[c]	[AP], 10^{-3} M	ϕ^o/ϕ
0.0	0.752	2.74	----
0.0129	0.540	1.97	1.39
0.0258	0.466	1.70	1.61
0.0387	0.390	1.42	1.93
0.0516	0.357	1.30	2.11

[a] 0.04 M ketone; RT, 313 nm, 2.5 hrs.

[b] 0.25 M VP actinometer: AP/C_{16} area ratio = 0.326; $[C_{16}]$ = 8.39 x 10^{-3} M.

[c] $[C_{21}]$ = 1.35 x 10^{-3} M; column #3, 195°.

Table 26. Quenching of 0.040 M o-Cyanovalerophenone by Pentadiene in Acetonitrile.[a]

$k_q\tau$ = 33, Φ_{II} = 0.54[b]

[Q], M	AP/C_{21} Area Ratio[c]	[AP], 10^{-3} M	ϕ^o/ϕ
0.0	1.70	2.44	----
0.0050	1.64	2.36	1.04
0.0100	1.37	1.97	1.24
0.0200	1.00	1.44	1.70
0.0300	0.843	1.21	2.02
0.0400	0.664	0.954	2.56

[a] RT, 313 nm, 1 hr.

[b] 0.10 M VP actinometer: AP/C_{16} area ratio = 0.160; [C_{16}] = 4.06 x 10^{-3} M.

[c] [C_{21}] = 5.32 x 10^{-4} M; column #2, 130°.

Table 27. Quenching of m-Cyanovalerophenone by Hexadiene in Benzene.[a]

Run #1: $k_q\tau = 19$, $\Phi_{II} = 0.17^b$

[Q], M	AP/C_{21} Area Ratio[c]	[AP], 10^{-3} M	ϕ^o/ϕ
0.0	2.73	9.66	----
0.0210	1.92	6.81	1.43
0.0420	1.55	5.50	1.76
0.0630	1.24	4.40	2.21
0.0840	1.07	3.80	2.56
0.105	0.894	3.17	3.06

[a] 0.041 M ketone; RT, 313 nm, 3.5 hrs.

[b] 0.050 M VP actinometer: AP/C_{16} area ratio = 5.06; $[C_{16}] = 1.50 \times 10^{-3}$ M.

[c] $[C_{21}] = 1.31 \times 10^{-3}$ M; column #4, 200°.

Run #2: $k_q\tau = 19$, $\Phi_{II} = 0.19^b$

[Q], M	AP/C_{19} Area Ratio[c]	[AP], 10^{-3}	ϕ^o/ϕ
0.0	1.45	2.35	----
0.0102	1.17	1.90	1.24
0.0204	1.04	1.69	1.40
0.0306	0.924	1.50	1.57
0.0409	0.824	1.34	1.76
0.0511	0.739	1.12	1.96

[a] 0.040 M ketone; RT, 313 nm, 8 hrs.

[b] 0.060 M VP actinometer: AP/C_{14} area ratio = 0.575; $[C_{14}] = 3.25 \times 10^{-3}$ M.

[c] $[C_{19}] = 6.76 \times 10^{-4}$ M; column #1, 150°.

Table 28. Quenching of 0.039 M m-Cyanovalerophenone by Hexadiene in Acetonitrile.[a]

$k_q\tau = 20$, $\Phi_{II} = 0.63$[b]

[Q], M	AP/C_{19} Area Ratio[c]	[AP], 10^{-3} M	ϕ^o/ϕ
0.0	0.763	1.87	----
0.00641	0.676	1.65	1.13
0.0128	0.598	1.46	1.26
0.0256	0.518	1.27	1.47
0.0385	0.430	1.05	1.77
0.0529	0.380	0.930	2.01
0.0769	0.296	0.725	2.58

[a] RT, 313 nm.

[b] 0.10 M VP actinometer: AP/C_{16} area ratio = 0.111; $[C_{16}] = 3.80 \times 10^{-3}$ M.

[c] $[C_{19}] = 1.02 \times 10^{-3}$ M; column #1, 142°, N_2 on 60 ml/min.

Table 29. Quenching of m-Cyanovalerophenone by Triethylamine in Benzene.[a]

Run #1: $k_q\tau$ = 22, Φ_{II} = 0.23[b], Φ_{max} = 0.65[b]

[Q], M	AP/C_{20} Area Ratio[c]	[AP], 10^{-3} M	ϕ^o/ϕ
0.0	1.37	2.11	----
0.0186	1.04	1.60	1.32
0.0372	0.778	1.20	1.77
0.0745	0.504	0.776	2.73
0.112	0.405	0.624	3.43
0, 0 pyr.	0.482	0.742	----

[a] 0.040 M ketone; 0.50 M pyridine; RT, 313 nm, 40 min.

[b] 0.10 M VP actinometer: AP/C_{16} area ratio = 0.348; $[C_{16}]$ = 1.28 x 10^{-3} M.

[c] $[C_{20}]$ = 6.16 x 10^{-4} M; column #1, 151°.

Run #2: $k_q\tau$ = 22, Φ_{II} = 0.22,[b]

[Q], M	AP/C_{20} Area Ratio[c]	[AP], 10^{-3} M	ϕ^o/ϕ
0.0	1.21	1.91	----
0.051	0.542	0.854	2.23
0.076	0.441	0.695	2.73
0.101	0.373	0.588	3.23
0.127	0.322	0.507	3.75
0, 0 pyr	0.662	1.04	----

[a] 0.040 M ketone; 0.049 M pyridine; RT, 313 nm, 1 hr.

[b] 0.10 M VP actinometer: AP/C_{16} area ratio = 0.0959; $[C_{16}]$ = 7.02 x 10^{-3} M.

[c] $[C_{20}]$ = 6.30 x 10^{-4} M; column #1, 148°.

Table 30. Quenching of m-Cyanovalerophenone by Triethylamine in Acetonitrile.[a]

Run #1: $k_q\tau$ = 10, Φ_{II} = 0.73[b]

[Q], M	AP/C_{20} Area Ratio[c]	[AP], 10^{-3} M	ϕ^o/ϕ
0.0	1.24	2.01	----
0.0124	1.14	1.85	1.09
0.0247	0.953	1.54	1.31
0.0494	0.833	1.35	1.49
0.0741	0.716	1.16	1.74
0.0988	0.625	1.01	1.99
0.148	0.483	0.783	2.58

[a] 0.040 M ketone; RT, 313 nm.

[b] 0.11 M VP Actinometer: AP/C_{16} area ratio = 0.358; $[C_{16}]$ = 1.15 x 10^{-3} M.

[c] $[C_{20}]$ = 6.48 x 10^{-4}; column #1, 138°.

Run #2: $k_q\tau$ = 10

[Q], M	AP/C_{19} Area Ratio[b]	[AP], 10^{-3} M	ϕ^o/ϕ
0.0	1.37	1.87	----
0.0091	1.29	1.77	1.06
0.0182	1.20	1.64	1.14
0.0365	0.978	1.34	1.40
0.0548	0.866	1.19	1.58
0.0730	0.814	1.11	1.68
0.109	0.618	0.846	2.21

[a] 0.036 M ketone; RT, 313 nm. [b] $[C_{19}]=5.95\times10^{-4}$ M; column #1, 140°.

Table 31. Quenching of p-Cyanovalerophenone by Hexadiene in Benzene.[a]

Run #1: $k_q\tau = 75$, $\Phi_{II} = 0.22$[b]

[Q], M	AP/C_{20} Area Ratio[c]	[AP], 10^{-3} M	ϕ^o/ϕ
0.0	0.772	2.33	----
0.00586	0.513	1.55	1.51
0.0117	0.423	1.28	1.82
0.0234	0.285	0.860	2.71
0.0352	0.212	0.639	3.64
0.0469	0.168	0.507	4.60

[a] 0.042 M ketone; RT, 313 nm, 2 hrs.

[b] 0.10 M VP actinometer: AP/C_{16} area ratio = 0.182; $[C_{16}] = 8.21 \times 10^{-3}$ M.

[c] $[C_{20}] = 1.16 \times 10^{-3}$ M; column #3, 190°.

Run #2: $k_q\tau = 73$, $\Phi_{II} = 0.20$[b]

[Q], M	AP/C_{19} Area Ratio[c]	[AP], 10^{-3} M	ϕ^o/ϕ
0.0	2.30	3.54	----
0.0193	1.01	1.55	2.28
0.0579	0.471	0.725	4.90
0.0772	0.348	0.536	6.61
0.0964	0.274	0.422	8.24

[a] 0.041 M ketone; RT, 313 nm, 8 hrs.

[b] 0.050 M VP actinometer: AP/C_{14} area ratio = 0.621; $[C_{14}] = 4.08 \times 10^{-3}$ M.

[c] $[C_{19}] = 5.92 \times 10^{-4}$ M; column #3, 190°.

Table 32. Quenching of 0.040 M p-Cyanovalerophenone by Hexadiene in Acetonitrile.[a]

$k_q\tau$ = 87, Φ_{II} = 0.80[b]

[Q], M	AP/C_{19} Area Ratio[c]	[AP], 10^{-3} M	ϕ^o/ϕ
0.0	0.950	2.26	----
0.00419	0.667	1.59	1.42
0.0168	0.406	0.966	2.34
0.0251	0.286	0.680	3.32
0.0335	0.246	0.585	3.84
0.0503	0.178	0.423	5.33

[a] RT, 313 nm, 1/2 hr.

[b] 0.10 M VP actinometer: AP/C_{16} area ratio = 0.191; $[C_{16}]$ = 2.12 x 10^{-3} M.

[c] $[C_{19}]$ = 9.91 x 10^{-4} M; column #1, 142°.

Table 33. Quenching of p-Cyanovalerophenone by Triethylamine in Benzene.[a]

Run #1: $k_q\tau = 86$

[Q], M	AP/C_{20} Area Ratio[b]	[AP], 10^{-3} M	ϕ^o/ϕ
0.0	1.41	1.06	----
0.00934	1.53	1.15	0.92
0.0187	1.09	0.822	1.30
0.0374	0.658	0.496	2.15
0.0561	0.484	0.365	2.92

[a] 0.021 M ketone; 0.50 M pyridine; RT, 313 nm, 20 min.

[b] $[C_{20}] = 2.90 \times 10^{-4}$ M; column #1, 150°.

Run #2: $k_q\tau = 96$, $\Phi_{0.25\text{ M pyr}} = 0.37^b$

[Q], M	AP/C_{20} Area Ratio	[AP], 10^{-3} M	ϕ^o/ϕ
0.0	1.39	1.41	----
0.0046	2.09	2.12	0.66
0.0093	1.63	1.65	0.85
0.0139	1.30	1.32	1.07
0.0186	1.06	1.07	1.31
0.0316	0.665	0.674	2.09
0.0557	0.532	0.539	2.61

[a] 0.040 M ketone; 0.25 M pyridine; RT, 313 nm, 30 min.

[b] 0.10 M VP actinometer: AP/C_{16} area ratio = 0.280; $[C_{16}] = 1.94 \times 10^{-3}$ M.

[c] $[C_{20}] = 3.90 \times 10^{-4}$ M; column #1, 150°.

Table 33. Continued.

Run #3: $k_q\tau = 91$

[Q], M	AP/C_{20} Area Ratio[b]	[AP], 10^{-3} M	ϕ^o/ϕ
0.0	1.25	1.01	----
0.0093	1.57	1.27	0.80
0.0187	1.03	0.836	1.21
0.0373	0.794	0.644	1.58
0.0560	0.417	0.338	3.00

[a] 0.020 M ketone; 0.50 M pyridine; RT, 313 nm, 20 min.

[b] $[C_{20}] = 3.12 \times 10^{-4}$ M; column #1, 150°.

Table 34. Quenching of 0.042 M p-Cyanovalerophenone by Low Concentrations of Triethylamine in Benzene.[a]

[Q], M	AP/C_{20} Area Ratio[b]	[AP], 10^{-3} M	ϕ^0/ϕ
0.0	1.44	1.88	----
0.0012	1.81	2.36	0.80
0.0024	2.29	2.99	0.63
0.0048	1.77	2.31	0.81
0.0072	1.67	2.18	0.87
0.0096	1.57	2.05	0.92
0.0143	1.42	2.05	1.0

[a] 0.54 M pyridine; RT, 313 nm, 50 min.

[b] $[C_{20}] = 5.02 \times 10^{-4}$ M; column #1, 135°.

Table 35. Quenching of 0.037 M p-Cyanovalerophenone by Triethylamine in Acetonitrile.[a]

$k_q\tau = 92$, $\Phi_{II} = 0.67$[b]

[Q], M	AP/C_{19} Area Ratio[c]	[AP], 10^{-3} M	ϕ^o/ϕ
0.0	0.914	1.66	----
0.000664	0.904	1.64	1.01
0.00133	0.858	1.56	1.06
0.00266	0.769	1.40	1.19
0.00398	0.694	1.26	1.32
0.00531	0.657	1.19	1.39
0.00797	0.579	1.05	1.58

[a] RT, 313 nm.

[b] 0.12 M VP actinometer: AP/C_{16} area ratio = 0.67; $[C_{16}] = 3.49 \times 10^{-3}$ M.

[c] $[C_{19}] = 7.56 \times 10^{-4}$ M; column #3, 180°.

Table 36. Quenching of 0.041 M p-Cyanobutyrophenone by Hexadiene in Benzene.[a]

$k_q\tau = 360$, $\Phi_{II} = 0.12$[b]

[Q], M	AP/C_{20} Area Ratio[c]	[AP], 10^{-3} M	ϕ^o/ϕ
0.0	1.66	3.00	----
0.00050	1.42	2.56	1.17
0.0010	1.22	2.22	1.36
0.0020	1.17	2.11	1.76
0.0040	0.654	1.18	2.54
0.0060	0.499	0.900	3.33

[a] RT, 313 nm, 2 hrs.

[b] 0.10 M VP actinometer: AP/C_{16} area ratio = 1.43; [C_{16}] = 2.56 x 10^{-3} M.

[c] [C_{20}] = 6.94 x 10^{-4} M; column #2, 110°.

Table 37. Quenching of 0.040 M p-Cyanobutyrophenone by Hexadiene in Benzene.[a]

$k_q\tau$ = 435, Φ_{II} = 0.12[b]

[Q], M	AP/C_{20} Area Ratio[c]	[AP], 10^{-3} M	ϕ^o/ϕ
0.0	1.88	3.71	----
0.000248	1.61	3.17	1.17
0.000496	1.48	2.92	1.27
0.000993	1.23	2.42	1.52
0.00149	1.11	2.19	1.69
0.00199	1.04	2.05	1.80
0.00298	0.87	1.71	2.16

[a] RT, 313 nm, 2-1/2 hrs.

[b] 0.10 M VP actinometer: AP/C_{16} area ratio = 2.26; [C_{16}] = 1.94 x 10^{-3} M.

[c] [C_{20}] = 7.58 x 10^{-4} M; column #2, 110°.

Table 38. Quenching of 0.037 M p-Cyano-γ-Methylvalerophenone by Hexadiene in Benzene.[a]

$k_q\tau$ = 18, Φ_{II} = 0.13[b]

[Q], M	AP/C_{20} Area Ratio[c]	[AP], 10^{-3} M	ϕ^o/ϕ
0.0	0.753	1.50	----
0.0050	0.644	1.28	1.17
0.0100	0.600	1.20	1.25
0.0201	0.583	1.16	1.32
0.0301	0.461	0.918	1.63

[a] RT, 313 nm, 2 hrs.

[b] 0.10 M VP actinometer: AP/C_{16} area ratio = 0.847; $[C_{16}]$ = 1.99 x 10^{-3} M.

[c] $[C_{20}]$ = 7.66 x 10^{-4} M; column #2, 120°.

Table 39. Quenching of o-Carbomethoxyvalerophenone by Hexadiene in Benzene.[a]

Run #1: $k_q\tau$ = 138, Φ_{II} = 0.04[b]

[Q], M	AP/C_{20} Area Ratio[c]	[AP], 10^{-4} M	ϕ^o/ϕ
0.0	0.955	7.26	----
0.00142	0.837	6.36	1.14
0.00283	0.724	5.50	1.32
0.00567	0.520	3.95	1.84
0.00850	0.440	3.34	2.17
0.0113	0.366	2.78	2.61
0.0170	0.277	2.11	3.45

[a] 0.043 M ketone; RT, 313 nm, 2 hrs.

[b] 0.10 M VP actinometer: AP/C_{16} area ratio = 1.16; [C_{16}] = 2.25 x 10^{-3} M.

[c] [C_{20}] = 3.04 x 10^{-4} M; column #1, 140°.

Run #2: $k_q\tau$ = 150,

[Q], M	AP/C_{20} Area Ratio[b]	[AP], 10^{-3} M	ϕ^o/ϕ
0.0	3.61	3.75	----
0.0101	1.49	1.55	2.42
0.0203	0.917	0.954	3.94
0.0304	0.695	0.723	5.19
0.0405	0.493	0.513	7.32

[a] 0.051 M ketone; RT, 313 nm, 1-1/2 hrs.

[b] [C_{20}] = 4.16 x 10^{-4} M; column #3, 180°.

Table 39. Continued.

Run #3: $k_q\tau = 120$

[Q], M	AP/C_{20} Area Ratio[b]	[AP], 10^{-3} M	ϕ^o/ϕ
0.0	3.71	1.50	----
0.00518	2.30	0.932	1.62
0.0102	1.65	0.668	2.25
0.0154	1.35	0.547	2.75
0.0205	1.12	0.454	2.03
0.0256	0.894	0.362	4.15

[a] 0.042 M ketone; RT, 313 nm, 2 hrs.

[b] $[C_{20}] = 1.62 \times 10^{-4}$ M; column #3, 180°.

Table 40. Quenching of 0.041 M o-Carbomethoxyvalerophenone by Hexadiene in Acetonitrile.[a]

$k_q\tau = 338$, $\Phi_{II} = 0.19$[b]

[Q], M	AP/C_{20} Area Ratio[c]	[AP], 10^{-3} M	ϕ^o/ϕ
0.0	1.28	1.62	----
0.000772	0.987	1.25	1.30
0.00154	0.829	1.05	1.54
0.00309	0.625	0.789	2.05
0.00463	0.482	0.609	2.66
0.00617	0.422	0.533	3.03
0.00926	0.304	0.384	4.22

[a] RT, 313 nm, 2-1/2 hrs.

[b] 0.10 M VP actinometer: AP/C_{16} area ratio = 0.340; $[C_{16}] = 3.58 \times 10^{-3}$ M.

[c] $[C_{20}] = 5.05 \times 10^{-4}$ M; column #1, 125°.

Table 41. Quenching of o-Carbomethoxyvalerophenone by Triethylamine in Benzene.[a]

Run #1: $k_q\tau = 60$, $\Phi_{max} = 0.13^b$

[Q], M	AP/C_{20} Area Ratio[c]	[AP], 10^{-3} M	ϕ^o/ϕ
0.0	1.24	2.41	----
0.00745	1.08	2.10	1.14
0.0149	0.854	1.66	1.46
0.0298	0.552	1.07	2.25
0.0447	0.415	0.807	3.00
0.0596	0.328	0.638	3.80

[a] 0.041 M ketone; RT, 313 nm, 4 hrs.

[b] 0.11 M VP actinometer: AP/C_{16} area ratio = 1.14; $[C_{16}] = 2.43 \times 10^{-3}$ M.

[c] $[C_{20}] = 7.78 \times 10^{-4}$ M; column #1, 135°.

Run #2: $k_q\tau = 57$, $\Phi_{max} = 0.10^b$

[Q], M	AP/C_{20} Area Ratio[c]	[AP], 10^{-3} M	ϕ^o/ϕ
0.0	1.89	2.78	----
0.00365	1.88	2.76	1.01
0.00729	1.86	2.73	1.03
0.0146	1.58	2.32	1.20
0.0292	1.04	1.53	1.82
0.0438	0.785	1.15	2.41

[a] 0.044 M ketone; RT, 313 nm, 4 hrs.

[b] 0.11 M VP actinometer: AP/C_{16} area ratio = 0.963; $[C_{16}] = 4.28 \times 10^{-3}$ M.

[c] $[C_{20}] = 5.88 \times 10^{-4}$ M; column #1, 135°.

Table 42. Quenching of o-Carbomethoxyvalerophenone by Triethylamine in Acetonitrile.[a]

Run #1: $k_q\tau = 89$, $\Phi_{II} = 0.11$[b]

[Q], M	AP/C_{20} Area Ratio[c]	[AP], 10^{-3} M	ϕ^0/ϕ
0.0	1.00	1.76	----
0.00251	0.826	1.45	1.21
0.00502	0.725	1.27	1.38
0.0100	0.55	0.974	1.81
0.0151	0.427	0.749	2.35
0.0201	0.350	0.614	2.87
0.0301	0.265	0.465	3.78

[a] 0.041 M ketone; RT, 313 nm, 4 hrs.

[b] 0.11 M VP actinometer: AP/C_{16} area ratio = 0.661; $[C_{16}] = 3.36 \times 10^{-3}$ M.

[c] $[C_{20}] = 7.02 \times 10^{-4}$ M; column #1, 131°.

Run #2: $k_q\tau = 78$, $\Phi_{II} = 0.10$[b]

[Q], M	AP/C_{20} Area Ratio[c]	[AP], 10^{-4} M	ϕ^0/ϕ
0.0	0.544	9.47	----
0.00135	0.495	8.61	1.10
0.00270	0.459	7.99	1.19
0.00540	0.392	6.82	1.39
0.00809	0.335	5.83	1.62
0.0108	0.294	5.12	1.85
0.0162	0.242	4.21	2.24

[a] 0.041 M ketone; RT, 313 nm, 1 hr, 40 min.

[b] 0.11 M VP actinometer: AP/C_{16} area ratio = 0.351; $[C_{16}] = 3.75 \times 10^{-3}$ M.

[c] $[C_{20}] = 6.96 \times 10^{-4}$ M; column #1, 135°.

Table 43. Quenching of m-Carbomethoxyvalerophenone by Hexadiene in Benzene.[a]

Run #1: $k_q\tau = 19$, $\Phi_{II} = 0.24$[b]

[Q], M	AP/C_{20} Area Ratio[c]	[AP], 10^{-3} M	ϕ^o/ϕ
0.0	1.02	2.08	----
0.0103	0.857	1.74	1.19
0.0206	0.721	1.47	1.41
0.0413	0.569	1.16	1.76
0.0619	0.458	0.932	2.22
0.0826	0.398	0.810	2.56

[a] 0.049 M ketone; RT, 313 nm, 1-1/2 hrs.

[b] 0.11 M VP actinometer: AP/C_{16} area ratio = 0.276; $[C_{16}] = 4.42 \times 10^{-3}$ M.

[c] $[C_{20}] = 8.14 \times 10^{-4}$ M; column #3, 185°.

Run #2: $k_q\tau = 17$, $\Phi_{II} = 0.26$[b]

[Q], M	AP/C_{20} Area Ratio[c]	[AP], 10^{-3} M	ϕ^o/ϕ
0.0	1.28	2.58	----
0.0110	1.11	2.24	1.15
0.0220	0.954	1.92	1.34
0.0450	0.742	1.50	1.72
0.0670	0.578	1.17	2.21

[a] 0.050 M ketone; RT, 313 nm, 1-3/4 hrs.

[b] 0.10 M VP actinometer: AP/C_{16} area ratio = 0.349; $[C_{16}] = 4.33 \times 10^{-3}$ M.

[c] $[C_{20}] = 8.07 \times 10^{-4}$ M; column #3, 190°.

Table 44. Quenching of m-Carbomethoxyvalerophenone by Pentadiene in Acetonitrile.[a]

Run #1: $k_q\tau = 21$, $\Phi_{II} = 0.90^b$

[Q], M	AP/C_{21} Area Ratio[c]	[AP], 10^{-3} M	ϕ^o/ϕ
0.0	2.06	5.72	----
0.0100	1.61	4.47	1.28
0.0200	1.39	3.86	1.48
0.0400	1.10	3.05	1.87
0.0500	0.991	2.75	2.08
0.0600	0.894	2.48	2.30
0.0800	0.779	2.16	2.64
0.100	0.654	1.81	3.15

[a] 0.040 M ketone; RT, 313 nm, 25 min.

[b] 0.10 M VP actinometer: AP/C_{16} area ratio = 0.204; $[C_{16}] = 3.80 \times 10^{-3}$ M.

[c] $[C_{21}] = 1.11 \times 10^{-3}$ M; column #2, 130°.

Run #2: $k_q\tau = 20$, $\Phi_{II} = 0.90^b$

[Q], M	AP/C_{21} Area Ratio[c]	[AP], 10^{-3} M	ϕ^o/ϕ
0.0	2.96	4.49	----
0.0100	2.53	3.84	1.17
0.0200	2.15	3.26	1.38
0.0400	1.59	2.41	1.86
0.0600	1.30	1.97	2.28
0.0800	1.15	1.75	2.58
0.100	1.05	1.59	2.82

[a] 0.040 M ketone; RT, 313 nm, 30 min. [b] 0.10 M VP actinometer; AP/C_{16} area ratio = 0.313; $[C_{16}] = 1.99 \times 10^{-3}$ M. [c] $[C_{21}] = 6.07 \times 10^{-4}$ M; column #2, 140°.

Table 45. Quenching of 0.040 M m-Carbomethoxyvalerophenone by Triethylamine in Benzene.[a]

$k_q\tau$ = 25, Φ_{II} = 0.25,[b] Φ_{max} = 0.54[b]

[Q], M	AP/C_{20} Area Ratio[c]	[AP], 10^{-3} M	ϕ^o/ϕ
0.0	1.92	3.53	----
0.0251	1.53	2.82	1.26
0.0502	1.10	2.02	1.74
0.0753	0.932	1.71	2.06
0.100	0.707	1.30	2.72
0.151	0.521	0.959	3.69
0, 0 pyr	0.898	1.65	----

[a] 0.50 M pyridine; RT, 313 nm, 30 min.

[b] 0.10 M VP actinometer: AP/C_{16} area ratio = 0.540; $[C_{16}]$ = 1.72 x 10^{-3} M.

[c] $[C_{20}]$ = 7.36 x 10^{-4} M; column #1, 140°.

Table 46. Quenching of p-Carbomethoxyvalerophenone by Hexadiene in Benzene.[a]

Run #1: $k_q\tau = 44$, $\Phi_{II} = 0.19$[b]

[Q], M	AP/C_{20} Area Ratio[c]	[AP], 10^{-3} M	ϕ^o/ϕ
0.0	0.841	1.73	----
0.00397	0.740	1.52	1.14
0.00794	0.605	1.24	1.39
0.0159	0.507	1.04	1.66
0.0238	0.400	0.822	2.10
0.0318	0.348	0.715	2.41

[a] 0.050 M ketone; RT, 313 nm.

[b] 0.10 M VP actinometer: AP/C_{16} area ratio = 0.264; $[C_{16}] = 4.90 \times 10^{-3}$M.

[c] $[C_{20}] = 8.22 \times 10^{-4}$ M; column #3, 190°.

Run #2: $k_q\tau = 40$, $\Phi_{II} = 0.19$[b]

[Q], M	AP/C_{20} Area Ratio[c]	[AP], 10^{-3} M	ϕ^o/ϕ
0.0	1.18	1.82	----
0.00327	1.06	1.63	1.12
0.00654	0.857	1.32	1.38
0.0131	0.885	1.36	1.34
0.0196	0.652	1.00	1.82
0.0262	0.619	0.953	1.91
0.0393	0.486	0.748	2.44

[a] 0.041 M ketone; RT, 313 nm, 1 hr.

[b] 0.11 M VP actinometer: AP/C_{16} area ratio = 0.452; $[C_{16}] = 3.09 \times 10^{-3}$ M.

[c] $[C_{20}] = 6.16 \times 10^{-4}$ M; column #1, 145°.

Table 47. Quenching of p-Carbomethoxyvalerophenone by Hexadiene in Acetonitrile.[a]

Run #1: $k_q\tau$ = 63

[Q], M	AP/C_{20} Area Ratio[b]	[AP], 10^{-3} M	ϕ^o/ϕ
0.0	1.62	2.97	----
0.00323	1.33	2.44	1.33
0.00647	1.09	2.00	1.49
0.0129	0.875	1.61	1.85
0.0194	0.748	1.37	2.17
0.0259	0.597	1.10	2.71
0.0388	0.496	0.910	3.26

[a] 0.041 M ketone; RT, 313 nm, 30 min.

[b] $[C_{20}]$ = 7.34 x 10^{-4} M; column #1, 140°.

Run #2: $k_q\tau$ = 53, Φ_{II} = 0.52[b]

[Q], M	AP/C_{20} Area Ratio[c]	[AP], 10^{-3} M	ϕ^o/ϕ
0.0	1.21	2.08	----
0.0050	1.02	1.75	1.19
0.0100	0.766	1.31	1.58
0.0200	0.568	0.974	2.13
0.0300	0.449	0.770	2.70
0.0400	0.403	0.691	3.01
0.0600	0.301	0.516	4.02

[a] 0.040 M ketone; RT, 313 nm, 30 min.

[b] 0.10 M VP actinometer: AP/C_{16} area ratio = 0.204; $[C_{16}]$ = 2.83 x 10^{-3} M.

[c] $[C_{20}]$ = 6.86 x 10^{-4} M; column #3, 160°.

Table 48. Quenching of p-Carbomethoxyvalerophenone by Triethylamine in Benzene.[a]

Run #1: $k_q\tau$ = 47, Φ_{II} = 0.22[b] Φ_{max} = 0.32[b]

[Q], M	AP/C_{20} Area Ratio[c]	[AP], 10^{-3} M	ϕ^o/ϕ
0.0	2.04	3.33	----
0.0130	1.86	3.03	1.10
0.0259	1.53	2.49	1.33
0.0389	1.11	1.81	1.84
0.0518	0.983	1.60	2.07
0.0777	0.700	1.14	2.91
0, 0 pyr	1.41	2.30	----

[a] 0.044 M ketone; 0.51 M pyridine; RT, 313 nm, 1 hr.

[b] 0.11 M VP actinometer: AP/C_{16} area ratio = 0.786; $[C_{16}]$ = 1.90 x 10^{-3} M.

[c] $[C_{20}]$ = 6.52 x 10^{-4} M; column #1, 140°.

Run #2: $k_q\tau$ = 44

[Q], M	AP/C_{20} Area Ratio[b]	[AP], 10^{-3} M	ϕ^o/ϕ
0.0	0.664	1.20	----
0.0056	0.997	1.80	0.67
0.0111	0.802	1.45	0.83
0.0445	0.395	0.713	1.68
0.0667	0.323	0.583	2.06

[a] 0.041 M ketone; 0.50 M pyridine; RT, 313 nm, 40 min.

[b] $[C_{20}]$ = 7.22 x 10^{-4} M; column #4, 140°.

Table 49. Quenching of p-Carbomethoxyvalerophenone by Triethylamine in Acetonitrile.[a]

Run #1: $k_q\tau = 93$

[Q], M	AP/C_{20} Area Ratio[b]	[AP], 10^{-3} M	ϕ^o/ϕ
0.0	1.56	2.70	----
0.00701	1.17	2.03	1.34
0.0140	0.848	1.47	1.84
0.0281	0.514	0.891	3.04
0.0561	0.297	0.515	5.25
0.0841	0.194	0.336	8.47

[a] 0.040 M ketone; RT, 313 nm, 25 min.

[b] $[C_{20}] = 6.93 \times 10^{-4}$ M; column #1, 138°.

Run #2: $k_q\tau = 91$, $\Phi_{II} = 0.75$[b]

[Q], M	AP/C_{20} Area Ratio[c]	[AP], 10^{-3} M	ϕ^o/ϕ
0.0	2.19	3.08	----
0.00272	2.12	2.98	1.04
0.00545	1.59	2.24	1.38
0.00817	1.46	2.06	1.50
0.0109	1.24	1.75	1.77
0.0163	1.01	1.42	2.16
0.0218	0.815	1.15	2.69

[a] 0.041 M ketone; RT, 313 nm, 30 min.

[b] 0.11 M VP actinometer: AP/C_{16} area ratio = 0.415; $[C_{16}] = 1.32 \times 10^{-3}$ M.

[c] $[C_{20}] = 5.63 \times 10^{-4}$ M; column #1, 140°.

Table 49. Continued.

Run #3: $k_q\tau$ = 89, Φ_{II} = 0.65[b]

[Q], M	AP/C_{20} Area Ratio[c]	[AP], 10^{-3}	ϕ^o/ϕ
0.0	4.10	5.72	----
0.0050	4.20	5.86	0.96
0.0100	3.16	4.41	1.30
0.0200	2.15	3.00	1.91
0.0300	1.57	2.19	2.61
0.0400	1.38	1.93	2.97
0.0600	0.997	1.39	4.11

[a] 0.040 M ketone; RT, 313 nm, 30 min.

[b] 0.10 M VP actinometer: AP/C_{16} area ratio = 0.329; $[C_{16}]$ = 3.84 x 10^{-3} M.

[c] $[C_{20}]$ = 5.58 x 10^{-4} M; column #2, 130°.

Table 50. Quenching of m-Divalerylbenzene by Hexadiene in Benzene.[a]

Run #1: $k_q\tau = 37$, $\Phi_{II} = 0.22$[b]

[Q], M	AP/C_{24} Area Ratio[c]	[AP], 10^{-3} M	ϕ^o/ϕ
0.0	1.67	3.34	----
0.0112	1.08	2.16	1.55
0.0224	0.851	1.70	1.96
0.0448	0.649	1.30	2.57
0.0671	0.464	0.928	3.59
0.0895	0.399	0.798	4.18
0.112	0.348	0.696	4.79

[a] 0.038 M ketone; RT, 313 nm, 1-1/2 hrs.

[b] 0.055 M VP actinometer: AP/C_{16} area ratio = 0.904; $[C_{16}]$ = 2.25 x 10^{-3} M.

[c] $[C_{24}]$ = 1.00 x 10^{-3} M; column #4, 195°.

Run #2: $k_q\tau = 38$

[Q], M	AP/C_{22} Area Ratio[b]	[AP], 10^{-3} M	ϕ^o/ϕ
0.0	1.85	2.26	----
0.0075	1.45	1.77	1.28
0.0150	1.18	1.44	1.57
0.0300	0.792	0.969	2.34
0.0450	0.765	0.936	2.42
0.0600	0.561	0.686	3.30

[a] 0.020 M ketone; RT, 313 nm, 1 hr.

[b] $[C_{22}]$ = 6.44 x 10^{-4} M; column #2, 170°.

Table 51. Quenching of 0.032 M m-Divalerylbenzene by Hexadiene in Acetonitrile.[a]

$k_q\tau = 46$, $\Phi_{II} = 0.70$[b]

[Q], M	AP/C_{22} Area Ratio[c]	[AP], 10^{-3} M	ϕ^o/ϕ
0.0	2.81	3.56	----
0.0037	2.50	3.17	1.12
0.0073	2.04	2.59	1.38
0.0146	1.69	2.14	1.67
0.0220	1.38	1.75	2.04
0.0293	1.17	1.48	2.39
0.0439	0.951	1.21	2.96

[a] RT, 313 nm, 20 min.

[b] 0.11 M VP actinometer: AP/C_{16} area ratio = 0.160; $[C_{16}] = 4.55 \times 10^{-3}$ M.

[c] $[C_{22}] = 6.67 \times 10^{-4}$ M; column #3, 170°.

Table 52. Quenching of 0.029 M m-Divalerylbenzene by Triethylamine in Benzene.[a]

$k_q\tau = 28$, $\Phi_{max} = 0.54$[b]

[Q], M	AP/C_{22} Area Ratio[c]	[AP], 10^{-3} M	ϕ^o/ϕ
0.0	0.813	2.09	----
0.0110	0.754	1.93	1.08
0.0220	0.637	1.63	1.28
0.0440	0.450	1.15	1.81
0.0660	0.340	0.872	2.39
0.0881	0.278	0.713	2.93
0.132	0.204	0.523	3.98

[a] 0.53 M pyridine; RT, 313 nm, 25 min.

[b] 0.11 M VP actinometer: AP/C_{16} area ratio = 0.160; $[C_{16}] = 3.49 \times 10^{-3}$ M.

[c] $[C_{22}] = 1.35 \times 10^{-3}$ M; column #1, 143°.

Table 53. Quenching of m-Divalerylbenzene by Triethylamine in Acetonitrile.[a]

Run #1: $k_q\tau$ = 33

[Q], M	AP/C_{22} Area Ratio[b]	[AP], 10^{-4} M	ϕ^o/ϕ
0.0	0.509	7.41	----
0.0050	0.458	6.67	1.11
0.0100	0.383	5.57	1.33
0.0200	0.307	4.47	1.66
0.0300	0.275	4.00	1.85
0.0400	0.214	3.12	2.38
0.0600	0.172	2.50	2.96

[a] 0.037 M ketone; RT, 313 nm, 20 min.

[b] $[C_{22}]$ = 7.66 x 10^{-4} M; column #2, 152°.

Run #2: $k_q\tau$ = 34

[Q], M	AP/C_{22} Area Ratio[b]	[AP], 10^{-3} M	ϕ^o/ϕ
0.0	1.15	1.32	----
0.0050	1.33	1.53	0.86
0.0100	0.835	0.960	1.38
0.0200	0.672	0.773	1.71
0.0300	0.610	0.701	1.89
0.0400	0.466	0.536	2.47
0.0600	0.396	0.455	2.90

[a] 0.035 M ketone; RT, 313 nm, 25 min.

[b] $[C_{22}]$ = 6.05 x 10^{-4} M; column #1, 138°.

Table 54. Quenching of p-Divalerylbenzene by Hexadiene in Benzene.[a]

Run #1: $k_q\tau = 188$

[Q], M	AP/C_{24} Area Ratio[b]	[AP], 10^{-3} M	ϕ^o/ϕ
0.0	1.25	2.27	----
0.00401	0.688	1.25	1.82
0.00803	0.504	0.915	2.47
0.0120	0.398	0.723	3.13
0.0161	0.297	0.539	4.20

[a] 0.040 M ketone; RT, 313 nm, 2 hrs.

[b] $[C_{24}] = 9.08 \times 10^{-4}$ M; column #4, 200°.

Run #2: $k_q\tau = 178$, $\Phi_{II} = 0.10$[b] $\Phi_{max} = 0.17$

[Q], M	AP/C_{24} Area Ratio[c]	[AP], 10^{-3} M	ϕ^o/ϕ
0.0	1.43	2.47	----
0.00417	1.07	1.84	1.34
0.00833	0.623	1.07	2.30
0.0125	0.429	0.740	3.33
0.0167	0.341	0.588	4.19
0, 1 M pyr	2.32	4.00	----

[a] 0.040 M ketone; RT, 313 nm, 2 hrs.

[b] 0.10 M VP actinometer: AP/C_{16} area ratio = 0.845; $[C_{16}] = 4.1 \times 10^{-3}$ M.

[c] $[C_{24}] = 8.62 \times 10^{-4}$ M; column #4, 200°.

Table 55. Quenching of p-Acetylvalerophenone by Hexadiene in Benzene.[a]

Run #1: $k_q\tau$ = 300, Φ_{II} = 0.10[b]

[Q], M	AP/C_{20} Area Ratio[c]	[AP], 10^{-3} M	ϕ^o/ϕ
0.0	1.23	1.79	----
0.000622	0.989	1.44	1.24
0.00124	0.819	1.19	1.50
0.00249	0.654	0.952	1.87
0.00373	0.650	0.946	1.89
0.00497	0.527	0.767	2.32

[a] 0.040 M ketone; RT, 313 nm, 2-1/2 hrs.

[b] 0.10 M VP actinometer: AP/C_{16} area ratio = 0.848; [C_{16}] = 2.96 x 10^{-3} M.

[c] [C_{20}] = 5.60 x 10^{-4} M; column #1, 135°.

Run #2: $k_q\tau$ = 400, Φ_{II} = 0.09[b]

[Q], M	AP/C_{20} Area Ratio[c]	[AP], 10^{-3} M	ϕ^o/ϕ
0.0	1.73	7.02	----
0.000599	1.28	5.19	1.35
0.00120	1.13	4.58	1.53
0.00180	1.01	4.10	1.72
0.00299	0.797	3.23	2.18

[a] 0.032 M ketone; RT, 313 nm, 3 hrs.

[b] 0.052 M VP actinometer: AP/C_{16} area ratio = 1.01; [C_{16}] = 1.94 x 10^{-3} M.

[c] [C_{20}] = 1.56 x 10^{-3} M; column #4, 195°.

Table 56. Quantum Yields for 0.040 M Trifluoromethylvalerophenones in Benzene.[a]

Ketone	AP/C_{13} or C_{16} Area Ratio[b]	[AP], 10^{-3} M	Φ_{II}[c]
o-CF_3	0.212	0.382	0.15
o-CF_3[d]	1.22[d]	2.33	0.89
o-CF_3[e]	1.25[e]	2.39	0.91
m-CF_3	0.224	0.495	0.19
m-CF_3[d]	0.993[d]	1.89	0.72
m-CF_3[e]	1.02[e]	1.95	0.74
p-CF_3	0.202	0.611	0.23
p-CF_3[d]	1.26[d]	2.40	0.92
p-CF_3[e]	1.43[e]	2.73	1.0

[a] RT, 313 nm, 30 min.

[b] for o-CF_3VP: $[C_{13}] = 1.06 \times 10^{-3}$ M; for m-CF_3VP: $[C_{13}] = 1.30 \times 10^{-3}$ M; for p-CF_3VP: $[C_{13}] = 1.78 \times 10^{-3}$ M; column #2, 71°.

[c] 0.10 M VP actinometer: AP/C_{16} area ratio = 0.170; $[C_{16}] = 2.21 \times 10^{-3}$ M.

[d] 0.050 M pyridine; $[C_{16}] = 9.54 \times 10^{-4}$ M; column #2, 71°.

[e] 0.10 M pyridine; $[C_{16}] = 9.54 \times 10^{-4}$ M; column #2, 71°.

Table 57. Disappearance Quantum Yields for Cyanovalerophenones in Benzene.[a]

For m-CNVP:

	VP/STD Area Ratio[b]	[VP], 10^{-2} M	Φ_{-K}[c]
Before hν:	1.43	4.35	----
After hν:	1.31	4.02	0.23

For p-CNVP:

	VP/STD Area Ratio[b]	[VP], 10^{-2} M	Φ_{-K}[c]
Before hν:	1.44	4.13	----
After hν:	1.32	3.80	0.23

[a] RT, 313 nm, 4 hrs.

[b] [n-Octadecyl benzoate] = 1.67 x 10^{-2} M; column #2, 145°.

[c] 0.10 M VP actinometer: AP/C_{16} area ratio = 0.322; [C_{16}] = 6.31 x 10^{-3} M.

Table 58. Disappearance Quantum Yields for Cyanovalerophenones in Benzene.[a]

For o-CNVP:

	VP/C_{26} Area Ratio[b]	[VP], 10^{-2} M	Φ_{-K}[c]
Before hν:	2.64	4.97	----
After hν:	2.45	4.62	0.14

For p-CNVP:

	VP/C_{26} Area Ratio[d]	[VP], 10^{-2} M	Φ_{-K}[c]
Before hν:	2.58	5.05	----
After hν:	2.18	4.27	0.31

[a] RT, 313 nm, 5 hrs.

[b] $[C_{26}] = 8.07 \times 10^{-3}$ M; column #2, 165°.

[c] 0.10 M VP actinometer: AP/C_{16} area ratio = 0.782; $[C_{16}] = 4.55 \times 10^{-3}$ M.

[d] $[C_{26}] = 8.37 \times 10^{-3}$ M; column #2, 165°.

Table 59. Disappearance Quantum Yields for Cyanovalerophenones in Acetonitrile.[a]

For o-CNVP:

	VP/C_{26} Area Ratio[b]	[VP], 10^{-2} M	Φ_{-K}[c]
Before hν:	2.18	5.02	----
After hν:	1.23	2.83	0.82

For m-CNVP:

	VP/C_{26} Area Ratio[b]	[VP], 10^{-2} M	Φ_{-K}[c]
Before hν:	2.08	4.97	----
After hν:	1.49	3.56	0.52

For p-CNVP:

	VP/C_{26} Area Ratio[b]	[VP],10^{-2} M	Φ_{-K}[c]
Before hν:	2.12	5.00	----
After hν:	1.34	3.17	0.68

[a] RT, 313 nm, 2-1/2 hrs.

[b] $[C_{26}] = 1.02 \times 10^{-2}$ M; column #2, 165°.

[c] 0.10 M VP actinometer: AP/C_{16} area ratio = 1.36; $[C_{16}] = 2.83 \times 10^{-3}$ M.

Table 60. Disappearance Quantum Yields for Carbomethoxyvalerophenones in Acetonitrile.[a]

For m-CO_2CH_3VP:

	VP/C_{26} Area Ratio[b]	[VP], 10^{-2} M	Φ_{-K}[c]
Before hν:	3.13	5.02	----
After hν:	2.27	3.63	1.0

For p-CO_2CH_3VP:

	Area Ratio[b]	[VP], 10^{-2} M	Φ_{-K}[c]
Before hν:	2.98	5.03	----
After hν:	2.30	3.89	0.83

[a] RT, 313 nm, 1-1/4 hrs.

[b] $[C_{26}] = 7.85 \times 10^{-3}$ M; column #2, 170°.

[c] 0.10 M VP actinometer: AP/C_{16} area ratio = 0.745; $[C_{16}] = 2.65 \times 10^{-3}$M.

Table 61. Disappearance Quantum Yields for Carbomethoxyvalerophenones in Acetonitrile.[a]

For o-CO_2CH_3VP:

	VP/C_{26} Area Ratio[b]	[VP], 10^{-2} M	Φ_{-K}[c]
Before hν:	2.43	4.04	----
After hν:	1.94	3.21	0.25

For m-CO_2CH_3VP:

	VP/C_{26} Area Ratio[b]	[VP], 10^{-2} M	Φ_{-K}[d]
Before hν:	2.06	4.00	----
After hν:	1.60	3.09	0.85

For p-CO_2CH_3VP:

	VP/C_{26} Area Ratio[b]	[VP], 10^{-2} M	Φ_{-K}[d]
Before hν:	2.35	4.07	----
After hν:	1.85	3.20	0.81

[a] RT, 313 nm, 4-1/2 hrs for o-CO_2CH_3VP, 1-1/4 hrs for m- and p-CO_2CH_3VP.

[b] $[C_{26}] = 8.29 \times 10^{-3}$ M; column #2, 170°.

[c] 0.10 M VP actinometer AP/C_{16} area ratio = 1.16; $[C_{16}] = 4.06 \times 10^{-3}$ M.

[d] 0.10 M VP actinometer: AP/C_{16} area ratio = 0.380; $[C_{16}] = 4.06 \times 10^{-3}$ M.

Table 62. Maximization of Φ_{II} for 0.040 M p-Cyanovalerophenone by Pyridine in Benzene.[a]

Φ_{II} = 0.21[b] Φ_{max} = 0.42[b]

[Pyr], M	AP/C_{20} Area Ratio[c]	[AP], 10^{-3}	Φ_{II}[b]
0.0	0.723	0.959	0.21
0.075	1.25	1.66	0.36
0.30	1.44	1.91	0.42
0.45	1.38	1.83	0.40
0.60	1.39	1.84	0.41
0.75	1.30	1.72	0.38
1.5	1.12	1.49	0.33
3.0	1.34	1.78	0.39

[a] RT, 313 nm, 30 min.

[b] 0.10 M VP actinometer: AP/C_{16} area ratio = 0.167; $[C_{16}]$ = 4.02 x 10^{-3} M.

[c] $[C_{20}]$ = 5.1 x 10^{-4} M; column #1, 145°.

Table 63. Maximization of Φ_{II} for 0.041 M p-Cyanovalerophenone by Dioxane in Benzene.[a]

$\Phi_{II} = 0.17^b$ $\Phi_{max} = 0.35^b$

[Dioxane], M	AP/C_{20} Area Ratio[c]	[AP], 10^{-3} M	Φ_{II}[b]
0.0	0.526	0.755	0.17
1.00	0.975	1.40	0.31
2.01	0.897	1.29	0.29
3.01	1.06	1.52	0.34
4.02	1.04	1.49	0.33
5.02	1.02	1.46	0.32
6.02	1.01	1.45	0.32
7.03	1.12	1.61	0.36

[a] RT, 313 nm, 40 min.

[b] 0.10 M VP actinometer: AP/C_{16} area ratio = 0.624; $[C_{16}] = 1.02 \times 10^{-3}$ M.

[c] $[C_{20}] = 5.52 \times 10^{-4}$ M; column #1, 145°.

Table 64. Maximization of Φ_{II} for 0.040 M p-Cyanovalerophenone by t-Butyl Alcohol in Benzene.[a]

Φ_{II} = 0.17[b] Φ_{max} = 0.33[b]

[t-BuOH], M	AP/C_{20} Area Ratio[c]	[AP], 10^{-3} M	Φ_{II}[b]
0.0	0.550	1.39	0.17
0.125	0.672	1.69	0.20
0.250	0.731	1.84	0.22
0.375	0.924	2.33	0.28
0.500	0.985	2.48	0.30
0.626	0.991	2.50	0.30
0.751	1.14	2.88	0.35
1.00	1.07	2.70	0.29

[a] RT, 313 nm, 1 hr, 20 min.

[b] 0.10 M VP actinometer: AP/C_{16} area ratio = 0.603; [C_{16}] = 1.99 x 10^{-3} M.

[c] [C_{20}] = 9.70 x 10^{-4} M; column #2, 140°.

Table 65. Maximization of Φ_{II} for 0.040 M p-Cyanobutyrophenone by Pyridine in Benzene.[a]

Φ_{II} = 0.13[b] Φ_{max} = 0.31[b]

[Pyr], M	AP/C_{20} Area Ratio[c]	[AP], 10^{-3} M	Φ_{II}[b]
0.0	1.11	1.75	0.13
0.50	2.70	4.29	0.31
1.0	2.97	4.34	0.31

[a] RT, 313 nm, 1 hr.

[b] 0.10 M VP actinometer: AP/C_{16} area ratio = 0.773; [C_{16}] = 2.56 x 10^{-3} M.

[c] [C_{20}] = 6.36 x 10^{-4} M; column #2, 120°.

Table 66. Effect of Ketone Concentration on Φ_{II} for p-Carbomethoxyvalerophenone in Acetonitrile.[a]

[Ketone], M	AP/C_{20} Area Ratio[b]	[AP], 10^{-3} M	Φ_{II}[c]
0.020	1.26	2.10	0.47
0.060	1.26	2.10	0.47
0.080	1.34	2.23	0.50
0.10	1.32	2.20	0.49
0.12	1.37	2.28	0.51
0.14	1.34	2.23	0.50
0.16	1.47	2.45	0.55

[a] RT, 313 nm, 20 min.

[b] $[C_{20}] = 6.66 \times 10^{-4}$ M; column #3, 165°.

[c] 0.10 M VP actinometer: AP/C_{16} area ratio = 0.691; $[C_{16}] = 9.30 \times 10^{-4}$ M.

Table 67. Intersystem Crossing Yield for 0.040 M p-Cyanoacetophenone in Benzene.[a]

Run #1: Φ_{ISC} = 1.0

[cis-P], M[b]	β[c]	Φ_{ISC}[d]
0.12 (act)	0.0753	1.00
0.12	0.0721	0.96
0.060 (act)	0.136	1.00
0.060	0.143	1.05

[a] RT, 313 nm, 1 hr.

[b] cis-P = cis 1,3-pentadiene.

[c] β = area trans/area trans + area cis; column #6, 55°.

[d] $\Phi_{ISC} = \beta_{ketone}/\beta_{act}$; 0.060 M acetophenone actinomer.

Run #2: Φ_{ISC} = 1.0

[cis-P], M[b]	β[c]	Φ_{ISC}[d]
0.060 (act)	0.0673	1.00
0.060	0.0740	1.10
0.030 (act)	0.118	1.00
0.030	0.129	1.09
0.0050 (act)	0.413	1.00
0.0050	0.404	0.98

[a] RT, 313 nm 45 min.

[b] cis-P = cis 1,3-pentadiene.

[c] β = area trans/area trans + area cis; column #6, 55°.

[d] $\Phi_{ISC} = \beta_{ketone}/\beta_{act}$; 0.060 M acetophenone actinometer.

Table 68. Intersystem Crossing Yield for 0.050 M p-Carbomethoxyvalerophenone in Benzene.[a]

$\Phi_{ISC} = 1.0$

[cis-P], M[b]	β[c]	Φ_{ISC}[d]
0.050 (act)	0.204	1.00
0.050	0.201	0.99
0.10 (act)	0.134	1.00
0.10	0.137	1.02

[a] RT, 313 nm, 2-1/2 hrs.

[b] [cis-P] = cis 1,3-pentadiene.

[c] β = area trans/area trans + area cis; column #6, 55°.

[d] $\Phi_{ISC} = \beta_{ketone}/\beta_{act}$; 0.050 M valerophenone actinometer.

Table 69. Quenching of 0.050 M p-Cyanoacetophenone by Naphthalene in Acetonitrile (1.0 M Toluene).[a]

$k_q\tau = 2.2 \times 10^4$

[Q], 10^{-4} M	BB/C_{21} Area Ratio[b]	[BB], 10^{-3} M[c]	ϕ^o/ϕ
0.0	1.58	2.16	----
0.501	0.712	0.972	2.21
1.00	0.489	0.668	3.22
1.50	0.376	0.513	4.19

[a] RT, 366 nm, 13 hrs.

[b] BB = bibenzyl; $[C_{21}] = 9.10 \times 10^{-4}$ M; column #2, 130°.

[c] Response factor for $C_{21}/BB = 1.5$.

Table 70. Photoreduction of 0.051 M p-Cyanoacetophenone by Toluene in Acetonitrile.[a]

Slope = 18.8, intercept = 1.8

[Toluene], M	BB/C_{21} Area Ratio[b]	[BB], 10^{-3} M[c]	Φ_{BB}, 10^{-2}[d]
0.250	0.234	0.351	0.996
0.500	0.476	0.714	2.02
0.625	0.646	0.969	2.74
0.750	0.718	1.08	3.13
0.875	0.831	1.25	3.53
1.00	0.850	1.28	3.61
1.25	1.10	1.65	4.67

[a] RT, 313 nm, 3 hrs.

[b] BB = bibenzyl; $[C_{21}] = 1.00 \times 10^{-3}$ M; column #2, 120°.

[c] Response factor for C_{21}/BB = 1.5.

[d] 0.10 M VP actinometer: AP/C_{16} area ratio = 1.25; $[C_{16}] = 4.02 \times 10^{-3}$ M.

Table 71. Quenching of 0.050 M p-Cyanoacetophenone by Naphthalene in Dry Acetonitrile (1.0 M p-Xylene).[a]

$k_q\tau$ = 4,750

[Q], 10^{-3} M	p-diTE/C_{16} Area Ratio[b]	[p-diTE], 10^{-3} M[c]	ϕ^o/ϕ
0.0	1.54	3.10	----
0.501	0.507	1.02	3.04
0.751	0.390	0.784	3.95
1.00	0.282	0.567	5.46
1.25	0.204	0.410	7.56
1.50	0.178	0.358	8.65

[a] RT, 366 nm, 7-1/2 hrs.

[b] p-diTE = p-ditolylethane; [C_{16}] = 2.01 x 10^{-3} M; column #5, 140°.

[c] Response factor for C_{16}/p-diTE = 1.0.

Table 72. Photoreduction of 0.050 M p-Cyanoacetophenone by p-Xylene in Dry Acetonitrile.[a]

Slope = 1.7, intercept = 8.5

[p-Xylene], M	p-diTE/C_{16} Area Ratio[b]	[p-diTE], 10^{-4} M	Φ_{BB}, 10^{-1}[d]
0.313	0.248	5.01	0.733
0.625	0.279	5.64	0.824
0.938	0.319	6.44	0.942
1.25	0.352	7.11	1.04
1.56	0.367	7.41	1.08
1.88	0.360	7.27	1.06
2.19	0.377	7.62	1.11

[a] RT, 313 nm, 30 min.

[b] p-diTE = p-ditolylethane; [C_{16}] = 2.02 x 10^{-3} M; column #5, 140°.

[c] Response factor for C_{16}/p-diTE = 1.0.

[d] 0.10 M VP actinometer: AP/C_{16} area ratio = 0.215; [C_{16}] = 4.55 x 10^{-3} M.

Table 73. Quenching of 0.040 M p-Carbomethoxyvalerophenone by β-Dimethylaminoethyl Benzoate in Benzene.[a]

$k_q\tau$ = 32, Φ_{II} = 0.29[b]

[Q], M	AP/C_{21} Area Ratio[c]	[AP], 10^{-3} M	$\phi°/\phi$
0.0	0.897	3.13	----
0.0300	1.07	3.73	0.84
0.0600	0.795	2.77	1.13
0.120	0.473	1.65	1.90
0.180	0.328	1.14	2.74
0.240	0.247	0.861	3.62

[a] 0.50 M pyridine; RT, 313 nm, 30 min.

[b] 0.10 M VP actinometer: AP/C_{16} area ratio = 0.667; $[C_{16}]$ = 2.34 x 10^{-3} M.

[c] $[C_{21}]$ = 1.34 x 10^{-3} M; column #2, 131°.

Table 74. Quenching of p-Carbomethoxyvalerophenone by β-Dimethylaminoethyl Benzoate in Acetonitrile.[a]

Run #1: $k_q\tau = 40$, $\Phi_{II} = 0.55$[b]

[Q], M	AP/C_{20} Area Ratio[c]	[AP], 10^{-3} M	$\phi°/\phi$
0.0	1.24	1.80	----
0.00250	1.74	2.52	0.71
0.0050	1.58	2.29	0.79
0.0100	1.36	1.97	0.91
0.0150	1.41	2.04	0.88
0.0200	1.17	1.70	1.06

[a] RT, 313 nm, 25 min.

[b] 0.10 M VP actinometer: AP/C_{16} area ratio = 0.169; $[C_{16}] = 2.78 \times 10^{-3}$ M.

[c] $[C_{20}] = 5.80 \times 10^{-4}$ M; column #3, 161°.

Run #2: $k_q\tau = 40$

[Q], M	AP/C_{20} Area Ratio[b]	[AP], 10^{-3} M	$\phi°/\phi$
0.0	2.83	4.05	----
0.0125	3.43	4.90	0.83
0.0250	2.95	4.22	0.96
0.0500	1.90	2.72	1.49
0.0750	1.42	2.03	2.00

[a] RT, 313 nm, 30 min.

[b] $[C_{20}] = 5.72 \times 10^{-4}$ M; column #3, 161°.

Table 75. Quenching of 0.040 M p-Carbomethoxyvalerophenone by γ-Dimethylaminopropyl Benzoate in Benzene.[a]

$k_q\tau$ = 26, Φ_{max} = 0.33[b]

[Q], M	AP/C_{20} Area Ratio[c]	[AP], 10^{-3} M	$\phi°/\phi$
0.0	1.31	2.32	----
0.0250	1.35	2.39	0.97
0.0500	0.958	1.70	1.37
0.100	0.619	1.10	2.12

[a] 0.50 M pyridine; RT, 313 nm, 40 min.

[b] 0.10 M VP actinometer: AP/C_{16} area ratio = 0.307; [C_{16}] = 3.31 x 10^{-3} M.

[c] [C_{20}] = 7.08 x 10^{-4} M; column #3, 170°.

Table 76. Quenching of 0.040 M p-Carbomethoxyvalerophenone by γ-Dimethylaminopropyl Benzoate in Acetonitrile.[a]

$k_q\tau = 47$, $\Phi_{II} = 0.50$[b]

[Q], M	AP/C_{20} Area Ratio[c]	[AP], 10^{-3} M	$\phi°/\phi$
0.0	2.52	3.56	----
0.0125	2.65	3.74	0.95
0.0250	1.96	2.77	1.29
0.0500	1.26	1.78	2.00
0.0750	0.962	1.36	2.62
0.100	0.732	1.03	3.45

[a] RT, 313 nm, 40 min.

[b] 0.10 M VP actinometer: AP/C_{16} area ratio = 0.881; $[C_{16}] = 1.19 \times 10^{-3}$ M.

[c] $[C_{20}] = 5.65 \times 10^{-4}$ M; column #3, 170°.

Table 77. Quenching of 0.040 M m-Carbomethoxyvalerophenone by β-Dimethylaminoethyl Benzoate in Acetonitrile.[a]

$k_q\tau = 8.0$

[Q], M	AP/C_{21} Area Ratio[b]	[AP], 10^{-3} M	$\phi°/\phi$
0.0	3.15	7.21	----
0.0100	3.35	7.66	0.94
0.0200	3.12	7.14	1.01
0.0300	2.83	6.48	1.11
0.0400	2.64	6.04	1.19
0.0600	2.45	5.61	1.28
0.0800	2.18	4.99	1.44

[a] RT, 313 nm, 20 min.

[b] $[C_{21}] = 8.80 \times 10^{-4}$ M; column #2, 130°.

Table 78. Quenching of p-Methoxyvalerophenone by Pentadiene in Benzene.[a]

Run #1: $k_q\tau$ = 4,860, Φ_{II} = 0.11[b]

[Q], 10^{-3} M	AP/C_{22} Area Ratio[c]	[AP], 10^{-3} M	$\phi°/\phi$
0.0	0.740	1.00	----
0.125	0.460	0.624	1.61
0.250	0.305	0.413	2.43
0.500	0.231	0.313	3.20
0.750	0.152	0.206	4.87
1.00	0.136	0.184	5.45

[a] 0.040 M ketone; RT, 313 nm, 1 hr, 20 min.

[b] 0.10 M VP actinometer: AP/C_{16} area ratio = 0.512; $[C_{16}]$ = 2.52 x 10^{-3} M.

[c] $[C_{22}]$ = 5.02 x 10^{-4} M; column #2, 130°.

Run #2: $k_q\tau$ = 3750

[Q], 10^{-3} M	AP/C_{22} Area Ratio[b]	[AP], 10^{-3} M	$\phi°/\phi$
0.0	1.58	2.80	----
0.125	0.964	1.71	1.64
0.250	0.894	1.58	1.77
0.500	0.697	1.23	2.27
0.750	0.433	0.767	3.65
1.00	0.360	0.638	4.40
1.50	0.241	0.427	6.56

[a] 0.040 M ketone; RT, 313 nm, 2 hrs.

[b] $[C_{22}]$ = 6.56 x 10^{-4} M; column #2, 145°.

Table 79. Quenching of p-Methoxyvalerophenone by Pentadiene in Acetonitrile.[a]

Run #1: $k_q\tau = 6{,}800$, $\Phi_{II} = 0.21^b$

[Q], 10^{-4} M	AP/C_{20} Area Ratio[c]	[AP], 10^{-3} M	$\phi°/\phi$
0.0	1.11	2.80	----
1.00	0.672	1.70	1.70
2.00	0.468	1.18	2.45
4.00	0.307	0.775	3.73
6.00	0.228	0.576	5.04

[a] 0.040 M ketone; RT, 313 nm, 6-1/2 hrs.

[b] 0.10 M VP actinometer: AP/C_{16} area ratio = 0.276; $[C_{16}] = 2.61 \times 10^{-3}$ M.

[c] $[C_{20}] = 1.01 \times 10^{-3}$ M; column #2, 140°.

Run #2: $k_q\tau = 6{,}000$

[Q], 10^{-4} M	AP/C_{22} Area Ratio[b]	[AP], 10^{-3} M	$\phi°/\phi$
0.0	0.515	2.81	----
0.500	0.410	2.24	1.25
1.00	0.324	1.77	1.59
2.00	0.228	1.24	2.26
3.00	0.193	1.05	2.67
4.01	0.147	0.802	3.54
6.01	0.111	0.605	4.64

[a] 0.040 M ketone; RT, 313 nm, 1-1/2 hrs.

[b] $[C_{22}] = 2.02 \times 10^{-3}$ M; column #2, 140°.

Table 80. Quenching of 0.040 M p-Methoxyvalerophenone by N,N-Dimethylaminopropyl Phenyl Ether in Acetonitrile.[a]

$k_q\tau = 202$

[Q], 10^{-2} M	AP/C_{22} Area Ratio[b]	[AP], 10^{-4} M	$\phi°/\phi$
0.0	0.936	8.69	----
0.400	0.944	8.77	0.99
0.801	0.656	6.09	1.43
1.60	0.435	4.04	2.15
2.40	0.293	2.72	3.20
3.20	0.233	2.16	4.03

[a] RT, 313 nm, 40 min.

[b] $[C_{22}] = 3.44 \times 10^{-4}$ M; column #2, 140°.

Table 81. Quenching of 0.020 M p-2VB by Pentadiene in Benzene.[a]

$k_q\tau = 9.4$ $\Phi_{II} = 0.068$[b]

[Q], M	AP/C_{24} Area Ratio[c]	[AP], 10^{-4} M	$\phi°/\phi$
0.0	0.877	8.07	----
0.0125	0.819	7.54	1.07
0.0250	0.767	7.06	1.14
0.0500	0.690	6.35	1.27
0.0750	0.590	5.43	1.49
0.100	0.520	4.78	1.69
0.150	0.424	3.90	2.07

[a] 0.40 M pyridine; RT, 313 nm, 2 hrs.

[b] 0.11 M VP actinometer: AP/C_{16} area ratio = 0.476; [C_{16}] = 3.58 x 10^{-3} M.

[c] [C_{24}] = 4.60 x 10^{-4} M; column #2, 170°.

Table 82. Quenching of 0.030 M p-2VB by Pentadiene in Benzene.[a]

$k_q\tau$ = 10.1, Φ_{II} = 0.077[b]

[q], M	AP/C_{24} Area Ratio[c]	[AP], 10^{-4} M	$\phi°/\phi$
0.0	0.729	8.78	----
0.0125	0.684	8.24	1.07
0.0250	0.639	7.69	1.14
0.0500	0.567	6.83	1.29
0.0750	0.485	5.84	1.50
0.100	0.432	5.20	1.69
0.150	0.327	3.94	2.23

[a] 0.40 M pyridine; RT, 313 nm, 2-1/4 hrs.

[b] 0.10 M VP actinometer: AP/C_{16} area ratio = 0.552; [C_{16}] = 2.96 x 10^{-3} M.

[c] [C_{24}] = 6.02 x 10^{-4} M; column #2, 170°.

Table 83. Quenching of 0.040 M p-2VB by Pentadiene in Benzene.

$k_q\tau$ = 10.6, Φ_{II} = 0.079[b]

[Q], M	AP/C_{24} Area Ratio[c]	[AP], 10^{-4} M	$\phi°/\phi$
0.0	0.649	8.59	----
0.0150	0.602	7.97	1.08
0.0300	0.562	7.44	1.15
0.0600	0.451	5.97	1.44
0.0900	0.396	5.24	1.64
0.120	0.335	4.44	1.94
0.180	0.249	3.30	2.61

[a] 0.40 M pyridine; RT, 313 nm, 2-1/2 hrs.

[b] 0.10 M VP actinometer: AP/C_{16} area ratio = 0.452; $[C_{16}] = 3.44 \times 10^{-3}$ M.

[c] $[C_{24}] = 6.62 \times 10^{-4}$ M; column #2, 170°.

Table 84. Quenching of 0.010 M p-2VB with Pentadiene in Acetonitrile.[a]

$k_q\tau$ = 13.6, Φ_{II} = 0.10[b]

[Q], M	AP/STD Area Ratio[c]	[AP], 10^{-4} M	$\phi°/\phi$
0.0	0.849	6.58	----
0.0125	0.828	6.42	1.16
0.0250	0.807	6.25	1.32
0.0500	0.713	5.53	1.62
0.0750	0.628	4.87	2.10
0.100	0.510	3.95	2.33
0.150	0.395	3.06	3.02

[a] RT, 313 nm, 30 min.

[b] 0.10 M VP actinometer: AP/C_{16} area ratio = 0.609; [C_{16}] = 1.46 x 10^{-3} M.

[c] [n-Octadecyl benzoate] = 3.10 x 10^{-4} M; column #2, 170°.

Table 85. Quenching of 0.020 M p-2VB by Pentadiene in Acetonitrile.[a]

$k_q\tau = 12.3$, $\Phi_{II} = 0.11$[b]

[Q], M	AP/STD Area Ratio[c]	[AP], 10^{-3} M	$\phi°/\phi$
0.0	1.46	1.33	----
0.0125	1.19	1.08	1.22
0.0250	1.08	0.983	1.35
0.0500	0.860	0.783	1.70
0.0750	0.809	0.736	1.81
0.100	0.691	0.629	2.11
0.150	0.522	0.475	2.80

[a] RT, 313 nm, 1 hr.

[b] 0.10 M VP actinometer: AP/C_{16} area ratio = 0.565; [C_{16}] = 3.09 x 10^{-3} M.

[c] [n-Octadecyl benzoate] = 3.64 x 10^{-4} M; column #2, 170°.

Table 86. Quenching of 0.040 M p-2VB by Pentadiene in Acetonitrile.[a]

$k_q\tau$ = 10.6, Φ_{II} = 0.11[b]

[Q], M	AP/STD Area Ratio[c]	[AP], 10^{-3} M	$\phi°/\phi$
0.0	1.03	1.97	----
0.0125	0.982	1.88	1.05
0.0250	0.936	1.79	1.10
0.0501	0.633	1.21	1.63
0.0751	0.572	1.09	1.80
0.100	0.501	0.957	2.05
0.150	0.378	0.722	2.72

[a] RT, 313 nm, 2-1/2 hrs.

[b] 0.10 M VP actinometer: AP/C_{16} area ratio = 0.561; [C_{16}] = 4.37 x 10^{-3} M.

[c] [n-Octadecyl benzoate] = 7.64 x 10^{-4} M; column #2, 170°.

Table 87. Quenching of 0.060 M p-2VB of Pentadiene in Acetonitrile.[a]

$k_q\tau$ = 8.6, Φ_{II} = 0.097[b]

[Q], M	AP/STD Area Ratio[c]	[AP], 10^{-3} M	$\phi°/\phi$
0.0	0.628	1.79	----
0.0125	0.557	1.59	1.13
0.0251	0.540	1.54	1.16
0.0501	0.465	1.33	1.35
0.0752	0.399	1.14	1.57
0.100	0.338	0.963	1.86
0.150	0.244	0.695	2.57

[a] RT, 313 nm, 3 hrs.

[b] 0.10 M VP actinometer: AP/C_{16} area ratio = 0.908; [C_{16}] = 3.00 x 10^{-3} M.

[c] [n-Octadicyl benzoate] = 1.14 x 10^{-3} M; column #2, 170°.

Table 88. Quenching of 0.080 M p-2VB by Pentadiene in Acetonitrile.[a]

$k_q\tau$ = 7.5, Φ_{II} = 0.068[b]

[Q], M	AP/STD Area Ratio[c]	[AP], 10^{-3} M	$\phi°/\phi$
0.0	1.23	2.32	----
0.0125	1.09	2.05	1.13
0.0250	1.07	2.02	1.15
0.0500	0.868	1.64	1.42
0.0750	0.804	1.52	1.53
0.100	0.695	1.31	1.77
0.150	0.589	1.11	2.09

[a] RT, 313 nm, 2-1/2 hrs.

[b] 0.10 M VP actinometer: AP/C_{16} area ratio = 1.53; [C_{16}] = 3.18 x 10^{-3} M.

[c] [n-Octadecyl benzoate] = 7.54 x 10^{-3} M; column #2, 170°.

Table 89. Quenching of 0.10 M p-2VB by Pentadiene in Acetonitrile.[a]

$k_q\tau = 7.3$, $\Phi_{II} = 0.078$[b]

[Q], M	AP/STD Area Ratio[c]	[AP], 10^{-3} M	$\phi°/\phi$
0.0	0.748	1.93	----
0.0125	0.744	1.92	1.01
0.0250	0.658	1.69	1.14
0.0500	0.542	1.40	1.38
0.0750	0.481	1.24	1.56
0.100	0.410	1.06	1.82
0.150	0.366	0.943	2.04

[a] RT, 313 nm, 2-1/2 hrs.

[b] 0.10 M VP actinometer: AP/C_{16} area ratio = 0.930; [C_{16}] = 3.84 x 10^{-3} M.

[c] [n-Octadecyl benzoate] = 1.03 x 10^{-3} M; column #2, 170°.

Table 90. Quenching of 0.020 M p-3VB by Pentadiene in Acetonitrile.[a]

$k_q\tau$ = 11.4, Φ_{II} = 0.13[b]

[Q], M	AP/STD Area Ratio[c]	[AP], 10^{-3} M	$\phi°/\phi$
0.0	1.57	1.51	----
0.0125	1.33	1.28	1.18
0.0250	1.22	1.17	1.29
0.0500	0.970	0.931	1.62
0.0750	0.848	0.814	1.85
0.100	0.707	0.679	2.22
0.150	0.611	0.587	2.57

[a] RT, 313 nm, 1 hr.

[b] 0.10 M VP actinometer: AP/C_{16} area ratio = 1.07; [C_{16}] = 1.46 x 10^{-3} M.

[c] [n-Octadecyl benzoate] = 3.84 x 10^{-4} M; column #2, 170°.

Table 91. Quenching of 0.040 M p-3VB by Pentadiene in Acetonitrile.[a]

$k_q\tau = 7.8$, $\Phi_{II} = 0.093$[b]

[Q], M	AP/STD Area Ratio[c]	[AP], 10^{-3} M	$\phi°/\phi$
0.0	1.10	2.04	----
0.0125	1.04	1.93	1.06
0.0250	0.911	1.69	1.20
0.0500	0.790	1.47	1.39
0.0750	0.701	1.30	1.57
0.100	0.600	1.11	1.83
0.150	0.497	0.922	2.21

[a] RT, 313 nm, 2 hrs.

[b] 0.10 M VP actinometer: AP/C_{16} area ratio = 0.879; [C_{16}] = 3.44 x 10^{-3} M.

[c] [n-Octadecyl benzoate] = 7.42 x 10^{-4} M; column #2, 170°.

Table 92. Quenching of 0.060 M p-3VB by Pentadiene in Acetonitrile.[a]

$k_q\tau = 7.5$, $\Phi_{II} = 0.071$[b]

[Q], M	AP/STD Area Ratio[c]	[AP], 10^{-3} M	$\phi°/\phi$
0.0	0.855	1.84	----
0.0125	0.817	1.76	1.05
0.0250	0.720	1.55	1.19
0.0500	0.578	1.24	1.48
0.0750	0.598	1.29	1.43
0.100	0.479	1.03	1.79
0.150	0.400	0.860	2.14

[a] RT, 313 nm, 2 hrs.

[b] 0.10 M VP actinometer: AP/C_{16} area ratio = 1.70; [C_{16}] = 2.08 x 10^{-3} M.

[c] [n-Octadecyl benzoate] = 8.60 x 10^{-4} M; column #2, 170°.

Table 93. Quenching of 0.10 M p-3VB by Pentadiene in Acetonitrile.[a]

$k_q\tau$ = 6.4, Φ_{II} = 0.082[b]

[Q], M	AP/STD Area Ratio[c]	[AP], 10^{-3} M	$\phi°/\phi$
0.0	0.905	2.51	----
0.0125	0.888	2.46	1.02
0.0250	0.787	2.18	1.15
0.0500	0.684	1.90	1.32
0.0750	0.598	1.66	1.51
0.100	0.551	1.53	1.64
0.150	0.466	1.29	1.94

[a] RT, 313 nm, 3 hrs, 40 min.

[b] 0.10 M VP actinometer: AP/C_{16} area ratio = 2.21; [C_{16}] = 1.90 x 10^{-3} M.

[c] [n-Octadecyl benzoate] = 1.11 x 10^{-3} M; column #2, 170°.

Table 94. Quenching of 0.020 M m-2VB by Pentadiene in Benzene.[a]

$k_q\tau$ = 15, Φ_{II} = 0.15[b]

[Q], M	AP/STD Area Ratio[c]	[AP], 10^{-3} M	$\phi°/\phi$
0.0	1.41	1.40	----
0.0125	1.20	1.19	1.17
0.0250	1.07	1.06	1.32
0.0500	0.850	0.842	1.66
0.0750	0.701	0.694	2.01
0.100	0.578	0.572	2.44
0.150	0.415	0.411	3.40

[a] RT, 313 nm, 50 min.

[b] 0.10 M VP actinometer: AP/C_{16} area ratio = 0.588; [C_{16}] = 2.30 x 10^{-3} M.

[c] [n-Octadecyl benzoate] = 3.96 x 10^{-4} M; column #2, 170°.

Table 95. Quenching of m-2VB by Pentadiene in Acetonitrile.[a]

Run #1: $k_q\tau$ = 24, Φ_{II} = 0.31[b]

[Q], M	AP/STD Area Ratio[c]	[AP], 10^{-3} M	$\phi°/\phi$
0.0	0.944	1.06	----
0.0125	0.704	0.789	1.34
0.0250	0.583	0.653	1.62
0.0500	0.426	0.477	2.22
0.0750	0.345	0.386	2.73
0.100	0.285	0.319	3.31
0.150	0.199	0.223	4.75

[a] 0.020 M ketone; RT, 313 nm, 35 min.
[b] 0.10 M VP actinometer: AP/C_{16} area ratio = 0.172; [C_{16}] = 3.44 x 10^{-3} M.
[c] [n-Octadecyl benzoate] = 4.48 x 10^{-4} M; column #2, 170°.

Run #2: $k_q\tau$ = 22, Φ_{II} = 0.31[b]

[Q], M	AP/STD Area Ratio[c]	[AP], 10^{-3} M	$\phi°/\phi$
0.0	2.04	1.96	----
0.0125	1.62	1.56	1.23
0.0250	1.36	1.31	1.46
0.0500	1.05	1.01	1.91
0.0750	0.851	0.817	2.34
0.100	0.691	0.663	2.95
0.150	0.535	0.514	3.81

[a] 0.020 M ketone; RT, 313 nm, 30 min.
[b] 0.10 M VP actinometer: AP/C_{16} area ratio = 0.674; [C_{16}] = 1.37 x 10^{-3} M.
[c] [n-Octadecyl Benzoate] = 3.84 x 10^{-4} M; column #2, 170°.

Table 96. Effect of Ketone Concentration on Φ_{II} for p-2VB and p-3VB in Acetonitrile.[a]

For p-2VB: $\Phi_{\infty} = 0.13^{b}$

For p-3VB: $\Phi_{\infty} = 0.11^{b}$

[p-2VB], M	AP/STD Area Ratio[c]	[AP], 10^{-3} M	Φ_{II}[c]
0.020	1.56	1.93	0.10
0.040	1.49	1.84	0.098
0.060	1.23	1.52	0.081
0.080	1.18	1.46	0.078
0.120	1.05	1.30	0.069

[p-3VB], M	AP/STD Area Ratio[c]	[AP], 10^{-3} M	Φ_{II}[c]
0.020	1.46	1.73	0.092
0.040	1.56	1.86	0.099
0.060	1.51	1.79	0.095
0.080	1.41	1.68	0.090
0.120	1.33	1.59	0.085

[a] RT, 313 nm, 1-1/2 hrs.

[b] 0.10 M VP actinometer: AP/C_{16} area ratio = 1.69; [C_{16}] = 1.59 x 10^{-3} M.

[c] [n-Octadecyl benzoate] = 4.95 x 10^{-4} M; column #2, 170°.

Table 97. Disappearance Quantum Yields for p-2VB and p-2AB in Acetonitrile.[a]

Run #1:

For p-2VB:

	VP/STD Area Ratio[b]	[VP], 10^{-2} M	Φ_{-K}[c]
Before hν:	1.60	4.00	----
After hν:	1.24	3.11	0.39

For p-2AB:	AP/STD Area Ratio[b]	[AP], 10^{-2} M	Φ_{-K}[c]
Before hν:	1.34	4.06	----
After hν:	1.02	3.08	0.43

[a] RT, 313 nm, 4 hrs.

[b] [n-Octadecyl benzoate] = 1.20 x 10^{-2} M; column #2, 170°.

[c] 0.10 M VP actinometer: AP/C_{16} area ratio = 0.852;[C_{16}] = 3.89 x 10^{-3} M.

Run #2:

For p-2VB:

	VP/STD Area Ratio[b]	[VP], 10^{-1} M	Φ_{-K}[c]
Before hν:	3.63	1.00	----
After hν:	1.55	0.426	0.50

[a] RT, 313 nm, 6 hrs.

[b] [n-Octadecyl benzoate] = 2.02 x 10^{-2} M; column #2, 170°.

[c] 0.10 M VP actinometer: AP/C_{16} area ratio = 4.87; [C_{16}] = 3.36 x 10^{-3} M.

Table 97. Continued.

p-2AB:

	AP/STD Area Ratio[b]	[AP], 10^{-2} M	Φ_{-K}[c]
Before hν:	3.00	2.00	----
After hν:	1.45	0.967	0.20

[a] RT, 313 nm, 3 hrs.

[b] [n-Octadecyl benzoate] = 4.04 x 10^{-3} M; column #2, 170°.

[c] 0.10 M VP actinometer: AP/C_{16} area ratio = 2.21; [C_{16}] = 3.36 x 10^{-3} M.

Run #3:

For p-2VB:

	VP/STD Area Ratio[b]	[VP], 10^{-3} M	Φ_{-K}[c]
Before hν:	2.63	5.08	----
After hν:	1.48	2.85	0.23

Since only 78% of hν was absorbed, then Φ_{-K} = 0.29.

For p-2AB:

	AP/STD Area Ratio[b]	[AP], 10^{-3} M	Φ_{-K}[c]
Before hν:	1.82	5.06	----
After hν:	1.60	4.46	0.06

Since only 89% of hν was absorbed, then Φ_{-K} = 0.07

[a] RT, 313 nm, 40 min. [b] [n-Octadecyl benzoate] = 1.36 x 10^{-3} M; column #2, 170°. [c] 0.10 M VP actinometer: AP/C_{16} area ratio = 0.886; [C_{16}] = 1.55 x 10^{-3} M.

Table 98. Quenching of 0.020 M p-MeO3E by Pentadiene in Acetonitrile.[a]

$k_q\tau$= 3.6 Φ_{II} = 0.030[b]

[Q], M	AP/C_{22} Area Ratio[c]	[AP], 10^{-3} M	$\phi°/\phi$
0.0	1.11	1.29	----
0.0200	0.617	0.718	1.80
0.0399	0.425	0.495	2.61
0.0599	0.354	0.412	3.13
0.0799	0.291	0.339	3.81
1.20	0.199	0.232	5.59
1.60	0.219	0.255	5.06
2.16	0.139	0.162	7.99

[a] RT, 313 nm, 2-1/2 hrs.

[b] 0.10 M VP actinometer: AP/C_{16} area ratio = 1.20; $[C_{16}]$ = 5.21 x 10^{-3} M.

[c] $[C_{22}]$ = 4.31 x 10^{-4} M; column #2, 165°.

Table 99. Quenching of p-3VE by Pentadiene in Benzene.[a]

Run #1: $k_q\tau = 2{,}900$, $\Phi_{max} = 0.22$[b]

[Q], 10^{-3} M	AP/C_{24} Area Ratio[c]	[AP], 10^{-3} M	$\phi°/\phi$
0.0	1.88	2.10	----
0.100	1.47	1.64	1.28
0.200	1.23	1.37	1.53
0.400	0.877	0.979	2.14
0.600	0.691	0.771	2.72
1.20	0.408	0.455	4.61

[a] 0.020 M ketone; 0.50 M pyridine; RT, 313 nm, 1 hr.

[b] 0.10 M VP actinometer: AP/C_{16} area ratio = 0.433; [C_{16}] = 3.09 x 10^{-3} M.

[c] [C_{24}] = 4.75 x 10^{-4} M; column #2, 165°.

Run #2: $k_q\tau = 3{,}025$, $\Phi_{II} = 0.07$[b]

[Q], 10^{-3} M	AP/C_{24} Area Ratio[c]	[AP], 10^{-4} M	$\phi°/\phi$
0.0	0.761	7.08	----
0.100	0.615	5.72	1.24
0.200	0.491	4.57	1.55
0.400	0.343	3.19	2.22
0.600	0.259	2.41	2.94
0.800	0.234	2.18	3.25
1.12	0.160	1.49	4.76

[a] 0.020 M ketone; RT, 313 nm, 1-1/2 hrs.

[b] 0.099 M VP actinometer: AP/C_{16} area ratio = 0.621; [C_{16}] = 2.21 x 10^{-3} M.

[c] [C_{24}] = 3.96 x 10^{-4} M; column #2, 165°.

Table 100. Quenching of Ketone Disappearance for p-3VE and p-2AE by Pentadiene in Acetonitrile.[a]

For p-3VE: $k_q\tau$ = 122

	[Q], 10^{-2} M	VP/C_{26} Area Ratio[b]	[VP], 10^{-2} M
Before hν:	0.0	2.39	2.00
After hν:	0.0	1.18	0.989
After hν:	1.25	1.91	1.60

[a] RT, 313 nm, 3 hrs.

[b] $[C_{26}]$ = 5.24 x 10^{-3} M; column #2, 150°.

For p-3AE; $k_q\tau$ = 176

	[Q], 10^{-2} M	AP/C_{24} Area Ratio[b]	[AP], 10^{-2} M
Before hν:	0.0	1.29	2.00
After hν:	0.0	0.61	0.952
After hν:	1.25	1.07	1.67

[a] RT, 313 nm, 3 hrs.

[b] $[C_{24}]$ = 6.67 x 10^{-3} M; column #2, 150°.

Table 101. Phosphorescence Lifetime for 1.0 x 10^{-4} M m-Carbomethoxybenzophenone and Φ_{rel} for 1.0 x 10^{-4} M m-2BB in CCl_4.[a]

$k_q\tau = 2.3 \times 10^5$

For m-CO_2CH_3BP:

[Diene], 10^{-6} M[b]	I	I°/I
0.0	60	----
2.0	43	1.40
4.0	36	1.67
6.0	26	2.31
8.0	18	3.33

For m-CO_2CH_3BP:

[Amine], 10^{-4} M[c]	I	I°/I
1.0	30	2.0

For m-2BB:

[Q], M	I
0.0	6.5

[a] RT, 290 nm, monitor at 426 nm.

[b] Diene = 2,5-dimethylhexa-2,4-diene.

[c] Amine = N,N-dimethylaminoethylbenzoate.

Table 102. Phosphorescence Lifetime for 1.0 x 10^{-4} M p-Carbomethoxybenzophenone and Φ_{rel} for 1.0 x 10^{-4} M p-2BB in CCl_4.[a]

$k_q\tau$ = 5.3 x 10^5

For p-CO_2CH_3BP:

[Diene], 10^{-6} M[b]	I	I°/I
0.0	574	----
4.0	192	3.0
8.0	106	5.4

For p-CO_2CH_3BP:

[Amine], 10^{-4} M[c]	I	I°/I
1.0	433	1.3

For p-2BB

[Q], M	I
0.0	51

---

[a] RT, 290 nm, monitor at 437 nm.

[b] Diene = 2,5-dimethylhexa-2,4-diene.

[c] Amine = N,N-dimethylaminoethylbenzoate.

Table 103. Phosphorescence Lifetime for 1.0 x 10^{-4} M p-2BB in CCl_4.[a]

Run #1: $k_q\tau$ = 2.6 x 10^4

[Diene], 10^{-4} M[b]	I	I°/I
0.0	127	----
0.8	77	1.65
1.2	22	5.8
1.6	25	5.1

[a] RT, 300 nm, monitor at 440 nm.

[b] Diene = 2,5-dimethylhexa-2,4-diene.

Run #2: k_q = 4.2 x 10^4

[Diene], 10^{-5} M[b]	I	I°/I
0.0	44	----
0.4	43	1.02
2.0	39	1.13
4.0	18	2.44
8.0	9	4.89

[a] RT, 290 nm, monitor at 475 nm.

[b] Diene = 2,5-dimethylhexa-2,4-diene.

Table 104. Quenching of 0.040 M Butyrophenone in CCl_4.[a]

$k_q\tau$ = 710, Φ_{II} = 0.34[b]

[Diene], 10^{-3} M	AP/C_{15} Area Ratio[c]	[AP], 10^{-3} M	$\phi°/\phi$
0.0	1.80	1.16	----
2.02	0.698	0.452	2.57
4.04	0.449	0.291	4.01
6.06	0.363	0.235	4.95

[a] RT, 313 nm, 40 min.

[b] 0.10 M VP actinometer: AP/C_{16} area ratio = 0.228; $[C_{16}] = 2.16 \times 10^{-3}$ M.

[c] $[C_{15}] = 3.01 \times 10^{-4}$ M; column #3, 125°.

$k_q\tau$ = 280

$[Et_3N]$, 10^{-3} M	AP/C_{15} Area Ratio[b]	[AP], 10^{-3} M	$\phi°/\phi$
0.0	1.80	1.16	----
1.00	1.67	1.08	1.08
2.00	1.44	0.932	1.25
3.00	1.12	0.725	1.61
4.00	0.757	0.490	2.37

[a] RT, 313 nm, 40 min.

[b] $[C_{15}] = 3.01 \times 10^{-4}$ M; column #3, 125°.

REFERENCES

1. A. Jablonski, *Z. Physik*, **94**, 38 (1935).

2. E. F. Ullman, *Accts. Chem. Res.*, **1**, 353 (1968).

3. N. J. Turro, "Molecular Photochemistry", W. A. Benjamin, Inc., N New York, 1967, Chapter 4.

4. (a) M. A. El-Sayed, *Accts. Chem. Res.*, **1**, 8 (1968).

   (b) P. M. Rentzepis and G. E. Busch, *Mol. Photochem.*, **4**, 353 (1972).

   (c) R. M. Hochstrasser, H. Lutz and G. W. Scott, *Chem. Phys. Lett.*, **24**, 162 (1974).

5. R. M. Hochstrasser and C. A. Marzzacco in "Molecular Luminescence", E. C. Lim, Ed., W. A. Benjamin, New York, 1969, p. 631.

6. M. A. El-Sayed, *Accts. Chem. Res.*, **4**, 23 (1971).

7. R. G. W. Norrish and M. E. S. Appleyard, *J. Chem. Soc.*, 874 (1947).

8. C. N. Bamford and R. G. W. Norrish, *ibid.*, 1504 (1935).

9. N. C. Yang and D. H. Yang, *J. Am. Chem. Soc.*, **80**, 2913 (1958).

10. (a) P. J. Wagner and G. S. Hammond, *ibid.*, **80**, 1245 (1966).

    (b) P. J. Wagner, *ibid.*, **89**, 5898 (1967).

    (c) P. J. Wagner, P. A. Kelso, and R. G. Zepp, *ibid.*, **94**, 7480 (1972).

11. (a) N. C. Yang, A Morduchowitz, and D. H. Yang, *ibid.*, **85**, 1017 (1963).

    (b) R. D. Rauh and P. A. Leermakers, *ibid.*, **90**, 2246 (1968).

    (c) F. D. Lewis, *ibid.*, **92**, 5602 (1970).

12. P. J. Wagner, I. E. Kochevar, and A. E. Kemppainen, *ibid.*, **94**, 7489 (1972).

13. P. J. Wagner, P. A. Kelso, A. E. Kemppainen, J. M. McGrath, H. N. Schott, and R. G. Zepp, *ibid.*, **94**, 7506 (1972).

14. P. J. Wagner and A. E. Kemppainen, *ibid.*, **94**, 7495 (1972).

15. J. N. Pitts, Jr., D. R. Burley, J. C. Mani, A. D. Broadbent, *ibid.*, **90**, 5900 (1968).

16. C. Walling and M. J. Gibian, *ibid.*, **87**, 3361 (1965).

17. P. J. Wagner, *Accts. Chem. Res.*, **4**, 168 (1971).

18. J. N. Murrell, "The Theory of the Electronic Spectra of Organic Molecules", Methven and Co., Ltd., London, 1963, pp. 206, 227.

19. S. Nagakura and J. Tanaka, *J. Chem. Phys.*, **22**, 236 (1954).

20. N. C. Yang and R. L. Dusenbery, *Mol. Photochem.*, **1**, 159 (1969).

21. G. Porter and P. Suppan, *Trans. Faraday Soc.*, **61**, 1664 (1965).

22. N. J. Turro and C. Lee, *Mol. Photochem.*, **4**, 427 (1972).

23. (a) N. C. Yang, D. S. McClure, S. L. Murov, J. J. Houser, and R. Dusenbery, *J. Am. Chem. Soc.*, **89**, 5466 (1967).

    (b) N. C. Yang and R. L. Dusenbery, *ibid.*, **90**, 5899 (1968).

24. M. Berger, E. McAlpine, and C. Steel, *ibid.*, **100**, 5147 (1978).

25. E. J. Baum, J. K. S. Wan, and J. N. Pitts, Jr., *ibid.*, **88**, 2652 (1966).

26. P. J. Wagner and A. E. Kemppainen, *ibid.*, **90**, 5898 (1968).

27. J. N. Pitts, Jr., D. R. Burley, J. C. Mani, and A. D. Broadbent, *ibid.*, **90**, 5902 (1968).

28. P. J. Wagner, A. E. Kemppainen, and H. N. Schott, *ibid.*, **95**, 5604 (1973).

29. P. J. Wagner, M. J. Thomas, and E. Harris, *ibid.*, **98**, 7675 (1976).

30. (a) D. R. Kearns and W. A. Case, *ibid.*, **88**, 5087 (1966).

    (b) A. A. Lamola, *ibid.*, **47**, 4810 (1967).

    (c) R. M. Hochstrasser and C. Marzzacco, *J. Chem. Phys.*, **49**, 971 (1968).

    (d) Y. H. Li and E. C. Lim, *Chem. Phys. Lett.*, **7**, 15 (1970).

31. S. Dym and R. M. Hochstrasser, *J. Chem. Phys.*, **51**, 2458 (1969).

32. N. J. Turro, *J. Chem. Ed.*, **43**, 13 (1966).

33. N. J. Turro, "Modern Molecular Photochemistry", Benjamin/Cummings Publishing Co., Inc., Menlo Park, CA, 1978, Ch. 9.

34. V. L. Ermolaev, *Soviet Physics, Upekhi*, **80**, 333 (1963).

35. P. J. Wagner and I. Kochevar, *J. Am. Chem. Soc.*, **90**, 2232 (1968).

36. P. J. Wagner and G. S. Hammond, in "Advances in Photochemistry", Vol. 5, W. A. Noyes, Jr., G. S. Hammond, and J. N. Pitts, Eds., Interscience, New York, 1968, p. 56.

37. N. J. Turro and Y. Tanimoto, *J. Photochem.*, **14**, 199 (1980).

38. G. R. DeMare, M. C. Fontaine, and M. Termonia, *Chem. Phys. Lett.*, **11**, 617 (1971).

39. P. J. Wagner, J. M. McGrath, and R. G. Zepp, *J. Am. Chem. Soc.*, **94**, 6883 (1972).

40. (a) P. A. Leermakers, G. W. Byers, A. A. Lamola, and G. S. Hammond, *ibid.*, **85**, 2670 (1963).

    (b) A. A. Lamola, P. A. Leermakers, G. W. Byers, and G. S. Hammond, *ibid.*, **87**, 2322 (1965).

41. (a) D. O. Cowan and A. A. Baum, *ibid.*, **92**, 2153 (1970).

    (b) D. O. Cowan and A. A. Baum, *ibid.*, **93**, 1153 (1971).

42. H. E. Zimmerman and R. D. McKelvey, *J. Am. Chem. Soc.*, **93**, 3638 (1971).

43. (a) R. A. Keller and L. J. Dolby, *ibid.*, **89**, 2768 (1967).

    (b) R. A. Keller and L. J. Dolby, *ibid.*, **91**, 1293 (1969).

44. (a) G. S. Hammond and W. M. Moore, *ibid.*, **81**, 6334 (1959).

    (b) J. G. Calvert and J. N. Pitts, Jr., "Photochemistry", J. Wiley, New York, 1966, Ch. 5.

    (c) P. J. Wagner and A. E. Puchalski, *J. Am. Chem. Soc.*, **102**, 7138 (1980).

45. E. J. Bowen and E. L. A. E. De La Praudiere, *J. Chem. Soc.*, 1503 (1934).

46. G. S. Hammond, W. P. Baker, and W. M. Moore, *J. Am. Chem. Soc.*, **83**, 2795 (1961).

47. G. S. Hammond and P. A. Leermaker, *ibid.*, **84**, 207 (1962).

48. S. G. Cohen and S. Aktipis, *Tetrahedron Lett.*, 579 (1965).

49. (a) S. G. Cohen and R. J. Baumgarten, *J. Am. Chem. Soc.*, **87**, 2996 (1965).

    (b) R. S. Davidson, *Chem. Commun.*, 575 (1966).

    (c) S. G. Cohen and R. J. Baumgarten, *J. Am. Chem. Soc.*, **89**, 3471 (1967).

50. For a review see J. C. Scaiano, *J. of Photochem.*, **2**, 81 (1973).

51. C. Walling and M. J. Gibian, *J. Am. Chem. Soc.*, **87**, 3361 (1965).

52. R. S. Davidson and P. F. Lambeth, *Chem. Commun.*, 1265 (1967).

53. S. G. Cohen and A. D. Litt, *Tetrahedron Lett.*, 579 (1965).

54. S. G. Cohen and B. Green, *J. Am. Chem. Soc.*, **91**, 3085 (1969).

55. W. E. Bachmann, *ibid.*, **55**, 391 (1933).

56. S. G. Cohen and J. I. Cohen, *ibid.*, **89**, 164 (1967).

57. S. G. Cohen, A. Parola, and G. H. Parsons, Jr., *Chem. Rev.*, **73**, 141 (1973).

58. S. G. Cohen and J. I. Cohen, *J. Phys. Chem.*, **72**, 3782 (1968).

59. A. Weller, *Pure Appl. Chem.*, **16**, 115 (1968).

60. D. Rehm and A. Weller, *Ber. Bunsenges. Phys. Chem.*, **73**, 834 (1969).

61. N. Mataga, T. Okada, and N. Yamamoto, *Chem. Phys. Lett.*, **1**, 119 (1967).

62. G. A. Davis, P. A. Carapellucci, K. Szoc, and J. D. Gresser, *J. Am. Chem. Soc.*, **91**, 2264 (1969).

63. S. G. Cohen and N. Stein, *ibid.*, **91**, 3690 (1969).

64. (a) J. B. Guttenplan and S. G. Cohen, *ibid.*, **94**, 4040 (1972).

    (b) J. B. Guttenplan and S. G. Cohen, *Tetrahedron Lett.*, **22**, 2163 (1972).

65. H. Knibbe, D. Rehm, and A. Weller, *Ber. Bunsenges. Physik. Chem.*, **73**, 839 (1969).

66. H. Leonhardt and A. Weller, *ibid.*, **67**, 791 (1963).

67. P. J. Wagner and B. J. Scheve, *J. Am. Chem. Soc.*, **99**, 1858 (1977)

68. P. J. Wagner and R. A. Leavitt, *ibid.*, **95**, 3669 (1973).

69. R. I. Bartholomew, R. S. Davidson, P. F. Lambeth, J. F. McKellar, and P. H. Turner, *J. Chem. Soc., Perkin II*, 577 (1972).

70. C. G. Shaefer and K. S. Peters, *J. Am. Chem. Soc.*, **102**, 7566, (1980).

71. E. Amouyal and R. Bensasson, *J. Chem. Soc., Faraday Trans. 1*, **73**, 1561 (1977).

72. F. I. Uilęsov, *Usp. Fiz. Nauk*, **81**, 669 (1963).

73. P. J. Wagner, A. E. Kemppainen, and T. Jellinek, *J. Am. Chem. Soc.*, **94**, 7512 (1972).

74. W. B. Mueller and P. J. Wagner, unpublished results, Michigan State University.

75. P. J. Wagner and A. E. Kemppainen, *J. Am. Chem. Soc.*, **91**, 3085 (1969).

76. I. E. Kochevar and P. J. Wagner, *ibid.*, **94**, 3859 (1972).

77. P. J. Wagner and R. A. Leavitt, *ibid.*, **95**, 3669 (1973).

78. S. G. Cohen and J. B. Guttenplan, *J. Org. Chem.*, **38**, 2001 (1973).

79. R. A. Clasen and S. Searles, Jr., *Chem. Commun.*, 289 (1966).

80. A. Padwa, E. Eisenhardt, R. Gruber, and D. Pashayan, *J. Am. Chem. Soc.*, **91**, 1857 (1969).

81. A. Padwa, F. Albrecht, P. Singh, and E. Vega, *ibid.*, **93**, 2928 (1971).

82. P. J. Wagner and D. A. Ersfeld, *ibid.*, **98**, 4515 (1976).

83. S. G. Cohen, G. A. Davis, and W. D. K. Clark, *ibid.*, **94**, 869 (1972).

84. M. A. Winnik and C. Hsiao, *Chem. Phys. Lett.*, **33**, 518 (1975).

85. A. Mar and M. A. Winnik, *ibid.*, **77**, 73 (1981).

86. H. Mashuhara, Y. Maeda, and N. Mataga, *Chem. Phys. Letts.*, **69**, 182 (1980).

87. P. J. Wagner in "Creation and Detection of the Excited State", Vol. 1 A, A. A. Lamola, Ed., Marcel Decker, New York, 1971, p. 173.

88. A. A. Lamola and G. S. Hammond, *J. Chem. Phys.*, **43**, 2129 (1965).

89. (a) D. R. Arnold, *Adv. Photochem.*, **6**, 301 (1968).

    (b) W. T. Leigh, D. R. Arnold, R. W. R. Humphreys and P. C. Wong, *Can. J. Chem.*, **58**, 2537 (1980).

90. (a) D. R. Arnold, J. R. Bolton, and J. A. Pederson, *J. Am. Chem. Soc.*, **94**, 2872 (1972).

    (b) M. L. May, Ph.D. Thesis, Michigan State University, 1977.

91. P. J. Wagner, I. E. Kochevar, and A. E. Kemppainen, *J. Am. Chem. Soc.*, **94**, 7489 (1977).

92. R. O. Loutfy and R. O. Loutfy, *Tetrahedron*, **29**, 2251 (1973).

93. P. J. Wagner, M. L. May and A. Haug, *Chem. Phys. Lett.*, **13**, 545 (1972).

94. R. Hoffmann and J. R. Swenson, *J. Phys. Chem.*, **74**, 415 (1970).

95. S. Wawzonek and A. Gundersen, *J. Electrochem. Soc.*, **107**, 537 (1960).

96. L. Nadjo and J. M. Savéant, *J. Electroanal. Chem.*, **30**, 41 (1971).

97. R. O. Loutfy and R. O. Loutfy, *J. Phys. Chem.*, **76**, 1650 (1972).

98. N. Hirota, T. C. Wong, E. T. Harrigan, and K. Nishimoto, *Mol. Phys.*, **29**, 903 (1975).

99. P. J. Wagner and M. L. May, *Chem. Phys. Lett.*, **39**, 350 (1976).

100. P. H. Rieger and G. K. Fraenkel, *J. Chem. Phys.*, **37**, 2795 (1962).

101. C. Santeajo and K. N. Houk, *J. Am. Chem. Soc.*, **98**, 3380 (1976).

102. D. R. Kearns, *J. Chem. Phys.*, **36**, 1608 (1962).

103. J. Petruska, *ibid.*, **34**, 1120 (1961).

104. H. Suzuki, "Electronic Absorption Spectra and Geometry of Organic Molecules", Academic Press, New York, 1967, p. 432.

105. P. H. Rieger, I. Bernal, W. H. Reinmuth, and G. Fraenkel, *J. Am. Chem. Soc.*, **85**, 683 (1963).

106. P. J. Wagner and G. Capen, *Mol. Photochem.*, **1**, 159 (1969).

107. R. W. Alder, R. Baker, and J. M. Brown, "Mechanism in Organic Chemistry", Wiley-Interscience, New York, 1971, p. 30.

108. Unpublished results by P. J. Wagner and M. J. Thomas.

109. "Handbook of Chemistry and Physics," R. C. Weast, ed., Chemical Rubber Company, Cleveland, OH, 1972, D-118, 119.

110. The term "merostabilization" describes the additional stabilization imparted to free radicals bearing substituents of opposite electron demand, as first suggested by R. W. Baldock, P. Hudson, A. R. Katrutzky, and F. Scoti, *J. Chem. Soc. Perkin Trans. I*, 1422 (1974).

111. D. A. Ersfeld, Ph.D. Thesis, Michigan State University, 1974.

112. F. J. Golemba and J. E. Guillet, *Macromol.*, **5**, 63 (1972).

113. C. K. Mann, *Anal. Chem.*, **36**, 2424 (1964).

114. D. I. Schuster and T. M. Weil, *Mol. Photochem.*, **4**, 447 (1972).

115. J. A. Riddick, "Techniques of Organic Chemistry", Vol. 2, A. Weisberger, Ed., John Wiley and Sons, New York, N.Y., second edition, 1970.

116. E. O. Forster, *J. Chem. Phys.*, **37**, 1021 (1962).

117. P. J. Wagner group, both published and unpublished syntheses.

118. W. Michaelis, J. H. Russel, and O. Schindler, *J. Med. Chem.*, **13**, 497 (1970).

119. W. F. Bruce, *Org. Syn.*, **2**, 139 (1943).

120. F. S. Alvarez, A. W. Watt, *J. Org. Chem.*, **33**, 2143 (1968).

121. P. L. de Benneville, *J. Org. Chem.*, **6**, 462 (1941).

122. M. S. Newman, H. G. Kuivila, and A. B. Garrett, *J. Am. Chem. Soc.*, **67**, 704 (1945).

123. J. W. Melton and H. R. Henze, *J. Am. Chem. Soc.*, **69**, 2018 (1947).

124. C. F. H. Allen and J. W. Gates, Jr., *Org. Syn.*, **3**, 140 (1955).